PHENOTYPIC ANALYSIS OF PLANT DWARFING INDUCED BY OVEREXPRESSION OF A TOBACCO *MYB* GENE

Thesis submitted for the degree of
Doctor of Philosophy
at the University of Leicester

by

Sasan Amirsadeghi
Department of Biology
University of Leicester

October 2000

ProQuest LLC
789 East Eisenhower Parkway
P.O. Box 1346
Ann Arbor, MI 48106-1346

for mama and baba

&

Azita

ABSTRACT

Phenotypic analysis of plant dwarfing induced by overexpression of a tobacco *MYb* gene

Sasan Amirsadeghi

The tobacco *NtmybAS1* gene encodes a novel anther-specific member of the Myb family of transcription factors. Overexpression of *NtmybAS1* driven by the CaMV35S promoter in tobacco resulted in dramatic alterations in plant architecture leading to a semi-dominant dwarf phenotype. Northern blot analysis demonstrated a direct relationship between the severity of dwarf phenotype and the level of *NtmybAS1* transcripts, which clearly indicated that the *NtmybAS1*-induced dwarfing is gene dosage dependent.

Analysis of cell morphology demonstrated that a severe reduction of cell elongation in hypocotyls was the major cause of *NtmybAS1*-induced dwarfing. In contrast, a dramatic increase in cell elongation and pronounced cell division was detected in palisade and mesophyll cells. Despite changes in cell morphology, the overall body organisation of *NtmybAS1* plants remained unaffected. Furthermore, phenotypic alterations in *NtmybAS1* overexpressing plants were not normalised by application of phytohormones or by grafting, indicating the involvement of non-hormonal factors and the cell autonomy of dwarfing.

Transient expression analyses of the N-terminal Myb domain derivatives fused to sGFP revealed the presence of a nuclear localisation signal, which efficiently targeted sGFP to the pollen nucleus.

Analysis of the cellular protein profiles of *NtmybAS1* plants by one and two-dimensional gel electrophoresis revealed two proteins that were highly induced in *NtmybAS1* plants. Tryptic peptides derived from these proteins by reversed-phase HPLC were sequenced and showed an exact match with two pathogenesis-related (PR) proteins, tobacco chitinase P (PR-P) and PR-1a. Induction of PR-P and PR-1a mRNAs in *NtmybAS1* plants was also confirmed by northern blot analysis. Activation of PR proteins in *NtmybAS1* plants was associated with the induction of tobacco *myb1* expression, which encodes a Myb-related component of the salicylic acid (SA) signal transduction pathway. However, RT-PCR analyses revealed that *NtmybAS1* was not induced by application of SA or by wounding. Results derived from these analyses led to the hypothesis that induction of PR-P, PR-1a and *myb1* expression in *NtmybAS1* plants is a consequence of increased phenylalanine ammonia lyase (PAL) activity, which catalyses the first step in the biosynthesis of SA. The results further suggested that the NtMybAS1 protein might act as a regulator of *gPAL1* expression in tobacco anthers. These hypotheses were supported by demonstration of expression of *gPAL1* in *NtmybAS1* plants above the wild type level and further establishment of a positive correlation between the induction of *NtmybAS1* mRNA and activation of *gPAL1* expression at early stages of anther development.

Taken together, the results presented here suggest that the *NtMybAS1* is an activator of *gPAL1* expression in anthers, and when overexpressed in vegetative tissues induces *gPAL1* expression leading to induction of PR-P and PR-1a via a salicylic acid-dependent signal transduction pathway.

Acknowledgements

I would like to thank my supervisors Prof. David Twell for excellent supervision, encouragement and patience and Dr. Mehdi Barghchi for his constant support throughout the course of this project.

I am grateful to Dr. Justin Sweetman for providing the *myb* cDNAs and plant material at the beginning of this project. I extend my special thanks to Dr. Jonathan Combe for his friendship, advice and technical assistance in all things and to Dr. Neil Bate and Dr. Man-Kim Cheung for their friendship and providing plasmids for the *myb* constructs. I also thank Dr. Luis Mur for his advice in sectioning and grafting.

I extend my gratitude to Dr. Ana Bras-Goldberg for protein analysis by two-dimensional gel electrophoresis and Dr. Kathryn Lilley for HPLC analysis and peptide sequencing.

I am grateful to members of Biology Department for their support during the course of this project. I would also like to thank Graham Benskin and June Saddington for maintenance and care of transgenic plants.

Many thanks to Azita especially for all she did for me from the beginning to the end of this project.

I acknowledge the financial support of AREEO and ICARDA.

Contents page

List of figures

Abbreviations

A	adenine
aa	amino acid
abaxial	lower surface
adaxial	upper surface
AMV	avian myeloblastosis virus
ATP	adenosine triphosphate
BAP	6-benzylaminopurine
bp	base pair
BR	Brassinosteroid
BSA	bovine serum albumin
°C	degrees centigrade
CAD	cinnamyl alcohol dehydrogenase
cDNA	complementary DNA
C4H	cinnamic acid 4-hydroxylase
CHI	chalcone isomerase
CHS	chalcone synthase
4CL	4-coumarate:coenzyme A ligase
cm	centimetre
cv	cultivar
dCTP	2'-deoxycytidine 5'-triphosphate
DEPC	diethyl pyrocarbonate
DNA	deoxyribonucleic acid
dNTP	deoxynucleotide triphosphate
DTT	dithiothreitol
EDTA	ethylenediaminetetraacetic acid
EGTA	ethylene glycol-bis(β-aminoethyl ether)N,N,N',N'-tetraacetic acid
g	gram
g	gravity
G	guanine

GA	gibberellic acid
GUS	β-glucuronidase
h	hour
HPLC	High Pressure Liquid Chromatography
IEF	isoelectric focusing
Kb	Kilobase pair
kDa	Kilodalton
l	litre
M	molar
mA	milliampere
MBS	Myb binding site
MES	2-(N-Morpholino)ethanesulfonic acid
μg	microgram
μl	microlitre
mg	milligram
ml	millilitre
mM	millimolar
min	minute
MOPS	3-(N-morpholino)propanesulfonic acid
mRNA	messenger RNA
MS	Murashige and Skoog
ng	nanogram
NLS	nuclear localisation signal
NMR	nuclear magnetic resonance
nt	nucleotide
OD	optical density
PAL	phenylalanine ammonia-lyase
PCR	polymerase chain reaction
PMSF	phenylmethylsulfonyl fluoride
PNACL	The protein and nucleic acid chemistry laboratory
PR protein	pathogenesis-related protein
RNA	ribonucleic acid

rpm	revolution per minute
R1R2R3	Myb repeats
RT	room temperature
RT-PCR	reverse transcriptase-PCR
SA	salicylic acid
SAR	systemic acquired resistance
SD	standard deviation
SDS	sodium dodecyl sulphate
SDS-PAGE	SDS-polyacrylamide gel electrophoresis
SDW	sterile distilled water
sec	second
sGFP	synthetic green fluorescent protein
TAE	tris-acetate EDTA
TEMED	N,N,N',N'-tetramethylethylenediamine
TFA	trifluoroacetic acid
Thr	threonine
TLC	thin layer chromatography
TMV	tobacco mosaic virus
Tris	tris(hydroxymethyl)aminomethane
Triton X-100	(t-Octylphenoxypolyethoxyethanol)
U	enzyme units
UTR	untranslated region
UV	ultra violet
V	volts
v/v	volume per volume
W	watts
WT	wild type
w/v	weight per volume

Chapter 1

Introduction

1. 1 Transcription machinery in eukaryotes

Three distinct RNA polymerases (RNAP I, RNAP II and RNAP III) have evolved in eukaryotes to transcribe different sets of nuclear genes. The genes encoding large ribosomal RNAs are transcribed by RNAP I. All the protein-coding messenger RNAs and small RNAs (snRNAs) are transcribed by RNAP II and finally RNAP III transcribes transfer RNA (tRNA), 5S RNA and U6 RNA. None of the eukaryotic polymerases is able to recognise their promoters and initiate transcription on its own. Distinct sets of promoter elements and protein factors which are required for promoter recognition and initiation of transcription by RNAPs have been identified in eukaryotes (reviewed in Zawel and Reinberg, 1995).

Recognition of promoter and initiation of transcription by RNAP II requires the function of general transcription factors (GTFs) including TFIIA, TFIIB, TFIID, TFIIE, TFIIF, TFIIH (Conaway and Conaway, 1997) which are highly conserved in eukaryotes. In addition a number of coactivators such as TAF, USA and CBP, which are able to increase gene expression *in vitro* and *in vivo* can stimulate transcription above basal levels (Roeder, 1996; Montminy, 1997).

Transcription initiation complex is primarily assembled by a mechanism known as nucleation. The TATA motif (generally 30 nucleotides upstream of the transcription start site) and the initiator motif (Smale and Baltimore, 1989), which contains the transcription start site, are the two core promoter elements that mediate nucleation in RNAPII promoters.

TFIID is a multiprotein complex, which binds to the TATA box. The 38-kDa subunit of TFIID known as TBF (TATA binding factor) contains two imperfect direct repeats of about 90 amino acids at the C-terminal domain, which recognise the TATA motif. This subunit is tightly associated with polypeptides known as TAFs (TBP-associated factors) that are tightly associated with TBP.

Once initiation complex assembly is nucleated by TFIID or initiator binding proteins (IBPs) on the core promoter elements, a single polypeptide known as TFIIB (Buratowski *et al.*, 1989; Maldonado *et al.*, 1990), which may act as a bridge links the RNAPII to the core promoter. It has been reported that the N-terminal domain of TFIIB is involved in interactions with TFIIF, which function to deliver the RNAPII

to the initiation complex and with complexes containing RNAPII. The C-terminal domain of TFIIB interacts with TFIID-DNA complex (Ha *et al.*, 1993, Roberts *et al.*, 1993). Studies on the components of yeast transcription machinery have established that the direct interaction of TFIIB with RNAPII plays a critical role in determining the transcription start site (Li *et al.*, 1994).

It has been shown that the TFIIA stimulates binding of TFIID to the TATA motif. The 32 kDa active polypeptide of TFIIB can specifically recognise a complex consisting of TFIID and TFIIA (DA complex) and form the DAB complex. Formation of this complex also requires the sequences downstream of the transcriptional start site (Maldonado *et al.*, 1990). Stable association of RNAPII with either complex (DAB or DB) on promoter is mediated by TFIIF. Two subunits of TFIIF (RAP 30 and RAP 74) are involved in recruitment of RNAPII to the promoter containing DAB complex. However, it has been shown that RAP 30 alone is sufficient for this process (Flores *et al.*, 1991; Zawel *et al.*, 1993).

Interaction of TFIIF with TFIIB (Ha *et al.*, 1993) and TFIIF with RNAPII (Killeen and Greenblatt, 1992) in solution have led to the suggestion that TFIIB and TFIIF cooperate for the recruitment of RNAPII to the promoter.

Initiation of transcription following recruitment of RNAPII to the promoter requires the function of two additional GTFs (TFIIE and TFIIH) and hydrolysis of β-γ bond of ATP. TFIH (Schaeffer *et al.*, 1994) and TFIIE (Inostroza *et al.*, 1991; Ohkuma *et al.*, 1990) are involved in modification of RNAPII. TFIIH is a multisubunit protein and is not only involved in transcription initiation, but also contains kinase, ATPase and helicase activity (reviewed in Drapkin *et al.*, 1994). The C-terminal domain (CTD) of the largest subunit of RNAPII contains tandem repeats of the heptapeptide sequence YSPTSPS, which is phosphorylated by TFIIH (Feaver *et al.*, 1991; Lu *et al.*, 1992; Serizawa *et al.*, 1992) at serine, threonine and/or tyrosine and results in generation of two hyperphosphorylated (RNAPIIO) and nonphosphorylated (RNAPIIA) isoforms of RNAPII (Dahmus, 1981; Cadena and Dahmus, 1987; Baskaran *et al.*, 1993). These two species of RNAPII are functionally different. The RNAPIIO is transcriptionally active and is involved in RNA chain elongation (Cadena and Dahmus, 1987; Weeks, 1993; O'Brien *et al.*, 1994) whereas RNAPIIA is preferentially involved in preinitiation complex assembly (Lu *et al.*,

1991; Chesnut *et al.*, 1992) and formation of short transcripts from sequences proximal to promoters due to a pause in transcription (O'Brien *et al.*, 1994).

Phosphorylation of RNAPII during the initiation complex assembly is believed to act as a signal for the transition from (transcription) initiation complex assembly to elongation (Zawel and Reinberg, 1992). Further demonstration of interaction of the nonphosphorylated CTD with TBP (Usheva *et al.*, 1992) and TFIIE (Maxon *et al.*, 1994) has led to a suggestion that phosphorylation of CTD mediates a conformational change in the initiation complex (Zawel and Reinberg, 1992). TFIIE is a heterodimer consisting of two 56-kDa and 34-kDa subunits, which is involved in the stable association of TFIIH with the preinitiation complex for transcription initiation and stimulation of both the kinase and ATPase activity of TFIIH (Lu et al., 1992; Ohkuma *et al.*, 1994; Serizawa *et al.*, 1994).

1. 2 Transcriptional activation *in vivo*: Triad model

The triad model of transcriptional activation (Struhl, 1996) provides a simplified view of the interaction between the components of transcription machinery for the activation of transcription *in vivo*. In this model, TFIID (TBP and associated proteins), poll II holoenzyme and activator proteins are considered as the three legs of a triad which interact with each other to form a stable triad and initiate transcription. Indeed the process of transcriptional activation is considered as the active recruitment of poll II to the initiation complex, which can be increased by the interaction between any two components of the triad. However, in this process the roles of activator proteins are more critical due to high affinity and specificity for particular DNA sequences in the promoter environments.

Recruitment of either TFIID or pol II by the activator protein results in formation of an intermediate state and when the third component is recruited, the resulting triad can initiate transcription. The protein-protein interactions or changes in chromatin structure by the function of chromatin remodelling factors SWI/Snf (reviewd in Carlson and Laurent, 1994) increases the stability of transcription apparatus at the promoter. Following the release of RNAPII from the initiation complex by CTD phosphorylation and elongation (section 1. 1) either a new triad can

be formed by the association an RNAPII molecule to the remainder of the partially dissociated triad, which allows multiple rounds of initiation or the triad complex could also be dissociated and reassembled for the next initiation event. The former mechanism is more likely to occur in light of the fact that transcription initiation occur every 6 seconds on active promoters of yeast and flies in which the pol II density reaches to one molecule per 100 bp (Struhl, 1996).

1. 3 Myb gene family of transcription factors

The *myb* gene was originally identified as a retroviral v-*myb* oncogene of the avian myeloblastosis virus (AMV) and its cellular homologue c-*myb* (Klempnauer *et al.*, 1982). The two forms of this avian retrovirus, AMV (reviewed in Baluda and Reddy, 1994) and E26 (Graf *et al.*, 1992) carrying different versions of the v-*myb* oncogene cause acute monoblastic and erythroblastic leukemia in chickens.

The discovery of the v-*myb* oncogene of AMV further led to identification of the *myb*-related genes in a wide variety of eukaryotes including human (Majello *et al.* 1986; Slamon *et al.*, 1986; Nomura *et al.*, 1988; Westin *et al.*, 1990), mouse (Gonda *et al.*, 1985; Lam *et al.*, 1992), bovine (Ishiguro *et al.*, 1994), chicken (Gonda and Bishop, 1983; Rosson and Reddy, 1986; Gerondakis and Bishop, 1986; Foos *et al.*, 1992), *Xenopus* (Bouwmeester *et al.*, 1992; Sleeman, 1993; Amaravadi and king, 1994), *Drosophila* (Katzen *et al.*, 1985, England *et al.*, 1992; Katzen *et al.*, 1998), cellular slime mold (Stober-Grasser *et al.*, 1992), fungi (Tice-Baldwin *et al.*, 1989; Ju *et al.*, 1990; Ohi *et al.*, 1994; Wieser and Adams, 1995), plants (reviewed in Martin and Paz-Ares, 1997; Romero *et al.*, 1998; Rabinowicz *et al.*, 1999; Kranz *et al.*, 2000), bryophytes (Leech *et al.*, 1993, Kranz *et al.*, 2000) and pteridophytes (Kranz *et al.*, 2000).

Despite the diversity of *myb*-related genes in different eukaryotic phyla, sequence analyses of the genome of the eubacteria *Hemophilus influenza* have not revealed the presence of any *myb*-related genes (Lipsick, 1996). Also the archaebacteria, whose transcription machinery shares many features with eukaryotes (Baumann *et al.*, 1995; Keeling and Doolittle, 1995; Langer *et al.*, 1995) have not been yet investigated for the presence of *myb*-related sequences.

1. 4 The Myb domain forms a helix-turn-helix structure

A conserved domain of approximately 50 amino acids present in one, two (R2, R3) or three (R1, R2 and R3) tandem repeats at the N-terminus of Myb proteins is the common structural feature of the Myb family of transcription factors which is known as the Myb domain. The structure of Myb domain varies to different degrees and is the major determinant of DNA binding specificity of Myb proteins.

In each Myb repeat three tryptophan residues are regularly spaced 18 or 19 amino acids apart and in some cases the first tryptophan of the third repeat is replaced with phenylalanine, isoleucine and tyrosine. In addition to tryptophans several other residues are well conserved in the Myb domain, which include a short acidic motif and a glycine between the first and second tryptophan, a short aliphatic motif and an arginine between the second and third tryptophan and a leucine beyond the third tryptophan (Lipsick, 1996). In the first and second Myb repeats a cysteine residue is highly conserved within a basic motif (KQCRER). This cysteine is involved in redox regulation of DNA binding (Abate *et al.*, 1990) and has been shown to be essential for the oncogenic transformation of myeloid cells and transcriptional activation *in vivo* (Grässer *et al.*, 1992). Furthermore mutation of cysteine to serine decreases the DNA binding affinity of the Myb oncoprotein (Myrset *et al.*, 1993)

The three-dimensional structure of the Myb repeats has been determined by nuclear magnetic resonance (NMR) spectroscopy (Ogata *et al.*, 1992; Jamin *et al.*, 1993; Ogata *et al.*, 1994; Ogata *et al.*, 1995). These analyses revealed that R2 and R3 form three helices and the third helix of each repeat serves as a recognition helix, which is closely packed in the major groove of DNA and overlap each other. Although this type of interaction with DNA has also been reported for the TFIIIA-type zinc fingers (Pavletich and Pabo, 1991; Pavletich and Pabo, 1993; Fairall *et al.*, 1993), the more closely packed positioning of the recognition helices in the major groove of DNA occurs exclusively in the Myb-DNA complexes.

The R1 partially covers the major groove of DNA. This domain is not tightly bound to either DNA or R2R3 and also does not change the conformation of DNA and R2R3. The results of NMR (Ogata *et al.*, 1994) and DNA binding studies

(Tanikawa *et al.*, 1993) has led to the suggestion that R1 is involved in enhancement of the stability of the R2R3-DNA complex.

Further NMR analyses of c-Myb revealed the presence of a cavity inside the hydrophobic core of R2. This cavity is exclusive to R2 and may play an important role in DNA recognition. Mutations affecting the structure of this cavity result in a reduced DNA binding and transcription activation (Ogata *et al.*, 1996).

In contrast to c-Myb in which the R2 and R3 represent a similar structure and the C-terminus of R2 forms a stable helix, the tertiary structure of R2 and R3 in B-Myb varies to a great extent and the C-terminus of R2 forms multiple conformations. This heterogeneity in conformation of B-Myb R2 is thought to be important in the control of gene expression (McIntosh *et al.*, 1998).

1. 5 The Myb domain binds DNA via sequence-specific interactions

Specific interactions of the R2R3 domain of mouse c-Myb with a double stranded 16-mer deoxyoligonucleotide (5'-CCTAACTGACACACAT-3') have been studied by NMR spectroscopy. Based on analysis of 25 structures of the R2R3-DNA complex, two major types of interactions between the amino acids of R2R3 with the DNA base pairs and with the phosphate backbone have been identified (Ogata *et al.*, 1994).

Interactions of Asparagine (183) and lysine (128) with A and G at the positions 4+ and 8+ and lysine (182) with G at position 6- (complementary strand) are the most specific contacts of R2R3 amino acids with the DNA bases. It has been shown by mutation analysis that the substitution of any of these DNA bases dramatically reduces (more than 500-fold) the DNA binding activity of R2R3 (Tanikawa *et al.*, 1993). Furthermore, two independent reports indicate that mutation of lysine (182) to glutamine (Saikumar *et al.*, 1990) and asparagine (183) to alanine (Gabrielsen *et al.*, 1991) causes loss of DNA biding activity.

The second type of interaction of R2R3 with DNA involves contacts between R2R3 amino acids and the phosphate backbone. The most frequent contacts have been found between lysine (92), tryptophan (115), serine (116), glutamine (129) and arginine (133) in R2 and asparagine (164) and tryptophan (166) in R3 with the

phosphate backbones (Ogata *et al.*, 1994). It has been shown that the mutation of certain residues interacting with the phosphate backbones abolishes DNA binding activity (Frampton *et al.*, 1991; Gabrielsen *et al.*, 1991). In addition to the interactions described above, the three arginine residues at positions 125, 133 and 176 interact with both phosphate backbones and by formation of salt bridges with glutamine acid (99), aspartic acid (100) and glutamic acid (151).

These data suggest that a loss of DNA binding activity due to the mutations in the DNA interacting amino acids of R2R3 may be the consequence of disruption of protein structure and backbone interactions (Ogata *et al.*, 1994).

1. 6 Myb domain is involved in trascriptional regulation

Several pieces of evidence described in sections 1. 4 and 1.5 represent the Myb repeats as a domain, which is specifically implicated in DNA binding in a sequence-specific manner. However, in some cases it has been shown that the Myb repeats are also involved in transcriptional regulation. Mutation of a conserved cysteine (C) to serine (S) at position 65 in the N-terminal DNA binding domain of v-Myb does not affect DNA binding ability and localisation of v-Myb in the nuclei of avian hematopoietic cells but this change abolishes *trans*-activation of the CAT reporter gene and transformation of yolk sac myeloid cells (Grässer *et al.*, 1992).

In comparison with c-*myb*, the second repeat of the DNA binding domain of AMV v-*myb* contains three point mutations resulting in substitution of asparagine to isoleucine, histidine to leucine and aspartic acid to valine at positions 91, 106 and 117 respectively. It has been shown that the reversion of any of these mutations to that of c-*myb* enables the oncogene to activate the *mim1* gene. Furthermore, back mutations of asparagine and histidine (91 and 106) change the phenotype of transformed monoblasts into promyelocytes with characteristic granules (Introna *et al.*, 1990).

Evidence of involvement of the Myb domain in transcriptional regulation is also derived from functional analyses of fusions of *Drosophila* Myb and v-Myb repeats, which demonstrate that one repeat of v-myb is essential for *trans*-activation and oncogenic transformation (Bin and Lipsick, 1993).

Furthermore, transcriptional activation of the *bronze-1* (*Bz-1*) promoter in maize requires the co-operation of C1 and a member of the MYC basic helix loop proteins including R or B. Analysis of interactions between maize C1 and B using *trans*-activation of β-galactosidase in yeast have revealed that the Myb repeats of C1 interact with the amino terminus of the B protein (Goff *et al.*, 1992). The evidence described above implies that the Myb domain is not only involved in DNA recognition and binding but also functions in transcriptional regulation of genes via specific interactions.

1. 7 Plant Myb proteins contain conserved motifs beyond the Myb domain

Phylogenetic analyses of plant Myb proteins based on a 320 amino acid sequence of 86 *Arabidopsis* and 35 other plant Myb proteins (Kranz *et al.*, 1998) revealed the presence of conserved motifs in a highly variable region beyond the Myb domain. This finding led to classification of plant Myb proteins into 22 different subgroups (Kranz *et al.*, 1998).

Based on this classification, the NtMybAS1 protein (Sweetman, 1996), the subject of this thesis, which shows strong sequence similarity to petunia PhMYB3 (Avila *et al.*, 1993) is classified in subgroup 18 (Kranz *et al.*, 1998). The conserved amino acid motif of this subgroup, QRaGLPxYPxE/S, in the NtMybAS1 protein is found immediately C-terminal (aa. 126-136) to the Myb domain in which the last glutamic acid (E) is substituted with an aspartic acid (D) (Figure 1. 1).

The conserved amino acid motifs beyond the Myb domain are mostly specific for Myb proteins. The conserved motif (lWVheDdFELSsLtxMMdF) of the *Arabidopsis* Myb proteins in subgroup 15 has not been yet identified in any other plant species. In contrast, the conserved amino acid motif (IDeSFWxE/Dxlstd) of subgroup 2 is also found in a plant virus protein (Kranz *et al.*, 1998). The functional significance of these motifs is largely unknown. However, deletion of this motif in *gl1-2* (Esch *et al.*, 1994), a mutant allele of *GL1*, results in a reduction of trichome development. Furthermore, *Drosophila* mutants containing a single amino acid substitution, glycine (G) to serine (S), in a highly conserved domain at the C-terminus of DmMyb protein develop defective wings with fewer cells and larger

nuclei due to a block in G2 to M and inability to prevent endoreplication (Katzen *et al.*, 1998). These data reflect to some extent the functional importance of the conserved motifs at the C-terminus of Myb proteins.

Some members of certain subgroups perform similar functions (subgroup 9) and show a similar pattern of gene expression (subgroup 10, 11 and 19). However, since the full range of functions of the Myb proteins in plants is unknown, it is not possible at this point to deduce whether the members of each subgroup are functionally homologous. The two members of subgroup 18 including HvMYBGa (Gubler *et al.*, 1995) and OsMYBGa (X98355) are involved in the GA response pathway leading to activation of α-amylase gene expression whereas petunia PhMYB3 (Avila *et al.*, 1993; Solano *et al.*, 1995) in this subgroup has a different function and is involved in flavonoid biosynthesis. Furthermore, a recent report (Yang *et al.*, 2000) indicates that the NtMybAS1 protein acts as an activator of phenylalanine ammonia-lyase expression in tobacco anthers that bears no similarity to the functions of GAMYBs described above. Although the functions of four other members of this subgroup including AtMyb 33, AtMyb 65, AtMyb 81 and AtMyb 101 are unknown, these data indicate that the members of each subgroup do not necessarily perform similar functions.

1. 8 Biological activity of Myb proteins is post-translationally regulated

Several lines of evidence indicate that the post-translational modifications such as phosphorylation and acetylation modulate Myb protein activity both *in vitro* and *in vivo*. Recent studies revealed the presence of a phosphorylated form of B-Myb in mouse fibroblasts. The phosphorylation of B-Myb was S phase-specific and inducible by a cyclin A/cdk2 when expressed in insect cells. (Robinson *et al.*, 1996).

It has been shown that the coexpression of B-Myb and cyclin A or cyclin E increases the number of cells in S phase of the cell cycle, transactivates CAT reporter gene expression and alters electrophoretic mobility of B-Myb as a result of formation of phosphorylated forms of B-Myb. Furthermore, transient transfection of B-Myb in human cell lines with high levels of cyclin A promotes cell proliferation leading to a significant increase of the number of cells in S phase of the cell cycle. These data led

to the conclusion that the cyclin-induced phosphorylation of human B-myb act as a positive regulator of B-Myb activity for the control of cell proliferation and trascriptional activation (Sala *et al.*, 1997).

The finding that the ability of cyclin A-Cdk2 to enhance *trans*-activation function of B-Myb in human cells is abolished in the presence of a dominant negative Cdk2 protein provided evidence that the kinase activity of cyclin A/Cdk2 complex stimulates *trans*-activation function of B-Myb. Transient expression and Western blot analysis has established a close correlation between the phosphorylation of B-myb and stimulation of B-Myb *trans*-activation function. The fact that deletion (aa. 562-704) of the C-terminal domain of B-Myb significantly increased the B-Myb *trans*-activation demonstrated that the B-Myb activity can be stimulated both by cyclin-dependent phosphorylation and deletion of the B-Myb C-terminus. Furthermore, analysis of cell cycle profiles of human cells transfected with the cyclin A, B-Myb and the CD20 cell surface protein using fluoroscein isothiocyanate-tagged CD20 antibody and propidium iodide in conjunction with flow cytometry has established the synergistic effect of cyclin A on B-Myb to promote cells into the S phase of the cell cycle (Lane *et al*, 1997).

Studies of phosphorylation of B-Myb *in vitro* using ^{32}P-ATP and cell extracts containing cyclin A/Cdk2, cyclin E/Cdk2 and D1/Cdk4 revealed the specific radiolabelling of B-Myb by the extract containing cyclin A/Cdk2 indicating that B-Myb is a substrate for cyclin A/Cdk2. It has been shown by TLC analysis that the tryptic phosphopeptides derived from *in vivo* ^{32}P-orthophosphate-labelled B-Myb have the same pattern of migration in TLC plates as those derived from *in vitro* phosphorylated B-Myb by cyclin A/Cdk2. Mutation analysis and two-dimensional phosphopeptide mapping has identified the Thr447, Thr490 and Thr497 and Ser581 as the sites of B-Myb phosphorylation by cyclinA-Cdk2. Furthermore, mutation of phosphorylation sites dramatically reduces *trans*-activation function of B-Myb. These data indicate that phosphorylation of B-Myb at cyclin A/Cdk2 sites directly modulate the B-Myb *trans*-activation function (Saville and Watson, 1998).

More recently the cyclin A/Cdk2 phosphorylation sites of B-Myb was determined by two-dimensional tryptic phosphopeptide analysis. It was shown that Thr443, Thr447, Thr490, Thr497 and Thr524 at the C-terminus of B-Myb are phosphorylated *in vivo*. Furthermore, the finding that substitution of Thr524 to an alanine dramatically reduced *trans*-activation activity of B-Myb led to the conclusion

that phosphorylation of Thr524 is crucial for the activation of B-Myb by cyclin A (Bartsch *et al.*, 1999).

Phosphorylation of Myb proteins has also been studied in the case of mouse A-Myb. Transactivation potential of A-Myb, which is modulated in a cyclin dependent manner, is suppressed by a dominant negative mutant of cyclin dependent kinase CDK2. Gel retardation assay revealed that the formation of slower migrating form of A-Myb as result of phosphorylation of A-Myb by the complexes containing cyclin-A or cyclin E and CDK2 is abolished by the dominant negative mutant of CDK2. The use of an *in vitro* phosphatase assay has established that the cyclin-induced alterations in gel mobility of A-Myb result from phosphorylation. Cyclin-dependent phosphorylation of A-Myb has also been shown *in vivo* using ^{32}P-ortophosphate. Incorporation of phosphate label into A-Myb is dramatically stimulated in the presence of cyclin A or cyclin E. The site of phosphorylation of A-Myb has been mapped to the C-terminal domain of this protein and its phosphorylation has been shown directly by *in vitro* kinase assay. Expression of A-Myb in a cell cycle-dependent manner and phosphorylation of A-Myb by cyclin A or cyclin E and CDK2 complexes has led to the conclusion that the function of A-Myb is regulated at two different levels leading to the maximum activity of A-Myb at the G1/S-transition and the S-phase of the cell cycle (Ziebold *et al.*, 1997).

In higher plants post-translational modification of the Myb proteins has been shown in the case of *Arabidopsis CCA1* gene product, which binds the *Lhcb1*3* promoter and is involved in phytochrome signal transduction and in the regulation of circadian rhythms (Wang and Tobin, 1998). Using the yeast two hybrid system a regulatory subunit of Ser/Thr kinase CK2, known as CKB3, was identified in *Arabidopsis*, which specifically interacts with CCA1 (Sugano *et al.*, 1998). CK2 enhances binding of CCA1 to the *Lhcb1*3* promoter *in vitro* and also phosphorylates CCA1 in the presence of both ATP and GTP as phosphodonors. Phosphorylation of CCA1 *in vitro* has also been shown using the *Arabidopsis* whole-cell extracts. This phosphorylation is necessary for the establishment of a DNA-protein complex containing CCA1 (Sugano *et al.*, 1998).

Study of DNA binding affinities of Myb305 and Myb340, synthesised in yeast, revealed that the Myb305 binds to a number of flavonoid biosynthetic gene

promoters more strongly than Myb340. Furthermore, *in vitro* synthesised Myb305 showed higher binding affinity to chalcone isomerase (CHI) promoter than the Myb340. The finding that dephosphorylation of Myb340 compared with Myb305 dramatically increased its binding to the CHI promoter led to the suggestion that the difference in binding affinity of Myb305 and Myb340 is a consequence of differential phosphorylation of these proteins *in vivo* which prevents binding of Myb340 to its target sites (Moyano *et al.*, 1996).

Myb proteins undergo another type of post-translational modification. More recently it was shown that the c-Myb is acetylated both *in vitro* and *in vivo* by a histone acetyl transferase, p300. The acetylation sites at the C-terminus of c-Myb have been mapped to three conserved lysine residues at positions 471, 480, 485. EMSA and transient expression assays revealed that the acetylation of c-Myb dramatically increases its DNA binding and *trans*-activation activities (Tomita *et al.*, 2000).

Taken together, this evidence indicates that post-translational modifications play an important role in modulation of *trans*-activation potential and cellular function of Myb proteins.

1. 9 Higher plants contain large number of *myb* genes

The genes encoding Myb-related proteins are widely found in eukaryotes. In contrast to vertebrates in which about 10 *myb* genes have been identified (reviewed in Lipsick, 1996), higher plants contain the largest number of *myb* genes among other eukaryotes. Two independent studies (Romero *et al.*, 1998; Kranz *et al.*, 1998) of the *myb* gene family in *Arabidopsis* revealed the presence of about 100 different *myb* genes which corresponds to 0.2-0.6% of the total estimated genes in *Arabidopsis* (Gibson and Sommerville 1993). The number of *myb* genes in other plant species is largely unknown. However, it has been estimated that *Petunia hybrida* contains at least 20-30 *myb* genes (Avila *et al.*, 1993) and one report indicates the isolation of 14 *myb*-related cDNAs from tomato (Lin *et al.*, 1996).

The majority of plant *myb* genes reported until 1998 were identified in dicots but later sequence analyses in the model monocot *Zea mays* revealed the presence

and expression of more than 82 *R2R3 Myb* genes (Rabinowicz *et al.*, 1999). Further identification of *myb*-related genes encoding three Myb repeats in bryophytes (moss), pteridophytes (fern) as well as in other monocots (*Hordeum vulgare* and *Secale cereale*) clearly demonstrated that *myb*-related genes exist in the genome of major plant evolutionary lineages (Kranz *et al.*, 2000). However, an accurate estimate of the number of *myb*-related genes in these plant lineages is not yet available.

Overall, sequence analyses in *Arabidopsis* and maize has revealed that the Myb family of transcription factors contains the largest number of members in plant genomes, which in turn reflects the extensive involvement of Myb proteins in regulation of gene expression during plant development. Although the proportion of the genes encoding zinc-finger proteins in human (1% of genes) and homeobox proteins in *Caenorhabditis elegans* (0.4% of genes) are higher than *myb*-related genes in *Arabidopsis*, they display much lower sequence similarity and higher diversity in DNA-binding specificity than Myb proteins (Romero *et al.*, 1998). Furthermore, phylogenetic studies on amino acid sequences of Myb proteins has led to a suggestion that Myb proteins are a polyphyletic group (Rosinski and Atchley, 1998).

1. 10 Myb proteins perform a broad range of functions in plants

A large body of functional evidence on a small proportion of plant Myb proteins indicate that the functions of Myb proteins in plants are extremely diverse (reviewed in Martin and Paz-Ares, 1997; Jin and Martin 1999). Functional data are available for 37 plant Myb proteins from three subgroups of one-repeat Myb, R2R3 Myb and R1R2R3Myb. However, the cellular targets of these proteins are largely unknown.

One-repeat Myb domain proteins are a relatively small subgroup of plant Myb proteins with at least 9 known members. In this subgroup the LHY (Schaffer *et al.*, 1998) regulates circadian clock and flowering time and CCA1 (Wang *et al.*, 1997; Wang and Tobin, 1998) is involved in phytochrome signal transduction and regulation of circadian clock. CPC1 (Wada *et al.*, 1997) regulates differentiation of

epidermal cells and root hair formation and PcMYB1 (Feldbrügge *et al.*, 1997) is involved in light-induced activation of the chalcone synthase promoter. Two other members of this subgroup, IBP1 (Lugert and Werr, 1994) and BPF1 (da Costa e Silva *et al.*, 1993) interact with specific DNA sequences related to the G-rich telomeric repeats. The MybP1 gene in *Perilla frutescens* is light inducible and plays a role in regulation of anthocyanin biosynthetic gene expression (Gong *et al.*, 1999). The functions of two other members of this subgroup including AtMybL2 (Kirik and Baumlein, 1996), which is preferentially expressed in *Arabidopsis* leaves and StMYB1 (Baranowskij *et al.*, 1994) are unknown. However, the results of transient expression analyses suggest that the StMYB1 may act as a transcriptional activator.

The most well characterised subgroup of plant Myb proteins is R2R3Myb. In this subgroup distinct functions have been assigned to 29 Myb-related proteins. A majority of 12 members of this subgroup including ZmMYBC1 (Cone *et al.*, 1986; Paz-Ares *et al.*, 1987), ZmMYBPL (Cone *et al.*, 1993), ZmMYBP (Grotewold *et al.*, 1994), ZmMYB1 and ZmMYB38 (Franken *et al.*, 1994), PhMYBAN2 (Quattrocchio *et al.*, 1999), PhMYB3 (Avila *et al.*, 1993; Solano *et al.*, 1995), AmMYB305, 340 (Jackson *et al.*, 1991), PsMYB26 (Uimari and Strommer, 1997), AmMYB308, 330 (Tamagnone *et al.*, 1998) are exclusively involved in regulation of different aspects of phenylpropanoid biosynthetic gene expression.

Another 8 members of this subgroup function in different developmental processes. AtMYBGL1 (Oppenheimer *et al.*, 1991) and CotMYBA (Loguerico *et al.*, 1999) are involved in trichome formation, AmMYBMIXTA (Noda *et al.*, 1994) regulates the conical cell shape of petal epidermis, AmMYBPHAN (Waites *et al.*, 1998) play a role in regulation of dorsoventrality of lateral organs, ZmMYBRS2 (Timmermans *et al.*, 1999) functions in repression of knox homeobox genes in maize lateral organ primordia, AtMYB13 (Kirik *et al.*, 1998) is involved in shoot morphogenesis, AtMYB werewolf (Lee and Schiefelbein, 1999) regulates position-dependent epidermal cell patterning and AtMYB103 (Li *et al.*, 1999) may play a role in anther development.

Six members of the R2R3 Myb subgroup are involved in different signal transduction pathways including AtMYB2 (Urao *et al.*, 1993) and cpm5, cpm7 and cpm10 (Iturriaga *et al.*, 1996), which function in response to dehydration and ABA

and GAMYB (Gubler *et al.*, 1995) in response to gibberellic acid. ATR1 (Bender and Fink, 1998) in this subgroup is involved in tryptophan biosynthesis.

In addition the functions of three members of this subgroup including NtMYB1 in plant disease resistance (Yang and Klessig, 1996), AtMYB30 in hypersensitive cell death (Daniel *et al.*, 1999) and AtCDC5 in regulation of cell cycle (Hirayama and Shinozaki, 1996) have been established.

The plant R1R2R3 Myb domain proteins are a newly discovered subgroup of Myb family of transcription factors with structural similarity to vertebrate c-Myb proteins. The first two members of this subgroup, pc-Myb1 and pc-Myb2 were originally discovered in *Arabidopsis* (Braun and Grotewold, 1999). Several other members of this subgroup have recently been identified in a wide variety of land plant species including *Arabidopsis*, monocots including *Hordeum vulgare* (barley) and *Secale cereale* (rye) as well as in bryophytes and pteridophytes (Kranz *et al.* 2000) and accordingly 33 different sequences of the plant R1R2R3 Myb genes have been submitted to current databases. Although functional data on these newly identified R1R2R3 Myb proteins are not yet available, an unpublished report cited in a recent review (Jin and Martin, 1999) indicates that at least one member of this subgroup in tobacco is involved in regulation of B-type cyclin genes.

Taken together, several pieces of evidence described above demonstrate that the Myb-related proteins containing one, two or three repeats in the Myb domain are extensively used by plant species for regulation of gene expression at transcriptional level in diverse processes during plant development. In addition, the structural similarities between plant and animal R1R2R3 Myb proteins (Braun and Grotewold, 1999; Kranz *et al.*, 2000) suggest that plants have retained *myb* genes encoding this subgroup from a common ancestor, which provide conserved functions including regulation of cell cycle and differentiation (reviewed in Lipsick, 1996).

1. 11 Pollen development and Myb-related transcription factors

The process of male gametogenesis in angiosperms represents a unique pathway enabling study of the sequence of biological events initiating from the biogenesis of sporogenous cells culminating in the formation of mature pollen and

release from the anthers. Developmental stages of anther have been well defined in tobacco (Koltunow *et al.*, 1990). Furthermore, microsporogenesis and microgametogenesis have been well described at the ultrastructural level (Owen and Makaroff, 1995).

Anther development is initiated by differentiation of the stamen primordium at the early stages of flower development, which give rise to a set of tissues consisting of epidermis, vascular tissue, archesporial cells and connective tissue. The archesporial cells undergo mitotic divisions and produce primary parietal cells and sporogenous cells. Further differentiation of parietal cells give rise to distinct anther wall layers including endothecium, middle layer and tapetum, which enclose four anther locules (pollen sacs) (Koltunow *et al.*, 1990; Bedinger, 1992).

The gametophytic phase of anther development is initiated by differentiation of sporogenous cells into the microsporocytes (pollen mother cell). Prior to meiotic division of microsporocytes the undifferentiated sporophytic microsporocytes within each anther locule secrete β−1,3 glucan (callose), which surrounds these cells. Following meiosis a tetrad of microspores separated by the callose walls is formed. Microspores are then released from tetrad upon degradation of callose wall by β-1,3-glucanase (callase) secreted by the tapetal cells into the anther locule (Pacini, 1990, Koltunow *et al.*, 1990; Bedinger, 1992)

Tapetal cells are metabolically active and perform other functions during microsporogenesis. These cells provide nutrition for the microspores, produce precursors of outer pollen wall (exine), which mainly consists of sporopollenin (complex polymers of long chain fatty acids and oxygenated aromatic rings) synthesised outside the tapetal cytoplasm (Scott, 1994). Tapetal cells release polysaccharides into the loculus, which are absorbed by the microspores. In addition they function in formation of a continuous, acetolysis-resistant membrane outside the tapetal protoplast, which may play a role in pollen dispersal (Pacini, 1990).

Tapetal cells are involved in formation of viscin threads, pollen kitt and tryphine. The viscin threads on exine surface join the neighbouring tetrads or pollen grains. The hydrophobic pollen kitt layer mainly consists of lipids and carotenoids resulting from plastids and degeneration of cytoplasms of tapetal cells. Tryphine consists of a mixture of hydrophobic and hydrophilic substances, including the

remainder of degenerated organelles. The viscin threads, pollen kitt and tryphine are also involved in holding the pollen grains together in clumps (Pacini, 1990).

Tapetal cells are also involved in formation of orbicules (Ubisch bodies) which consist of lipid bodies developed from the tapetal cytoplasm and coated with sporopollenin (Scott, 1994) polymerised outside the tapetal cytoplasm. Moreover, tapetal cells secrete sporophytic proteins, which may be deposited in aperture regions and interaperturate areas (Pacini, 1990). Recently the enzyme xylanase was identified in maize pollen coat. It was shown by Northern blot and *in situ* hybridisation analyses that the xylanase gene (*Xyl*) is specifically expressed in tapetum (Bih *et al.*, 1999).

The uninucleate microspores released from tetrads undergo an asymmetric division when the microspore nucleus migrates to a specific position at the cell periphery leading to formation of bicellular pollen containing a larger vegetative cell and a smaller generative cell. This asymmetric division known as pollen mitosis I (PMI) is considered as a developmental switch required for the differentiation of generative cell and initiation of a gametophytic pathway (Bedinger, 1992; Twell, 1994; Twell and Howden 1998; Twell *et al.*, 1998). During microspore mitosis metabolic activity increases and major changes in rate of mRNA (Stinson *et al.*, 1987; Schrauwen *et al.*, 1990; McCormick, 1991) protein (Tupy *et al.*, 1983, Bedinger and Edgerton, 1990; Eady *et al.*, 1994) and starch biosynthesis (Tupy *et al.*, 1983) occur within pollen grains.

As pollen grains mature the tapetal layer is degraded and the cell contents are released into the locule and deposited onto pollen surface. In tobacco this layer shrinks following separation of microspores at the stage 3 of flower development when corollas emerge from the calyx (Koltunow *et al.*, 1990). Biological significance of metabolites such as flavonoids, which are released from tapetum in the process of pollen germination, tube growth and fertility, is discussed in section 1. 13.

In the majority (70%) of flowering plants including tobacco mature pollen is bicellular containing a vegetative and a generative cell. After pollen germination within the pollen tube the generative cell undergoes a mitotic division known as pollen mitosis II (PMII) leading to formation of two sperm cells. In a minority (30%)

of plant species including maize and *Arabidopsis thaliana* mature pollen is tricellular and PMII occurs before pollen germination (Brewbaker, 1967).

Interaction of mature pollen with the stigma surface and rehydration of pollen results in germination and emergence of the pollen tube from a pore on exine surface. Pollen germination and tube growth is a rapid process. In maize, pollen germination occurs within 5 min of landing on the silk and the pollen tube can grow 50 cm in 24-36 hr with a rate of 1 cm/hr (Barnabas and Fridvalszky, 1984). Within the style the pollen tube grows along the transmitting tissue and through the micropyle approaches the embryo sac. The pollen tube then penetrates one of the synergids and after rupturing the tube, the sperm cells are delivered into the embryo sac where double fertilisation occurs. One sperm cell fuses with the haploid egg cell to produce the diploid zygote and the other sperm cell fuses with the diploid central cell to form the triploid endosperm nucleus (Mascarenhas, 1989).

1.12 Gene expression in the male gametophyte

Study of the total complexity of tobacco anther mRNA led to an estimation that about 26,000 genes are active in anther tissues among which 15,500 are also expressed in leaf (Kamalay and Goldberg, 1980). The total number of genes expressed in the male gametophyte of *Tradescantia* and maize has been estimated based on the kinetics of hybridisation of ^{3}H-cDNA with poly (A) RNA in excess. These analyses revealed the presence of about 20,000 and 24,000 different mRNA sequences in mature pollen grains of *Tradescantia* and maize respectively. Of these 60% are also expressed in shoots (Willing *et al.*, 1998; Willing and Mascarenhas, 1984). These estimates provided evidence for the complexity of genes expressed late in pollen development. However, there exist a number of genes, which are activated at the early stages of microspore development or soon after meiosis and their transcripts is reduced or become undetectable later at mature pollen. Examples of these genes are the ribosomal RNA (rRNA) and transfer RNA (tRNA) genes (reviewed in Mascarenhas, 1990).

Study of isozyme profiles of vegetative tissues and pollen in tomato, maize, barley and *Populus* species has revealed extensive overlap in gene expression

between pollen and sporophyte tissues. Results derived from colony hybridisation of cDNA libraries of pollen poly (A) RNA hybridised with vegetative tissues and pollen ^{32}P-cDNAs led an estimate that in maize and *Tradescantia* pollen approximately 10% and 20% of the total expressed sequences are pollen specific (Stinson *et al.*, 1987).

In mature pollen presynthesised mRNAs are highly abundant. Analysis of expression pattern of pollen-specific genes in maize and *Tradescantia* revealed transcripts of two sets of genes known as early and late genes, which are detectable at two different developmental stages. The mRNA transcripts of the early genes are detectable in microspores soon after meiosis and release from tetrad whereas transcripts of the late genes are detectable after microspore mitosis and accumulate until pollen maturity (Mascarenhas, 1990).

The developmental pattern of expression of anther/pollen-specific genes has been determined by Northern blot analysis using gene specific probes and by transformation of plants with the constructs harbouring putative regulatory sequences fused to the GUS reporter gene. The latter approach has also allowed quantitative *in planta* determination of transcriptional activity of regulatory sequences, cell-specificity of gene expression using histochemical analysis and the time of activation of pollen-specific genes.

Promoter analyses of a number of anther/pollen specific genes have determined precisely the location of *cis*-acting elements, which confer anther/pollen specificity (reviewed in Twell, 1994; Tsuchiya *et al.*, 1994; Tebbutt *et al.*, 1994; Eyal *et al.*, 1995; Wetering *et al.*, 1995; Bate and Twell, 1998).

Despite identification of *cis*-regulatory elements in the anther/pollen-specific gene promoters, transcription factors interacting with these elements are unknown. Isolation of genes encoding putative transcription factors specifically expressed in anther/pollen has been largely based on screening of cDNA or genomic libraries using probes corresponding to the most conserved domain of the known transcription factors. Using this approach several anther/pollen-specific transcription factors have been isolated from both monocot and dicot species.

The snapdragon MADS box gene, DEFH125 is specifically expressed in pollen and in nuclei of transmitting tissue of carpel and might be involved in

regulation of late pollen gene expression (Zachgo *et al.*, 1997). Two members of MADS box genes have also been identified in rice, *OsMADS2* and *OsMADS4* (Chung *et al.*, 1995).

The PLIM (SF3) gene of sunflower, which encodes a protein containing two zinc finger domains is specifically expressed in pollen at late stage and binds to both its promoter and RNA transcripts *in vitro* (Baltz *et al.*, 1992; Baltz *et al.*, 1996; Baltz *et al.*, 1999). Seven members of zinc-finger family of transcription factors with 2, 3, and 4 zinc finger motifs are expressed sequentially from tetrad stage to anther dehiscence. (Kobayashi *et al.*, 1998). Recently, two members of the LIM gene family, NTPLIM1a and NTPLIM1b, were isolated from tobacco pollen and are specifically expressed in mature and germinating pollen and may have a regulatory function during pollen development (Sweetman *et al.*, 2000).

Among the members of the *myb* gene family of transcription factors three anther-specific genes have been identified so far. The *Atmyb103* gene of *Arabidopsis* has been shown to be expressed in tapetum and middle layer of anthers (Li *et al.*, 1999). The *NtmybAS1* and *NtmybAS2* of tobacco are expressed in tapetum, stomium, mature and germinating pollen (Yang *et al.*, 2000) and when overexpressed in tobacco cause a dwarf phenotype (Sweetman, 1996).

Despite isolation and characterisation of several anther/pollen-specific transcription factors in a variety of plant species described above the target genes which may be regulated by these factors are unknown. However, the results presented in this work and those reported recently (Yang *et al.*, 2000) demonstrate the activation potential of NtMybAS1 and led to identification of *gPAL1* as a putative target of NtMybAS1. Therefore, based on the evidence described above *NtmybAS1* represents the most well characterised anther-specific transcription factor, which is involved in regulation of phenylpropanoid biosynthetic genes during anther development.

The metabolites synthesised in the phenylpropanoid pathway (Hahlbrock and Scheel, 1989; Dixon and Paiva, 1995) play important roles during pollen development, germination, tube growth and fertility. Therefore, the biological significance of this group of metabolites is discussed in more detail in the following section.

1. 13 Phenylpropanoid metabolites and pollen development

The functional significance of the phenylpropanoid metabolites during pollen development has been well documented. The first enzyme of the phenylpropanoid pathway phenylalanine ammonia-lyase (PAL) catalyses the conversion of phenylalanine to *trans*-cinnamic acid, which is the precursor for the synthesis of all the phenylpropanoid metabolites. PAL activity plays an important role in the development of microspores.

It has been shown that the PAL activity in fertile anthers of broccoli after release of the microspores is higher than in a male sterile strain. Immunohistochemical studies have revealed that PAL is predominantly localised in the tapetal cells. Furthermore, it has been found that the PAL activity in immature anthers is positively correlated with the pollen fertility (Kishitani *et al.*, 1993).

Disruption of normal PAL activity affects pollen fertility. It has been reported that the sense and antisense expression of a PAL cDNA of sweet potato in tobacco using a tapetum-specific promoter result in formation of abnormal pollen grains devoid of starch and flavonols, which are not able to germinate and this defect further leads to a partial male sterility. In addition a positive correlation has been established between the level of PAL activity in anthers and the number of fertile pollen grains (Matsuda *et al.*, 1996).

In addition to PAL activity, which is a key regulatory point for the control of biosynthesis of phenylpropanoids, other phenylpropanoid metabolites have been shown to play an important role during pollen development and fertility. Flavonoids are a highly abundant class of phenylpropanoid metabolites in plants, which are initially synthesised by the enzyme chalcone synthase. This involves the condensation of *p*-coumaroyl-CoA with three molecules of malonyl-CoA, which result in formation of chalcone. Isomerisation of chalcones by the enzyme chalcone isomerase (CHI) results in formation of flavonones. The enzyme flavonone-3-hydroxylase (F3H) catalyses hydroxylation of flavonones to form dihydroflavonols and these are then converted to flavonols by a dioxygenase, flavonol synthase (FLS) (reviewed in Dixon and Steele, 1999).

The basic structure of flavonoids contains two carbon rings, which are interconnected by three carbon atoms. Both flavonols and flavones are recognised by the presence of a double C2-C3 bond in the C ring. The flavonols are further recognised from flavones by the presence of a hydroxyl group at the 3-position (Mo *et al.*, 1992).

Early evidence of involvement of the flavonoids in pollen development derived from the finding that the mutation (wp, white pollen) in a chalcone synthase gene of maize results in formation of sterile white pollen (Coe *et al.*, 1981). It has also been shown that the antisense suppression of chalcone synthase expression in petunia severely affects pollen germination and tube growth. This defect can be biochemically complemented by application of flavonols. Due to lack of flavonols the resulting pollen grains are not functional in self-crosses but their function is restored in out crosses and therefore, this phenomenon is known as conditional male fertility (CMF). This finding implied the importance of flavonoid synthesis in the sporophyte for fertility (Taylor and Jorgensen, 1992).

Conditional male fertility has also been studied in maize. This phenomenon in maize and petunia is to some extent similar in that both require flavonols for pollen tube growth and fertility (Mo *et al.*, 1992). However, in maize, chalcone synthase is transcribed but not translated in seedlings and male florets (Pollak *et al.*, 1995) whereas in petunia chalcone synthase transcript is not detectable in conditional male fertile stigmas (Vogt *et al.*, 1994). Unlike petunia, in maize chalcone synthase-deficient pollen grains are able to germinate and grow both *in vitro* and *in vivo* in the absence of flavonols. The pollen tube growth is abolished within 12-24 h post pollination within the silk and this is associated with the swelling and bursting of the tip of pollen tube. Normal pollen growth can be restored by the addition of flavonols at pollination (Pollak *et al.*, 1995). Analysis of flavonols by HPLC in wild type petunia stigma (Pollak *et al.*, 1993) revealed the presence of flavonols, which are able to rescue the conditional male fertile pollen. In contrast, in maize it has been shown that the silk extracts do not stimulate germination of conditional male fertile petunia pollen suggesting the absence of flavonols. Furthermore, it has been shown by HPLC analysis that the petunia pollen does not contain flavonol aglycones (Pollak *et al.*, 1993) whereas maize pollen contain flavonol aglycone (quercetin), which is

able to rescue the the conditional male fertile petunia pollen (Pollak *et al.*, 1995). In addition the major flavonol content of petunia and maize pollen is different. In Petunia anthers the presence of both kaempferol and quercetin have been identified (Pollak *et al.*, 1993) whereas maize pollen predominantly contain quercetin and quercetin glycosides (Pollak *et al.*, 1995).

Study of the effects of tobacco and petunia pollen diffusates on pollen function revealed that the anther derived flavonols including kaempferol, quercetine and myricetin in the diffusates from the *in situ* matured pollen can strongly stimulate pollen germination and tube growth *in vitro* (Ylstra *et al.*, 1992).

A more direct evidence of the involvement of flavonoids in male gametophyte development was the isolation and identification of kaempferol, a flavonol aglycone from the wild type petunia stigma and the demonstration of restoration of pollen germination and tube growth *in vitro* and *in vivo* by application of kaempferol. Furthermore, it has been shown that the presence of keto group at position 4 and an unglycosylated hydroxyl group at position 3 in the C ring of flavonoids is absolutely required for the biochemical restoration of pollen function (Mo *et al.*, 1992).

It has been reported that the antisense inhibition of chalcone synthase activity in tapetum using the anther box motif found in the promoters of flavonoid biosynthetic genes (van Tunen *et al.*, 1988) result in male sterile plants. Furthermore, establishment of a positive correlation between the inhibition of anther pigmentation, leading to a white collapsed phenotype and the severe reduction in chalcone synthase transcript in anthers implied the importance of flavonoid biosynthesis for normal pollen development (van der Meer *et al.*, 1992).

Lack of flavonols in petunia as a result of suppression of chalcone synthase activity affects the structure of pollen tube leading to the sudden disruption of the pollen tube apex and release of its content. This defect can be overcome by the addition of flavonol aglycones but not with the glycosylated flavonols such as rutin (quercetin 3-*O*-rhamnoglucoside). Furthermore, the flavone, apigenin inhibits pollen tube growth. These data indicate the structural role of a specific group of flavonols (aglycones) in the membranes of the male gametophytes during the process of pollen tube growth (Ylstra *et al.*, 1994).

Several lines of evidence described above clearly demonstrate that flavonoids play an essential role in the process of pollen development and fertility in both monocot (maize) and dicot (petunia and tobacco) species. These data support the hypothesis that plant species generally require flavonoids for pollen development and fertility. However, study of flavonoid-deficient mutants of *Arabidopsis* has provided compelling evidence, which argue against this hypothesis.

Eleven loci known as *transparent testa* (*tt*) have been identified in *Arabidopsis*, which contain the genes encoding the enzymes of the flavonoids biosynthesis pathway. Mutations in these loci result in a reduction or lack of flavonoids. However, the mutant plants do not show aborted seeds and are self-fertile (Shirley *et al.*, 1995). It has been shown that the lack of flavonols in pollen and reproductive organs of *Arabidopsis tt4* mutants does not affect the amount of pollen germination and tube growth *in vivo* and results in the formation of fully fertile plants (Ylstra *et al.*, 1996). A mutation at the 3' splice acceptor site in *tt4* locus which encodes the enzyme, chalcone synthase results in complete disruption of chalcone synthase activity. Although the results of HPLC analyses demonstrated that the *tt4* flowers and stamens are completely devoid of flavonoids, the formation of normal seed set in these plants indicate that lack of flavonoids in *Arabidopsis* does not affect plant fertility (Burbulis *et al.*, 1996).

In sharp contrast to petunia, tobacco and maize, the evidence described above conclude that at least in *Arabidopsis* the flavonoids do not play an essential role in pollen germination, tube growth and fertility and therefore, the flavonoid requirement for plant reproduction may not be necessarily similar in different species.

1. 14 Manipulation of expression of *myb* genes result in a dwarf phenotype

Dwarfing phenomena in higher plants have been the centrepiece of intense investigations. Spontaneous mutations affecting plant height have long been identified in a broad range of plant species. The dwarf features of many of these mutants resulted from a defect in the biosynthesis or perception/signal transduction of the phytohormone, gibberellic acid (GA) (Reviewed in Reid, 1986). Dwarf

mutants have also been generated by physical (radiation) and chemical mutagens and by T-DNA insertion mutagenesis (Feldmann *et al.*, 1989, Feldmann, 1992; Redei and Koncz, 1992).

Among the mutants in which a genetic defect reduces plant height the gibberellic acid mutants have received the most attention. These mutants not only have provided fundamental insight into the GA biosynthesis pathway and into developmental processes which are regulated by GAs (reviewed in Reid 1986; Hooley, 1994; Hedden, 1997) but also have used for agricultural purposes. The GA-regulated processes can be classified in three major groups consisting of (1) cell growth, (2) flower and fruit development and (3) seed reserve mobilisation (Hooley, 1994). The reduced elongation growth of GA mutants result in a dwarf or semidwarf phenotype and this characteristic has been employed in plant breeding programs to develop dwarf varieties of crop plants. The basic idea that reducing the height of the wheat plants would prevent lodging and reduce wind and rain damage had later a great impact on global wheat yield. Breeding a number of GA insensitive mutants and most remarkably Norin 10 containing the mutant loci, *Rht1* and *Rht2*, on commercial wheat lines developed the semidwarf high-yielding wheat lines resistant to lodging. Incorporation of these mutant alleles into Mexican wheat dramatically increased the wheat grain yield and led to the 'Green Revolution' (reviewed in Hoisington *et al.*, 1999; Silverstone and Sun, 2000).

Apart from the mutations influencing biosynthesis and perception/signal transduction of phytohormones, genetic manipulation in many cases has resulted in altered plant architecture leading to a dwarf phenotype. The examples of genes causing such phenotypic alterations have been described in chapter 4. Among the members of the *myb* gene family manipulation of expression of four genes have been reported to reduce plant extension growth and confer a short stature. These include overexpression of the *NtmybAS1* (Sweetman, 1996), AmMYB308 and AmMYB330 (Tamagnone *et al.*, 1998) and MIXTA (Glover *et al.*, 1998) genes in tobacco. Although the dwarf features of plants overexpressing the genes described above are to some extent similar, major phenotypic differences exist among these plants. The general reduction of size of plant organs and the reduced internode length of *NtmybAS1* plants resemble the phenotypes described for the AmMYB308,

AmMYB330 overexpressing plants. However, the *NtmybAS1* plants do not show the characteristic features of the AmMYB308 and AmMYB330 plants including early senescence and areas of white dead tissues in leaves mainly as a result of depletion of phenolic acids and monolignols (Tamagnon *et al.*, 1998).

Reduced apical dominance and short stature of *NtmybAS1* plants also show similarities to those described for the MIXTA overexpressing plants. However, the MIXTA plants develop rolled leaves, paler corollas and cornet- shaped flowers whereas in *NtmybAS1* plants the leaves do not roll and the flower color intensity is not significantly different from wild type.

Despite the fact that overproduction of a number of Myb proteins described above in the original or heterologous species result in a dwarf phenotype in neither case has the mechanisms underlying dwarfing been described.

1. 15 Background to the project

In higher plants the number and functions of protein factors regulating gene expression during male gametogenesis are largely unknown. An effort to identify the pollen-specific transcriptional regulators of gene expression in tobacco led to isolation and characterisation of two cDNA clones (*NtmybAS1* and *NtmybAS2*) from a tobacco pollen cDNA library with structural similarity to Myb family of transcription factors (Sweetman, 1996). The *NtmybAS1* and *NtmybAS2* gene products showed the highest sequence similarity to PhMyb3 from *Petunia hybrida*, (Figure 1. 1), which has been show to play a role in regulation of flavonoid biosynthetic genes (Avila *et al.*, 1993; Solano *et al.*, 1995).

Investigation of the genomic organisation of *NtmybAS1* and *NtmybAS2* in tobacco by Southern blot analysis indicated that both *NtmybAS1* and *NtmybAS2* are single copy genes in the genome of *N. tabacum* and its parental lines, *N. tomentosiformis* and *N. sylvestris*.

A detailed analysis of spatial and temporal expression of *NtmybAS1* revealed that *NtmybAS1* is specifically expressed in mature and germinating pollen. Furthermore, *in planta* expression of *NtmybAS1* revealed that the overproduction of

Figure 1. 1

Sequence alignment of NtMYBAS1 and PhMYB3

-The R2 and R3 Myb repeats are boxed. Asterisks show the tryptophan (W) and phenylalanine (F) residues in R2 and R3.

-Dots represent the identical amino acids.

-Bars indicate mismatches.

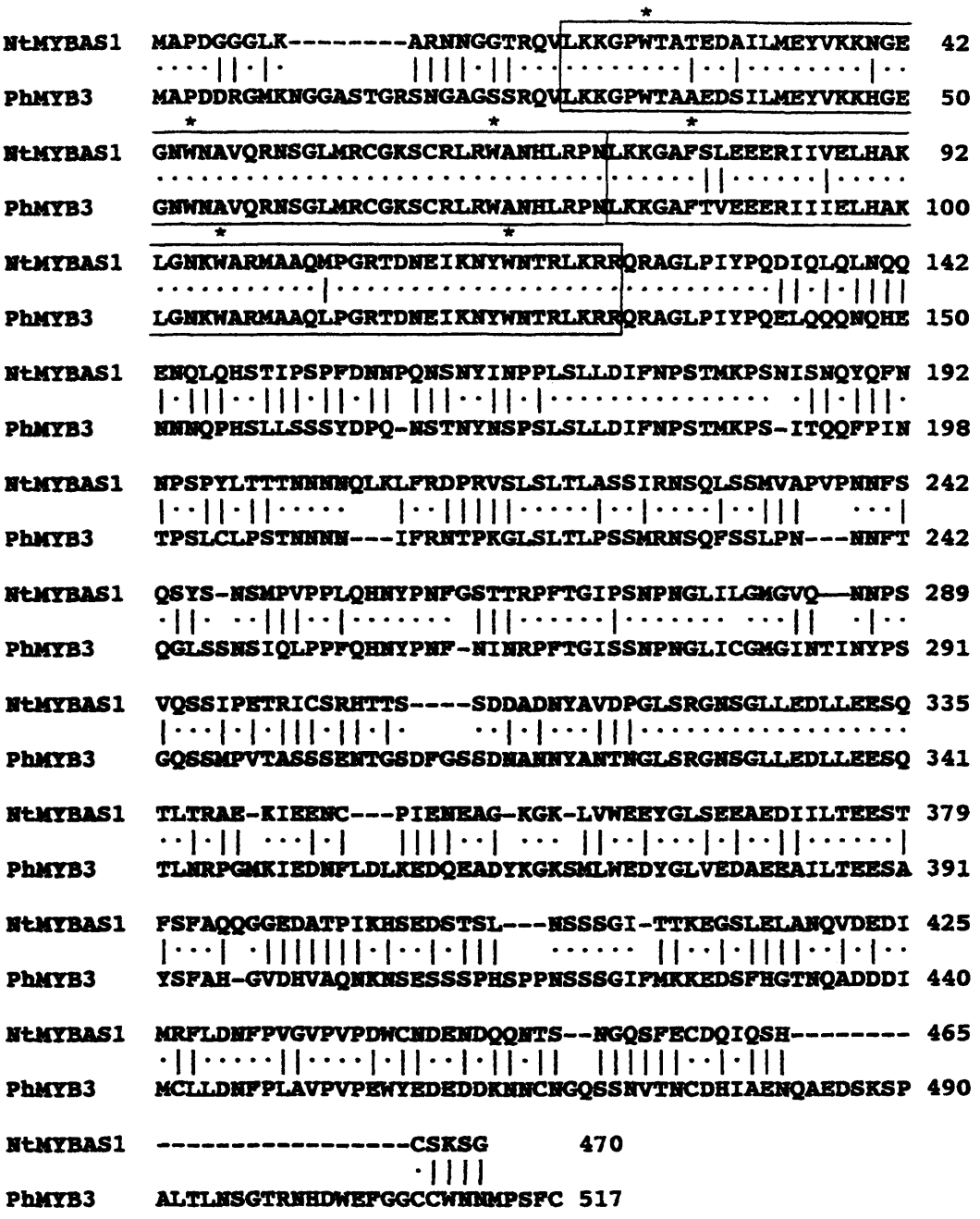
NtMYBAS1 MAPDGGGLK--------ARNNGGTRQVLKKGPWTATEDAILMEYVKKNGE 42
PhMYB3 MAPDDRGMKNGGASTGRSNGAGSSRQVLKKGPWTAAEDSILMEYVKKHGE 50
NtMYBAS1 GNWNAVQRNSGLMRCGKSCRLRWANHLRPNLKKGAFSLEEERIIVELHAK 92
PhMYB3 GNWNAVQRNSGLMRCGKSCRLRWANHLRPNLKKGAFTVEEERIIIELHAK 100
NtMYBAS1 LGNKWARMAAQMPGRTDNEIKNYWNTRLKRRQRAGLPIYPQDIQLQLNQQ 142
PhMYB3 LGNKWARMAAQLPGRTDNEIKNYWNTRLKRRQRAGLPIYPQELQQQNQHE 150
NtMYBAS1 ENQLQHSTIPSPFDNNPQNSNYINPPLSLLDIFNPSTMKPSNISNQYQFN 192
PhMYB3 NNNQPHSLLSSSYDPQ-NSTNYNSPSLSLLDIFNPSTMKPS-ITQQFPIN 198
NtMYBAS1 NPSPYLTTTNNNNQLKLFRDPRVSLSLTLASSIRNSQLSSMVAPVPNNFS 242
PhMYB3 TPSLCLPSTNNNN---IFRNTPKGLSLTLPSSMRNSQFSSLPN---NNFT 242
NtMYBAS1 QSYS-NSMPVPPLQHNYPNFGSTTRPFTGIPSNPNGLILGMGVQ--NNPS 289
PhMYB3 QGLSSNSIQLPPFQHNYPNF-NINRPFTGISSNPNGLICGMGINTINYPS 291
NtMYBAS1 VQSSIPETRICSRHTTS----SDDADNYAVDPGLSRGNSGLLEDLLEESQ 335
PhMYB3 GQSSMPVTASSSENTGSDFGSSDNANNYANTNGLSRGNSGLLEDLLEESQ 341
NtMYBAS1 TLTRAE-KIEENC---PIENEAG-KGK-LVWEEYGLSEEAEDIILTEEST 379
PhMYB3 TLNRPGMKIEDNFLDLKEDQEADYKGKSMLWEDYGLVEDAERAILTEESA 391
NtMYBAS1 FSFAQQGGEDATPIKHSEDSTSL---NSSSGI-TTKEGSLELANQVDEDI 425
PhMYB3 YSFAH-GVDHVAQNKNSESSSPHSPPNSSSGIFMKKEDSFHGTNQADDDI 440
NtMYBAS1 MRFLDNFPVGVPVPDWCNDENDQQNTS--NGQSFECDQIQSH-------- 465
PhMYB3 MCLLDNFPLAVPVPEWYEDEDDKNNCNGQSSNVTNCDHIAENQAEDSKSP 490
NtMYBAS1 ----------CSKSG 470
PhMYB3 ALTLNSGTRNHDWEFGGCCWNNMPSFC 517

NtmybAS1 in tobacco affects plant height leading to a dwarf phenotype (Sweetman, 1996).

Demonstration of expression of the *myb*-related genes in tobacco pollen provided new insight into identity of the proteins, which may function as a regulator of gene expression in tobacco pollen. Furthermore, the specific expression of *NtmybAS1* and *NtmybAS2* in mature and germinating pollen and the induction of dwarfing as a result of overexpression of *NtmybAS1* in vegetative tissues of tobacco suggested that the *NtmybAS1* encoded protein plays an important role during pollen development in tobacco.

Taken together, the work described above provided a basis to further investigate the dwarfing phenomenon and to gain insight into the function of NtMybAS1 in tobacco pollen.

1. 16 The aims of thesis

The work presented in this thesis was essentially performed in continuation of the previous work described in section 1. The major objective of this project was to elucidate the mechanisms underlying *NtmybAS1*-induced dwarfing and to further gain insight into the function of *NtmybAS1* during tobacco pollen development.

In the first part of this project the specific aims of the experiments were to determine (1) the functional domains of *NtmybAS1*, (2) the relationship between the level of *NtmybAS1* expression and reduction of plant height and (3) the cellular localisation of NtMybAS1 protein. This involved ectopic overexpression of the full length and truncated versions of *NtmybAS1* in tobacco and a detailed characterisation of the phenotype of the resulting transformants, analysis of transgene expression and transient expression of NtMybAS1-sGFP fusion protein in tobacco pollen (Chapter 3).

In the second part of this study the specific objectives of the experiments were to determine (1) the effect of phytohormones and their inhibitors on the dwarf phenotype, (2) the cell autonomy of dwarfing and (3) cellular changes in *NtmybAS1* overexpressing plants. This involved feeding phytohormones and their inhibitors into *NtmybAS1* overexpressing plants and a detailed characterisation of the resulting

phenotype, analysis of the effects of *NtmybAS1* root and shoot systems on dwarfing phenomenon by grafting and investigation of cell morphology by sectioning and light microscopy (Chapter 4).

In the final part of this project special emphasis was placed on investigation of the molecular basis of *NtmybAS1*-induced dwarfing. The specific objectives of the experiments were to determine (1) the proteins that are differentially expressed (putative NtMybAS targets) as a result of overexpression of *NtmybAS1* in tobacco and (2) the relationship between the levels of expression of *NtmybAS1* and induction/suppression of the putative target genes. This involved the analysis of cellular protein profiles of *NtmybAS1* plants by one and two-dimensional gel electrophoresis, in-gel digestion of the differentially expressed proteins with trypsin, separation and purification of the resulting tryptic peptides by reversed-phase HPLC and N-terminal sequencing of the tryptic peptides. Furthermore, Northern blot and RT-PCR were adopted to established differential gene expression in *NtmybAS1* overexpressing plants at mRNA level (Chapter 5).

Taken together, using the strategies described above compelling evidence was provided to support the regulatory function of NtMybAS1 protein during anther development and to explain several aspects of *NtmybAS1*-induced dwarfing in tobacco. The results derived from these analysis further led to propose a model in which the NtMybAS1-mediated activation of *gPAL1* induces expression of two pathogenesis-related (PR) proteins via a salicylic acid-dependent signal transduction pathway.

Chapter 2

Materials and Methods

2. 1 Materials

Materials used in this work were obtained from the suppliers as follows: Chemicals: Sigma, Fisher Chemicals, GIBCO BRL, BDH, Fisons, Melford Laboratories Ltd; Molecular biology enzymes and reagents: GIBCO BRL, Boehringer Mannheim, Stratagene, Promega, Pharmacia, Perkin Elmer; Plant tissue culture salts and hormones: Flow Laboratories, Sigma; Agar and related products: Difco laboratories; Bacterial media: Unipath Ltd; Historesin embedding kit: Leica Instruments GmbH; DNA purification kits: Bio101 Ltd, GENOMED GmbH and Promega; Radiolabelled compounds and Hybond membranes: Amersham; NucTrap Push columns: Stratagene; RT-PCR kit: Advanced Biotechnologies Ltd; ProtoGel: National Diagnostics; Microconcentrators: Amicon; Two-dimensional (2-D) gel electrophoresis materials: Amersham Pharmacia Biotech; Disposable plastic materials: Sterilin, Nunc and Sarstedt; Filters and Acrodiscs: Millipore, Calbiochem and Galman Sciences.

2. 2 Bacterial culture and storage

2 . 2. 1 Strains and genotypes

Escherichia coli (*E. coli*)

XL1-Blue: *recA 1*, *endA1*, *gyrA96*, *thi*, *hsdR17*, *supE44*, *relA1*, *lac*, {*F'*, *proAB*, *lacIq*, *ZDM15*, *Tn10*, (tet^R)} (Bullock *et al.*, 1987).

Agrobacterium tumefaciens (*A. tumefaciens*)

LBA4404: containing Ti plasmid pAL4404 (Ooms *et al.*, 1982).

2. 2. 2 Antibiotics for bacterial selection

Ampicillin (100 mg/l), kanamycin (50 mg/l) and tetracyclin (10 mg/l) was used for growth and selection of *E. coli*.

Kanamycin (50 mg/l) and rifampicin (50 mg/l) was used for growth and selection of *A. tumefaciens*.

2. 2. 3 Bacterial media and growth condition

Luria Bertani (LB): Bacto-tryptone 1% (w/v), bacto-yeast extract 0.5 % (w/v), NaCl 1% (w/v). pH adjusted to 7.0 with 1 M NaOH and autoclaved for 15 min at 120 °C. Solidified LB medium (LB agar) was prepared by incorporating 1.5% (w/v) agar into LB medium .

2YT: Bacto-tryptone 1.6% (w/v), bacto-yeast extract 1% (w/v) and NaCl 0.5% (w/v). pH adjusted to 7.0 with 1 M NaOH and autoclaved 15 min at 120 °C.

E. coli and *A. tumefaciens* cultures were grown at 37 °C and 28 °C respectively. Liquid cultures were grown on an orbital shaker at 200 rpm until the required optical density was obtained.

2. 2. 4 Long term storage of bacterial strains

A 0.5 ml aliquot of an overnight bacterial culture (*E. coli* and *A. tumefaciens*) was transferred to a cryogenic storage tube. 0.5 ml of filter sterilised 50% (v/v) glycerol was added, mixed and stored at -80 °C. To recover the single colonies of each strain a small portion of the frozen culture was streaked on solidified media containing selective antibiotic and grown as described in section 2. 2. 3.

2. 3 Bacterial transformation

2. 3. 1 Preparation of competent *E. coli*

2XL broth: 2YT (section 2. 2. 3), 1% (v/v) Glucose 18%. Autoclaved 15 min at 120 °C.

$Ca^{2+}Mg^{2+}$ solution: Sodium acetate 40 mM, $CaCl_2$ 100 mM, $MnCl_2$ 70 mM. pH adjusted to 5.5 with 1 M HCl and filter sterilised.

Preparation of competent *E. coli* cells was performed as described by Hanahan (1983). A single colony of XL1-Blue was grown in 25 ml of 2XL broth containing tetracycline (10 mg/ml) at 30 °C. A 1-ml aliquot of the overnight culture was inoculated into 100 ml of pre-warmed 2XL broth containing tetracycline and grown until an OD_{600} of 0.2 was obtained. Filter sterilised 1 M $MgCl_2$ was added to a final concentration of 20 mM (2 ml) and the culture grown until an OD_{600} of 0.45-0.55 was obtained.

The bacterial culture was transferred to a 50 ml sterile tube, placed on ice for 2 hours and centrifuged at 3000 *g*, 4 °C, for 5 min. The supernatant was discarded, the bacterial pellet was gently resuspended in 50 ml of $Ca^{2+}Mg^{2+}$ solution, which had been pre-chilled to 4 °C and incubated on ice for 45 min. The bacterial culture was centrifuged as mentioned above, the supernatant was discarded and the pellet was gently resuspended in 5 ml of $Ca^{2+}Mg^{2+}$ solution containing 15% glycerol. The cells were quickly divided in 0.2 ml aliquots, transferred to 1.5 ml pre-chilled microfuge tubes, flash frozen in liquid nitrogen and stored at -80 °C.

2. 3. 2 Transformation of *E. coli*

An aliquot of competent *E. coli* (section 2. 3. 1) was thawed on ice, plasmid DNA resulting from ligation reaction (section 2. 5. 4) was added, gently mixed by flicking the tube and incubated on ice for 30 min. The cells were heat shocked at 37 °C for 5 min, transferred to 1 ml of LB (without antibiotic selection) in a universal tube and grown on a shaker at 200 rpm for 1 h at 37 °C. Generally, two aliquots of the resulting cells were spread on LB agar plates containing antibiotic selection, allowed to dry and incubated overnight at 37 °C. The resulting transformants were identified by restriction digests (section 2. 5. 1) or colony PCR (section 2. 6. 3).

2. 3. 3 Preparation of competent *A. tumefaciens*

$T_{10}E_1$ (pH 7.5) medium: Tris-HCl (pH 7.5) 10 mM, EDTA (pH 8) 1 mM.

A single colony of A. *tumefaciens* was grown in 10 ml of 2YT broth with selective antibiotic on a shaker (200 rpm) at 28 °C. The overnight culture was inoculated into 200 ml of 2YT broth and grown for 4 hours as before. The bacterial culture was centrifuged at 3000 *g*, 4 °C for 10 min. The supernatant was discarded and the pellet was washed with 20 ml of pre-chilled (4 °C) $T_{10}E_1$. The pellet was recovered by centrifugation as before, the supernatant was removed and the pellet was gently resuspended in 20 ml of pre-chilled (4 °C) 2YT broth. The cells were quickly divided in 0.5 ml aliquots, transferred to 1.5 ml pre-chilled (4 °C) microfuge tubes, flash frozen in liquid nitrogen and stored at –80 °C.

2. 3. 4 Transformation of *A. tumefaciens*

An aliquot of competent *A. tumefaciens* (section 2. 3. 3) was thawed on ice, 0.5-1 µg of plasmid DNA in a volume of 10 µl of SH_2O was added and mixed by gentle flicking. The cells were incubated on ice for 5 min, frozen in liquid nitrogen for further 5 min and thawed at 37 °C for 5 min. The cells were inoculated into 1 ml of 2YT broth (without antibiotic selection) in a universal tube and grown on a shaker at 200 rpm for 2-4 h at 28 °C. Generally, two aliquots of the resulting cells were spread on LB agar plates containing antibiotic selection, allowed to dry and incubated at 28 °C for 2 days.

2. 4 Isolation and purification of nucleic acids

2. 4. 1 Small scale isolation of plasmid DNA

Solution I: Glucose 50 mM, Tris-HCl (pH 8.0) 25 mM and EDTA (pH 8.0) 10 mM.

Autoclaved 15 min at 120 °C

Solution II: NaOH 0.2 N, SDS 1% (w/v)

Solution III: Potassium acetate 5M, glacial acetic acid 11.5% v/v. Autoclaved 15 min at 120 °C.

Phenol/chloroform: isoamyl alcohol (24:1): 100 ml phenol (Fisons), 100 ml chloroform and 4.16 ml isoamyl alcohol.

A 1.5 ml aliquot of an overnight culture (5 ml) grown from a single colony was transferred to a 1.5 ml microfuge tube and centrifuged at 14000 *g*, for 5 min. The supernatant was discarded and the pellet was resuspended in 100 µl of solution I. Following addition of 200 µl of solution II, the tube was gently inverted 5 times to lyse the bacteria. After lysis, 150 µl of solution III was added to the lysate, mixed and centrifuged at 14000 *g* for 5 min. The supernatant was transferred to a fresh tube, an equal volume of phenol chloroform was added, vortexed and centrifuged at 14000 *g* for 5 min. The top aqueous layer was transferred to a fresh tube, 2.5 volumes of absolute ethanol was added and centrifuged at 14000 *g*, for 5 min at RT to precipitate the crude plasmid. The supernatant was removed, the pellet was washed with 100 µl of 70% v/v ethanol and centrifuged at 14000 *g*, for 1 min. The supernatant was discarded, the pellet was vacuum dried for 10-15 min and resuspended in 25 µl of SDW.

The method described above was also used to isolate plasmid DNA from *A. tumefaciens* except that the volume of overnight culture selected was increased to 4.5 ml.

2. 4. 2 Medium and large scale preparation of plasmid DNA

A 50 µl aliquot of an overnight bacterial culture grown from a single colony was inoculated into 50 ml of LB with selective antibiotic and grown as described in section 2. 2. 3. The overnight culture was transferred to a 50 ml centrifuge tube and the bacterial pellet was recovered by centrifugation at 10000 g for 10 min at RT. The supernatant was removed and the pellet was resuspended in 2 ml of solution I and

lysed with 3 ml of solution II by gently inverting the tube 3-4 times. Following lysis 2.5 ml of solution III was added mixed and the white bacterial debris was precipitated by centrifugation at 10,000 *g* for 5 min at RT. The supernatant was transferred through a Miracloth (Calbiochem) into a fresh centrifuge tube to remove the remaining debris. The resulting supernatant was mixed with an equal volume of isopropanol, centrifuged at 10,000 *g* for 10 min at 4 °C to precipitate the nucleic acid. The supernatant was removed, the pellet was resuspended in 300 µl of SDW and transferred to a 1.5 ml microfuge tube. To precipitate the large RNA molecules, 300 µl of 8 M LiCl was added, vortexed and centrifuged at 14000 *g* for 5 min at RT. The supernatant was transferred to a fresh microfuge tube containing 600 µl of isopropanol, vortexed and centrifuged at 14000 *g* for 5 min at RT. The supernatant was removed and the pellet was resuspended in 500 µl of SDW. To remove the remaining RNA molecules 10 µl of RNAse A (20 mg/ml) was added, briefly vortexed and incubated at 37 °C for 1 hour. The RNAse was removed by phenol/chloroform as described in section 2 Following RNAse treatment 500 µl of phenol/chloroform was added, vortexed and centrifuged at 14000 g for 5 min at RT. The top aqueous phase was transferred to a fresh microfuge tube and the phenol/chloroform step was repeated. To the resulting aqueous phase 100 µl of 5 M ammonium acetate and two volumes of absolute ethanol was added, vortexed and centrifuged at 14000 *g* for 5 min at RT to precipitate the plasmid. The supernatant was removed, the pellet was washed with 200 ml of 70% ethanol followed by a brief spin (1 min). The ethanol was removed, the pellet was vacuum dried for 10-15 min and resuspended in appropriate volume of SDW. The resulting plasmid DNA was quantified by agarose gel electrophoresis (section 2. 8. 1)

Bacterial cultures for large-scale isolation of plasmid DNA were essentially prepared as described in section 2. except that the volume of the cultures was increased to 400 ml, the bacterial pellet was recovered in 200 ml centrifuge tubes and 8, 12 and 10 ml of solutions I, II and III were used for cell lysis respectively.

Following precipitation of the nucleic acid pellet with isopropanol the pellet

was resuspended in 3 ml of SDW and transferred to a 50 ml centrifuge tube. To remove the large RNA molecules 3 ml of 8 M LiCl was added, vortexed and centrifuged at 10,000 *g* for 10 min at 4 °C. The supernatant was transferred to a fresh centrifuge tube, mixed with an equal volume of isopropanol and centrifuged as before. The supernatant was discarded, the resulting pellet was resuspended in 500 µl SDW and transferred to a 1.5 ml microfuge tube. RNAse A treatment, phenol/chloroform extraction and ethanol precipitation of the plasmid DNA were performed as described in section 2. 4. 5.

2. 4. 3 Isolation of total RNA

Total RNA was isolated from mature leaves and pollen using TRIZOL reagent (GIBCO BRL). Plant tissues were ground to a fine powder in liquid nitrogen, TRIZOL reagent was added to a volume that gave a TRIZOL: tissue ratio of 10:1 v/w and briefly vortexed to homogenise the sample. 1 m of the homogenised sample was transferred to a 1.5 ml microfuge tube and incubated at 15-30 °C for 5 min. 0.2 ml of chloroform (per 1 ml TRIZOL) was added, vortexed for 15 seconds and incubated at 15-30°C for 2-3 min. The samples were centrifuged at 12000 *g* for 15 min at 2-8 °C to separate the total RNA in aqueous phase. The supernatant was transferred to a fresh tube, 0.5 ml of isopropyl alcohol (per 1 ml TRIZOL) was added, mixed and incubated at 15-30 °C for a 10 min. The samples were centrifuged at 12000 *g* for 10 min at 2-8 °C. The supernatant was discarded, the RNA pellet was washed with 1 ml of 75% ethanol (per 1 ml TRIZOL) and centrifuged at 7500 *g* for 5 min at 2-8 °C. The supernatant was discarded and the RNA pellet was vacuum dried for 5-10 min. Total RNA was partially dissolved in DEPC treated water by several pipetting, incubated for 10 min at 55-60 °C and quantified spectrophotometrically (section 2. 4. 6).

2. 4. 4 Purification of DNA fragments from agarose gels

DNA fragments required for cloning or preparation of radioactive probes were purified from agarose gel using DNA purification kits Geneclean (Bio 101 Ltd.) and JETsorb (GENOMED GmbH) for DNA fragments larger than 0.2 kb and Mermaid (Bio 101 Ltd) for DNA fragments less than 0.2 kb according to manufacturers instructions.

2. 4. 5 Purification of DNA

Following enzymatic manipulation of DNA, to remove the proteins from DNA solutions, an equal volume of phenol/chloroform: isoamyl alcohol (24:1) (section 2. 4. 1) was added to the reaction mixture, vortexed and centrifuged at 14000 g for 5 min. The aqueous phase was transferred to a fresh tube, two volumes of absolute ethanol and sodium acetate (3.0 M, pH 5.2) to a final concentration of 0.3 M were added, vortexed and centrifuged at 14000 g for 20 min. The supernatant was removed, the pellet was washed with 1ml of 70% (v/v) ethanol and centrifuged at 14000 g for 1 min. The supernatant was removed, the pellet was vacuum dried for 10-15 min and resuspended in SDW.

2. 4. 6 Quantification of nucleic acids

The concentration of nucleic acid was determined by measuring the UV absorbance of a DNA or RNA sample at wavelengths of 260 nm and 280 nm using a Philips (PU 8740 UV/VIS) scanning spectrophotometer. The concentration of nucleic acid in the sample was calculated on the basis that an OD of 1 corresponds to 50 µg/ml of double-stranded DNA, 40 µg/ml of single stranded DNA and RNA, and 20 µg/ml of single stranded oligonucleotides.

2. 5 Enzymatic manipulation and purification of DNA

2. 5. 1 Digestion of DNA with restriction endonucleases

DNA digests were normally set up using 10 U of restriction endonucleases in a total volume of 30 µl for 3-4 hours. The amount of enzymes used for digests was less than 0.1 volume of the final reaction mixture to avoid inhibition of enzyme activity by glycerol. The restriction endonuclease buffer and incubation temperature was selected according to manufacturers instructions. In cases where reaction condition was not favourable for simultaneous digests, DNA was purified (section 2. 4. 5) after the first digest and the condition was set up for the next restriction endonuclease.

2. 5. 2 Phosphorylation and annealing of oligonucleotides

1-10 µg of each purified oligonucleotide was phosphorylated in a 30 µl reaction containing 50 mM Tris-HCl (pH 7.5), 10 mM $MgCl_2$, 5 mM DTT, 1 mM ATP, 20 unit of T4 kinase and 50 ng/µl BSA. The reaction was incubated at 37 ^{o}C for 1 h. The volume of reaction was adjusted to 100 ml with SDW, the phosphorylated oligonucleotides were purified as described in section 2. 4. 5 and the resulting oligonucleotide pellet were resuspended in 10 µl of SDW. A 5 µl aliquot of each complementary oligonucleotide was transferred to 1.5 ml microfuge tube, mixed and annealed at 65 ^{o}C for 1 min.

2. 5. 3 Dephosphorylation of linearised plasmid DNA

10x dephosphorylation buffer:

$ZnCl_2$ 10 mM, $MgCl_2$ 10 mM, Tris-HCl (pH 8.3) 100 mM

To suppress self-ligation of the linearised plasmid DNA, the 5'-phosphates was removed using calf intestinal alkaline phosphatase (CIP). Following complete digestion of plasmid DNA (5-10 µg) with a desired restriction endonuclease, to a 50 µl reaction mixture, 0.5 unit of CIP, 10 µl of 10x CIP dephosphorylation buffer and 40 µl SDW were added to give a final volume of 100 µl. The reaction was incubated

at 37 °C for 30 min. The dephosphorylated DNA was purified by phenol/chloroform extraction and ethanol precipitation (section 2. 4. 5).

2. 5. 4 Ligation of DNA fragments

Plasmid vector and insert required for a recombinant plasmid were ligated in a 10 µl ligation reaction using 2 units (0.5 µl) of T4 ligase (GIBCO BRL), 2 µl of 5X T4 ligase buffer with the concentration of termini of the insert approximately 3 fold higher than the plasmid vector. Approximately 30-60 ng of the vector DNA and in the case of low copy number binary vector (pBIN19) 100 ng of vector was used in ligations.

The ligations were incubated overnight at RT and a 0.2-0.4 µl aliquot of each ligation was used for bacterial transformation as described in sections 2. 3. 2 and 2. 3. 4.

2. 6 Amplification of DNA by polymerase chain reaction (PCR)

2. 6. 1 Purification of oligonucleotide primers

Oligonucleotide primers obtained from PNACL (synthesised by ABI 3808 or ABI 394 DNA synthesiser) were purified as described by Sawadogo and Van Dyke (1991). A 100 µl aliquot of an oligonucleotide primer was transferred to a 1.5 microfuge tube, 1ml of butan-1-ol was added, vortexed for 15 sec and centrifuged at 14000 *g*, room temp, for 1 min. The supernatant was carefully removed, the pellet was resuspended in 100 µl of SDW and the purification step with the butan-1-ol was repeated. The supernatant was discarded and the pellet was vacuum dried for 30 min. The pellet was resuspended in 100 µl of SDW and quantified spectrophotometrically (section 2. 4. 6).

Oligonucleotide primers obtained from Bioline were not purified. The pellet was resuspended in appropriate volumes of SDW as recommended by the supplier and used directly.

2. 6. 2 General PCR

Standard PCR was performed to amplify the desired DNA fragments. The PCR reaction mixture consisted of 5-10 ng of purified DNA template, 50 ng of purified primers, 200 µM of dNTPs, 1x *Taq* buffer and 1.0 U of *Taq* polymerase was prepared in a 0.5 ml microfuge tube to a final volume of 50 µl. The PCR reaction was mixed, spun briefly and overlaid with two drops of paraffin oil. The DNA fragment was amplified for 30 cycles using the following thermal conditions: Denaturing DNA template 94 °C for 1 min, Primer annealing 50 °C for 1 min, DNA synthesis 72 °C for 1 min. The PCR product was analysed by agarose gel electrophoresis (section 2. 8. 1).

2. 6. 3 Colony PCR

A small portion of a single colony was inoculated into a 50 µl PCR reaction (section 2. 6. 2) using a sterile toothpick and overlaid with a drop of mineral oil. Initially, the bacteria were incubated at 95 °C for 5 min to lyse the cells and then the standard PCR amplification was performed as described in section 2. 6. 2.

2. 6. 4 Reverse transcription and PCR amplification of RNA (RT-PCR)

RT-PCR was performed using the ABgene R*everse-i* T™ One Step system RT-PCR Kit (AB-0845) to detect RNA transcripts in tobacco leaf and pollen. The RNA template used for RT-PCR was isolated with TRIZOL reagent (GIBCO BRL) as described in section 2.

The RT-PCR reaction mixture consisted of 2x ReddyMix ™ Master Mix 25 µl, RNA template (1 µg/ml) 1 µl, primer (10 µM) 1 µl, reverse transcriptase blend 1 µl was prepared in a 0.5 ml microfuge tube and made up to 50 µl with DEPC treated water. The RT-PCR reaction was mixed, spun briefly and overlaid with 30 µl of mineral oil.

The RNA was reverse transcribed and PCR amplified using the following thermal conditions: first strand cDNA synthesis 47 °C for 30 min (1 cycle), reverse transcriptase inactivation and initial denaturation 94 °C for 2 min (1 cycle), Denaturation 94 °C for 20 sec, annealing 55 °C for 30 sec, extension 72 °C for 5 min (40 cycles), final extension 72 °C for 5 min (1 cycle). The presence of target template was detected by analysing an aliquot (10-20 µl) of the RT-PCR product using agarose gel electrophoresis (section 2. 8. 1).

2. 7 DNA sequencing by ABI PRISM ™ Dye terminator cycle sequencing

Automated dideoxy-mediated chain termination sequencing method was performed using The ABI PRISM™ BigDye Terminator Cycle Sequencing Ready Reaction kit with Ampli-Taq DNA polymerase FS (Promega). Plasmid DNA was prepared using the Wizard plus SV mini prep DNA purification system (Promega) according to manufacturers instructions.

For each sequencing reaction, 8.0 µl of terminator ready reaction mix, 200-500 ng of double stranded DNA, 3.2 pmol of primer were added to a 0.5 ml PCR tube and made up to a final volume of 20 µl with SDW. The sequencing reaction was mixed, spun briefly and overlaid with a drop of mineral oil. The tubes were placed in a Perkin Elmer thermal cycler model 480 and the amplification was performed in 25 cycles using the following thermal conditions: rapid thermal ramp to 96 °C, 96 °C for 30 sec; rapid thermal ramp to 50 °C, 50 °C for 15 sec; rapid thermal ramp to 60 °C, 60 °C for 4 min; rapid thermal ramp to 4 °C.

The extension reaction was transferred to a fresh 1.5 ml microfuge tube, 0.2 µl of 3 M sodium acetate (pH 4.6) and 50 µl of 95% ethanol was added, vortexed and placed on ice for 10 min. The tubes were centrifuged at 14000 g for 15-30 min. The supernatant was removed, the pellet was washed with 250 µl of 70% ethanol (v/v), vortexed briefly and spun at 14000 *g* for 5 min. The supernatant was removed and the pellet was vacuum dried for 10-15 min. The purified extension products were

analysed using ABI PRISM sequencer (ABI 373) by PNACL at Leicester University. The sequencing data obtained as chromatograms were analysed using the Sequence Editor 1.0.3 (Applied Biosystems) and Gene Jockey II (Biosoft) softwares.

2. 8 Gel electrophoresis

2. 8. 1 Agarose gel electrophoresis for separation of DNA

50x TAE buffer: Tris base 242 g, glacial acetic acid 57.1 ml, EDTA 0.5 M (pH 8.0) 100 ml.
Gel loading buffer: orange G 0.5% w/v, glycerol 50% v/v

Agarose gels were prepared by melting the appropriate amount of agarose in 100 ml of 1x TAE buffer and cooled to 60 ^{o}C. The ethidium bromide was added to the molten gel to a final concentration of 0.5 µg/ml, mixed thoroughly and poured into a mould with an appropriate comb. The gel was allowed to set for 30 min at room temp, the comb was carefully removed and the mould was placed into an electrophoresis tank containing 1x TAE buffer.

The DNA samples were mixed with 10x gel loading buffer to a final concentration of 1x and loaded into wells. An aliquot of a standard DNA ladder was used as a control. A voltage of 8 V/cm was applied and the gel was run until complete separation of the DNA fragments. After electrophoresis, DNA was visualised using a UVP (TM-40) DUAL-INTENSITY transilluminator and Gel Print 2000 *i* device, and the size and quantity of the DNA fragments was determined by comparing with the known mass and size fragments of a 1 kb standard DNA ladder (GIBCO BRL).

2. 8. 2 Agarose gel electrophoresis for separation of RNA

10x Mops buffer: Mops 0.2 M, sodium acetate 50 mM, EDTA 10 mM. pH adjusted to 7.0 with 5M NaOH, autoclaved 15 min at 120 ^{o}C.

RNA gel-loading buffer: formamide 64.5% v/v, formaldehyde (37%) 22.5% v/v, 10x Mops 13% v/v, Bromophenol blue 0.25 mg/ml.

To prepare an RNA gel, 1.2 g of agarose was melted in 87 ml SDW and cooled to 60 °C. 10 ml of 10x mops and 5.1 ml of 37% formaldehyde was added, mixed thoroughly and poured into a mould with an appropriate comb. The gel was allowed to set for at least 30 min at room temp, the comb was carefully removed and the mould was placed into an electrophoresis tank containing 1x Mops buffer.

In a 1.5 ml microfuge tube, 30-40 µg of total RNA was mixed with 3.5 volumes of RNA gel loading buffer to give a final concentration of 1x Mops, 50% formamide and 2.2 M formaldehyde. The samples were incubated at 65 °C for 15 min, chilled on ice and spun briefly. 1 µl of ethidium bromide (1 mg/ml DEPC treated water) was added to each sample, mixed and loaded. The gel was run at 80 V and the RNA was visualised as described in section 2. 8. 1

2. 9 Northern blotting

10x SSC: NaCl 1.5 M, trisodium citrate 150 mM. pH adjusted to 7.0 and autoclaved 15 min at 120 °C.

Following electrophoretic separation of RNA (section 2. 8. 2), the gel was carefully placed into 400 ml solution of 1x SSC, 80 mg NaOH for 20 min. Two pieces of Whatman 3MM filter paper (larger than gel) were placed on a stack of sponges inside a dish containing 10x SSC. When the filter papers were wet, the air bubbles between the sponge and the filter papers were removed using a sterile glass pipette. The gel was placed on top of the filter papers, the area of the gel above the wells was cut using a sterile razor blade and the air bubbles between the gel and the filter papers were removed as before. A piece of Hybond N membrane (Amersham) was cut and placed on top of the gel and covered with the two pieces of filter paper soaked in 10x SSC. The remaining air bubbles was removed as before, the gel was surrounded with Nescofilm (Whatman) and a stack of paper towels were placed on

top of the filter papers contact of which with the sponges was prevented by the Nescofilm. A 500 g weight was applied to the top of the paper towels and left overnight (16 h) enabling capillary transfer of RNA to the Hybond N membrane to proceed.

After transfer, the bottom left-hand corner of the Hybond N membrane was cut which enabled the membrane to be orientated correctly. The membrane, soaked once in 2x SSC and then in DEPC treated water to remove any remaining pieces of agarose. The membrane was dried between two pieces of filter paper and the RNA was UV cross-linked to the membrane using an UV Stratalinker (Stratagene).

2. 10 Radioactive labelling of DNA probes and hybridisation

2. 10. 1 Preparation of ^{32}P labelled DNA probe

Double stranded DNA probes were radioactively labelled with α-^{32}P-dCTP using an Oligolabelling kit (Amersham Pharmacia Biotech). DNA probe (25-50 ng) dissolved in SDW was denatured at 95-100 ^{o}C for 2-3 min, immediately incubated on ice for 2 min and centrifuged briefly. The volume of DNA probe was adjusted to 34 µl, 10 µl of Reagent Mix, 5 µl of α-^{32}P-dCTP and 1 µl of Klenow fragment was added to a final volume of 50 µl. The reaction mixture was gently mixed, centrifuged briefly and incubated at 37 ^{o}C for 60 min. The resulting radiolabelled probe was purified as described in section 2. 10. 2.

2. 10. 2 Purification of ^{32}P labelled DNA probe

STE buffer: NaCl 100 mM, Tris 10 mM, EDTA.2H_2O 1mM. pH adjusted to 7.5 with HCl and autoclaved 15 min at 120 ^{o}C.

Unincorporated nucleotides were separated from the ^{32}P-dCTP radiolabelled DNA probe using the Nuctrap Probe Purification Column and Push Column Beta Shield Device (Stratagene).

A 70 µl aliquot of STE buffer was loaded onto a Nuctrap Push column and passed through the column using a 10 ml Luer luck syringe. The syringe was disassembled, the ^{32}P labelled probe was carefully loaded on to the pre-wet column under a Push Column Beta Shield and passed through the column as before. The purified probe was retrieved by passing a 70 µl aliquot of STE buffer through the column and collecting the follow-through in a 1.5 ml screw-cap tube.

2. 10. 3 Hybridisation of DNA probes

1 M Na_2HPO_4 (pH 7.2) solution: Na_2HPO_4 1M 72 ml, NaH_2PO_4 1M 28 ml pH adjusted to 7.2.

Prehybridisation/hybridisation solution: Na_2HPO_4 (pH 7.2) 0.25 M, SDS 7%.

Church wash I: Na2HPO4 (pH 7.2) 20 mM, SDS 5% (Church and Gilbert, 1984).

Church wash II: Na2HPO4 (pH 7.2) 20 mM, SDS 1% (Church and Gilbert, 1984).

Prehybridisation, hybridisation and washing of RNA immobilised on the Hybond N membrane was performed at 65 ^{o}C.

The UV cross-linked membrane (section 2. 9) was placed into a Hybaid hybridisation bottle. The side of membrane carrying RNA faced towards the interior of the Hybaid bottle enabling RNA to be exposed to the radioactive probe. Prehybridisation solution (15-20 ml) was added and incubated in a Hybaid oven for 1-2 hours. Prehybridisation solution was removed and 5 ml of fresh prehybridisation solution was added. The radioactive probe (sections 2. 10. 1 and 2. 10. 2) was added directly to the prehybridisation solution and incubated overnight in a Hybaid oven.

The probe was transferred to a 50 ml Falcon tube and stored at –20. The membrane was washed twice with 15-20 ml of each of Church wash I and Church wash II solution for 20-30 min. After washing, the membrane was sealed in a plastic

bag and transferred to a Phosphorimager cassette. The intensity of the radioactive signal was determined using a Molecular dynamics phosphorimaging system 425E and Image Quant software.

2. 11 Transient expression assay by microprojectile bombardment

Tobacco leaf and pollen was bombarded essentially as described by Twell *et al.* (1989a) using a biolistic gun (Klein *et al.*, 1987).

2. 11. 1 Preparation of plant tissues

Pollen germination medium (PGM) (Tupy *et al.*, 1991): Sucrose 0.3 M, H_3BO_3 1.6 mM, Ca $(NO_3)_2$ 3 mM, $MgSO_4$ 0.8 mM, KNO_3 1 mM, MES 25 mM. pH adjusted to 5.9 with 1 M KOH and autoclaved 15 min at 120 °C.

Tobacco leaf used for microprojectile bombardment was selected from approximately 6 week-old greenhouse grown plant. A leaf disk of 2 cm squares was cut, placed adaxial surface up on the centre of an MSO plate and used directly for microprojectile bombardment.

Mature pollen collected as described in section 2. 14 was resuspended in liquid pollen germination medium (Tupy *et al.*, 1991) to a final concentration of 50 mg/ml. For transient expression analysis of sGFP fusion proteins (section 3. 8), the concentration of pollen was reduced to 30 mg/ml.

A 7 cm Whatman No. 1 filter paper was placed on the surface of a solidified PGM plate and a 2 cm square Hybond N membrane was placed on top of the filter paper. A 0.4 ml aliquot of the pollen suspension was spread onto surface of the Hybond N membrane, allowed to set and used quickly for microprojectile bombardment.

2. 11. 2 Preparation of M10 tungsten microprojectiles

The M10 tungsten microprojectiles were added to ethanol to a final concentration of 50 mg/ml. The slurry was vortexed, a 0.5 ml aliquot was taken immediately before rapid precipitation of tungsten microprojectiles and transferred to a 1.5 microfuge tube. To obtain aliquots with the same concentration of tungsten microprojectiles, the remaining slurry was vortexed before taking the next aliquot. The microprojectiles were precipitated by centrifugation at 14000 *g*, room temp for 5 min. The supernatant was discarded, 0.5 ml of SDW was added, vortexed and centrifuged as before. Two more washes were carried out as before and the M10 tungsten microprojectiles were resuspended in 0.5 ml of SH_2O and stored at –20 ^{o}C.

2. 11. 3 Preparation of macroprojectiles and bombardment of plant tissues

The M10 tungsten microprojectile suspension (section 2. 11. 2) was vortexed and a 25 µl aliquot was transferred into a 1.5 ml microfuge tube. 5 µg of plasmid DNA, 25 µl of 1 M $CaCl_2$ and 10 µl of 0.1 M spermidine free base were added separately, mixed by rapid pipetting before adding the next solution. The mixture was left at RT for 10 min to allow precipitation of the plasmid DNA onto M10 tungsten microprojectiles to proceed. After precipitation 25 µl of the supernatant was discarded and the mixture was sonicated using a horn type sonicator (Soniprep 150 MSE) to disperse the M10 tungsten microprojectiles.

A 2 µl aliquot of the mixture was quickly transferred onto the surface of a macroprojectile. The macroprojectile containing DNA-coated tungsten microprojectiles was placed upside down into the barrel of a biolistic gun using a forceps and was pushed into the barrel by a 1.5 cm metal rod. A 0.22 blank charge was placed in the barrel above the macroprojectile and the firing apparatus was assembled.

A stopping plate was fitted into the chamber on a metal plate beneath the barrel. The plate containing plant tissue was fitted into the chamber on a metal plate 7.5 cm away from the stopping plate. The chamber was evacuated using a vacuum pump to a pressure of 25 inches of mercury. The charge was fired resulting in bombardment of plant tissue with the DNA coated microprojectiles. Each

bombardment was performed in duplicate. After bombardment the vacuum was released, the plate was sealed with Nescofilm and incubated under constant light for 16 hours at 25 ^{o}C.

2. 12 Analysis of protein expression

2. 12. 1 Isolation of total protein

Homogenisation buffer:
MOPS (pH 7.2) 500 µl, 2M NaCl 250 µl, 0.5 M EDTA100 µl, 0.1 M EGTA 500 µl, glycerol 1 ml, β-Mercaptoethanol 9.8 µl, 100 mM PMSF 50 µl, Aprotinin 10 µl, Leupeptin 10 µl, Pepstatin 10 µl.

To extract total soluble proteins from tobacco leaf, the tissues were ground to a fine powder in liquid nitrogen and transferred to a 1.5 ml microfuge tube. Two volumes (v/w) of a freshly made ice cold homogenisation buffer was added, immediately vortexed and centrifuged at 14000 *g* for 10 min at 4 ^{o}C. The supernatant was transferred to a fresh tube, centrifuged as before to precipitate the remaining debris. The supernatant was transferred to a fresh tube and stored at -80 ^{o}C.

2. 12. 2 Quantification of protein

Based on a method described by Bradford (1976), the concentration of proteins was determined using Bradford reagent (Sigma). This reagent causes a shift in the absorption (maximum from 465 to 595), which is proportional to the concentration of protein. A 100 µl aliquot of the standard solutions of BSA (ranging from 100 µg/ml-1000 µg/ml) was loaded in duplicate into the wells of a 96 well NUNC plate in conjunction with the protein samples and SDW as a control. A 100 µl aliquot of the Bradford reagent was added to each well, mixed and left for 5 min. The absorbance values were measured using a Dynatech MR5000 microtitre plate reader

bombardment was performed in duplicate. After bombardment the vacuum was released, the plate was sealed with Nescofilm and incubated under constant light for 16 hours at 25 °C.

2. 12 Analysis of protein expression

2. 12. 1 Isolation of total protein

Homogenisation buffer:
MOPS (pH 7.2) 500 µl, 2M NaCl 250 µl, 0.5 M EDTA100 µl, 0.1 M EGTA 500 µl, glycerol 1 ml, β-Mercaptoethanol 9.8 µl, 100 mM PMSF 50 µl, Aprotinin 10 µl, Leupeptin 10 µl, Pepstatin 10 µl.

To extract total soluble proteins from tobacco leaf, the tissues were ground to a fine powder in liquid nitrogen and transferred to a 1.5 ml microfuge tube. Two volumes (v/w) of a freshly made ice cold homogenisation buffer was added, immediately vortexed and centrifuged at 14000 *g* for 10 min at 4 °C. The supernatant was transferred to a fresh tube, centrifuged as before to precipitate the remaining debris. The supernatant was transferred to a fresh tube and stored at -80 °C.

2. 12. 2 Quantification of protein

Based on a method described by Bradford (1976), the concentration of proteins was determined using Bradford reagent (Sigma). This reagent causes a shift in the absorption (maximum from 465 to 595), which is proportional to the concentration of protein. A 100 µl aliquot of the standard solutions of BSA (ranging from 100 µg/ml-1000 µg/ml) was loaded in duplicate into the wells of a 96 well NUNC plate in conjunction with the protein samples and SDW as a control. A 100 µl aliquot of the Bradford reagent was added to each well, mixed and left for 5 min. The absorbance values were measured using a Dynatech MR5000 microtitre plate reader

and the protein concentration was determined by comparing the average of absorbance values against the standard curve.

2. 12. 3 SDS polyacrylamide gel electrophoresis (SDS-PAGE)

12% Resolving gel for a single 16x18 cm gel: SDW 13.2 ml, 30% acrylamide/bisacrylamide 16 ml, 1.5 M Tris (pH 8.8) 10 ml, 10% SDS 400 µl, 10% ammonium persulphate 400 µl, TEMED 16 µl.
Stacking gel: SDW 5.54 ml, 30% acrylamide/bisacrylamide 1.66 ml, 1.5 M Tris (pH 8.8) 2.52 ml, 10% SDS 100 µl, 10% ammonium persulphate 100 µl, TEMED 10 µl.
10x SDS running buffer: Tris 30.2 g, glycine 188 g, SDS 10 g. made up to 1 l with SDW.
3x loading buffer: 0.5 M Tris HCl (pH 6.8) 40 ml, SDS 6 g, glycerol 30 ml, SDW 15 ml, bromophenol blue trace. 8.5 ml of the buffer was mixed with 1.5 ml of β-mercaptoethanol.
Coomassie Brilliant Blue R 250: Methanol 45 ml, glacial acetic acid 10 ml, SDW 45 ml Coomassie Brilliant Blue R 250 0.25 gr. The solution filtered through a Whatman No. 1 filter paper.
Destain solution: Methanol 30% v/v, acetic acid 10% v/v.

Total soluble proteins extracted from tobacco leaves were separated using a Hoefer SE 600 unit for vertical slab gel electrophoresis. The unit was assembled according to the manufacturers instructions. Approximately 30 ml of resolving gel was poured between two glass plates (16x18 cm) with 1.5 mm spacers, overlaid with isopropanol and allowed to polymerise.

After polymerisation the casting stand was tilted to remove the overlaying isopropanol, the surface of the gel was rinsed and the remaining SDW was dried using a Whatman 3MM filter paper. A 15-teeth comb was inserted between the two glass plates, the stacking gel was poured above the polymerised resolving gel allowed to set. The comb was removed and the wells were washed with 1x running buffer to remove unpolymerised acrylamide. The gel sandwich was fitted into the electrophoresis tank and 1x running buffer was added.

One volume of the protein samples (section 2. 12. 1) were mixed with two volumes of 3x loading buffer and, boiled at 95 °C for 3 min, The samples were cooled, centrifuged briefly and loaded. A 10 µl aliquot of a 10 kDa protein ladder (Gibco BRL) was used as a control. The gel was run at 30 ma until the tracking dye reached to the bottom of the gel. The gel apparatus was disassembled, the gel was stained with Coomassie Brilliant Blue on a rotary platform for 4 hours and destained overnight.

2. 12. 4 Two-dimensional gel electrophoresis (2-D electrophoresis)

Rehydration solution: 8 M Urea 12.0 g, 0.5% Triton X-100 0.13 ml, pharmalyte (3-10) 0.5 ml, DTT 50 mg. made up to 25 ml with SDW and incubated at 37 °C to dissolve.

Sample solution: Urea 13.5 g, 2-mercaptoethanol 0.5 ml (or DTT 250 mg), Pharmalyte (3-10) 0.5 ml, Triton X-100 0.13 ml. Traces of bromophenol blue was added, made up to 25 ml with distilled water and stored at –20 °C.

Tris-HCl stock solution (2 M): Tris 6.1 g. dissolved in 30 ml of SDW, pH adjusted to 6.8 and made up to 100 ml with SDW.

Equilibration solution 1: Tris-HCl stock solution 2.5 ml, urea 36 g, glycerol 30 ml, SDS 1 g, Made up to 100 ml with SDW. DTT 50 mg/10 ml was added and mixed.

Equilibration solution 2: Tris-HCl stock solution 2.5 ml, urea 36 g, glycerol 30 ml, SDS 1 g. Made up to 100 ml with SDW. iodoacetamide 0.45 g/10 ml and traces of bromophenol blue was added and mixed.

Total soluble protein was analysed in more detail by two-dimensional gel electrophoresis using a Multiphor II horizontal system (Amersham Pharmacia Biotech) for 2-D electrophoresis. In the first dimension step, isoelectric focusing (IEF), the proteins were separated according to their isoelectric points (pI) and in the second dimension step the proteins were separated on a SDS-polyacrylamide gel according to their molecular weights.

The first dimension (IEF) step was performed on a 180 mm Immobiline DryStrip consisting of a precast polyacrylamide gel with an immobilised pH gradient (3-10) on a plastic support. The Immobiline DryStips were placed in a reswelling cassette and rehydrated overnight in rehydration solution.

Total protein samples used for 2-D electrophoresis were desalted using a Microcon 3 microconcentrator (Amicon) at 14000 *g*, 4 °C. One volume of each sample containing 30 µg of total protein quantified by Bradford assay (section 2. 12. 2.) was mixed with 4 volumes of sample solution. The IEF gel apparatus was assembled according to the manufacturers instructions and the protein samples were loaded into sample cups adjusted above each Immobiline DryStrip. The first dimension gel was run for 16 hours at three phases as following: Phase 1: 500 V, 1 mA, 5 W, 1 h; Phase 2: 500 V, 5 W, 5 h; Phase 3: 3500 V, 1 mA, 5 W, 10 h to give a total number of Volt-hours of 45500.

After the first dimension run was completed the gel apparatus was disassembled and the Immobiline DryStrips were removed. Since one 18 mm Immobiline DryStrip can be run at a time in the second dimension, the unused strip was wrapped carefully in aluminium foil and stored at –80 until further use. The strip to be run in the second dimension was placed into a petri dish with the gel side facing inwards and the plastic support film facing towards the wall of the petri dish. The Immobiline DryStrip was equilibrated with 20 ml of the equilibration solution 1 for 10 min and then with 20 ml of the equilibration solution 2 for 10 min on a rotary platform. After equilibration placing the Immobiline DryStrip vertically on its edge on a piece of moistened filter paper without any contact of the gel with the filter paper drained the excess of equilibration solution 2. The equilibrated strip was immediately run in the second dimension.

The second dimension was performed using a 245X180 mm ExcelGel XL SDS 12-14, which consisted of a 0.5 mm thin precast polyacrylamide gel with a gradient of 12-14 cast on a plastic support film. The buffer ions required for the gel was supplied from the precast anodic and cathodic SDS buffer strips. The equilibrated Immobiline DryStrip was placed on the second dimension gel and the gel apparatus was assembled according to the manufacturers instructions. A 10 ml aliquot of 10 kDa protein ladder (GIBCO BRL) was included as a control. The

second dimension gel was run at three steps as following: Step 1: 1000 V, 20 mA, 40 W, 45 min; Step 2 1000 V, 40 mA, 40 W, 5 min; Step 3 1000 V, 40 mA, 40W, 160 min. After the first step was completed the Immobiline DryStrip was removed and a short run for 5 min (step 2) was performed. The cathodic buffer strip was transferred to the place of removed Immobiline DryStrip and electrophoresis was continued as described for step 3. Following electrophoresis, the gel apparatus was disassembled, the gel was removed and immediately stained as described in section 2. 12. 5.

2. 12. 5 Silver staining of ExcelGel XL SDS 12-14 gels

Fixing solution: ethanol 400 ml, Acetic acid 100 ml. made up to 1.0 litre with SDW.

Incubation solution: ethanol 75 ml, sodium acetate. $3H_2O$17.0 g, glutaraldehyde (25% w/v) 1.3 ml, sodium thiosufate ($Na_2S_2O_3.5H_2O$) 0.5 g. made up to 250 ml with SDW.

Silver solution: silver nitrate 0.25 g, formaldehyde 50 µl. made up to 250 ml with SDW.

Developing solution: sodium carbonate 6.25 g, formaldehyde 25 ml. made up to 250 ml with SDW.

Stop solution: EDTA-Na_2. $2H_2O$ 3.65 g. made up to 250 ml with SH_2O

Preserving solution: Glycerol 20 ml. made up to 250 ml with SDW.

To detect the proteins on Excell Gel SDS 12-14, a silver staining method was adopted using 400 ml of solutions for each gel in a tray standing on a rotary platform. All steps were performed at RT.

Following electrophoresis the gel was immediately immersed in fixing solution for 30 min to precipitate the proteins and diffuse out the SDS. The gel was placed in incubation solution for 30 min and then washed three times for 5 min with SDW. The gel was transferred to silver solution for 40 min, rinsed for 30 sec with 50 ml of developing solution and immersed in fresh developing solution for 15 min. As soon as the protein bands with the desired intensity were developed, placing the gel in stopping solution for 5-10 min stopped the reaction. The gel was washed three

times with SDW for 5-10 min and transferred to preserving solution for 20 min. The gel was placed on a glass plate with the gel side up, covered with a cellophane preserving sheet soaked in preserving solution and allowed to dry at RT.

2. 13 Protein sequencing

2. 13. 1 In-gel digestion of proteins

Tryptic peptides required for the N-terminal sequencing of proteins were obtained by in-gel digestion of proteins with trypsin. Protein bands corresponding to a protein of interest were cut from the commassie stained gel (section 2. 12. 3), placed in a microfuge tube and destained by washing with two 0.5 ml aliquots of 50% acetonitrile in 200 mM ammonium bicarbonate buffer for 30 min or until the bands appeared colourless. The gel slices were further washed with a 0.5 ml aliquot of 100 mM ammonium bicarbonate for 60 min. The supernatant was discarded, 0.15 ml of 100 mM ammonium bicarbonate and 10 µl of 45 mM DTT was added and incubated for 30 min at 60 ^{o}C. After cooling to RT, 10 µl of 100 mM iodoacetamide was added and incubated at RT for 30 min in the dark. The supernatant was discarded and the gel slices was washed with shaking in 50% acetonitrile and 50% 100 mM ammonium bicarbonate for 60 min. The gel slices were removed, cut into 5 squares each and transferred to the same microfuge tube. A 50 µl aliquot of acetonitrile was added and incubated at RT for 15 min. Following incubation when the gel slices were opaque in appearance, the supernatant was removed and the gel slices were desiccated in a speed vac for 5-10 min.

The gel slices were reswelled with a 10 µl aliquot of 25 mM ammonium bicarbonate/5 mM $CaCl_2$ solution containing Promega modified trypsin at a concentration which gave a protein: trypsin ratio of 10:1. After 10-15 min another 10 µl aliquot of 25 mM ammonium bicarbonate/5 mM $CaCl_2$ solution was added to cover the gel pieces and to ensure they stay wet during the digestion. The digests were incubated overnight at 37 ^{o}C. The tubes were centrifuged at 13000 rpm for 5 min and the supernatant was transferred to a fresh tube. The peptides were extracted

by 2x 20 min incubation at RT with 50 µl of 60% acetonitrile and 0.1% TFA. The peptides were dried in a speed vac or freeze dried for 2-3 hours.

2. 13. 2 Separation of tryptic peptides by reversed phase chromatography (RPC)

A rapid and efficient HPLC technique, the reversed phase chromatography (RPC) was used for separation and purification of tryptic peptides derived from the in-gel digestion of proteins (section 2. 13. 1). In this method the peptides are separated on stationary phases normally consist of silica-based supports modified with alkyl chains, which provides the hydrophobic surface for separation. The peptides are then eluted using mobile phases typically consist of volatile organic solvents (e.g., acetonitrile). The mobile phases also facilitate sample concentration and solvent removal prior to solute analysis. In this type of HPLC, the retention of peptides and proteins is considered to be a function of their relative hydrophobicities.

To dissolve the freeze dried tryptic peptides derived from in-gel digestion of proteins (section 2. 13. 1), a 60 µl aliquot of 0.1% TFA was added to each tube, sonicated for 10 min and spun at 14000 rpm for 10 min. The peptides were separated and purified by an HPLC (Hewlett Packard 1100) using a C-8 reversed phase column (2.1x220 mm, Applied Biosystems). The peptides were eluted from the column with a gradient of 0-50% of solvent B (80% acetonitrile, 0.1% TFA) for 20 minutes and 50-100% of solvent B for 15 minutes in single peaks. The eluted peptides were freeze dried and stored at -20 ^{o}C until required.

2. 13. 3 Coupling of tryptic peptide fraction and Sequelon-AA disc

carbodiimide solution: 1 mg water-soluble carbodiimide in 100 µl of coupling buffer

To prepare the tryptic peptides derived from RPC (section 2. 13. 2) for the N-terminal sequencing, each tryptic peptide fraction was covalently attached to a Sequelon-AA disc (Millipore). Sequelon-AA disc consists of a PVDF (polyvinylidene difluoride) matrix that has been derivatized with aryl amine groups.

This matrix provides a surface capable of reacting with both the C-terminal and side chain carboxyl groups of peptides and the reaction is activated by carbodiimide.

A freeze dried tryptic peptide fraction, separated and purified by RPC (section 2. 13. 2), was dissolved thoroughly in a 10 µl aliquot of acetonitrile, 0.1% TFA solution, briefly vortexed and sonicated at 55°C for 10 min. A sequelon-AA disk was placed on a sheet of Mylar (or glass slide) on a heater block at 55°C. A 5 µl aliquot of the dissolved tryptic peptide was applied to the Sequelon-AA disk, allowed to dry for 10-15 min. A second 5 µl aliquot of the same was added and dried as before. The Mylar sheet containing the Sequelon-AA disk was carefully removed from the heater without touching the disk. A 5 µl aliquot of a freshly prepared carbodiimide solution was applied to the disk and allowed the reaction to proceed at RT for 20 min. The disks were immediately used for N-terminal sequencing or stored in a microfuge tube at –20°C until required.

2. 13. 4 N-terminal sequencing by automated Edman degradation

The sequence of tryptic peptides was determined by automated Edman degredation using an Applied Biosystems (ABI 476) protein sequencer. This method is based on a stepwise removal of amino acid residues from the N-terminus of a (poly)peptide. At the first stage (coupling), the reaction of phenyl isothiocyanate (PITC), C_6H_5-N=C=S, with the N-terminus of a peptide leads to formation of phenylthiocarbamyl (PTC) peptide. At the second stage (cleavage), in the presence of trifluoroacetic acid (TFA) the sulfur atom attack on the carbonyl carbon of the terminal peptide which results in removal of the PITC and the first N-terminal residue from the rest of peptide and formation of a thiazolinone intermediate. The remainder of peptide chain with one less residue containing a new N-terminus is released. Finally at the last stage (conversion), the thiazolinone intermediate is hydrolysed to phenylthiocarbamyl derivative of the N-terminal amino acid and then cyclised to form the phenylthiohydantoin amino acid (PTH-aa). The cycle of degradation is repeated for the remaining peptide and after each cycle a new PTH-aa is produced.

The PTH-aa's produced by each cycle of Edman degradation is injected into an HPLC, which is integral to the sequencer and contains a C18 reversed phase column. The PTH-aa's are eluted using a gradient of solvent A (tetrahydrofuran, sodium acetate) and solvent B (acetonitrile) with increasing solvent B. PTH-aa's eluting from the column are detected by their absorbance at 269 nm. Each PTH-aa has a characteristic elution time, which is determined by injecting all 19 PTH-aa's (except cysteine as this is destroyed during Edman Degradation) at the beginning of the sequencing of any sample. PTH-aa's usually elute in the following order DNSQTGEAHYRPMVWFIKL. Each new PTH-aa eluted is therefore determined based on its elution time relative to the known standard PTH's.

2. 14 Plant material and growth conditions

Surface sterilised tobacco seeds required for tissue culture were obtained by soaking the seeds in 1 ml of 70% (v/v) ethanol for 1 min, 2 ml of 10% (v/v) Domestos (Lever Industrial, Runcorn, UK) for 10-15 min and four times wash with 2 ml of SDW. Sterilisation was performed in a laminar flow hood.

Nicotiana tabacum cv. SR1 leaf explants, seedlings and plantlets in culture media were grown in a growth room at 25 ^{o}C with continuous fluorescent light. Plants transferred to soil were either grown under normal greenhouse condition with a 16-h photoperiod or in a growth cabinet at 25 ^{o}C with 16-h light/8- h dark cycles.

Tobacco pollen samples used for total RNA analysis and microprojectile bombardment were collected from greenhouse grown plants using a vacuum cleaner containing a 20 μm mesh (obtained from R. Cadisch and Sons, Arcadia Avenue, Finchley, London N32JZ) to retain pollen.

Tobacco anthers used for RNA analysis were collected at five developmental stages from flower buds (10-12, 12-16, 17-30, 30-40 and 40-50 mm) of greenhouse grown plants. Plant material were used directly or stored at –80 ^{o}C until required.

2. 15 Tobacco transformation

2. 15. 1 Media

MSO medium (liquid): MS basal salts (Murashige and Skoog, 1962) 0.44% (w/v), sucrose 3% (w/v). pH adjusted to 5.8 with 5 M KOH and autoclaved for 15 min at 120 °C.

MSO medium (solidified): MSO, agar 0.8%. Autoclaved for 15 min at 120 °C.

2. 15. 2 Preparation of leaf discs

Tobacco leaves were excised from approximately 6 week-old plants grown under normal greenhouse condition and soaked in 10% (v/v) Domestos in a sterile casserole dish for 15 min. The leaves were transferred to a new sterile casserole dish and rinsed four times with 400 ml aliquots of SDW. Tobacco leaves were cut into 2 cm squares and transferred to a 14 mm petri dish containing 50 ml of liquid MSO to protect the edges from desiccation before transformation.

2. 15. 3 Preparation of *A. tumefaciens* and leaf disc transformation

A single colony of *A. tumefaciens* was inoculated into 10 ml of LB medium with antibiotic selection and grown overnight at 28 °C. The overnight culture was diluted five fold with liquid MSO medium in a 14 mm petri dish. The sterile leaf disks prepared as described in section 2. 15. 2 were transferred into the *A. tumefaciens* suspension and left for 5 min. The excess of *A. tumefaciens* suspension was removed from the leaf disks by placing them between sterile Whatman No.1 filter papers. The leaf disks were transferred adaxial side up onto MSO medium and gently flattened onto the medium using a sterile forceps ensuring that the edges are in contact with the medium. The plates were sealed with Nescofilm and leaf disks cocultivated with the *A. tumefaciens* were incubated under constant light at 25 °C for 2 days. The leaf discs were then transferred onto fresh MSO medium containing 1 mg/l BAP, 200 mg /l cefotaxime and 50 mg/l kanamycin in which within 2-4 weeks calli and shoots were developed. Regenerated calli were transferred to a fresh

medium as above to develop new shoots. Regenerated shoots as putative transformants were transferred to MSO medium containing 50 mg/l kanamycin in the magenta boxes until roots were developed. After root growth the plantlets were transferred to soil and grown to maturity under greenhouse condition.

Seeds derived from primary transformants and their progenies were surface sterilised as described in section 2. 14 and plated on the MSO medium supplemented with kanamycin (50 mg/l). The segregation ratio for resistance to kanamycin was determined by scoring the kanamycin resistant seedlings with developed roots and green leaves against the sensitive seedlings with undeveloped roots, lack of true leaves and bleached cotyledons.

2. 16 Application of phytohormones and ethylene inhibitors

Silver thiosulphate solution (1.25 mg/ml): A silver nitrate solution (2.5 mg/ml) was added dropwise and mixed with equal volume of sodium thiosulphate pentahyhrate solution (14.6 mg/ml) and filter sterilised (Clarke *et al.*, 1992).

Based on a method described by Schmülling *et al.* (1993) a 10 µl aliquot of aqueous solutions of GA_3 (10 µl of 2.5 and 0.25 mM) was applied to the shoot apex of 45 day-old greenhouse grown plants and repeated every four days until flowering.

Brassinosteroids (0.1, 0.5 and 1 mM solutions of epibrassinolide and homobrassinolide in chloroform), cobalt chloride (0.1, 1, 10 and 50 mM) and silver thiosulphate (5 mg/l) were incorporated directly into the MSO medium. Surface sterilised tobacco seeds were plated in these media, the plates were sealed with Nescofilm and incubated as described in section 2. 14.

In order to facilitate measurement of hypocotyl and root lengths, the MSO plates supplemented with brassinosteroids were placed vertically on a stand allowing contact of roots with medium without penetrating into the agar. Hypocotyl and root length of 30 seedlings was measured after 3 weeks.

2. 17 Sectioning and light microscopy

Toluidine blue staining solution (Regan and Moffatt, 1990): Toluidine blue 1% (w/v), sodium borate 1% (w/v). Filtered through Whatman No.1 filter paper and diluted 20 fold to a final concentration of 0.05% (w/v).

Hypocotyls, cotyledons and first true leaves from four week-old seedlings grown on MSO medium at 25 °C under constant fluorescent light were embedded using a Historesin embedding kit (Leica Instruments GmbH).

The tissues were fixed in 4% *p*-formaldehyde, vacuum infiltrated for 5 min and left overnight at 4 °C in fresh fixative. The fixative was removed, 70% ethanol was added and incubated for 2-4 h at 4 °C. The 70% ethanol was removed, 95% ethanol was added and incubated overnight at 4 °C. A series (3:1, 2:1, 1:1,1:2, 1:3 and 100% infiltration solution) of 95% ethanol: infiltration solution (50 ml basic resin and 0.5 g activator) were added to the tissues, vacuum infiltrated for 20 min with each solution and left for a minimum of 4 h or overnight at 4 °C. The tissues were placed in the required orientation in the beem cones filled with embedding solution (15 ml infiltration solution and 1 ml hardener) and left overnight to allow the embedding solution to be polymerised.

Longitudinal sections (5 µm) of hypocotyls (parallel to the apical-basal axis), cotyledons and first true leaves (perpendicular to adaxial-abaxial axis) were prepared using a microtome (Bright 5030). The sections were stained with 0.1% toluidine blue for 1 min, rinsed with SDW and dried on a heating block. The sections were mounted with DPX (Fisons) mounting medium. Cell size was measured parallel and perpendicular to the apical-basal axis in hypocotyls and to adaxial-abaxial axis in cotyledons and first true leaves using a Zeiss axiophot microscope. Images were captured as described in section 2. 21.

2. 18 Grafting

Tobacco plants used for grafting were grown in a growth cabinet as described in section 2. 14. Eighty day-old homozygote *NtmybAS1* scions were grafted onto 40

day-old wild type rootstocks. This difference in plant age allowed *NtmybAS1* plants to grow more and provided a reasonably sized scion for grafting. Heterozygote scions and rootstocks (for reciprocal grafting) of an intermediate size were the same age (50 day-old) as wild type when grafted. Wild type scions were grafted onto wild type rootstocks as a control.

The leaves near the grafting point were removed using a scalpel blade. The centre of the stem in rootstock was cut longitudinally (about 1-1.5 cm), the cut end of the scion was given a wedge shape edge and introduced into the slit made in the rootstock. The area around grafting point was sealed with Nescofilm and grafted plants were kept under plastic bags for one week to prevent drying of scions. For aeration of plants several holes were made in plastic bags. Plant height was measured at first flower stage in grafted and control plants.

2. 19 Callose staining

Based on a method described by Currier and Strugger (1956) tobacco leaves were stained to visualise callose deposition. The tissue was placed in 1% glutaraldehyde, 5 mM citric acid, 90 mM Na_2HPO_4 (pH 7.4) and fixed overnight. The fixing solution was removed and the tissue was cleared and dehydrated in absolute ethanol. The tissue was placed sequentially in 50% ethanol and in 67 mM K_2HPO_4 (pH 12) and stained for 1 h in 0.01% aniline blue in 67 mM K_2HPO_4 (pH 12). The stained tissue was placed in 70% glycerol, 30% stain and callose deposition was examined under a Nikon Optiphot UV microscope (section 2. 21).

2. 20 Chlorophyll measurement

Chlorophyll was measured in four uniformly grown tobacco plants at first flower stage. Two leaf discs of 1 cm square were cut from between the veins of four fully expanded leaves along the main stem. Each leaf disk was placed in a 1.5 ml microfuge tube containing 1 ml of N, N-dimethylformamide and incubated in the dark at 4 ^{o}C for 48 h. The extracted chlorophyll was transferred to 1 ml cuvettes and

the absorbance values read at 664 and 647 nm using a Philips (PU 8740 UV/VIS) scanning spectrophotometer. The concentration of chlorophyll was determined according to Moran (1982).

Chlorophyll a = 12.7 A_{664} – 2. 79 A_{647} in μg/ml

Chlorophyll b = 20.7 A_{664} – 4.62 A_{647} in μg/ml

Total chlorophyll = 7.04 A_{664} – 20.27 A_{647} in μg/ml

To avoid chlorophyll destruction by light exposure the samples were wrapped in aluminium foil during measurements.

2. 21 Image processing

In order to visualise the localisation of sGFP, pieces of bombarded pollen was removed from the Hybond N membrane (section 2. 11. 1), placed in 2-3 drop of liquid PGM (section 2. 11. 1) and spread over a microscope slide. Expression of sGFP was detected using a Nikon Optiphot UV microscope with a 470-490 nm excitation filter and a 480 nm barrier filter.

Deposition of callose in tobacco leaves was examined using the same set of filters described above. Hypocotyl, cotyledon and leaf sections were analysed under normal light.

Images were captured directly using a CCD camera (JVC KYF55B) and Imagegrabber software (Neotec).

Chapter 3

In planta overexpression of *NtmybAS1*

3. 1 Introduction

Isolation and characterisation of two members (*NtmybAS1* and *NtmybAS2*) of the *myb* gene family from tobacco pollen and specific expression of *NtmybAS1* in mature and germinating pollen led to the suggestion that *NtmybAS1* acts as a pollen specific transcription factor regulating gene expression in tobacco pollen (Sweetman, 1996). The function of *NtmybAS1* was initially characterised by ectopic expression of *NtmybAS1* in transgenic tobacco (Sweetman, 1996). The resulting dwarf phenotype provided a basis for studying the functional domains of *NtmybAS1* and it's role during pollen development.

To further characterise the functional domains of *NtmybAS1*, the full length and truncated versions of *NtmybAS1* were overexpressed in tobacco and phenotypic characteristics of the resulting transformants were analysed in the first and second generation. Cellular localisation of the NtMybAS1 protein in tobacco pollen was investigated by transient assay using the sGFP (Chiu *et al.*, 1996) reporter gene. A recent study on DNA binding, activation potential and localisation of *NtmybAS1* in anthers provided evidence for the regulatory role of the NtMybAS1 protein in activation of *PAL* expression (Yang *et al.*, 2000). Therefore, the relationship between the expression of *NtmybAS1* and induction of *gPAL1* (Fukasawa-Akada *et al.*, 1996) mRNA in anther during different stages of development and in *NtmybAS1* overexpressing lines was investigated.

This chapter demonstrates that a full length *NtmybAS1* is required for dwarfing. Dwarfing is gene dosage dependent and is directly related to the level of *NtmybAS1* expression. NtMybAS1 is a nuclear protein which contains a nuclear localisation signal (NLS) at the N-terminal Myb domain. Establishment of a relationship between the expression of *NtmybAS1* and induction of *gPAL1* mRNA in anthers revealed that *NtmybAS1* is anther-specific and probably functions as an activator of *gPAL1* expression during anther development. Despite high level expression of *NtmybAS1* in mature pollen *gPAL1* expression is suppressed in pollen. A model is proposed to show the potential mechanisms by which *gPAL1* expression is activated in anthers and suppressed in mature pollen.

3. 2 Construction of plasmids for ectopic overexpression of *NtmybAS1* in tobacco

Four T-DNA constructs were built in a binary plant transformation vector, pBIN19 (Bevan, 1984), for overexpression of a full length, two C-terminally truncated *NtmybAS1* proteins and for root specific expression of *NtmybAS1*. A double cauliflower mosaic virus 35S promoter (*2CaMV35S5'*) (Töpfer *et al.*, 1987), tobacco etch virus 5'UTR (*TEV5'UTR*) (Carrington and Freed, 1990), cauliflower mosaic virus 35S transcript polyadenylation sequence (*CaMV35S3'*) (Töpfer *et al.*, 1987) were used in these constructs except in the construct used for root-specific expression of *NtmybAS1* in which a region from –90 to +1 of the *CaMV35S* promoter was used (*-90 CaMV35S5'*). It has been shown by β–glucuronidase (GUS) fusion analysis that this region confers root specific expression of GUS reporter protein (Benfey and Chua, 1990).

The T-DNA constructs consisted of two gene cassettes between the right and left borders of T-DNA. The first cassette consisted individually of the two full length and two C-terminally truncated versions of *NtmybAS1* controlled by *2CaMV35S5'* and the *–90CaM35S5'* and *CaMV35S3'* (C3'). The second cassette consisted of the neomycin phosphotransferase (*nptII*) gene for selecting kanamycin resistant plants controlled by the nopaline synthase promoter (*nos5'*) and polyadenylation sequence (*nos3'*). The T-DNA constructs were transferred to *Agrobacterium tumefaciens* LB4404 (Ooms *et al.*, 1982) and used to transform *N. tabacum* using the leaf disk method (section 2. 15. 3).

3. 2. 1 Construction of the pBIN19mybAS1 plasmid

Construction of the pBIN19mybAS1 plasmid for the ectopic overexpression of *NtmybAS1* in tobacco is shown in Figure 3. 1. A fragment consisting of *2CaMV35S5'-TEV5'UTR-NtmybAS1-CaMV35S3'* was excised from the pRT2-mybAS1 plasmid (Sweetman, 1996) as a *SalI-SphI* fragment, cloned into the *SalI-SphI* cut pSL301 plasmid (Invitrogen), which resulted in the pSLmybAS1 plasmid.

Figure 3. 1

Construction of the pBIN19mybAS1 plasmid

The *2CaMV35S5'-TEV5'UTR-NtmybAS1-CaMV35S3'* excised from pRT2mybAS1 as a *SalI-SphI* fragment was cloned into pSL301 (Invitrogen), recovered as a *SalI-SacI* fragment and cloned into pBIN19.

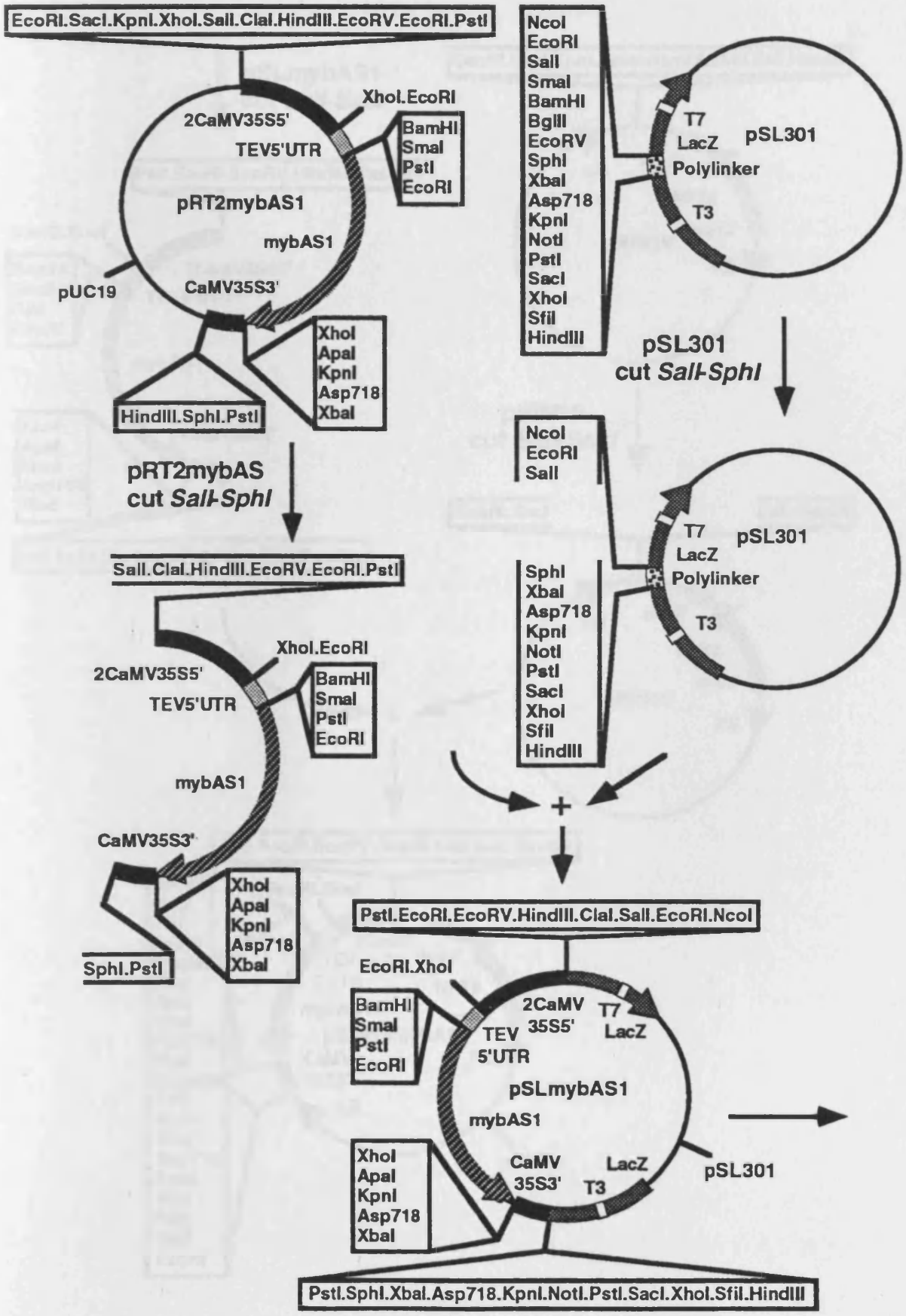
EcoRI.SacI.KpnI.XhoI.SalI.ClaI.HindIII.EcoRV.EcoRI.PstI
2CaMV35S5'
TEV5'UTR
XhoI.EcoRI
BamHI
SmaI
PstI
EcoRI
pRT2mybAS1
mybAS1
pUC19
CaMV35S3'
XhoI
ApaI
KpnI
Asp718
XbaI
HindIII.SphI.PstI
pRT2mybAS
cut SalI-SphI
SalI.ClaI.HindIII.EcoRV.EcoRI.PstI
2CaMV35S5'
TEV5'UTR
XhoI.EcoRI
BamHI
SmaI
PstI
EcoRI
mybAS1
CaMV35S3'
XhoI
ApaI
KpnI
Asp718
XbaI
SphI.PstI
NcoI
EcoRI
SalI
SmaI
BamHI
BglII
EcoRV
SphI
XbaI
Asp718
KpnI
NotI
PstI
SacI
XhoI
SfiI
HindIII
T7
LacZ
pSL301
Polylinker
T3
pSL301
cut SalI-SphI
NcoI
EcoRI
SalI
T7
LacZ
pSL301
Polylinker
T3
SphI
XbaI
Asp718
KpnI
NotI
PstI
SacI
XhoI
SfiI
HindIII
+
PstI.EcoRI.EcoRV.HindIII.ClaI.SalI.EcoRI.NcoI
EcoRI.XhoI
BamHI
SmaI
PstI
EcoRI
2CaMV
35S5'
TEV
5'UTR
T7
LacZ
pSLmybAS1
mybAS1
XhoI
ApaI
KpnI
Asp718
XbaI
CaMV
35S3'
T3
LacZ
pSL301
PstI.SphI.XbaI.Asp718.KpnI.NotI.PstI.SacI.XhoI.SfiI.HindIII

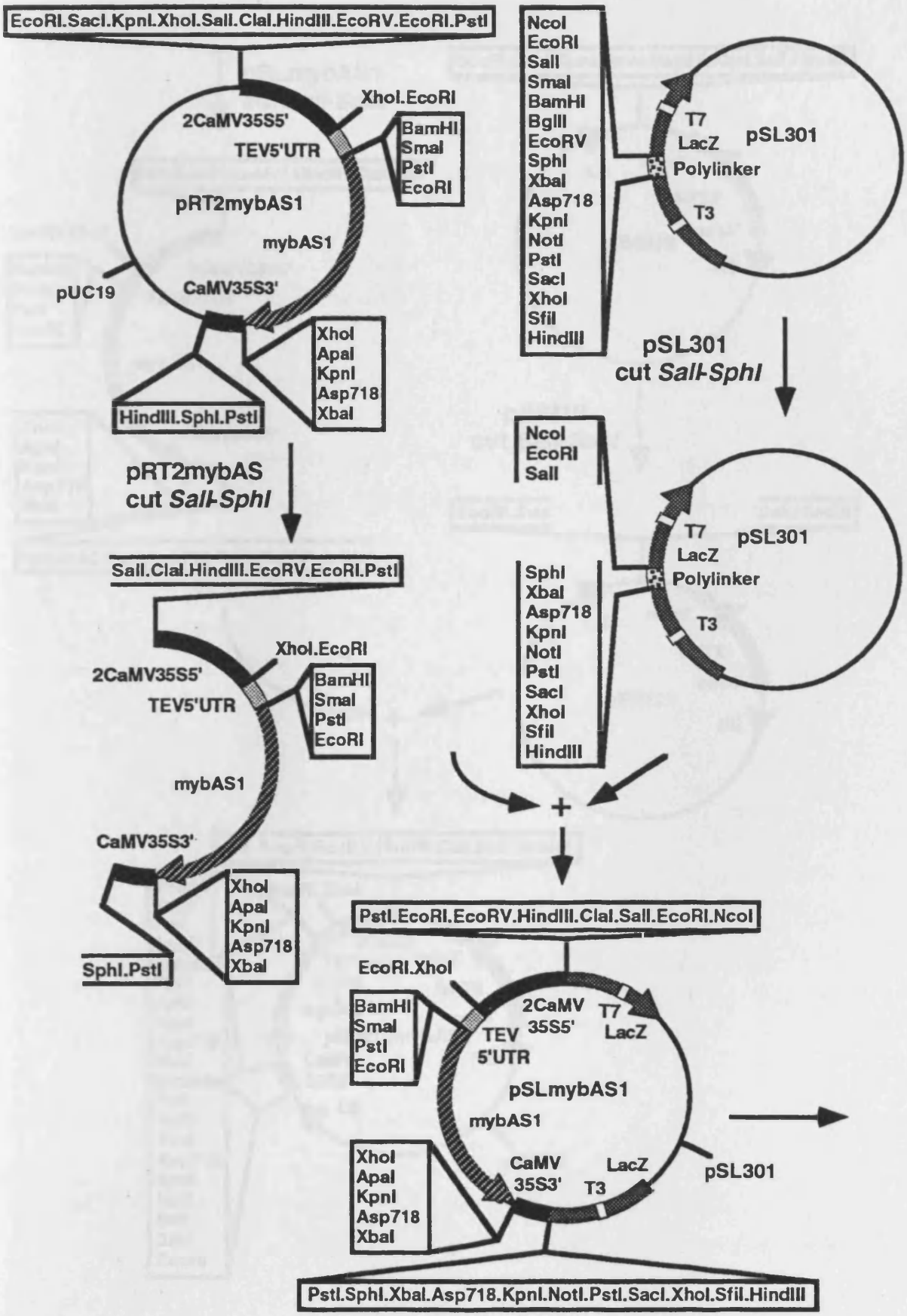
EcoRI.SacI.KpnI.XhoI.SalI.ClaI.HindIII.EcoRV.EcoRI.PstI
2CaMV35S5'
TEV5'UTR
XhoI.EcoRI
BamHI
SmaI
PstI
EcoRI
pRT2mybAS1
mybAS1
pUC19
CaMV35S3'
XhoI
ApaI
KpnI
Asp718
XbaI
HindIII.SphI.PstI
pRT2mybAS
cut SalI-SphI
SalI.ClaI.HindIII.EcoRV.EcoRI.PstI
2CaMV35S5'
TEV5'UTR
XhoI.EcoRI
BamHI
SmaI
PstI
EcoRI
mybAS1
CaMV35S3'
XhoI
ApaI
KpnI
Asp718
XbaI
SphI.PstI
NcoI
EcoRI
SalI
SmaI
BamHI
BglII
EcoRV
SphI
XbaI
Asp718
KpnI
NotI
PstI
SacI
XhoI
SfiI
HindIII
T7
LacZ
pSL301
Polylinker
T3
pSL301
cut SalI-SphI
NcoI
EcoRI
SalI
T7
LacZ
pSL301
Polylinker
T3
SphI
XbaI
Asp718
KpnI
NotI
PstI
SacI
XhoI
SfiI
HindIII
+
PstI.EcoRI.EcoRV.HindIII.ClaI.SalI.EcoRI.NcoI
EcoRI.XhoI
BamHI
SmaI
PstI
EcoRI
2CaMV
35S5'
T7
LacZ
TEV
5'UTR
pSLmybAS1
mybAS1
XhoI
ApaI
KpnI
Asp718
XbaI
CaMV
35S3'
LacZ
T3
pSL301
PstI.SphI.XbaI.Asp718.KpnI.NotI.PstI.SacI.XhoI.SfiI.HindIII

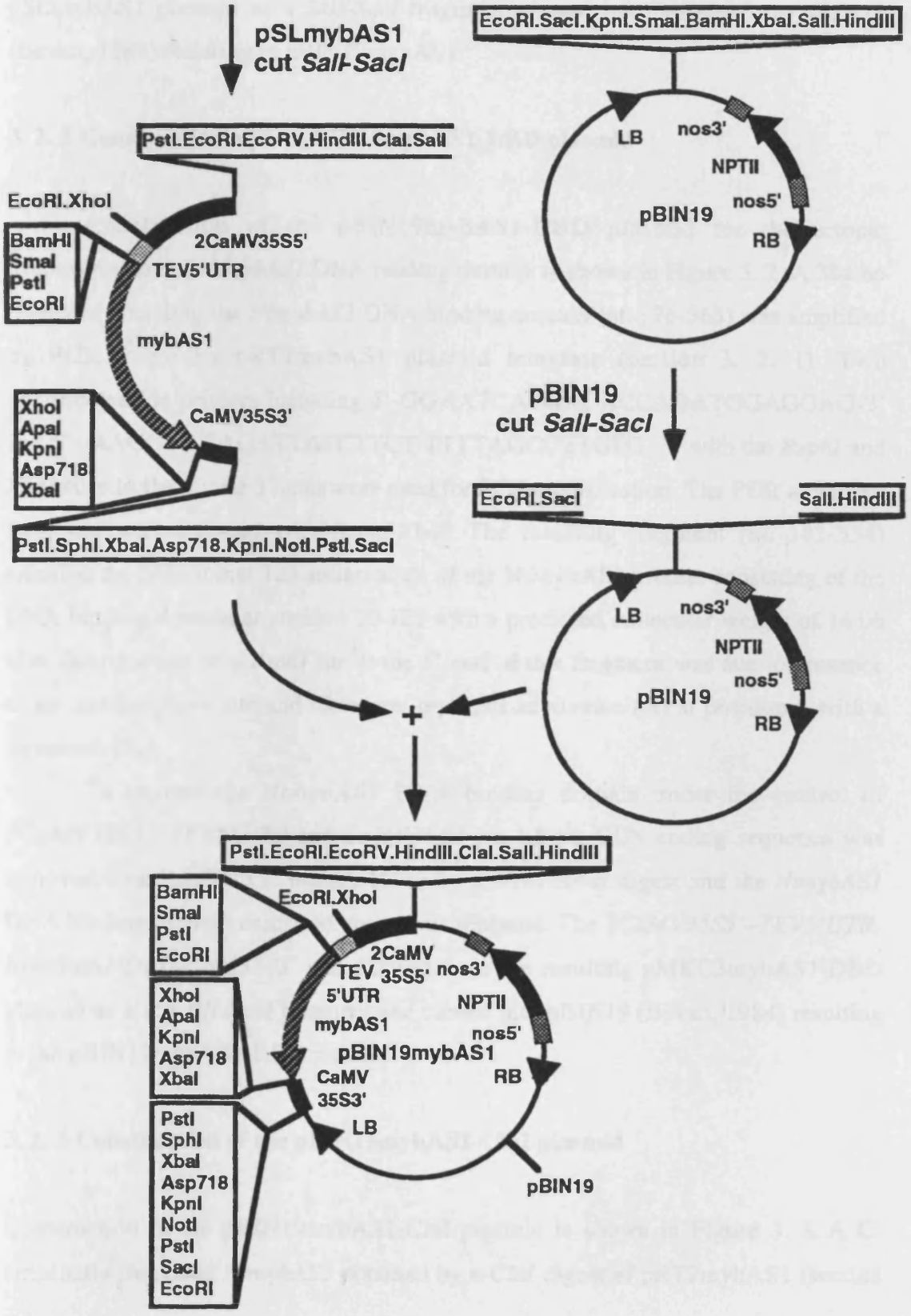
pSLmybAS1
cut Sall-SacI
PstI.EcoRI.EcoRV.HindIII.ClaI.SalI
EcoRI.XhoI
BamHI
SmaI
PstI
EcoRI
2CaMV35S5'
TEV5'UTR
mybAS1
XhoI
ApaI
KpnI
Asp718
XbaI
CaMV35S3'
PstI.SphI.XbaI.Asp718.KpnI.NotI.PstI.SacI
EcoRI.SacI.KpnI.SmaI.BamHI.XbaI.SalI.HindIII
LB
nos3'
NPTII
nos5'
pBIN19
RB
pBIN19
cut Sall-SacI
EcoRI.SacI
SalI.HindIII
+
PstI.EcoRI.EcoRV.HindIII.ClaI.SalI.HindIII
2CaMV
TEV 35S5'
5'UTR
mybAS1
pBIN19mybAS1
CaMV
35S3'
PstI
SphI
XbaI
Asp718
KpnI
NotI
PstI
SacI
EcoRI

The *2CaMV35S'-TEV-NtmybAS1-CaMV35S'* fragment was excised from the pSLmybAS1 plasmid as a *SalI-SacI* fragment, cloned into *SalI-SacI* cut pBIN19 (Bevan, 1984) resulting in pBIN19mybAS1.

3. 2. 2 Construction of the pBIN19mybAS1-DBD plasmid

Construction of the pBIN19mybAS1-DBD plasmid for the ectopic overexpression of *NtmybAS1* DNA binding domain is shown in Figure 3. 2. A 388 bp fragment encoding the *NtmybAS1* DNA binding domain (nt. 176-563) was amplified by PCR from the pRT2mybAS1 plasmid template (section 3. 2. 1). Two oligonucleotide primers including 5'-GGAATCATGACACCAGATGGAGGAG-3' and 5'- AACCTC TAGATTATCTTCT TTTTAGCCTTGTG- 3' with the *BsphI* and *XbaI* sites in the 5' and 3' ends were used for PCR amplification. The PCR amplified fragment was digested with *BsphI-XbaI*. The resulting fragment (nt. 181-554) encoded the N-terminal 123 amino acids of the NtMybAS1 protein consisting of the DNA binding domain at position 20-123 with a predicted molecular weight of 14.06 kDa. Introduction of a *BsphI* site at the 5' end of this fragment was due to presence of an internal *NcoI* site and therefore, replaced an alanine (A) at position 2 with a threonine (T).

To express the *NtmybAS1* DNA binding domain under the control of *2CaMV35S'*, *TEV5'UTR* and *CaMV35S'*, a 1.8 kb GUS coding sequence was removed from pMKC3 (Cheung, 1998) by a *NcoI-XbaI* digest and the *NtmybAS1* DNA binding domain described above was replaced. The *2CaMV35S'–TEV5'UTR-NtmybAS1 DBD-CaM35S'* was excised from the resulting pMKC3mybAS1-DBD plasmid as a *HindIII-SacI* fragment and cloned into pBIN19 (Bevan, 1984) resulting in the pBIN19mybAS1-DBD plasmid.

3. 2. 3 Construction of the pBIN19mybAS1-ClaI plasmid

Construction of the pBIN19mybAS1-ClaI plasmid is shown in Figure 3. 3. A C-terminally truncated *NtmybAS1* obtained by a *ClaI* digest of pRT2mybAS1 (section

Figure 3. 2

Construction of the pBIN19mybAS1-DBD plasmid

The *NtmybAS1* DNA binding domain was amplified by PCR, digested with *BsphI-XbaI* and cloned into pMKC3 (Cheung, 1998) after removing the GUS coding sequence. pMKC3mybAS1-DBD was digested with *HindIII-SacI* and the resulting *2CaMV35S5'-TEV5'UTR-NtmybAS1DBD-CaMV35S3'* fragment was cloned into pBIN19 plasmid.

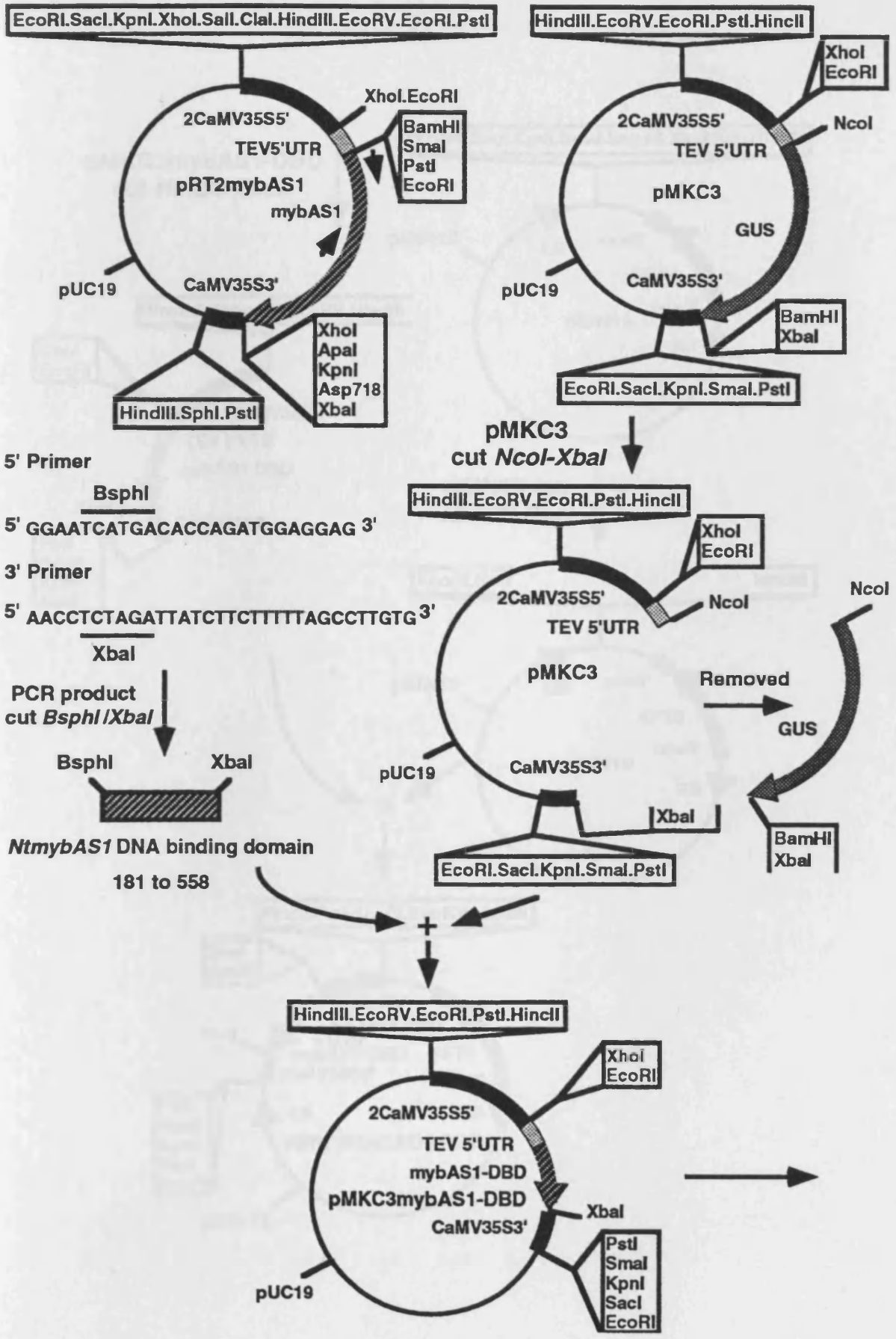
EcoRI.SacI.KpnI.XhoI.SalI.ClaI.HindIII.EcoRV.EcoRI.PstI
XhoI.EcoRI
2CaMV35S5'
TEV5'UTR
BamHI
SmaI
PstI
EcoRI
pRT2mybAS1
mybAS1
pUC19
CaMV35S3'
XhoI
ApaI
KpnI
Asp718
XbaI
HindIII.SphI.PstI
HindIII.EcoRV.EcoRI.PstI.HincII
XhoI
EcoRI
2CaMV35S5'
NcoI
TEV 5'UTR
pMKC3
GUS
pUC19
CaMV35S3'
BamHI
XbaI
EcoRI.SacI.KpnI.SmaI.PstI
pMKC3
cut NcoI-XbaI
5' Primer
BsphI
5' GGAATCATGACACCAGATGGAGGAG 3'
3' Primer
5' AACCTCTAGATTATCTTCTTTTTAGCCTTGTG 3'
XbaI
PCR product
cut BsphI/XbaI
BsphI
XbaI
NtmybAS1 DNA binding domain
181 to 558
HindIII.EcoRV.EcoRI.PstI.HincII
XhoI
EcoRI
2CaMV35S5'
NcoI
TEV 5'UTR
pMKC3
Removed
GUS
pUC19
CaMV35S3'
XbaI
EcoRI.SacI.KpnI.SmaI.PstI
NcoI
BamHI
XbaI
+
HindIII.EcoRV.EcoRI.PstI.HincII
XhoI
EcoRI
2CaMV35S5'
TEV 5'UTR
mybAS1-DBD
pMKC3mybAS1-DBD
XbaI
CaMV35S3'
PstI
SmaI
KpnI
SacI
EcoRI
pUC19

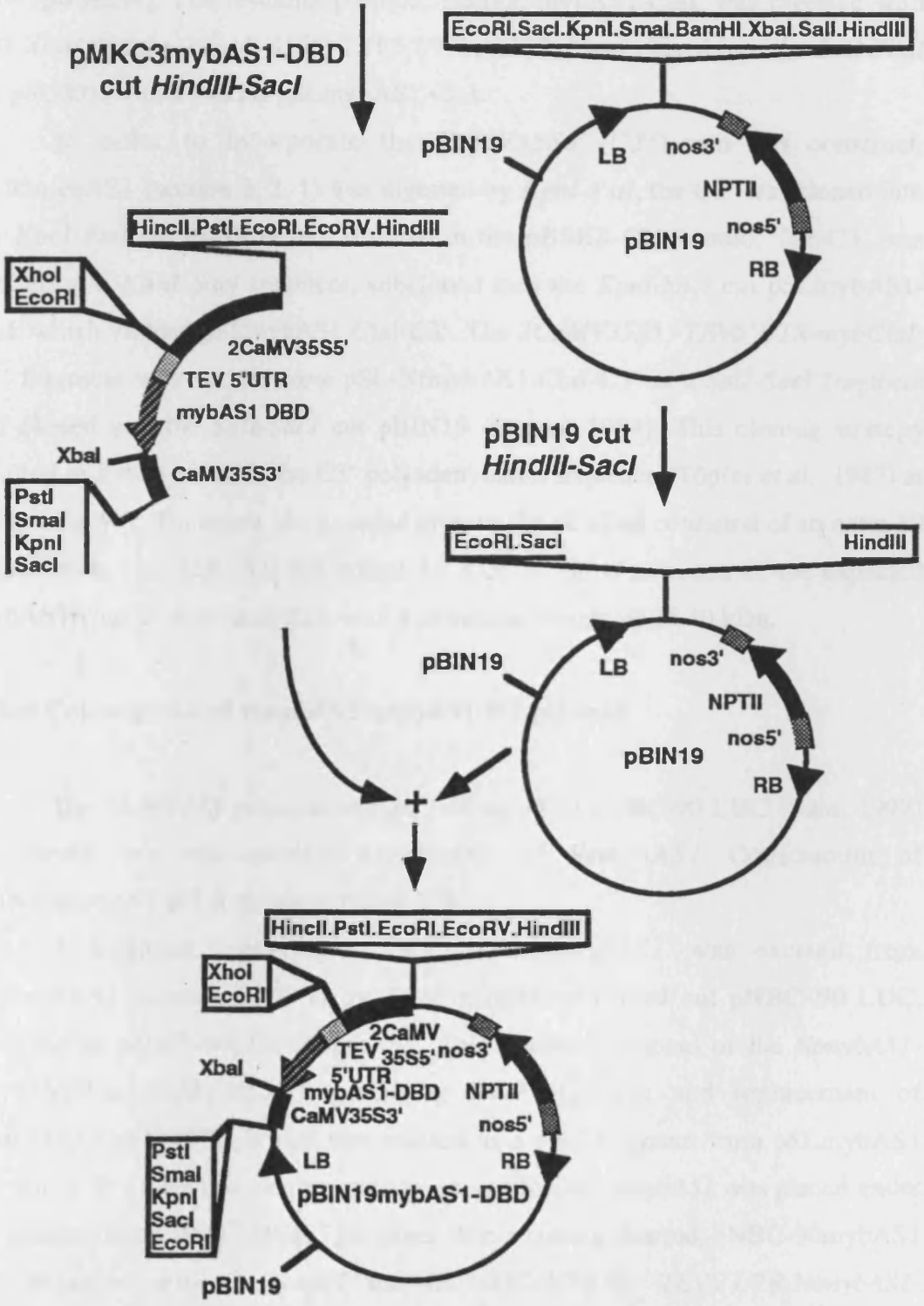
pMKC3mybAS1-DBD
cut HindIII-SacI
EcoRI.SacI.KpnI.SmaI.BamHI.XbaI.SalI.HindIII
pBIN19
LB
nos3'
NPTII
nos5'
pBIN19
RB
HincII.PstI.EcoRI.EcoRV.HindIII
XhoI
EcoRI
2CaMV35S5'
TEV 5'UTR
mybAS1 DBD
XbaI
CaMV35S3'
PstI
SmaI
KpnI
SacI
pBIN19 cut
HindIII-SacI
EcoRI.SacI
HindIII
pBIN19
LB
nos3'
NPTII
nos5'
pBIN19
RB
+
HincII.PstI.EcoRI.EcoRV.HindIII
XhoI
EcoRI
2CaMV
TEV 35S5'
nos3'
XbaI
5'UTR
mybAS1-DBD
NPTII
CaMV35S3'
nos5'
PstI
SmaI
KpnI
SacI
EcoRI
LB
RB
pBIN19mybAS1-DBD
pBIN19

3. 2. 1) enabled removal of 0.99 kb from the C-terminus of the *NtmybAS1* cDNA. The *2CaMV35S5'-TEV5'UTR-mybClaI* was cloned into the *ClaI* site of pBluscript II KS+ (pBSKS+). The resulting plasmid, pBSKS-mybAS1-ClaI, was digested with *SalI-XbaI* and the *2CaMV35S5'-TEV5'UTR-mybClaI* was cloned into the *SalI-XbaI* cut pSL301, which yielded pSLmybAS1-ClaI.

In order to incorporate the *CaMV35S3' (C3')* into this construct, pRT2mybAS1 (section 3. 2. 1) was digested by *KpnI-PstI*, the C3' was cloned into the *KpnI-PstI* cut pBSKS+ and resulted in the pBSKS-C3'plasmid. The C3' was excised as a *KpnI-SacI* fragment, subcloned into the *KpnI-SacI* cut pSLmybAS1-ClaI, which yielded pSLmybAS1-ClaI-C3'. The *2CaMV35S5'-TEV5'UTR-mybClaI-C3'* fragment was excised from pSL-NtmybAS1-ClaI-C3' as a *SalI-SacI* fragment and cloned into the *SalI-SacI* cut pBIN19 (Bevan, 1984). This cloning strategy resulted in a stop codon in the C3' polyadenylation sequence (Töpfer *et al.*, 1987) at nucleotide 549. Therefore, the encoded protein (29.48 kDa) consisted of an extra 39 amino acids (aa. 224-262) and added 4.1 kDa to the C-terminus of the expected MybAS1-ClaI protein (aa 1-223) with a molecular weight of 25.40 kDa.

3. 2. 4 Construction of the pBIN19mybAS1-RT plasmid

The *CaMV35S* promoter region –90 to +1 in pNBC-90 LUC (Bate, 1997) was used for root-specific expression of *NtmybAS1*. Construction of pBIN19mybAS1-RT is shown in figure 3. 4.

A fragment consisting of *TEV5'UTR-NtmybAS1* was excised from pSLmybAS1 (section 3. 2. 1) by *XhoI*, cloned into *XhoI* cut pNBC–90 LUC, resulting in pNBC–90LUC2TmybAS1. This allowed removal of the *NtmybAS1-TEV5'UTR-luc-CaMV35S3'* fragment by *PstI* digestion and replacement of *NtmybAS1-CaMV35S3'*, which was excised as a *PstI* fragment from pSLmybAS1 (section 3. 2. 1). By this cloning strategy expression of *NtmybAS1* was placed under the control of the *–90 CaMV35S* promoter. The resulting plasmid, pNBC-90mybAS1 was digested with *SalI-sacI* and the *–90CaMV35S5'-TEV5'UTR-NtmybAS1-CaMV35S3'* fragment was cloned into *SalI-SacI* cut BIN19 (Bevan, 1984).

Figure 3. 3

Construction of the pBIN19mybAS1-ClaI plasmid

The *2CaMV35S5'-TEV5'UTR-NtmybAS1ClaI* fragment excised from pRT2mybAS1 as a *ClaI* fragment was cloned into pBluescript+ (pBSKS+) (Stratagene), recovered as a *SalI-XbaI* fragment and subcloned into pSL301 (Invitrogen). The *CaMV35S3'* fragment excised as a *KpnI-PstI* fragment from pRT2mybAS1 was cloned into pBSKS+, recovered as a *KpnI-SacI* fragment and subcloned into pSLmybAS1-ClaI. The *2CaMV35S5'-TEV5'UTR-NtmybAS1 ClaI-CaMV35S3'* fragment excised as a *SalI-SacI* fragment from pSLmybAS1-ClaI-C3' was cloned into pBIN19.

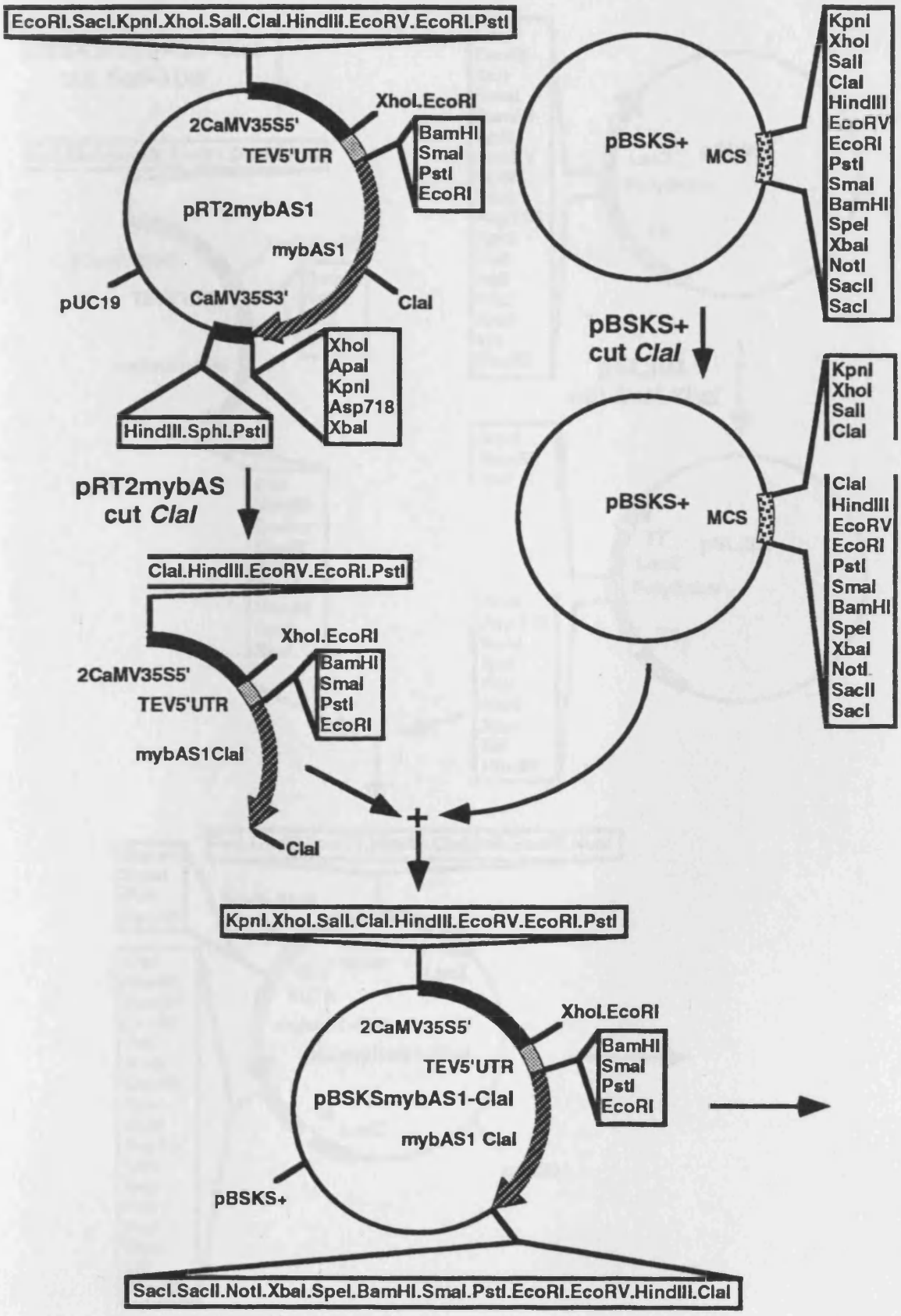
EcoRI.SacI.KpnI.XhoI.SalI.ClaI.HindIII.EcoRV.EcoRI.PstI
2CaMV35S5'
TEV5'UTR
XhoI.EcoRI
BamHI
SmaI
PstI
EcoRI
pRT2mybAS1
mybAS1
pUC19
CaMV35S3'
ClaI
XhoI
ApaI
KpnI
Asp718
XbaI
HindIII.SphI.PstI
pRT2mybAS
cut ClaI
ClaI.HindIII.EcoRV.EcoRI.PstI
XhoI.EcoRI
2CaMV35S5'
TEV5'UTR
BamHI
SmaI
PstI
EcoRI
mybAS1ClaI
ClaI
pBSKS+
MCS
KpnI
XhoI
SalI
ClaI
HindIII
EcoRV
EcoRI
PstI
SmaI
BamHI
SpeI
XbaI
NotI
SacII
SacI
pBSKS+
cut ClaI
pBSKS+
MCS
KpnI
XhoI
SalI
ClaI
ClaI
HindIII
EcoRV
EcoRI
PstI
SmaI
BamHI
SpeI
XbaI
NotI
SacII
SacI
+
KpnI.XhoI.SalI.ClaI.HindIII.EcoRV.EcoRI.PstI
2CaMV35S5'
TEV5'UTR
XhoI.EcoRI
BamHI
SmaI
PstI
EcoRI
pBSKSmybAS1-ClaI
mybAS1 ClaI
pBSKS+
SacI.SacII.NotI.XbaI.SpeI.BamHI.SmaI.PstI.EcoRI.EcoRV.HindIII.ClaI

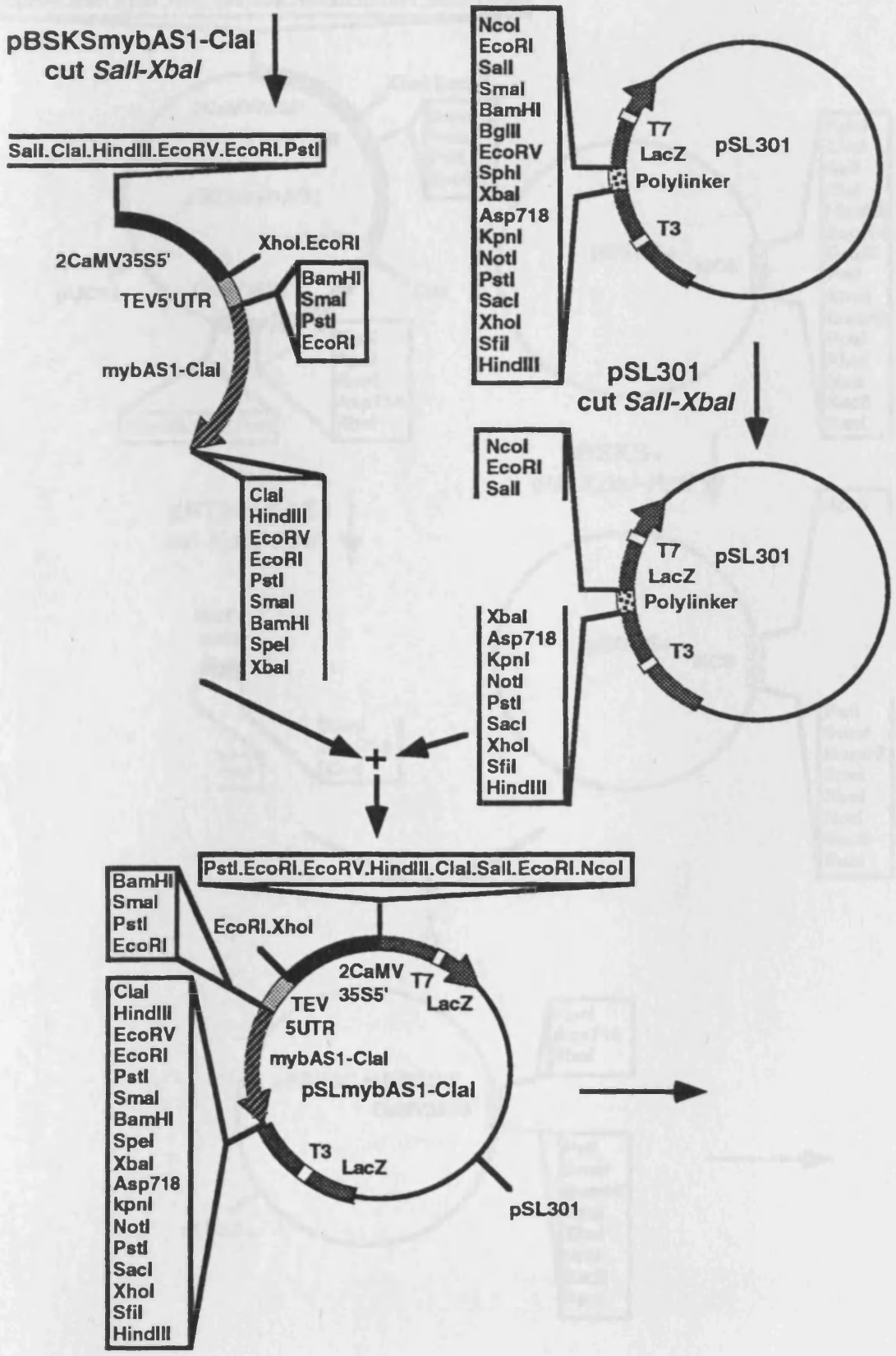
pBSKSmybAS1-ClaI
cut SalI-XbaI
SalI.ClaI.HindIII.EcoRV.EcoRI.PstI
2CaMV35S5'
XhoI.EcoRI
TEV5'UTR
BamHI
SmaI
PstI
EcoRI
mybAS1-ClaI
ClaI
HindIII
EcoRV
EcoRI
PstI
SmaI
BamHI
SpeI
XbaI
NcoI
EcoRI
SalI
SmaI
BamHI
BglII
EcoRV
SphI
XbaI
Asp718
KpnI
NotI
PstI
SacI
XhoI
SfiI
HindIII
T7
LacZ
pSL301
Polylinker
T3
pSL301
cut SalI-XbaI
NcoI
EcoRI
SalI
T7
LacZ
pSL301
Polylinker
T3
XbaI
Asp718
KpnI
NotI
PstI
SacI
XhoI
SfiI
HindIII
+
PstI.EcoRI.EcoRV.HindIII.ClaI.SalI.EcoRI.NcoI
BamHI
SmaI
PstI
EcoRI
EcoRI.XhoI
ClaI
HindIII
EcoRV
EcoRI
PstI
SmaI
BamHI
SpeI
XbaI
Asp718
kpnI
NotI
PstI
SacI
XhoI
SfiI
HindIII
2CaMV
35S5'
T7
LacZ
TEV
5UTR
mybAS1-ClaI
pSLmybAS1-ClaI
T3
LacZ
pSL301

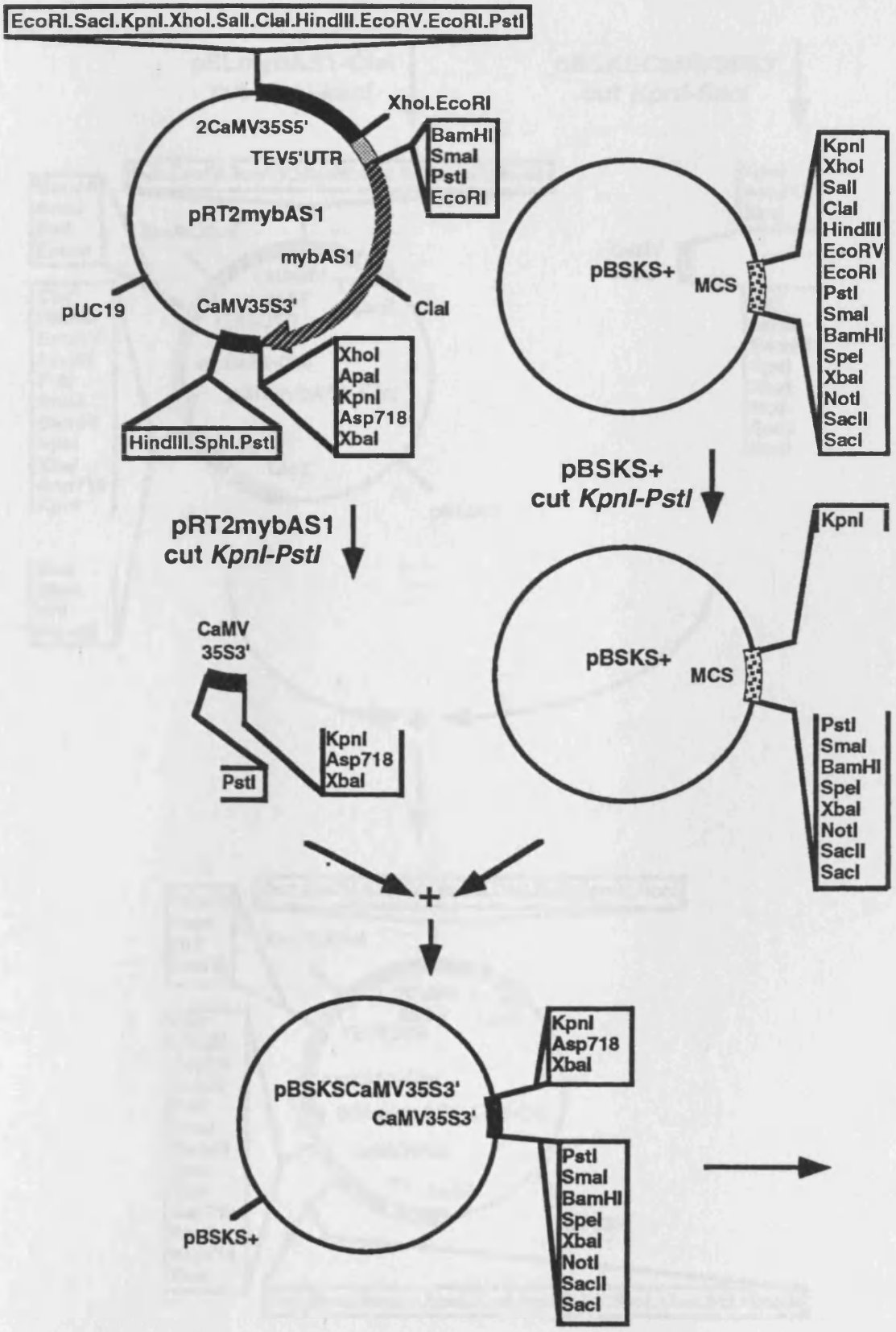
EcoRI.SacI.KpnI.XhoI.SalI.ClaI.HindIII.EcoRV.EcoRI.PstI
2CaMV35S5'
TEV5'UTR
XhoI.EcoRI
BamHI
SmaI
PstI
EcoRI
pRT2mybAS1
mybAS1
pUC19
CaMV35S3'
ClaI
XhoI
ApaI
KpnI
Asp718
XbaI
HindIII.SphI.PstI
pBSKS+
MCS
KpnI
XhoI
SalI
ClaI
HindIII
EcoRV
EcoRI
PstI
SmaI
BamHI
SpeI
XbaI
NotI
SacII
SacI
pBSKS+
cut KpnI-PstI
pRT2mybAS1
cut KpnI-PstI
CaMV
35S3'
KpnI
Asp718
XbaI
PstI
pBSKS+
MCS
KpnI
PstI
SmaI
BamHI
SpeI
XbaI
NotI
SacII
SacI
+
pBSKSCaMV35S3'
CaMV35S3'
KpnI
Asp718
XbaI
PstI
SmaI
BamHI
SpeI
XbaI
NotI
SacII
SacI
pBSKS+

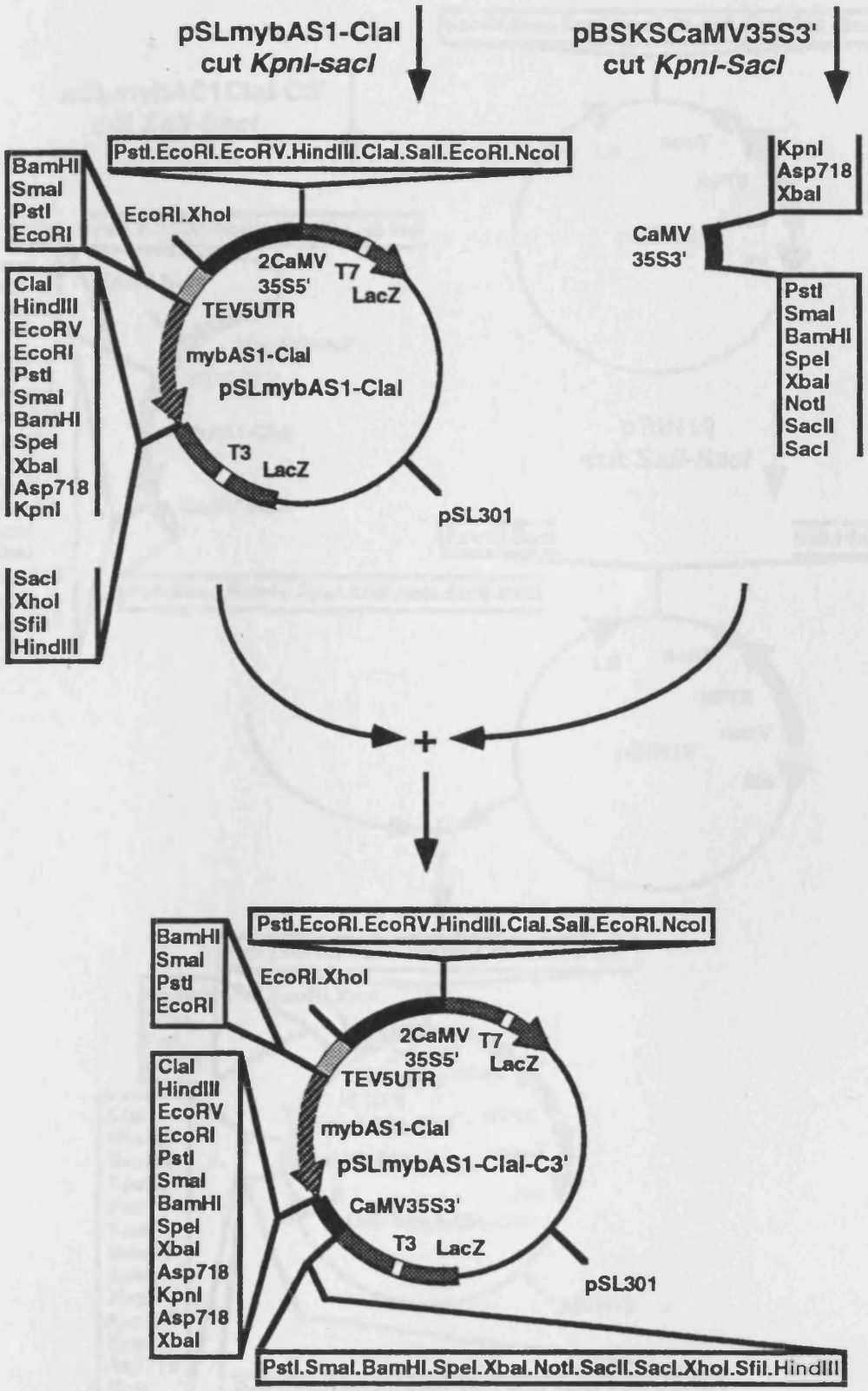
pSLmybAS1-ClaI
cut KpnI-SacI
pBSKSCaMV35S3'
cut KpnI-SacI
PstI.EcoRI.EcoRV.HindIII.ClaI.SalI.EcoRI.NcoI
BamHI
SmaI
PstI
EcoRI
EcoRI.XhoI
ClaI
HindIII
EcoRV
EcoRI
PstI
SmaI
BamHI
SpeI
XbaI
Asp718
KpnI
SacI
XhoI
SfiI
HindIII
2CaMV
35S5'
T7
LacZ
TEV5UTR
mybAS1-ClaI
pSLmybAS1-ClaI
T3
LacZ
pSL301
KpnI
Asp718
XbaI
CaMV
35S3'
PstI
SmaI
BamHI
SpeI
XbaI
NotI
SacII
SacI
+
PstI.EcoRI.EcoRV.HindIII.ClaI.SalI.EcoRI.NcoI
BamHI
SmaI
PstI
EcoRI
EcoRI.XhoI
ClaI
HindIII
EcoRV
EcoRI
PstI
SmaI
BamHI
SpeI
XbaI
Asp718
KpnI
Asp718
XbaI
2CaMV
35S5'
T7
LacZ
TEV5UTR
mybAS1-ClaI
pSLmybAS1-ClaI-C3'
CaMV35S3'
T3
LacZ
pSL301
PstI.SmaI.BamHI.SpeI.XbaI.NotI.SacII.SacI.XhoI.SfiI.HindIII

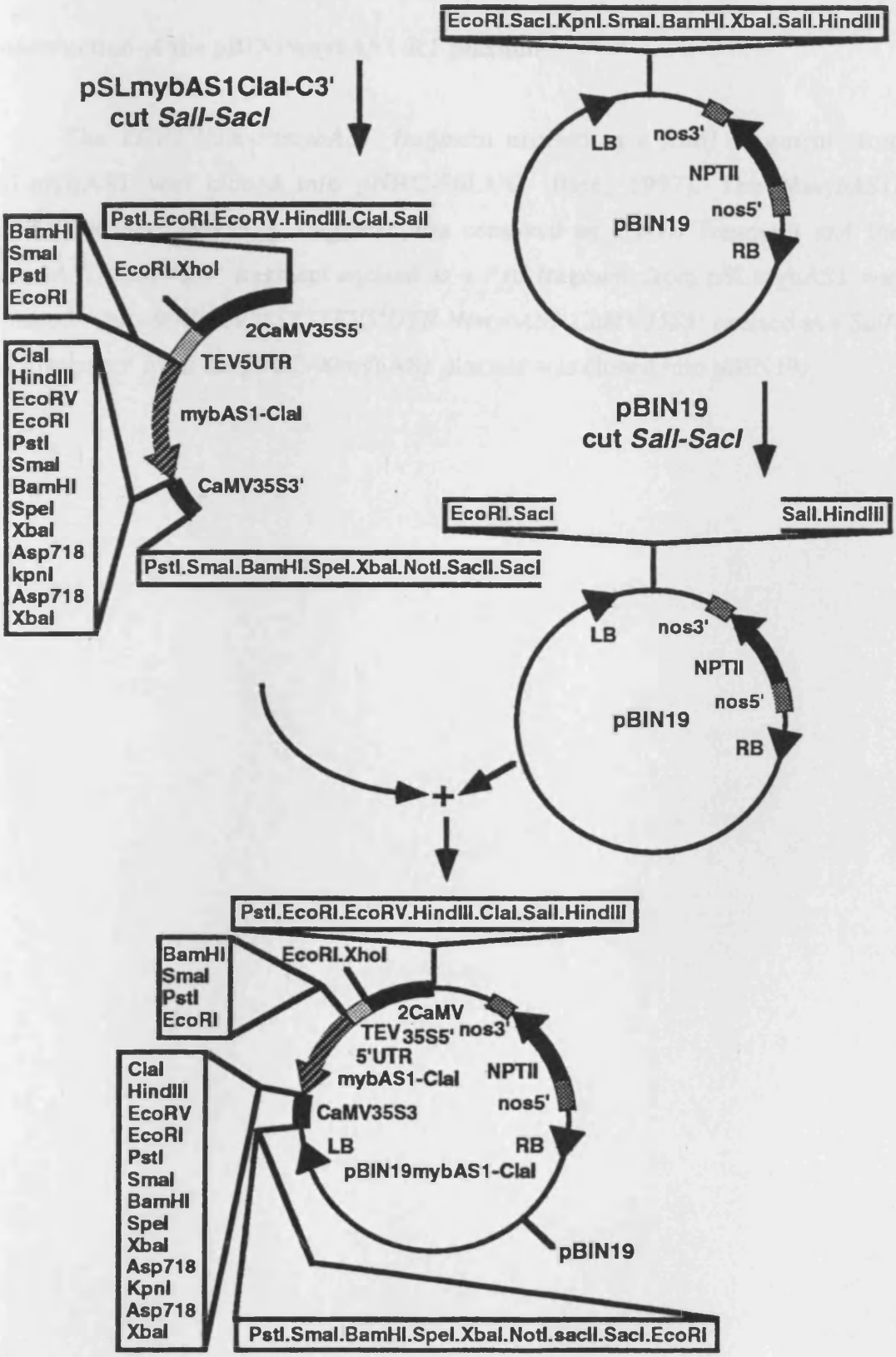
EcoRI.SacI.KpnI.SmaI.BamHI.XbaI.SalI.HindIII
pSLmybAS1ClaI-C3'
cut SalI-SacI
LB
nos3'
NPTII
nos5'
pBIN19
RB
PstI.EcoRI.EcoRV.HindIII.ClaI.SalI
BamHI
SmaI
PstI
EcoRI
EcoRI.XhoI
2CaMV35S5'
TEV5UTR
ClaI
HindIII
EcoRV
EcoRI
PstI
SmaI
BamHI
SpeI
XbaI
Asp718
kpnI
Asp718
XbaI
mybAS1-ClaI
CaMV35S3'
PstI.SmaI.BamHI.SpeI.XbaI.NotI.SacII.SacI
pBIN19
cut SalI-SacI
EcoRI.SacI
SalI.HindIII
LB
nos3'
NPTII
nos5'
pBIN19
RB
+
PstI.EcoRI.EcoRV.HindIII.ClaI.SalI.HindIII
BamHI
SmaI
PstI
EcoRI
EcoRI.XhoI
2CaMV
TEV 35S5'
5'UTR
nos3'
mybAS1-ClaI
NPTII
nos5'
CaMV35S3
LB
RB
pBIN19mybAS1-ClaI
pBIN19
ClaI
HindIII
EcoRV
EcoRI
PstI
SmaI
BamHI
SpeI
XbaI
Asp718
KpnI
Asp718
XbaI
PstI.SmaI.BamHI.SpeI.XbaI.NotI.sacII.SacI.EcoRI

Figure 3. 4

Construction of the pBIN19mybAS1-RT plasmid

The *TEV5'UTR-NtmybAS1* fragment excised as a *XhoI* fragment from pSLmybAS1 was cloned into pNBC-90LUC (Bate, 1997). The *NtmybAS1-TEV5'UTR-luc-CaMV35S3'* fragment was removed as a *PstI* fragment and the *NtmybAS1-CaMV353'* fragment excised as a *PstI* fragment from pSLmybAS1 was replaced. The *–90CaMV35S5'-TEV5'UTR-NtmybAS1-CaMV35S3'* excised as a *SalI-SacI* fragment from the pNBC-90mybAS1 plasmid was cloned into pBIN19.

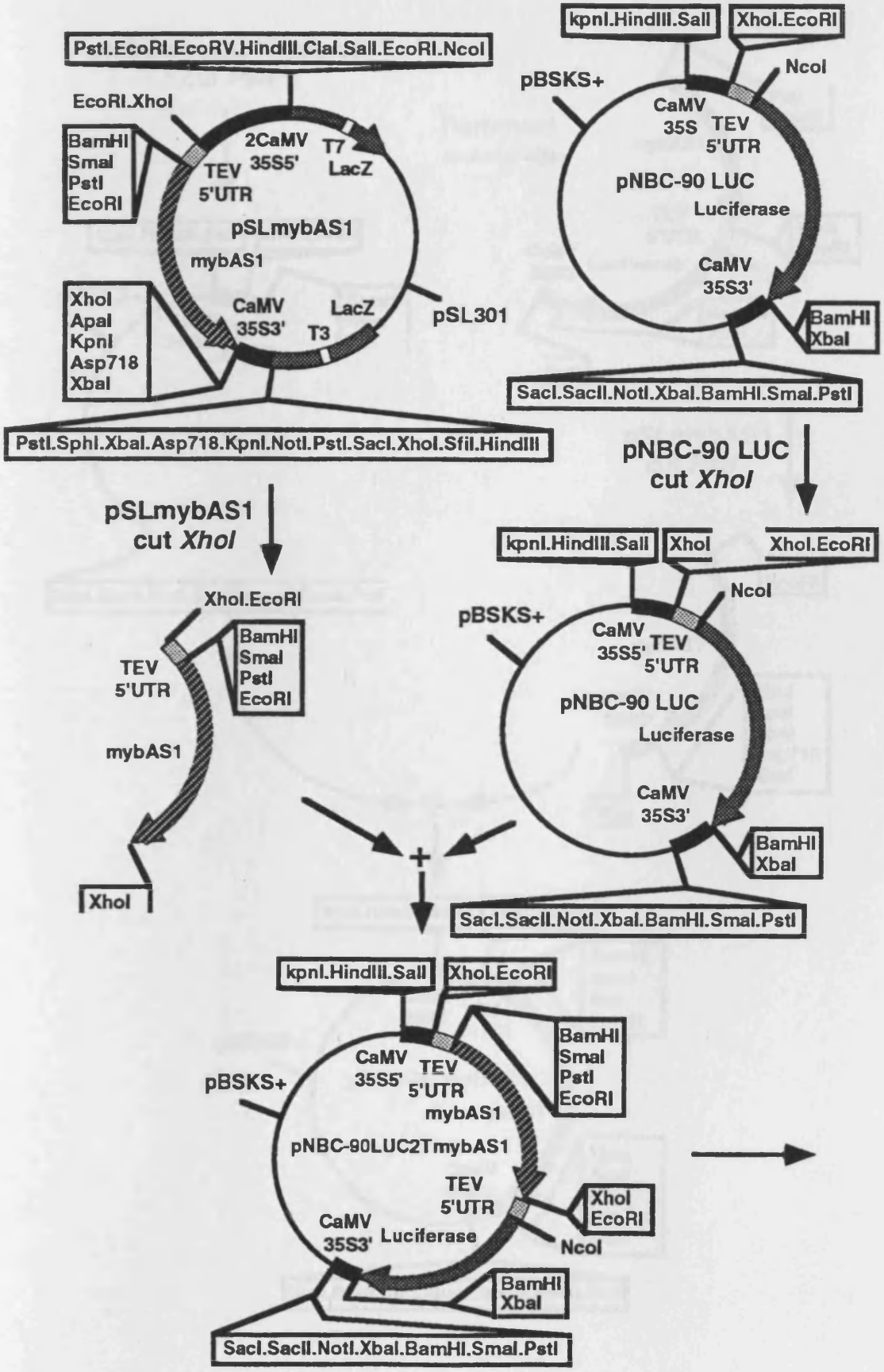
PstI.EcoRI.EcoRV.HindIII.ClaI.SalI.EcoRI.NcoI
EcoRI.XhoI
BamHI
SmaI
PstI
EcoRI
2CaMV 35S5'
T7
LacZ
TEV 5'UTR
pSLmybAS1
mybAS1
XhoI
ApaI
KpnI
Asp718
XbaI
CaMV 35S3'
LacZ
T3
pSL301
PstI.SphI.XbaI.Asp718.KpnI.NotI.PstI.SacI.XhoI.SfiI.HindIII
kpnI.HindIII.SalI
XhoI.EcoRI
NcoI
pBSKS+
CaMV 35S
TEV 5'UTR
pNBC-90 LUC
Luciferase
CaMV 35S3'
BamHI
XbaI
SacI.SacII.NotI.XbaI.BamHI.SmaI.PstI
pSLmybAS1 cut XhoI
pNBC-90 LUC cut XhoI
XhoI.EcoRI
BamHI
SmaI
PstI
EcoRI
TEV 5'UTR
mybAS1
XhoI
kpnI.HindIII.SalI
XhoI
XhoI.EcoRI
NcoI
pBSKS+
CaMV 35S5'
TEV 5'UTR
pNBC-90 LUC
Luciferase
CaMV 35S3'
BamHI
XbaI
SacI.SacII.NotI.XbaI.BamHI.SmaI.PstI
+
kpnI.HindIII.SalI
XhoI.EcoRI
BamHI
SmaI
PstI
EcoRI
pBSKS+
CaMV 35S5'
TEV 5'UTR
mybAS1
pNBC-90LUC2TmybAS1
TEV 5'UTR
CaMV 35S3'
Luciferase
XhoI
EcoRI
NcoI
BamHI
XbaI
SacI.SacII.NotI.XbaI.BamHI.SmaI.PstI

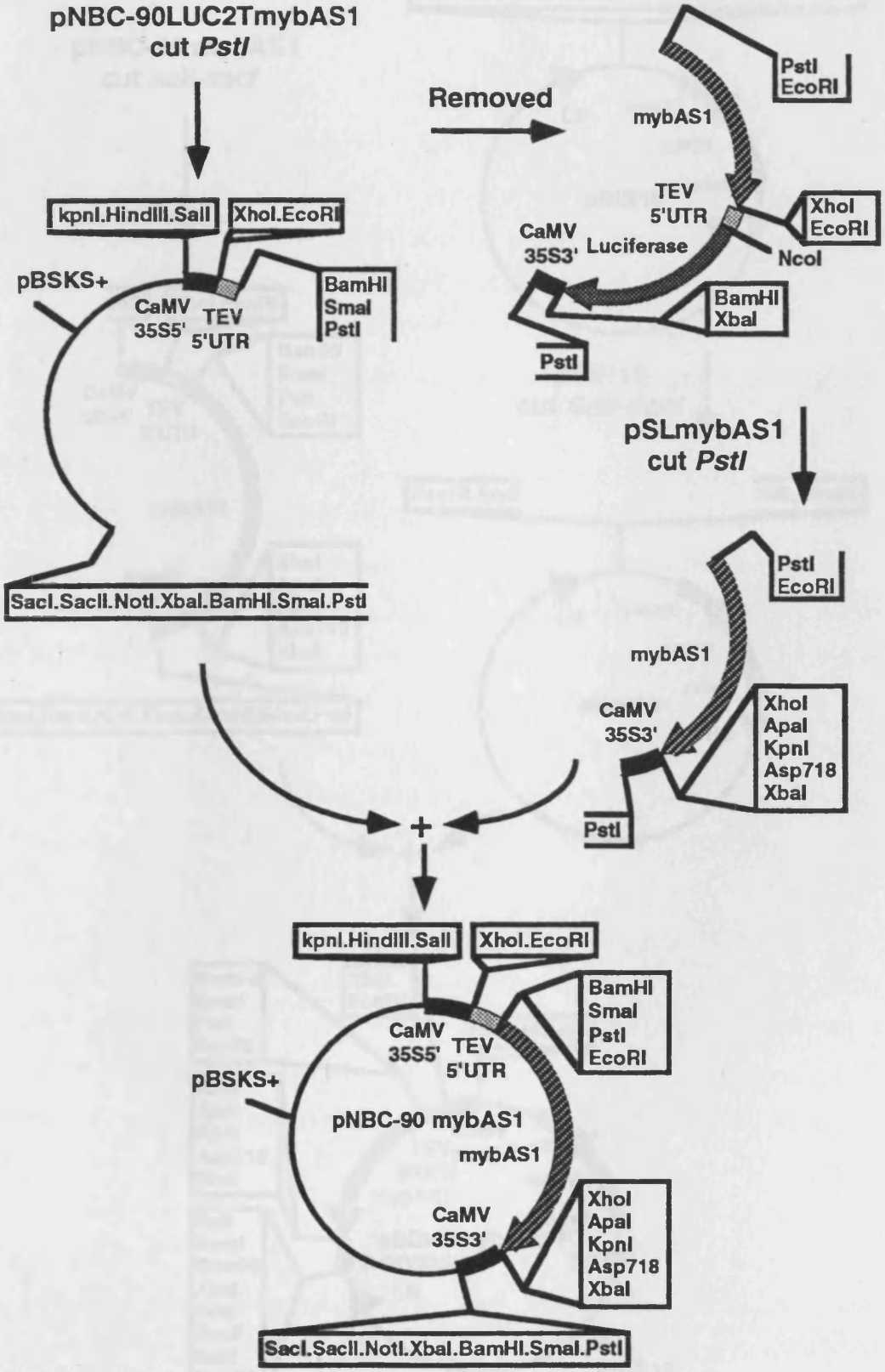
pNBC-90LUC2TmybAS1
cut PstI
Removed
PstI
EcoRI
mybAS1
TEV
5'UTR
XhoI
EcoRI
CaMV
35S3'
Luciferase
NcoI
BamHI
XbaI
PstI
kpnI.HindIII.SalI
XhoI.EcoRI
pBSKS+
CaMV
35S5'
TEV
5'UTR
BamHI
SmaI
PstI
SacI.SacII.NotI.XbaI.BamHI.SmaI.PstI
pSLmybAS1
cut PstI
PstI
EcoRI
mybAS1
CaMV
35S3'
XhoI
ApaI
KpnI
Asp718
XbaI
PstI
+
kpnI.HindIII.SalI
XhoI.EcoRI
BamHI
SmaI
PstI
EcoRI
CaMV
35S5'
TEV
5'UTR
pBSKS+
pNBC-90 mybAS1
mybAS1
CaMV
35S3'
XhoI
ApaI
KpnI
Asp718
XbaI
SacI.SacII.NotI.XbaI.BamHI.SmaI.PstI

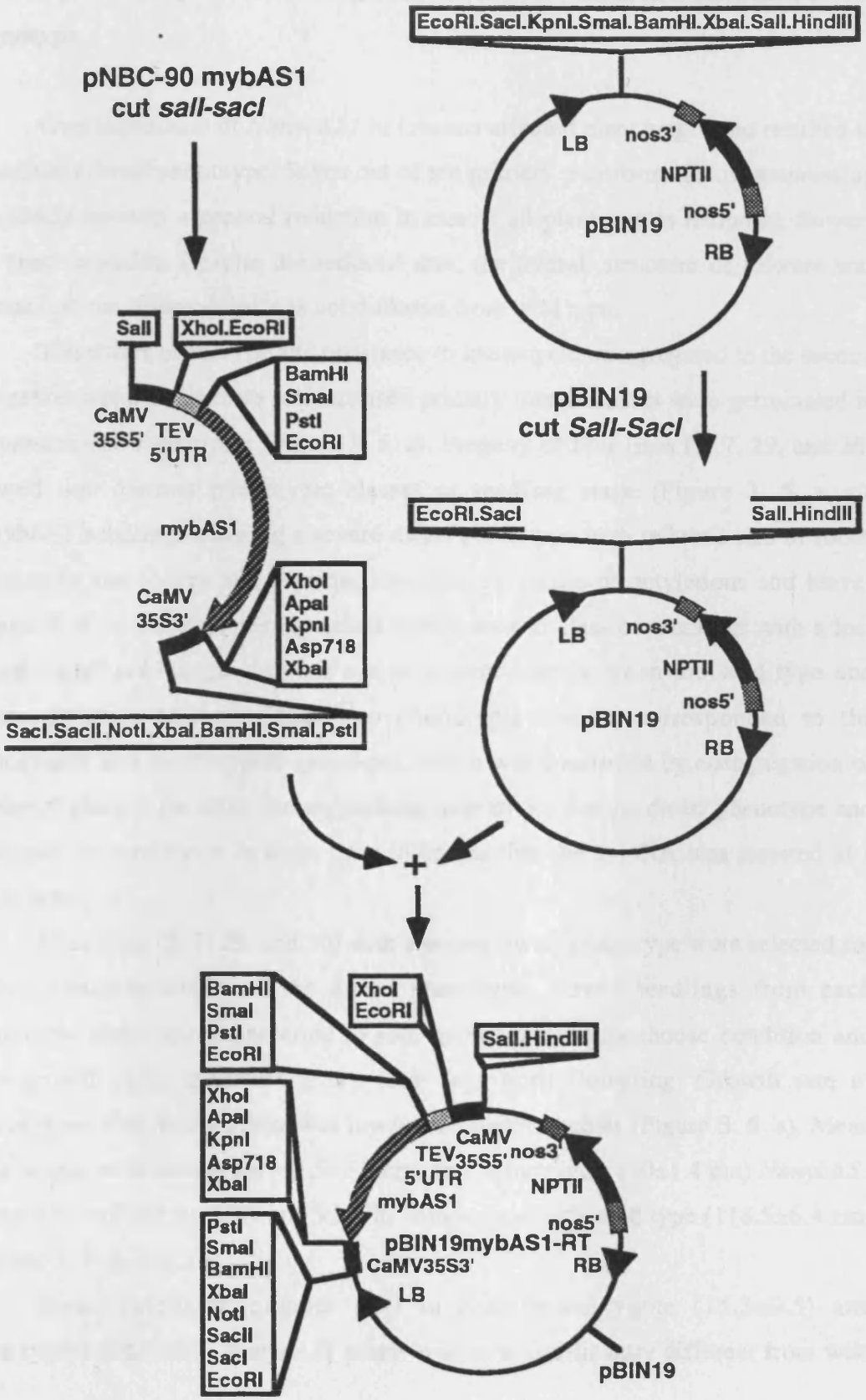
pNBC-90 mybAS1
cut sall-sacI
SalI
XhoI.EcoRI
BamHI
SmaI
PstI
EcoRI
CaMV
35S5'
TEV
5'UTR
mybAS1
CaMV
35S3'
XhoI
ApaI
KpnI
Asp718
XbaI
SacI.SacII.NotI.XbaI.BamHI.SmaI.PstI
EcoRI.SacI.KpnI.SmaI.BamHI.XbaI.SalI.HindIII
LB
nos3'
NPTII
nos5'
pBIN19
RB
pBIN19
cut SalI-SacI
EcoRI.SacI
SalI.HindIII
LB
nos3'
NPTII
nos5'
pBIN19
RB
+
BamHI
SmaI
PstI
EcoRI
XhoI
EcoRI
SalI.HindIII
XhoI
ApaI
KpnI
Asp718
XbaI
PstI
SmaI
BamHI
XbaI
NotI
SacII
SacI
EcoRI
CaMV
TEV
35S5'
nos3'
5'UTR
NPTII
mybAS1
nos5'
pBIN19mybAS1-RT
CaMV35S3'
RB
LB
pBIN19

3. 3 Ectopic overexpression of *NtmybAS1* in tobacco results in a dominant dwarf phenotype

Overexpression of *NtmybAS1* in tobacco affected plant height and resulted in a dominant dwarf phenotype. Seven out of ten primary transformants overexpressing *NtmybAS1* showed a general reduction in size of all plant organs including flowers and seed capsules. Despite the reduced size, the overall structure of flowers was normal and the flower color was not different from wild type.

The dwarf phenotype and resistance to kanamycin cosegregated in the second generation when seeds from self fertilised primary transformants were germinated in the presence of kanamycin (Figure 3. 5. a). Progeny of four lines (3, 7, 29, and 30) showed two distinct phenotypic classes at seedling stage (Figure 3. 5. a, c). *NtmybAS1* seedlings showing a severe dwarf phenotype with reduced size of roots, hypocotyls and leaves and a unique epinastic curvature of cotyledons and leaves (Figure 3. 5. b) could be distinguished from a second class of seedlings with a less severe dwarf phenotype showing a size intermediate between the wild type and severe dwarf seedlings. These two phenotypic classes corresponded to the homozygote and heterozygote genotypes, which was confirmed by cosegregation of the dwarf phenotype. Also, the segregation ratio of 3:1 for the dwarf phenotype and resistance to kanamycin in these lines indicated that the T-DNA was inserted at a single locus.

Four lines (3, 7, 29, and 30) with a severe dwarf phenotype were selected for further characterisation of the dwarf phenotype. Seven seedlings from each phenotypic class were transferred to soil, grown under greenhouse condition and their growth rates measured every four days until flowering. Growth rate of homozygote *NtmybAS1* plants was lower than heterozygotes (Figure 3. 6. a). Mean plant height in heterozygote (49.5±2.2 cm) and homozygote (10±1.4 cm) *NtmybAS1* plants was reduced by 58% and 92% in comparison with wild type (118.5±6.4 cm) (Figures 3. 5. d, 3. 6. b).

Mean internode number (IN) in both heterozygote (15.3±0.5) and homozygote (16.0±0.7) *NtmybAS1* plants were not significantly different from wild

Figure 3. 5

Phenotypic characteristics of *NtmybAS1* overexpressing plants

(a) Segregation of the dwarf phenotype and resistance to kanamycin in *NtmybAS1* overexpressing seedlings in the second generation. Arrows indicate a representative of wild type (WT), heterozygote (Het) and homozygote (Hom) *NtmybAS1* seedlings.

(b) Severe epinastic curvature of leaves in homozygote *NtmybAS1* seedlings.

(c) Two phenotypic classes resulting from overexpression of *NtmybAS1* in the second generation. Left: wild type plants, middle: heterozygote *NtmybAS1* plants, right: homozygote *NtmybAS1* plants.

(d) Comparison of plant height in wild type (left), heterozygote (middle) and homozygote (left) *NtmybAS1* plants.

(e) Reduced stem length and increased axillary growth in a heterozygote *NtmybAS1* plant. Left: Wild type stem, Right: Heterozygote *NtmybAS1* stem. Both plants are at first flower stage.

(f) Reduced leaf size and paler areas (mottling) of the *NtmybAS1* leaf. Left: Wild type leaf, Right: Heterozygote *NtmybAS1* leaf

(g) Bushy phenotype of a heterozygote *NtmybAS1* plant at flowering stage.

(h) Severe dwarfing in a homozygote *NtmybAS1* plant at flowering stage.

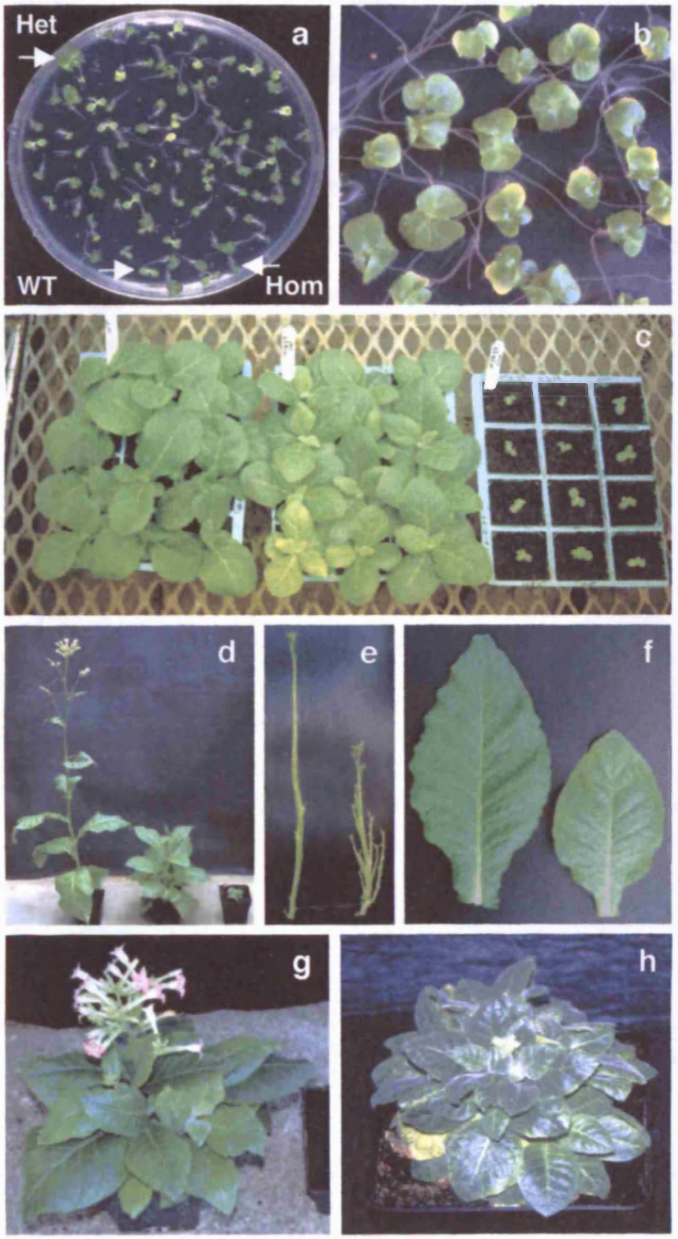
Het
a
WT
Hom
b
c
d
e
f
g
h

Figure 3. 6

Comparison of growth rate, mean number and mean length of internodes in wild type, heterozygote and homozygote *NtmybAS1* plants.

(a) Growth rate of wild type (WT), heterozygote and homozygote *NtmybAS1* plants. Results shown are the mean plant height ± SD measured for six plants at the day 33 after plating seeds in four-day intervals.

(b) Mean internode number (IN) and mean internode length (IL) of wild type, heterozygote and homozygote *NtmybAS1* plants.
Results shown are the mean internode number ± SD and mean internode length ± SD measured for six plants at first flower stage.

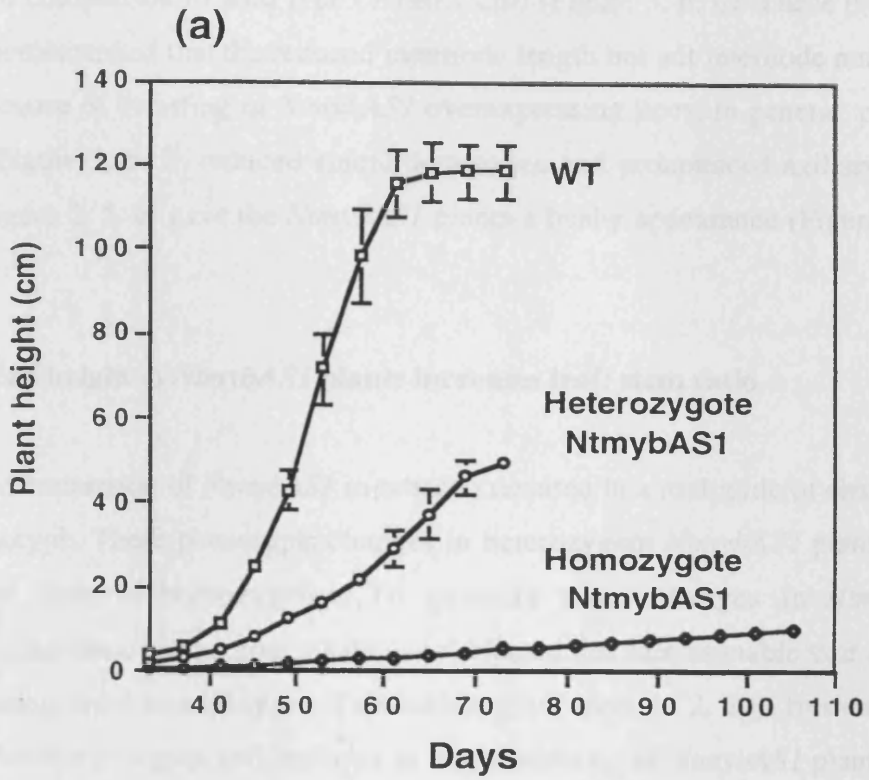
(a)
Plant height (cm)
140
120
100
80
60
40
20
0
WT
Heterozygote
NtmybAS1
Homozygote
NtmybAS1
40
50
60
70
80
90
100
110
Days

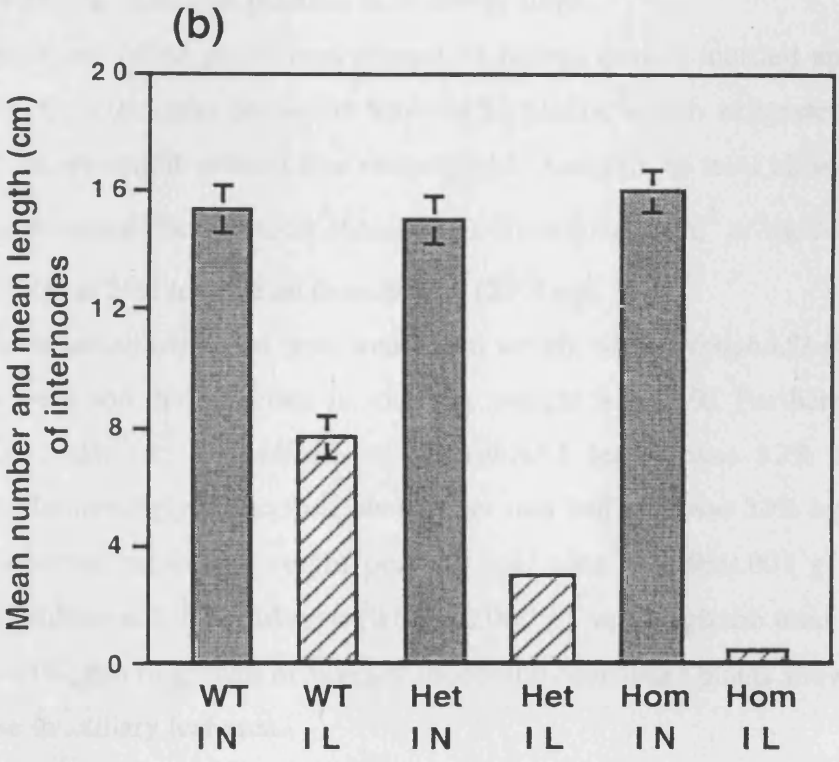
(b)
Mean number and mean length (cm)
of internodes
20
16
12
8
4
0
WT
IN
WT
IL
Het
IN
Het
IL
Hom
IN
Hom
IL

type (15±0.8). In contrast, mean internode length (IL) in heterozygote (2.95±0.2 cm) and homozygote (0.48±0.04 cm) *NtmybAS1* plants dramatically decreased by 62% and 99% in comparison to wild type (7.7±0.7 cm) (Figure 3. 6. b). These pieces of evidence demonstrated that the reduced internode length but not internode number is the major cause of dwarfing in *NtmybAS1* overexpressing lines. In general, reduced leaf size (Figure 3. 5. f), reduced apical dominance and pronounced axillary shoot growth (Figure 3. 5. e) gave the *NtmybAS1* plants a bushy appearance (Figures 3. 5. g, 3. 5. h).

3. 4 Reduced height in *NtmybAS1* plants increases leaf: stem ratio

Overexpression of *NtmybAS1* in tobacco resulted in a multitude of changes in plant phenotype. These phenotypic changes in heterozygote *NtmybAS1* plants were less severe than in homozygotes. To quantify these changes in *NtmybAS1* overexpressing lines, heterozgote plants were selected due to reasonable size and the same flowering time as wild types. Total chlorophyll (section 2. 20), fresh and dry weights of different organs and leaf area in four heterozygote *NtmybAS1* plants were compared with four wild type plants at first flower stage.

Paler areas in the green background of leaves gave a mottled appearance (Figure 3. 5. f) to the older leaves of *NtmybAS1* plants, which suggested that the *NtmybAS1* leaves might contain less chlorophyll. Analysis of total chlorophyll in these plants revealed that the total chlorophyll content in 1 cm^2 of the *NtmybAS1* leaves (22.7 μg) is 24% lower than in wild type (29.4 μg).

In comparison with wild type, total fresh weight of the *NtmybAS1* plants was reduced by 44% and the reduction in total dry weight was 53%. Furthermore, the reduction in fresh and dry weights of *NtmybAS1* leaves was 32% and 45% respectively. Interestingly, mean fresh weight per unit leaf area was 50% higher than wild type whereas mean dry weight per unit leaf area (0.009±0.001 g) was not significantly different from wild type (0.008±0.000 g). Although the total leaf area reduced by 43%, due to growth of axillary shoots the *NtmybAS1* plants showed a 35-fold increase in axillary leaf area.

As a result of the severe decrease in plant height (58%) due to a 62% decrease in mean internode length, fresh and dry weights of the *NtmybAS1* stem was reduced by 63% and 68%, which consequently increased the leaf: stem weight ratio by 75% and 65% in fresh and dry condition respectively.

3. 5 NtMybAS1 DNA binding domain alone, is not sufficient for dwarfing

Tobacco transformation with the NtmybAS1–DBD construct (section 3. 2. 2) was performed to investigate the effect of high level expression of *NtmybAS1* DNA binding domain on plant phenotype. Seventeen primary transformants overexpressing the *NtmybAS1* DNA binding domain were phenotypically normal. Although three primary transformants were slightly shorter than wild types, none of them showed the dwarf features described for the *NtmybAS1* overexpressing lines (sections 3. 3 and 3. 4). Progeny of 10 primary transformants segregated 3:1 for resistance to kanamycin. To further characterise the phenotype of these lines, fourteen kanamycin resistant progeny of each primary transformant were transferred to soil and their growth rates under normal greenhouse condition were measured every four days until flowering.

General features and growth rate of the majority of these plants were similar to wild type (Figure 3. 6) except for some of the progeny of three primary transformants, which showed a delay in growth at early stages. These plants were nearly half the size of the untransformed plants without showing a general reduction in leaf size but at later stages before flowering they grew to the same height as wild type. To determine whether the shorter phenotype of these plants results from higher levels of transgene expression in the homozygote genotype, seeds derived from these plants were germinated in the presence of kanamycin and their segregation for resistance to kanamycin was analysed. Segregation of these progenies for resistance and sensitivity to kanamycin demonstrated that the plants with a shorter phenotype were not homozygotes and this effect may be due to variation in growth of the selected individuals.

These analyses indicated that the overexpression of *NtmybAS1* DNA binding domain alone is not sufficient to cause a dwarf phenotype and therefore, the

putativeNtMybAS1 transcription activator domain is essential for its function.

3. 6 Dwarfing is gene dosage dependent

The relationship between the levels of *NtmybAS1* expression and severity of dwarfing in heterozygote and homozygote *NtmybAS1* plants was investigated by Northern blot analysis (Figure 3. 7). An RNA gel blot was prepared from 30 μg total RNA samples isolated from two wild type (WT1, WT2), two heterozygote (3 Het, 7 Het) and two homozygote (3 Hom, & 7 Hom) lines overexpressing *NtmybAS1* and four homozygote lines (9, 10, 14, 21) overexpressing *NtmybAS1-DBD*. A probe consisted of the 1.8 kb *NtmybAS1* cDNA was excised as a *BamHI-XbaI* fragment from the pRT2mybAS1 plasmid. The probe was gel purified (section 2. 4. 4), radioactively labelled with α^{32}P-dCTP (sections 2. 10. 1 and 2. 10. 2) and used for hybridisation analysis (section 2. 10. 3).

The level of expression of *NtmybAS1* in homozygote lines (3 Hom, 7 Hom) was proportionally higher than in heterozygotes (3 Het, 7 Het) (Figure 3. 7). This difference in expression of *NtmybAS1* between the homozygote (severe dwarf) and heterozygote (semi-dwarf) *NtmybAS1* plants clearly demonstrated that the severity of dwarfing is directly related to the level of expression of *NtmybAS1* and therefore, dwarfing is gene dosage dependent. The *NtmybAS1* transcript was not detectable in wild type (WT1, WT2) plants (Figure 3. 7).

Expression of *NtmybAS1* DNA binding domain in four homozygote lines (9, 10, 14, and 21) was examined (Figure 3. 7) and was higher than the expression of *NtmybAS1* in homozygote lines (3 Hom, 7 Hom). However, lack of phenotype in these lines (section 3. 5) indicated that the *NtMybAS1* DNA binding domain alone is not functional.

3. 7 Overexpression of a C-terminally truncated *NtmybAS1* does not result in a dwarf phenotype

Ectopic overexpression of *NtmybAS1-ClaI* in tobacco, which encoded a

Figure 3. 7

Northern blot analysis of *NtmybAS1* and *NtmybAS1* DNA binding domain expression

Total RNA (30 μg per lane) was prepared from mature leaves of wild type, heterozygote and homozygote lines overexpressing *NtmybAS1* and homozygote lines overexpressing *NtmybAS1* DNA binding domain. RNA gel blot was hybridised with a 1.8 kb fragment of the *NtmybAS1* cDNA (section 3. 6).

(a) Homozygote lines (3 Hom and 7 Hom) show a higher level of *NtmybAS1* expression than heterozygotes (3 Het and 7 Het). The level of *NtmybAS1-DBD* transcript in homozygote lines (9, 10, 14 and 21) is higher than the level of *NtmybAS1* transcript. No *NtmybAS1* transcript is detectable in wild type leaf (WT1 and WT2).

(b) Total RNA fractionated on a formaldehyde-agarose gel stained with ethidium bromide indicates the equivalent loading.

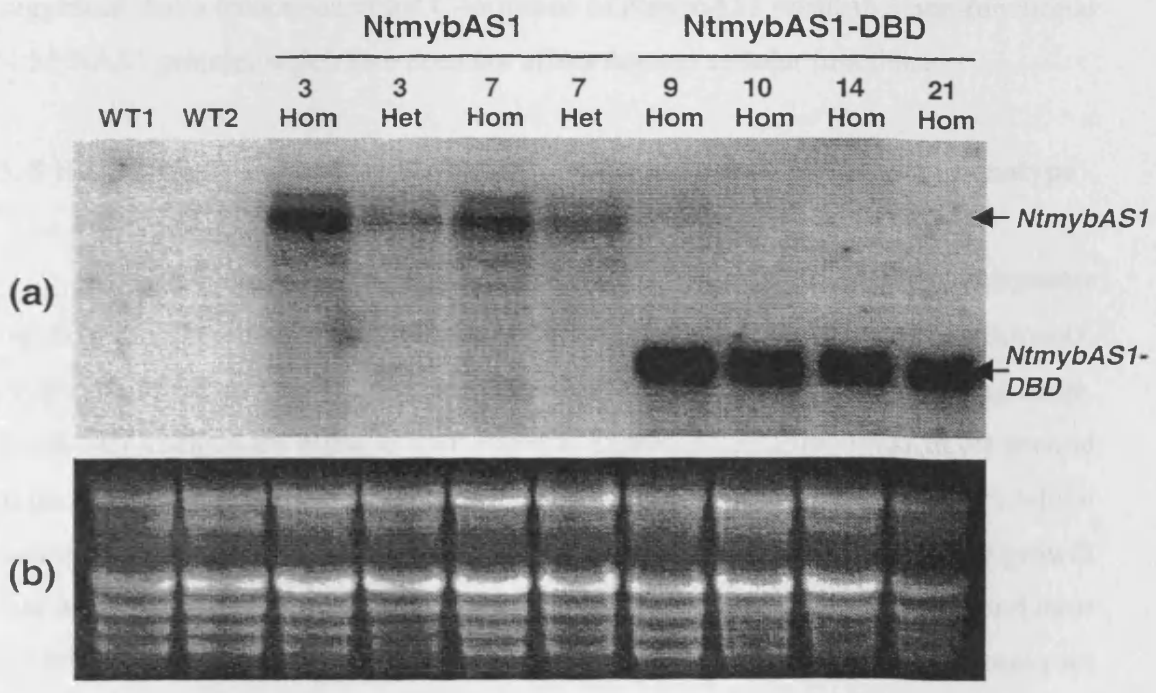
NtmybAS1
NtmybAS1-DBD
3 Hom
3 Het
7 Hom
7 Het
9 Hom
10 Hom
14 Hom
21 Hom
WT1
WT2
(a)
NtmybAS1
NtmybAS1-DBD
(b)

predicted 29.5 kDa C-terminally truncated NtMybAS1 protein (section 3. 2. 3) did not affect plant phenotype. Thirty-two primary transformants generated using the pBIN19mybAS1-ClaI construct (section 3. 2. 3) were phenotypically normal and plant height was not significantly different from wild type. Progenies of nineteen primary transformants segregated 3: 1 for resistance to kanamycin indicating the insertion of T-DNA at a single locus. None of the progenies of the primary transformants showed the dwarf features described for the *NtmybAS1* overexpressing lines. In addition the phenotype of six kanamycin resistance progenies of two primary transformants grown to maturity was not different from wild type. Results suggested that a truncation at the C-terminus of *NtmybAS1* result in a non-functional NtMybAS1 protein, which also does not affect normal cellular functions.

3. 8 Root-specific expression of *NtmybAS1* does not result in a dwarf phenotype

Expression of *NtmybAS1* driven by the –90 region of the *CaMV35S* promoter (section 3. 2. 4) did not affect the phenotype of twenty-seven primary transformants. Progenies of the primary transformants did not show a phenotype at seedling stage. To further analyse the effect of root-specific expression of *NtmybAS1* in the second generation plants, twelve progenies of twenty one primary transformants, which segregated 3:1 for resistance to kanamycin were transferred to soil and their growth rate were compared to wild types. These plants showed a normal phenotype and their growth rate was not different from wild type (Figure 3. 6. a). In addition, total root mass of 10 plants examined was similar to wild type indicating that the expression of *NtmybAS1* in roots does not result in a reduction in root mass. Therefore, root-specific expression of *NtmybAS1* is not sufficient to induce a dwarf phenotype.

3. 9 Analysis of NtMybAS1 nuclear localisation signal (NLS)

Import of the majority of proteins to the nucleus requires an NLS to be recognised by the nuclear import machinery (Raikhel, 1992; Merkle and Nagy, 1997). A short motif (119-RLKRRQR-125) in the NtMybAS1 protein containing five basic residues is similar to known monopartite NLSs. The role of this motif in

the nuclear import of the green fluorescent protein (GFP) was investigated by transient expression of GFP fusion proteins in tobacco pollen using particle bombardment (section 2. 11). Based on localisation of GFP fusion proteins in pollen, a domain in the NtMybAS1 protein that is necessary for nuclear targeting was identified.

3. 9. 1 Construction of pLAT52-sGFP plasmids

The control plasmid, pLAT52-sGFP (Figure 3. 8), used to direct expression of green fluorescent protein (GFP) in pollen consisted of the pollen-specific LAT52 promoter (Twell *et al.*, 1989b), the tobacco etch virus translational enhancer sequence (TEV-L), sGFP coding sequence (Chiu *et al.*, 1996) and the cauliflower mosaic virus 35S polyadenylation/terminator sequence (*CaMV35S3'*) in pUC19. This plasmid contains a unique *NcoI* site between the *TEV5'UTR* and sGFP, which allows the DNA fragments with compatible ends to be translationally fused to sGFP.

3. 9. 2 Construction of pLAT52-sGFPM1 fusion plasmid

The fusion plasmid pLAT52-sGFPM1 (Figure 3. 8) was constructed to determine whether the primary *NtMybAS1* sequence (nt. 182 to 556) encoding the N-terminal 125 amino acids of NtMybAS1 protein could direct sGFP to the pollen nucleus. This sequence contains the predicted monopartite nuclear localisation signal, RLKRRQR at position 119-125. Due to presence of a *NcoI* site in the *NtmybAS1* sequence (nt. 251-256) this fragment was amplified from the pRT2-NtmybAS1 plasmid (section 3. 2. 1) using two oligonucleotide primers including 5'-GGAATCATGACACCAGATGGAG GAG -3' and 5'- GGCATCATGACTCTTTG TCTTCTTTTTAGC -3' with a compatible *BsphI* site at both ends. These oligonucleotides correspond to nucleotides 176-200 (coding strand) and 538-567 (complementary strand) of *NtmybAS1* cDNA. The PCR amplified fragment (0.392 kb) was digested with *BsphI*, gel purified and cloned into the compatible *NcoI* site of pLAT52-sGFP plasmid (3. 9. 1). This cloning strategy allowed the N-terminal 126

Figure 3. 8

Construction of pLAT52sGFPM1

A *NtmybAS1* cDNA fragment (nt. 176-567) was amplified by PCR, digested with *BsphI* and the resulting fragment (181-558) encoding the N-terminal 126 amino acids of the NtMybAS1 protein was cloned into pLAT52sGFP.

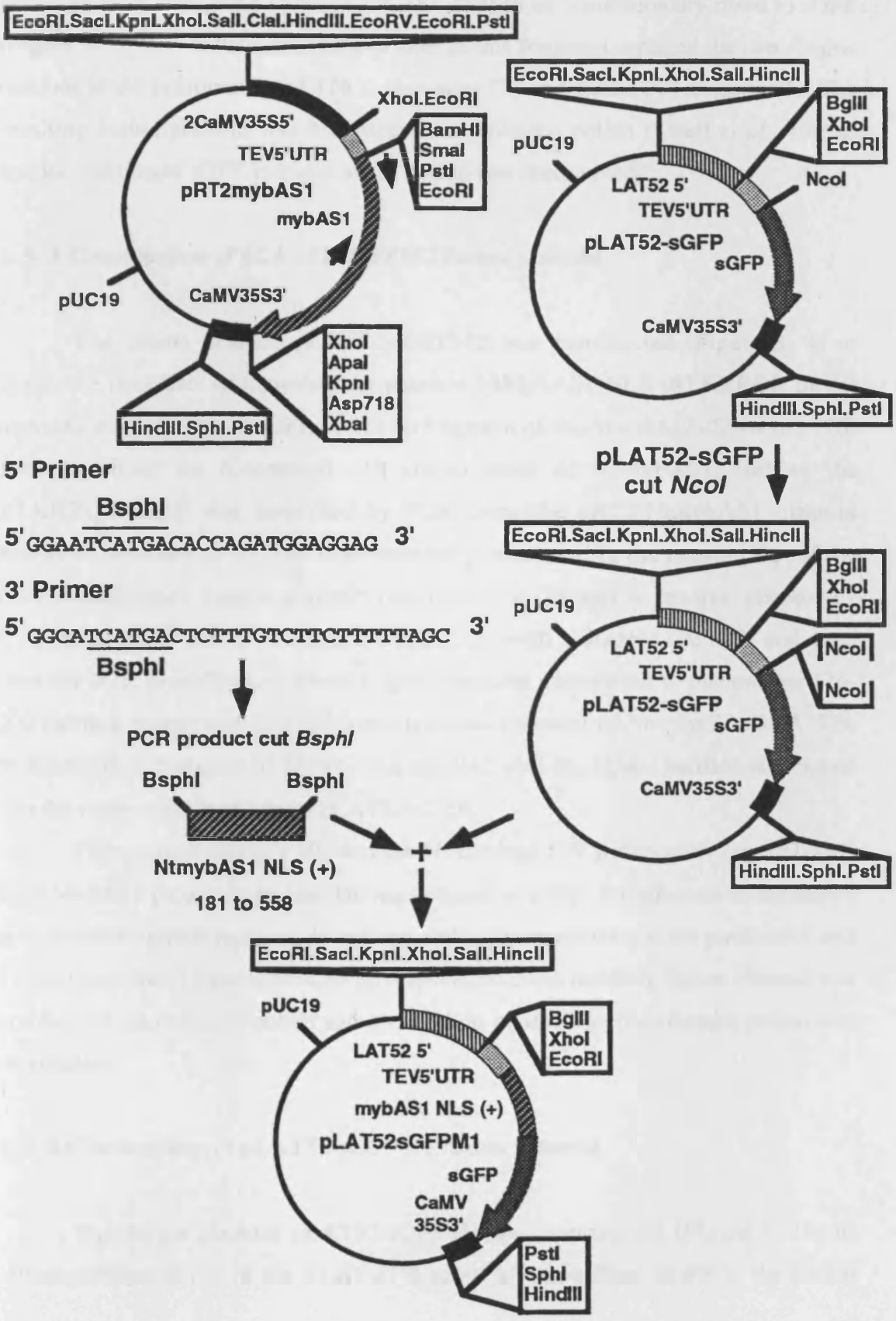
EcoRI.SacI.KpnI.XhoI.SalI.ClaI.HindIII.EcoRV.EcoRI.PstI
XhoI.EcoRI
2CaMV35S5'
TEV5'UTR
pRT2mybAS1
mybAS1
BamHI
SmaI
PstI
EcoRI
pUC19
CaMV35S3'
XhoI
ApaI
KpnI
Asp718
XbaI
HindIII.SphI.PstI
EcoRI.SacI.KpnI.XhoI.SalI.HincII
BglII
XhoI
EcoRI
pUC19
NcoI
LAT52 5'
TEV5'UTR
pLAT52-sGFP
sGFP
CaMV35S3'
HindIII.SphI.PstI
pLAT52-sGFP
cut NcoI
5' Primer
BsphI
5' GGAATCATGACACCAGATGGAGGAG 3'
3' Primer
5' GGCATCATGACTCTTTGTCTTCTTTTTAGC 3'
BsphI
PCR product cut BsphI
BsphI
BsphI
NtmybAS1 NLS (+)
181 to 558
EcoRI.SacI.KpnI.XhoI.SalI.HincII
pUC19
LAT52 5'
TEV5'UTR
mybAS1 NLS (+)
pLAT52sGFPM1
sGFP
CaMV
35S3'
BglII
XhoI
EcoRI
PstI
SphI
HindIII

amino acids of NtMybAS1 protein (nt. 181-558) to be translationally fused to sGFP (Figure 3. 8). Introduction of the *BsphI* sites in this fragment replaced the two alanine residues at the positions 2 and 126 to threonine (T) and valine (V) respectively. The resulting fusion plasmid was bombarded into tobacco pollen (Twell *et al.*, 1989a) and localisation of sGFP in transformed pollen was determined.

3. 9. 3 Construction of pLAT52-sGFPM2 fusion plasmid

The fusion plasmid pLAT52-sGFPM2 was constructed (Figure 3. 9) to determine the effect of removing the putative NtMybAS1 NLS (RLKRRQR motif) upon nuclear targeting of sGFP. A 371 bp fragment of the *NtmybAS1* cDNA (nt. 176-546) encoding the N-terminal 119 amino acids of NtMybAS1, lacking the RLKRRQR motif was amplified by PCR from the pRT2-NtmybAS1 plasmid template (section 3. 2. 1). The same forward primer used in the construction of the pLAT52-sGFPM1 fusion plasmid (section 3. 9. 2) and a reverse primer 5'-CTTTTCATGATTGTGTTCCAGTAATTC -3' with a *BspH1* site at 3' end were used for PCR amplification. These oligonucleotides correspond to nucleotides 176-200 (coding strand) and 520-546 (complementary strand) of *NtmybAS1* cDNA. The PCR amplified fragment (0.371 kb) was digested with *BsphI*, gel purified and cloned into the compatible *NcoI* site of pLAT52-sGFP.

This cloning strategy allowed the N-terminal 119 amino acids (nt. 181-537) of NtMybAS1 protein to be translationally fused to sGFP. Introduction of the *BsphI* sites in this fragment replaced the alanine and arginine residues at the positions 2 and 119 to threonine (T) and isoleucine (I) respectively. The resulting fusion plasmid was bombarded into tobacco pollen and localisation of sGFP in transformed pollen was determined.

3. 9. 4 Construction of pLAT52-sGFPM3 fusion plasmid

The fusion plasmid pLAT52-sGFPM3 was constructed (Figure 3. 10) to investigate the ability of the RLKRRQR motif alone to direct sGFP to the pollen

Figure 3. 9

Construction of pLAT52sGFPM2

A *NtmybAS1* cDNA fragment (nt. 176-546) was amplified by PCR, digested with *BsphI* and the resulting fragment (nt. 181-537) encoding the N-terminal 119 amino acids of NtMybAS1 was cloned into pLAT52sGFP.

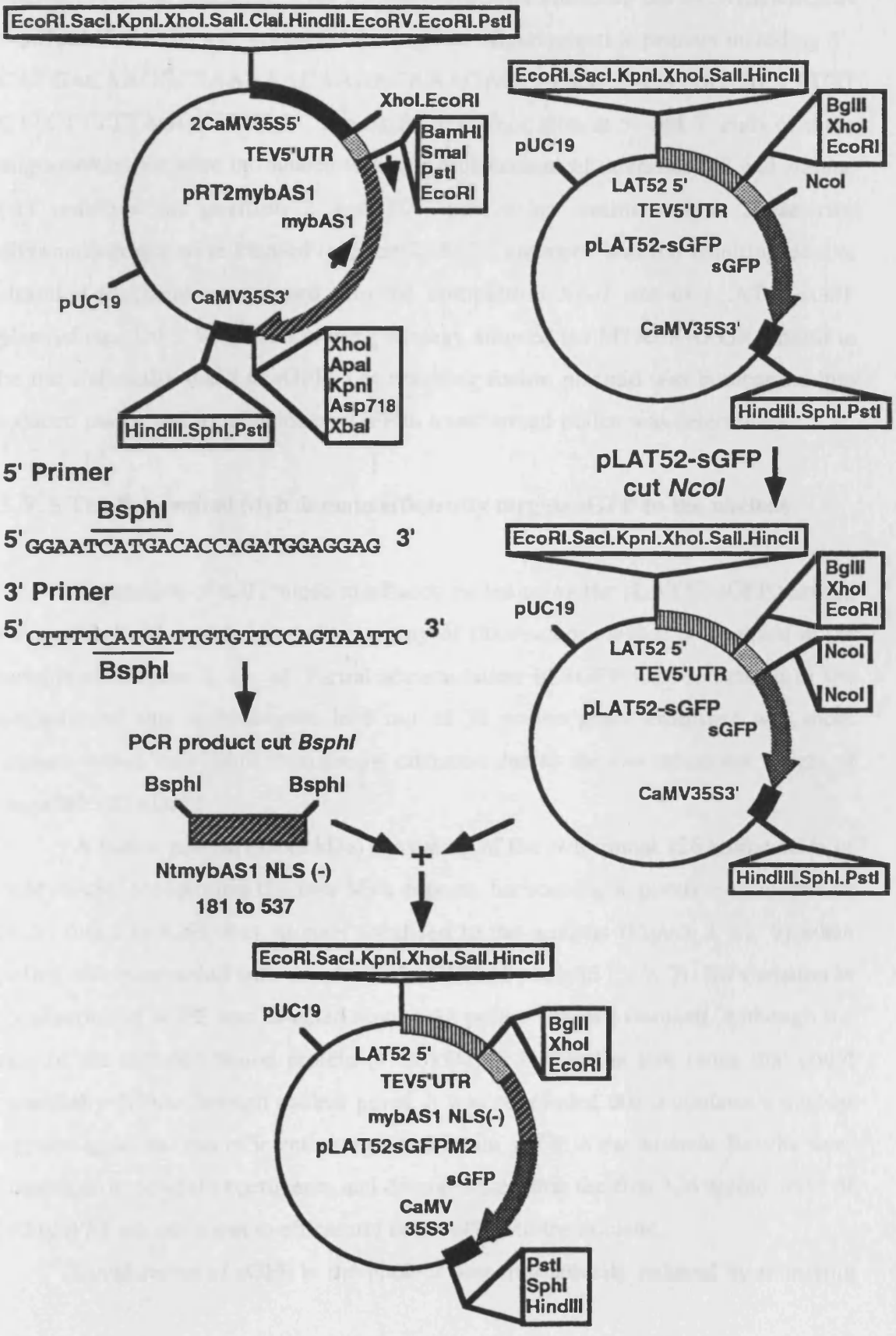
EcoRI.SacI.KpnI.XhoI.SalI.ClaI.HindIII.EcoRV.EcoRI.PstI
2CaMV35S5'
TEV5'UTR
pRT2mybAS1
mybAS1
XhoI.EcoRI
BamHI
SmaI
PstI
EcoRI
pUC19
CaMV35S3'
XhoI
ApaI
KpnI
Asp718
XbaI
HindIII.SphI.PstI
5' Primer
BsphI
5' GGAATCATGACACCAGATGGAGGAG 3'
3' Primer
5' CTTTTCATGATTGTGTTCCAGTAATTC 3'
BsphI
PCR product cut BsphI
BsphI
BsphI
NtmybAS1 NLS (-)
181 to 537
EcoRI.SacI.KpnI.XhoI.SalI.HincII
BglII
XhoI
EcoRI
pUC19
LAT52 5'
TEV5'UTR
mybAS1 NLS(-)
pLAT52sGFPM2
sGFP
CaMV
35S3'
PstI
SphI
HindIII
EcoRI.SacI.KpnI.XhoI.SalI.HincII
BglII
XhoI
EcoRI
NcoI
pUC19
LAT52 5'
TEV5'UTR
pLAT52-sGFP
sGFP
CaMV35S3'
HindIII.SphI.PstI
pLAT52-sGFP
cut NcoI
EcoRI.SacI.KpnI.XhoI.SalI.HincII
BglII
XhoI
EcoRI
pUC19
LAT52 5'
TEV5'UTR
NcoI
NcoI
pLAT52-sGFP
sGFP
CaMV35S3'
HindIII.SphI.PstI

nucleus. A 30 bp fragment of the *NtmybAS1* cDNA encoding the MTRLKRRQRA motif (nt. 529-558) was synthesised using two oligonucleotide primers including 5'-CATGACAAGGCTAAAAAGAAGACAAAGAGC-3'and 5'-CATGGCTCTTTGT CTTCTTTTTAGCCTTGT-3'. The *BsphI* and *NcoI* sites at 5' and 3' ends of these oligonucleotides were introduced to avoid replacement of threonine (T) and alanine (A) residues (at position 2 and 10) with other amino acids. These two oligonucleotides were kinased (section 2. 5. 2), annealed and the resulting double stranded fragment was cloned into the compatible *NcoI* site of pLAT52-sGFP plasmid (section 3. 9. 1). This cloning strategy allowed the MTRLKRRQRA motif to be translationally fused to sGFP. The resulting fusion plasmid was bombarded into tobacco pollen and localisation of sGFP in transformed pollen was determined.

3. 9. 5 The N-terminal Myb domain efficiently targets sGFP to the nucleus

Expression of sGFP alone in tobacco pollen using the pLAT52-sGFP plasmid (section 3. 9. 1) revealed that the majority of fluorescence signal is localised in the cytoplasm (Figure 3. 11. a). Partial accumulation of sGFP was detectable in the nucleus and this accumulation in 8 out of 38 pollen grain examined was more intense, which may result from simple diffusion due to the low molecular weight of the sGFP (27 kDa).

A fusion protein (41.43 kDa) consisting of the N-terminal 126 amino acids of NtMybAS1 (containing the two Myb repeats harbouring a putative monopartite NLS) fused to sGFP was strongly localised to the nucleus (Figure 3. 11. b) when pollen was bombarded with the pLAT52-sGFPM1 plasmid (3. 9. 2). No variation in localisation of sGFP was detected among 32 pollen grains examined. Although the size of the encoded fusion protein (41.4 kDa) is within the size range that could potentially diffuse through nuclear pores, it was concluded that it contains a nuclear import signal that can efficiently target and retain sGFP in the nucleus. Results were consistent in several experiments and demonstrated that the first 126 amino acids of NtMybPS1 are sufficient to efficiently target sGFP to the nucleus.

Localisation of sGFP in the nucleus was dramatically reduced by removing

Figure 3. 10

Construction of the pLAT52sGFPM3

Two oligonucleotide primers with a *BsphI* and a *NcoI* site in the 5'and 3' ends were kinased and annealed. The resulting double stranded oligonucleotide encoding the MTRLKRRQRA motif was cloned into pLAT52-sGFP.

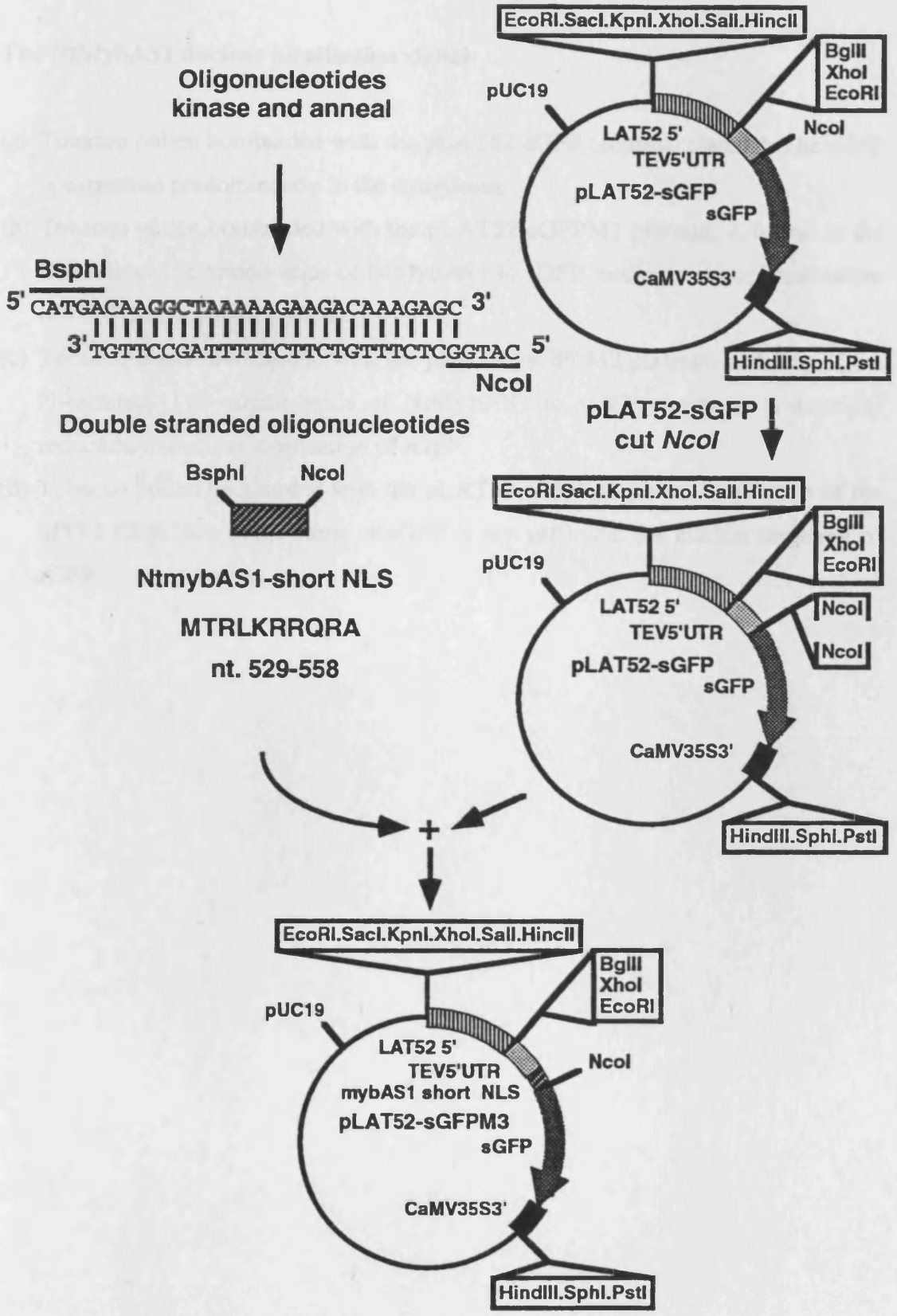
Oligonucleotides
kinase and anneal
BspHI
5' CATGACAAGGCTAAAAAGAAGACAAAGAGC 3'
3' TGTTCCGATTTTTCTTCTGTTTCTCGGTAC 5'
NcoI
Double stranded oligonucleotides
BspHI
NcoI
NtmybAS1-short NLS
MTRLKRRQRA
nt. 529-558
EcoRI.SacI.KpnI.XhoI.SalI.HincII
BglII
XhoI
EcoRI
pUC19
NcoI
LAT52 5'
TEV5'UTR
pLAT52-sGFP
sGFP
CaMV35S3'
HindIII.SphI.PstI
pLAT52-sGFP
cut NcoI
NcoI
+
mybAS1 short NLS
pLAT52-sGFPM3

Figure 3. 11

The NtMybAS1 nuclear localisation signal

(a) Tobacco pollen bombarded with the pLAT52-sGFP (control) plasmid. The sGFP is expressed predominantly in the cytoplasm.

(b) Tobacco pollen bombarded with the pLAT52-sGFPM1 plasmid. A fusion of the N-terminal 126 amino acids of NtMybAS1 to sGFP results in strong localisation of sGFP in the pollen nucleus.

(c) Tobacco pollen bombarded with the pLAT52-sGFPM2 plasmid. A fusion of the N-terminal 119 amino acids of NtMybAS1 to sGFP results in a dramatic reduction in nuclear localisation of sGFP.

(d) Tobacco pollen bombarded with the pLAT52-sGFPM3 plasmid. A fusion of the MTRLKRRQRA motif alone to sGFP is not sufficient for nuclear targeting of sGFP.

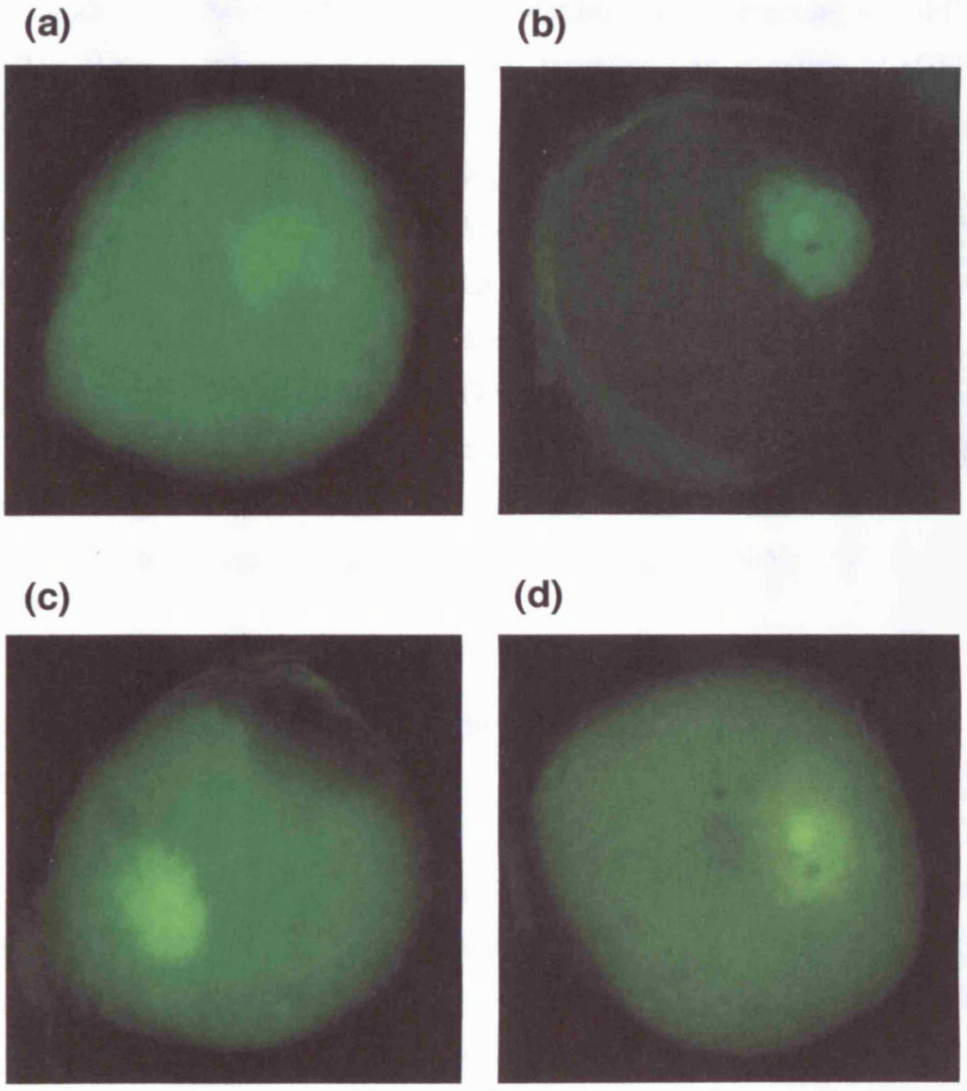
(a)
(b)
(c)
(d)

the RLKRRQR motif from the N-terminal Myb domain. A fusion protein (40.45 kDa) consisting of the N-terminal 119 amino acids of NtMybAS1 fused to sGFP was unable to efficiently localise sGFP in the nucleus (Figure 3. 11 .c) when pollen was bombarded with the pLAT52-sGFPM2 plasmid (section 3. 9. 3). Reduced localisation of sGFP in 44 pollen grains examined demonstrated that the first 119 amino acids of the NtMybAS1 is not sufficient for nuclear targeting of sGFP and the RLKRRQR motif is essential for efficient targeting and retention of sGFP in the nucleus.

Bombardment of pollen with the pLAT52-sGFPM3 plasmid (section 3. 9. 4) revealed that the RLKRRQR motif alone is not sufficient to direct sGFP to the nucleus. A fusion of the MTRLKRRQRA motif to sGFP (28.29 kDa) was not able to fully direct sGFP to the nucleus (Figure 3. 11. d). However, in 57 pollen grains examined a subnuclear localisation of sGFP was detected (Figure 3. 11. d).

These analyses demonstrated that the NLS of NtMybAS1 protein is not monopartite and therefore, efficient targeting of the NtMybAS1 to the nucleus (Figure 3. 11. b) also requires the upstream elements in the NtMybPS1 DNA binding domain.

3. 10 Expression of NtmybAS1 in anthers coincides with the induction of gPAL1 mRNA

Demonstration of localisation of NtmybAS1 transcript in tapetum, binding of the NtMybAS1 protein to the PAL promoter and activation of GUS reporter gene in tobacco protoplasts (Yang *et al.*, 2000) led to the hypothesis that the NtMybAS1 protein act as a regulator of PAL expression in tapetum. To test this hypothesis, expression of *NtmybAS1* and *gPAL1* were analysed in different stages of anther development and in mature pollen.

An RNA gel blot was prepared from 40 µg total RNA samples isolated from anthers during five stages of development when flower buds were 10-12, 12-16, 17-30, 30-40 and 40-50 mm, mature pollen and wild type leaf as a control (Figure 3. 12). To prepare a probe for detecting *gPAL1* expression, reverse transcription and PCR amplification (section 2. 6. 4) of *gPAL1* mRNA was performed using two

oligonucleotide primers including 5'–GCTGAATCCTTAAGAGGGAGTCATTTG G-3' and 5' –CAAGCCATTGTGGAGATGTTCGGAG- 3' to amplify a 0.994 kb (nt. 85-1054) fragment of *gPAL1* cDNA. These oligonucleotides corresponded to nucleotides 85-112 (coding strand) and 1054-1078 (complementary strand) of the *gPAL1* cDNA (Fukasawa-Akada, 1996). The 0.994 kb amplified fragment was gel purified (section 2. 4. 4), radioactively labelled with α ^{32}P-dCTP (sections 2. 10. 1 and 2. 10. 2) and used as a probe to hybridise the RNA gel blot described above. To analyse the expression of *NtmybAS1* in this blot, the same *NtmybAS1* probe described in section 3. 6 was used to hybridise the blot.

These analyses revealed that the *gPAL1* mRNA is induced at early stages of anther development (Figure 3. 12. a) when the flower buds are 10-12 and 12-16 mm. After this stage a decrease in *gPAL1* expression was detectable until the last stages of anther development (flower buds 40-50 mm). No *gPAL1* transcript was detectable in mature pollen.

Induction of *NtmybAS1* expression at early stages of anther development when flower buds were 10-12 and 12-16 mm (Figure 3. 12. b) coincided with the activation of *gPAL1* expression. A rapid decrease in *NtmybAS1* transcript was detectable in anthers when flower buds were 17-30 mm. After this stage an increase in *NtmybAS1* expression (flower buds 30-40 and 40-50) was detectable reaching the highest levels in mature pollen.

Establishment of a relationship between the expression of *NtmybAS1* and induction of *gPAL1* expression in anthers strongly suggested that the NtMybAS1 protein acts as an activator of *gPAL1* expression in tobacco anthers.

3. 11 *gPAL1* mRNA is induced in *NtmybAS1* overexpressing lines

Evidence of regulatory function of NtMybAS1 as an activator of *gPAL1* expression in tobacco anthers (section 3. 10) suggested that the high level expression of *NtmybAS1* would result in a similar induction of *gPAL1* mRNA in *NtmybAS1* overexpressing lines. Therefore, the expression of *gPAL1* in *NtmybAS1* overexpressing lines (3, 7) was determined by Northern blot analysis (Figure 3. 13).

Figure 3. 12

Northern blot analysis of *gPAL1* and *NtmybAS1* expression in anther and mature pollen

Total RNA (40 μg per lane) was prepared from the mature leaves of wild type, anthers at five developmental stages when flower buds were 10-12, 12-16, 17-30, 30-40 and 40-50 mm long and mature pollen. The RNA gel blot was hybridised with a 0.994 kb fragment of the *gPAL1* cDNA (section 3. 10). The blot was stripped and rehybridised with a 1.8 kb fragment of *NtmybAS1* cDNA (section 3. 6).

(a) The *gPAL1* transcript is induced at early stages of anther development (flower buds 10-12 and 12-16 mm) and is not detectable in mature pollen.

(b) Induction of *NtmybAS1* transcript at early stages of anther development (flower buds 10-12 and 12-16 mm) correlates with the induction of *gPAL1* mRNA and shows a maximum level in mature pollen.

(c) Total RNA fractionated on a formaldehyde-agarose gel stained with ethidium indicates the equivalent loading.

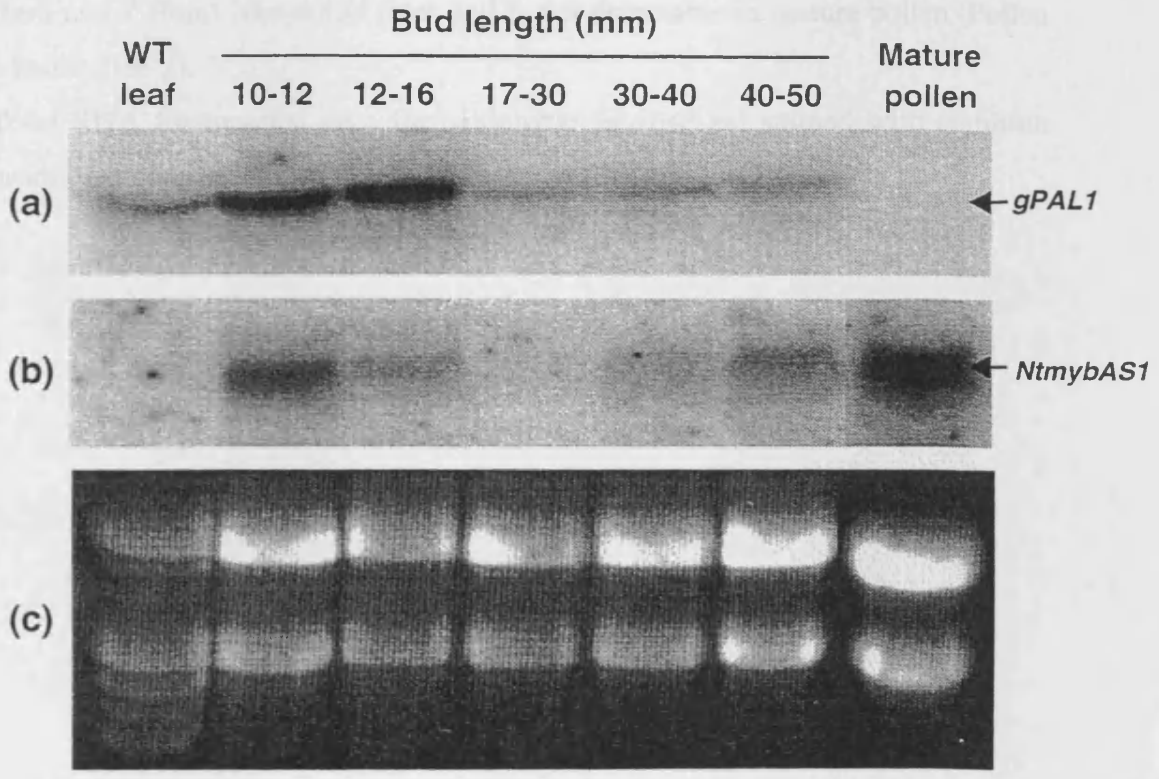
Bud length (mm)
WT leaf
10-12
12-16
17-30
30-40
40-50
Mature pollen
(a)
gPAL1
(b)
NtmybAS1
(c)

Figure 3. 13

Northern blot analysis of *gPAL1* expression in *NtmybAS1* plants

Total RNA (40 μg per lane) was prepared from mature pollen, mature leaves of wild type, heterozygote and homozygote *NtmybAS1* lines. The RNA gel blot was hybridised with a 0.99 kb fragment of the *gPAL1* cDNA (section 3. 10).

(a) The *gPAL1* mRNA is clearly induced above the wild type level in homozygote (3 Hom and 7 Hom) *NtmybAS1* lines and is not detectable in mature pollen (Pollen 1 and Pollen 2).

(b) Total RNA fractionated on a formaldehyde-agarose gel stained with ethidium bromide indicates the equivalent loading.

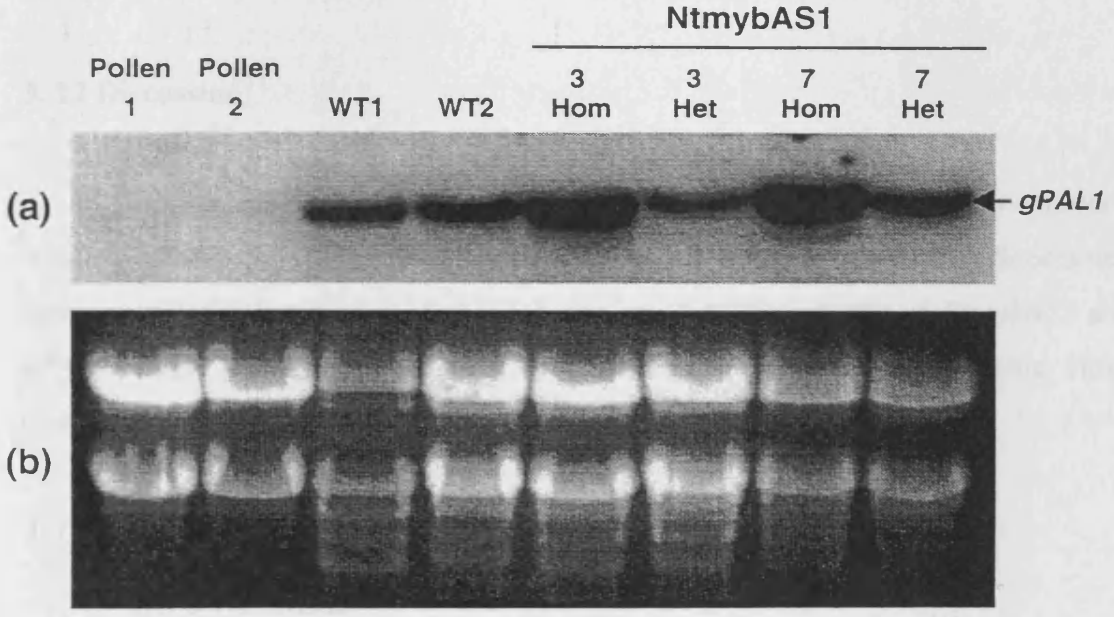
NtmybAS1
Pollen 1
Pollen 2
WT1
WT2
3 Hom
3 Het
7 Hom
7 Het
(a)
gPAL1
(b)

An RNA gel blot was prepared from 40 µg total RNA samples isolated from mature leaves of wild type (WT1 and WT2), heterozygote (3 Het and 7 Het) and homozygote (3 Hom and 7 Hom) *NtmybAS1* lines and from two pollen samples (Pollen1 and Pollen2) as controls. To detect *gPAL1* expression, the blot was hybridised with the same *gPAL1* probe described in section 3. 10.

This analysis revealed that the *gPAL1* transcript is induced in two homozygote *NtmybAS1* lines (Figure 3. 13). However, the level of *gPAL1* expression in two heterozygote lines was not clearly higher than in wild type. The *gPAL1* transcript was not detectable in mature pollen. Induction of *gPAL1* mRNA in homozygote *NtmybAS1* plants provided further evidence supporting the regulatory function of NtMybAS1 protein as an activator of *gPAL1* expression.

3. 12 Discussion

To gain insight into the function of *NtmybAS1*, an overexpression approach was adopted. Cellular localisation of NtMybAS1 protein in pollen was determined through transient expression of sGFP fusion proteins. Expression of *NtmybAS1* and *gPAL1* were analysed during anther development and in transgenic lines overexpressing *NtmybAS1*.

3. 12. 1 A full length *NtmybAS1* is required for dwarfing

Ectopic overexpression of *NtmybAS1* in tobacco resulted in dramatic alterations in plant architecture. A short stature, reduced leaf area, reduced apical dominance, pronounced axillary shoot growth and a bushy appearance were the most outstanding features of the *NtmybAS1* phenotype in the second generation (section 3. 3, Figure 3. 5).

Characterisation of two phenotypic classes, a semidwarf and a severe dwarf, in four lines (3, 7, 29 and 30) overexpressing *NtmybAS1* (section 3. 3, Figure 3. 5) and further establishment of a direct relationship between the level of *NtmybAS1* transcript and the severity of dwarfing (section 3. 6, Figure 3. 7) clearly demonstrated that dwarfing is gene dosage dependent.

A similar correlation between the levels of transgene expression and the severity of a dwarf phenotype has been reported for the *myb308* gene of *Antirrhinum* (Tamagnone *et al.*, 1998). Despite some similarities in dwarf features of the tobacco plants overexpressing the *NtmybAS1* and *myb308*, lack of early senescence and white dead tissues in leaves, which are characteristic of the myb308 phenotype indicated that the *NtmybAS1* is not involved in repression of the phenolic acids and lignin biosynthesis. Also overexpression of *myb308* had no effect on axillary shoot growth whereas, *NtmybAS1* overexpressing lines show increased axillary growth (Figure 3. 5).

Overexpression of the *NtmybAS1* DNA binding domain (section 3. 5, Figure 3. 2) and a C-terminally truncated version of *NtmybAS1* (*NtmybAS1-ClaI*) did not affect plant phenotype (section 3. 7, Figure 3. 3). Although expression of *NtmybAS1-DBD* in four homozygote lines (Figure 3. 7) was confirmed by Northern blot analysis, lack of phenotype in *NtmybAS1-DBD* and in *NtmybAS1-ClaI* overexpressing lines indicated that the C-terminus of *NtmybAS1* is essential for its function and this was consistent with the result reported for the overexpression of a C-terminally truncated version of the *MIXTA* gene of *Antirrhinum* (Glover *et al.*, 1998). These data further support the role of NtMybAS1 as a transcription factor whose function is abolished upon partial or complete loss of the transcription activation domain at the C-terminus.

Root-specific expression of *NtmybAS1* using –90 to +1 region of the *CaMV35S* promoter did not affect the phenotype of 27 primary transformants and of the progeny of 21 lines examined in the second generation (section 3. 8). Results derived from these analyses suggested that the level of expression of *NtmybAS1* by the *-90CaMV35S* promoter might be lower than the levels required causing a dwarf phenotype. Alternatively, expression of *NtmybAS1* even at high levels in specific tissues such as roots may be insufficient for dwarfing.

3. 12. 2 The N-terminal Myb domain contains an NLS

A NLS mediates import of the majority of proteins into the nucleus. Three classes of NLS in plants are similar to those found in yeast and animal systems

(Raikhel, 1992; Merkle and Nagy, 1997). The role of NLSs in the nuclear import of Myb proteins has been studied in B-Myb. Two separate NLSs, a monopartite (NLS1) in the central region and a bipartite (NLS2) in the C-terminal basic region of B-Myb protein have been shown to be necessary for nuclear targeting of B-Myb (Takemoto *et al.*, 1994).

The predicted NLS (119-RLKRRQR-125) of the NtMybAS1 protein resembled the known monopartite NLSs consisting of a short motif rich in basic amino acids. The N-terminal 126 amino acids of NtMybAS1 fused to sGFP strongly localised the sGFP to the nucleus (Figure 3. 11. b) whereas sGFP alone remained predominantly in the cytoplasm (Figure 3. 11. a). The fact that the removing of RLKRRQR motif from the N-terminal Myb domain severely reduced the nuclear import of sGFP (Figure 3. 11. c) demonstrated that this domain is necessary for nuclear import of NtMybAS1 protein. However, this domain alone was not sufficient to fully direct sGFP to the nucleus (Figure 3. 11. d). Analysis of surface probability of NtMybAS1 protein using the MacVector Sequence Analysis Software (Oxford Molecular Group PLC) predicted the NtMybAS1 domains with the higher probability of being exposed at the surface of the protein. These domains are shown above the axis in Figure 3. 14. The arginine at position 122 (within the 119-RLK**R**RQR-125 motif) was predicted to have the highest surface probability along the length of NtMybAS1 protein (Figure 3. 14. b). This implies that the six amino acids surrounding this arginine have the highest probability of being exposed at the protein surface and therefore, being recognised by the nuclear import machinery. This computer-assisted prediction further supported the conclusion that the RLKRRQR motif acts as an NLS in the NtMybAS1 protein.

Results derived from these analyses demonstrated that the N-terminal 126 amino acids of NtMybAS1 are sufficient for nuclear targeting of sGFP and suggest that the NtMybAS1 NLS lie within the DNA binding domain. The nuclear targeting of NtMybAS1 may depend on the co-operative function of the predicted NLS with an upstream element in the DNA binding domain. Co-operative function of the bipartite and multiple NLSs to direct a fusion protein into the nucleus have also been reported in potyviral NIa protein (Carrington *et al.*, 1991) and B-Myb (Takemoto *et al.*, 1994).

Figure 3. 14

Analysis of surface probability of the NtMybAS1 protein

The surface probability value of each amino acid that is calculated by the MacVector sequence analysis software (Oxford Molecular Group PLC) does not exceed 1.0. Based on this calculation the surface probability values of 1.0 and 0.0 never occur. A surface probability value of 1.0 for any residue indicates that a hexapeptides centred about this residue is absolutely exposed at the surface of the protein whereas a surface probability value of 0.0 for any residue indicates that the hexapeptide is buried inside the protein.

(a) The regions of NtMybAS1 protein, which have the higher probability to lie on the protein surface, are above the axis.

(b) Surface probability of amino acids 100 to 150 in the NtMybAS1 protein. The arginine (R) residue at position 122 within the predicted RLKRRQR motif (boxed) shows the highest surface probability along the length of the NtMybAS1 protein.

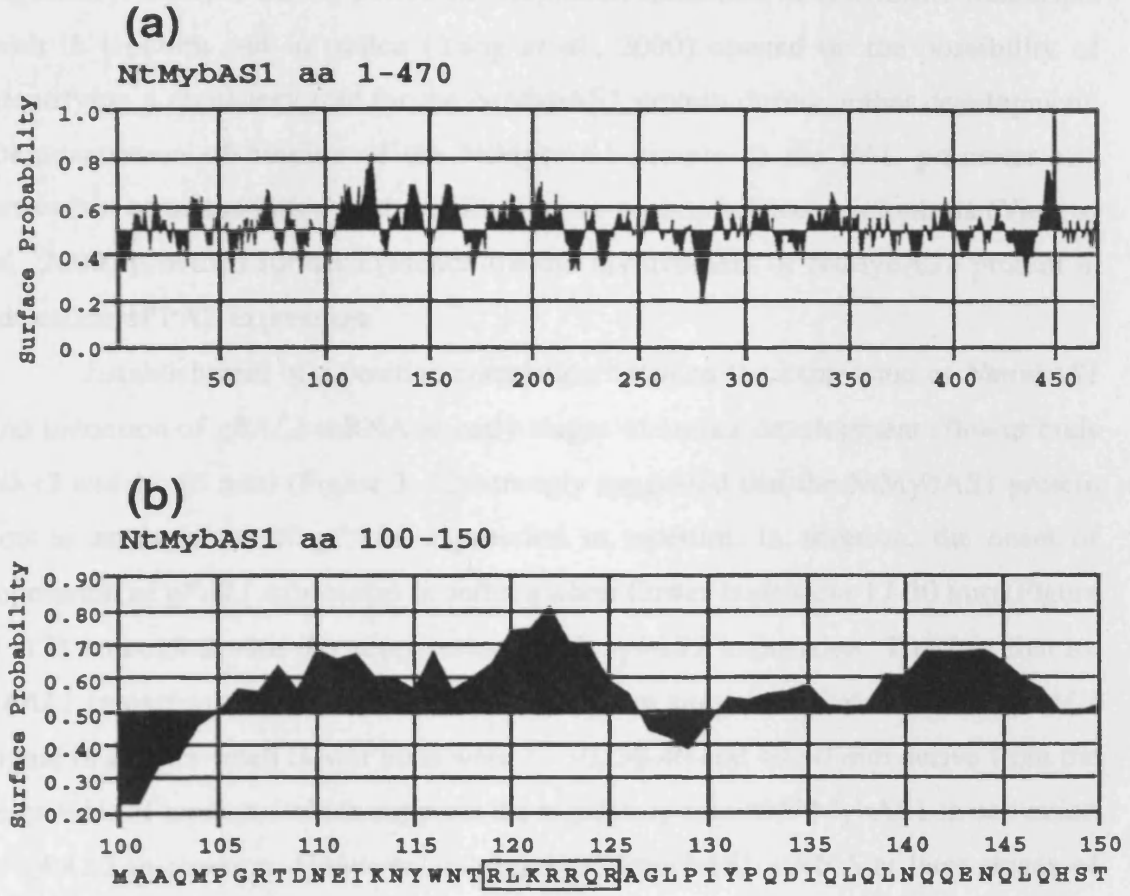
(a)
NtMybAS1 aa 1-470
Surface Probability
1.0
0.8
0.6
0.4
0.2
0.0
50
100
150
200
250
300
350
400
450
(b)
NtMybAS1 aa 100-150
Surface Probability
0.90
0.80
0.70
0.60
0.50
0.40
0.30
0.20
100
105
110
115
120
125
130
135
140
145
150
MAAQMPGRTDNEIKNYWNTRLKRRQRAGLPIYPQDIQLQLNQQENQLQHST

3. 12. 3 The NtMybAS1 protein is a regulator of *gPAL1* expression in tobacco anthers

Tissue specificity of expression of *NtmybAS1* in mature and germinating pollen as described by Sweetman (1996) suggested that the NtMybAS1 protein has a regulatory function during pollen development. Detection of *NtmybAS1* transcripts both in tapetum and in pollen (Yang *et al.*, 2000) opened up the possibility of identifying a regulatory role for the NtMybAS1 protein during anther development. Demonstration of binding of the NtMybAS1 protein to the PAL promoter and activation of transcription of the GUS reporter gene in tobacco protoplasts (Yang *et al.*, 2000) provided further evidence for the involvement of NtMybAS1 protein in activation of PAL expression.

Establishment of a positive correlation between the expression of *NtmybAS1* and induction of *gPAL1* mRNA at early stages of anther development (flower buds 10-12 and 12-16 mm) (Figure 3. 12) strongly suggested that the NtMybAS1 protein acts as an activator of *gPAL1* expression in tapetum. In addition, the onset of repression of *gPAL1* expression in anthers when flower buds were 17-30 mm (Figure 3. 12) coincided with the suppression of *NtmybAS1* expression. The fact that no *gPAL1* transcript was detectable in mature pollen suggested that the weak *gPAL1* signal in anthers when flower buds were 17-30, 30-40 and 40-50 mm derive from the remainder of tapetum, which supports the regulatory role of NtMybAS1 in activation of *gPAL1* in tapetum. However, induction of *NtmybAS1* mRNA at later stages of anther development (flower buds 30-40 and 40-50 mm) reaching to a maximum level in mature pollen suggested that the *NtmybAS1* might also perform other regulatory function in mature pollen.

A model is presented in Figure 3. 15 to illustrate the regulatory role of NtMybAS1 in activation of *gPAL1* expression in anther and possible mechanisms of repression of *gPAL1* expression in mature pollen. In this model induction of *gPAL1* mRNA in anthers is mediated by direct (Figure 3. 15. a) or indirect (via a cofactor) binding (Figure 3. 15. b) of NtMybAS1 protein to the Myb binding sequences (MBSs) in the *gPAL1* promoter. Demonstration of binding of the NtmybAS1 protein to both the MBSI and MBSII motifs and with higher affinity to MBSI (Yang *et al.*,

2000) supports this hypothesis. In addition, activation of gene expression through co-operation with other transcription factors has been shown for Myb proteins. Activation of transcription of HIS4 in yeast by BAS1 requires interaction with a homeodomain protein, BAS2 (Tice-Baldwin *et al.*, 1989). Furthermore, the chicken c-Myb and v-Myb proteins activate *mim1* expression by interaction with bZIP transcription factors like C/EBP (Burk *et al.*, 1993).

In mature pollen suppression of *gPAL1* expression may be due to presence of a repressor which can bind either to *gPAL1* promoter or to NtMybAS1 protein and block transcription from *gPAL1* promoter (Figure 3. 15. c). The absence of a cofactor in mature pollen, which is required for the NtMybAS1 to function, may suppress *gPAL1* transcription (Figure 3. 15. d). Post-translational modifications such as phosphorylation may abolish binding of NtMybAS1 to *gPAL1* promoter (Figure 3. 15. e). Protein modifications such as phosphorylation and acetylation have been reported for Myb proteins (Robinson *et al.*, 1996; Vorbrueggen *et al.*, 1996; Lane *et al.*, 1997; Sala *et al.*, 1997; Ziebold *et al.*, 1997; Saville and Watson, 1998; Sugano *et al.*, 1998; Johnson *et al.*, 1999; Bartsch *et al.*, 1999; Tomita *et al.*, 2000). DNA modifications such as methylation (Robertson and Jones, 2000) in *gPAL1* promoter may also inhibit binding of NtMybAS1 protein to the *gPAL1* promoter (Figure 3. 15. f) leading to transcriptional repression of *gPAL1*. Suppression of gene expression by methylation of metallothionein gene promoter has been shown in rat (Ghoshal *et al.*, 2000). In plants DNA methylation within the 0.2 kb promoter region of the *Spm* transposons result in an inactive transposon (Fedoroff, 1999). High level of methylation prevents transcription of *Spm* transposons (Banks *et al.*, 1988; Fedoroff, 1999).

3. 12. 4 A dwarf phenotype results from altered *gPAL1* expression

Demonstration of expression of *NtmybAS1* and induction of *gPAL1* mRNA at early stages of anther development (Figure 3. 12) strongly suggest that the *gPAL1* is a native target of NtMybAS1 protein in tobacco anther. This conclusion is further supported by the demonstration of induction of *gPAL1* mRNA in *NtmybAS1* plants

Figure 3. 15

Schematic representation of the mechanisms of induction and repression of *gPAL1* in anther and mature pollen

In anther the NtMybAS1 protein binds directly (a) or via a cofactor (b) to MBSI and MBSII motifs in *gPAL1* promoter and activates *gPAL1* transcription.

In mature pollen the presence of a repressor (c), lack of a cofactor (d), post translational modification of the NtMybAS1 protein such as phosphorylation (e) and DNA modifications such as methylation in *gPAL1* promoter (f) may prevent binding of the NtMybAS1 protein to *gPAL1* promoter and therefore block induction of *gPAL1* expression.

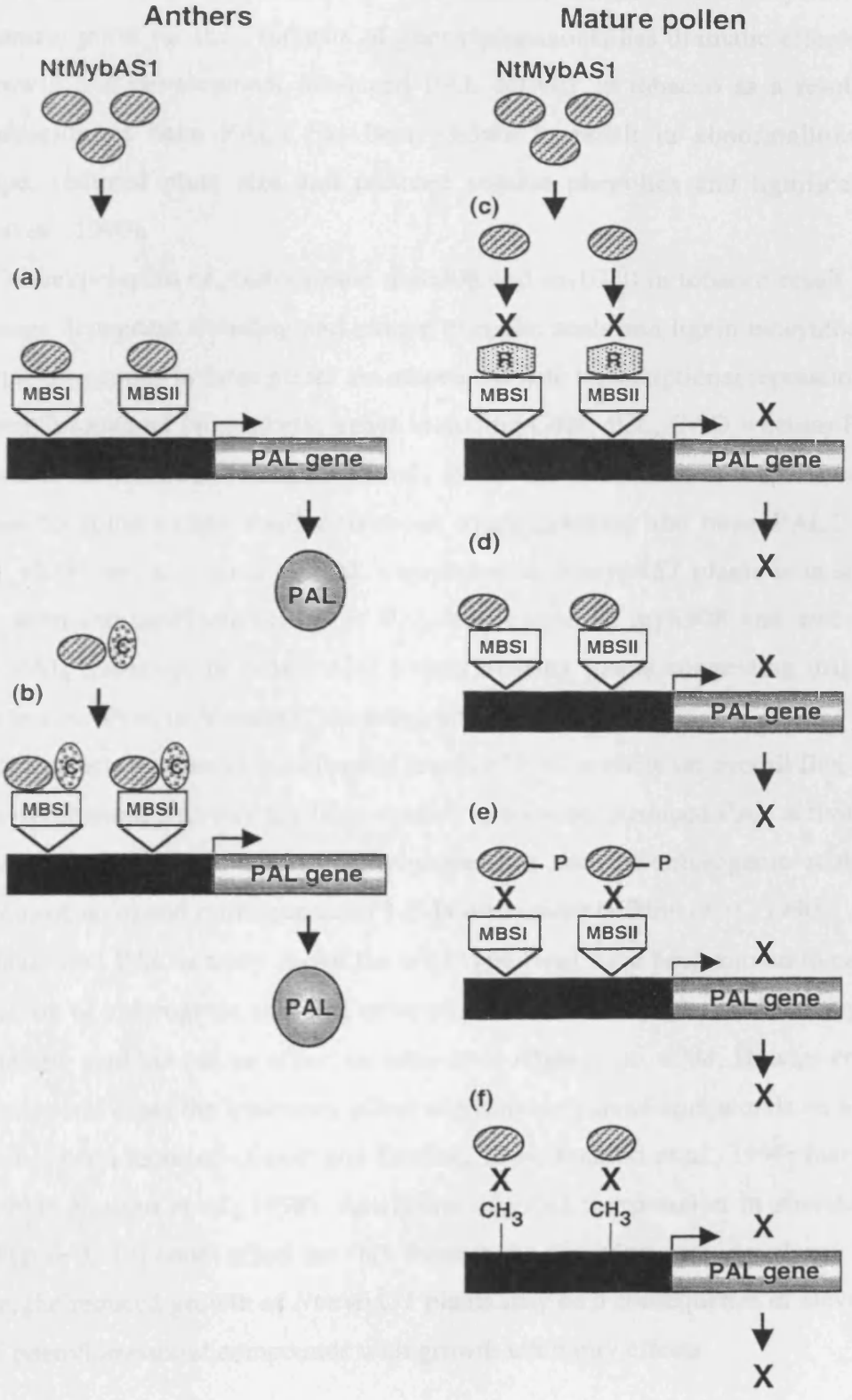
Anthers
Mature pollen
NtMybAS1
NtMybAS1
(a)
(b)
(c)
(d)
(e)
(f)
MBSI
MBSII
PAL gene
PAL
R
C
P
X
CH_3

(Figure 3. 13). The fact that an increase in PAL transcription generally results in an increase in PAL enzyme activity (Edwards *et al.*, 1985; Fritzemeier *et al.*, 1987; Lawton and Lamb, 1987; Orr *et al.*, 1993) suggests that *NtmybAS1* overexpressing lines have higher levels of PAL activity. Disruption of normal PAL activity that is a major control point for the synthesis of phenylpropanoids has dramatic effects on plant growth and development. Reduced PAL activity in tobacco as a result of overexpression of bean PAL2 has been shown to result in abnormalities in phenotype, reduced plant size and reduced soluble phenolics and lignification (Elkind *et al.*, 1990).

Overexpression of *Antirrhinum* myb308 and myb330 in tobacco result in a gene dosage dependent dwarfing and reduce phenolic acids and lignin biosynthesis. Phenotypic alterations in these plants are associated with transcriptional repression of three phenylpropanoid biosynthetic genes including C4H, 4CL, CAD whereas PAL expression is not affected (Tamagnone *et al.*, 1998). Dwarf features of the *NtmybAS1* plants are to some extent similar to those overexpressing the bean PAL2 and myb308. However, activation of PAL expression in *NtmybAS1* plants is in sharp contrast with the unaffected level of PAL expression in myb308 and with the reduced PAL transcript in bean PAL2 overexpressing plants suggesting that the mechanisms involved in *NtmybAS1* dwarfing are different.

The effect of reduced and elevated levels of PAL activity on overall flux into the phenylpropanoid pathway has been studied in tobacco. Reduced PAL activity is associated with reduced levels of phenylpropanoids such as chlorogenic acid (3-caffeoylquinic acid) and rutin (quercetin 3-β-D-rutinoside) (Elkind *et al.*, 1990).

Increased PAL activity above the wild type level have been shown to cause accumulation of chlorogenic acid and other phenolics such as β-glucoside conjugate of 4-coumaric acid but has no effect on rutin level (Bate *et al.*, 1994, Howles *et al.*, 1996). In several cases the inhibitory effect of phenylpropanoid compounds on plant growth have been reported (Kefeli and Dashek, 1984; Inamori *et al.*, 1991; Inamori *et al.*, 1993; Kusano *et al.*, 1998). Activation of *gPAL1* expression in *NtmybAS1* plants (Figure 3. 13) could affect the flux through the phenylpropanoid pathway and therefore, the reduced growth of *NtmybAS1* plants may be a consequence of elevated levels of phenylpropanoid compounds with growth inhibitory effects.

Chapter 4

Physiological and cellular analysis of *NtmybAS1*-induced dwarfing in *Nicotiana tabacum*

4. 1 Introduction

In higher plants a broad range of genetic defects can result in abnormal plant growth and development leading to a dwarf phenotype. Outstanding amongst these are mutations in genes involved in biosynthesis and perception/signal transduction of phytohormones including gibberellic acid (GA) (Reid 1986; Swain and Olszewski, 1996) and brassinosteroids (BRs) (reviewed in Altmann, 1998a, b). In addition, dwarf phenotypes have been reported for *Arbidopsis* mutants with insensitivity to auxin (Wilson *et al.*, 1990; Timpte *et al.*, 1992) and with constitutive activation of the ethylene response (Kieber *et al.*, 1993). Furthermore mutations that constitutively increase salicylic acid (SA) levels and induce expression of pathogenesis-related (PR) proteins cause a dwarf phenotype (Bowling *et al.*, 1994; Bowling *et al.*, 1997).

Overexpression of several genes in plants has been shown to result in diverse morphological alterations, in which dwarfing is a common feature. These include overexpression of *rolA* and *rolC* genes of *Agrobacterium rhizogenes* in tobacco and potato (Schmülling *et al.*, 1988; Sinkar *et al.*, 1988; Fladung, 1990), bean *PAL2* (Elkind *et al.*, 1990), rice *OsMADS1* (Chung *et al.*, 1994) *Antirrhinum MIXTA* (Glover *et al.*, 1998), *myb308* and *myb330* (Tamagnone *et al.*, 1998), homeobox genes including rice *OSH1* (Kusaba *et al.*, 1998) and tobacco *NTH15* (Tamaoki *et al.*, 1997; Tanaka-Ueguchi *et al.*, 1998) in tobacco and phytoene synthase in tomato (Fray *et al.*, 1995). Antisense suppression of GA20-oxidase (*AtGA20ox1*) reduces elongation growth via limiting bioactive GA levels (Coles *et al.*, 1999). In *Arabidopsis* insertion of a *Dissociation* (*Ds*) transposon in the untranslated leader of *TINY*, which encodes a putative transcription factor with similarity to APETALA2 (Jofuku *et al.*, 1994) results in overexpression of *TINY* and induction of a gene dosage dependent dwarfing (Wilson *et al.*, 1996).

To further understand the basis of dwarfing in *NtmybAS1* plants, the effects of phytohormones and their inhibitors on the phenotype of *NtmybAS1* plants were investigated. The physiological basis of action of NtMybAS1 protein was investigated through grafting and the effects of *NtmybAS1* root and shoot systems on dwarfing was determined. The cellular anatomy of *NtmybAS1* plants was analysed to determine the effects of overproduction of NtMybAS1 protein on cell morphology.

This chapter demonstrates that the ectopic overexpression of *NtmybAS1* in tobacco does not interfere with GA or BR biosynthesis and the epinastic curvature of leaves does not result from elevated ethylene levels. Grafting experiments established the cell autonomy of dwarfing. The phenotypes associated with the overproduction of NtMybAS1 protein in tobacco result from dramatic changes at the cellular level, which affect both cell expansion and cell division. Results further suggest that the mechanisms controlling the overall leaf shape is independent of the ones controlling cell expansion and cell division.

4. 2 GA_3 feeding does not fully normalise the dwarf phenotype of *NtmybAS1* plants

To determine whether the overproduction of NtMybAS1 protein in tobacco interferes with components of the GA biosynthesis pathway, the effect of GA_3 on the phenotype of homozygote *NtmybAS1* plants was investigated. Aqueous solutions (2.5, 0.25 mM) of GA_3 were fed to shoot apices (section 2. 16) of wild type and homozygote *NtmybAS1* plants (Figure 4. 1. a, b) and their growth rates analysed. Homozygote *NtmybAS1* plants showed a greater response to GA_3 than wild type. Mean plant height in *NtmybAS1* plants increased to 6.8 fold (GA_3 0.25 M) whereas wild type plants only showed a 1.25 fold increase in mean plant height (Figure 4. 1. c). A 10-fold increase in GA_3 concentration (2.5 mM) did not significantly increase plant height both in wild type (1.3 fold) and *NtmybAS1* (8 fold) plants indicating that the plants are almost saturated by 0.25 mM GA_3. Despite the greater response of *NtmybAS1* plants to GA_3, the phenotype of these plants was not normalised to wild type. Demonstration of inability of GA_3 to normalise the *NtmybAS1* phenotype, lack of dark green color (characteristic of GA deficient mutants) and normal germination of *NtmybAS1* seeds in the absence of GA suggested that the dwarf phenotype of *NtmybAS1* plants does not result from GA deficiency.

Figure 4. 1

Effects of GA_3 feeding on *NtmybAS1* phenotype and comparison of growth rates of wild type and *NtmybAS1* plants

(a) Response of homozygote *NtmybAS1* plants to GA_3 feeding at early stage of growth.

Left: Homozygote *NtmybAS1* plants treated with 0.25 mM GA_3

Middle: Homozygote *NtmybAS1* Control (no GA_3)

Right: Homozygote *NtmybAS1* plants treated with 2.5 mM GA_3

(b) Phenotypes of untreated and GA_3-treated homozygote *NtmybAS1* plants at mature stage

Left: Homozygote *NtmybAS1* Control (no GA_3)

Middle: Homozygote *NtmybAS1* plants treated with 0.25 mM GA_3

Right: Homozygote *NtmybAS1* plants treated with 2.5 mM GA_3

(c) Comparison of growth rates of untreated and GA_3-treated wild type and homozygote *NtmybAS1* plants

Results shown are mean plant height ± SD measured for six plants.

(a)

(b)

(c)

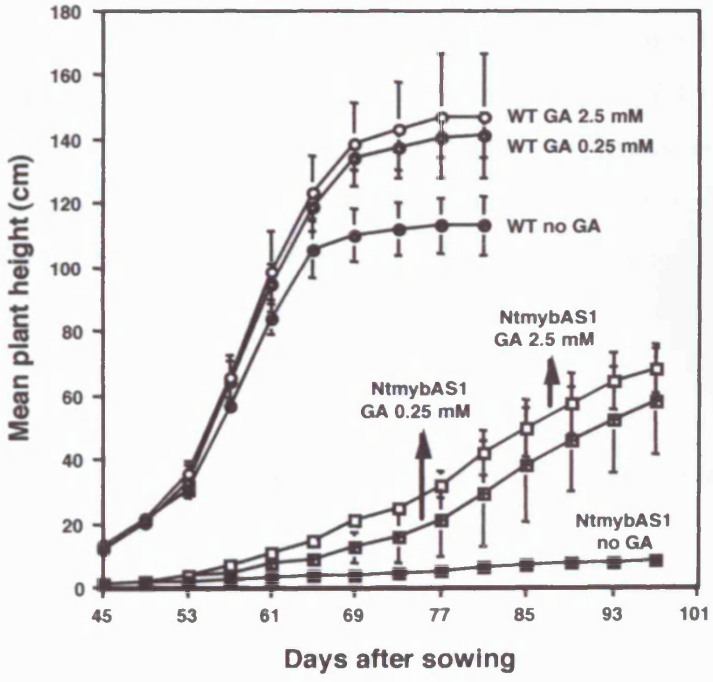
Mean plant height (cm)
180
160
140
120
100
80
60
40
20
0
45
53
61
69
77
85
93
101
Days after sowing
WT GA 2.5 mM
WT GA 0.25 mM
WT no GA
NtmybAS1
GA 2.5 mM
NtmybAS1
GA 0.25 mM
NtmybAS1
no GA

4. 3 The *NtmybAS1* plants do not respond differentially to brassinosteroids

Cell elongation defects leading to dwarfing may be due to a block in brassinosteroid biosynthesis. It has been shown that the dwarf phenotype of the brassinosteroid mutants of *Arabidopsis* can be restored to that of wild type by exogenous application of brassinosteroids (Takahashi *et al.*, 1995; Bishop *et al.*, 1996; Kauschmann *et al.*, 1996; Li *et al.*, 1996; Szekeres *et al.*, 1996; Nomura *et al.*, 1997; Choe *et al.*, 1998). To determine the effect of brassinosteroids on the *NtmybAS1* phenotype, brassinosteroid-feeding experiments were performed using epibrassinolide and homobrassinolide (section 2. 16).

Brassinosteroid feeding reduced root growth and stimulated hypocotyl elongation in both wild type and *NtmybAS1* seedlings. In addition, both wild type and *NtmybAS1* seedlings showed a greater response to epibrassinolide than to homobrassinolide. Root growth in *NtmybAS1* seedlings was not differentially reduced in response to brassinosteroids. Epibrassinolide and homobrassinolide reduced root length by 2.2-fold and 1.8 fold in both wild type and *NtmybAS1* seedlings. However, in response to epibrassinolide and homobrassinolide, wild type hypocotyls elongated more (6.4 and 2.4-fold) than *NtmybAS1* hypocotyls (4.6 and 1.9-fold). The lack of differential response in roots and insensitivity of *NtmybAS1* hypocotyls to brassinosteroids examined suggested that reduced growth of *NtmybAS1* plants does not result from brassinosteroid deficiency. Therefore, it is unlikely that the NtMybAS1 protein interferes with the brassinosteroid biosynthesis pathway.

4. 4 Epinastic curvature of *NtmybAS1* leaves does not result from elevated ethylene levels

Severe downward curvature (epinasty) of cotyledons and leaves was a major characteristic of *NtmybAS1* seedling (Figure 3. 5. b). Epinastic curvature of leaves is one of the well characterised effects of ethylene in plants. Therefore, it was hypothesised that the epinastic curvature of *NtmybAS1* leaves may results from an increase in endogenous ethylene levels. To test this hypothesis, the effects of

ethylene inhibitors including cobalt chloride ($CoCl_2$) and silver thiosulfate (STS) on growth of *NtmybAS1* seedlings were investigated (section 2. 16).

Epinastic curvature of leaves was not normalised when the *NtmybAS1* seeds were germinated in the presence of 0.1 mM $CoCl_2$. Higher concentrations of $CoCl_2$ (1, 10 and 50 mM) reduced growth and prevented seed germination. Epinastic curvature of *NtmybAS1* seedlings was not also normalised when seeds were germinated in the presence of 5 mg l^{-1} STS. However, STS (5 mg l^{-1}) promoted growth of both wild type and *NtmybAS1* seedlings. The inability of two ethylene inhibitors to reverse the epinastic curvature of *NtmybAS1* leaves to the wild type phenotype strongly suggested that the severe leaf curvature in *NtmybAS1* seedlings is not a consequence of elevated ethylene levels.

4. 5 Dwarf phenotype is not normalised by grafting

Grafting experiments have provided fundamental insights into gene function, translocation of assimilates, phytohormones, other graft transmissible substances in plants and also into effects of root systems on shoots and vice versa.

To investigate the response of *NtmybAS1* plants to grafting, the homozygote and heterozygote *NtmybAS1* scions were grafted onto wild type rootstocks. Reciprocal grafting was performed to determine the effect of the *NtmybAS1* root system on wild type shoot. Self-grafts of wild type (Figure 4. 2. a), heterozygote *NtmybAS1* and non-grafted plants were used as controls. The effect of grafting on phenotype was quantified by measuring plant height at first flower stage for each combination of grafting (Figure 4. 2. c).

The dwarf phenotype of *NtmybAS1* scions was not normalised by grafting onto wild type rootstocks. However, partial stem elongation in three (out of five) homozygote *NtmybAS1* scions grafted onto wild type rootstocks may be due formation of a better graft union (Figure 4. 2. b). No stem elongation was observed in six heterozygote *NtmybAS1* scions grafted onto wild type rootstocks. The fact that graft transmissible substances did not affect the dwarf phenotype both in

Figure 4. 2

Effect of grafting on phenotype and plant height in wild type and *NtmybAS1* plants

(a) Wild type scions grafted onto wild type rootstock

Left: Wild type control (no grafting)

Right: Wild type scion grafted onto wild type rootstock. Lower leaves were removed to show the grafting point denoted by arrow.

(b) Homozygote *NtmybAS1* scions grafted onto wild type rootstocks. Arrow indicates the grafting point.

(c) Plant height at first flower stage in control and grafted plants

Orientation of grafting: scions/rootstocks

WT: Wild type

Het: Heterozygote *NtmybAS1* plant

Hom: Homozygote *NtmybAS1* plant

(a)

(b)

(c)

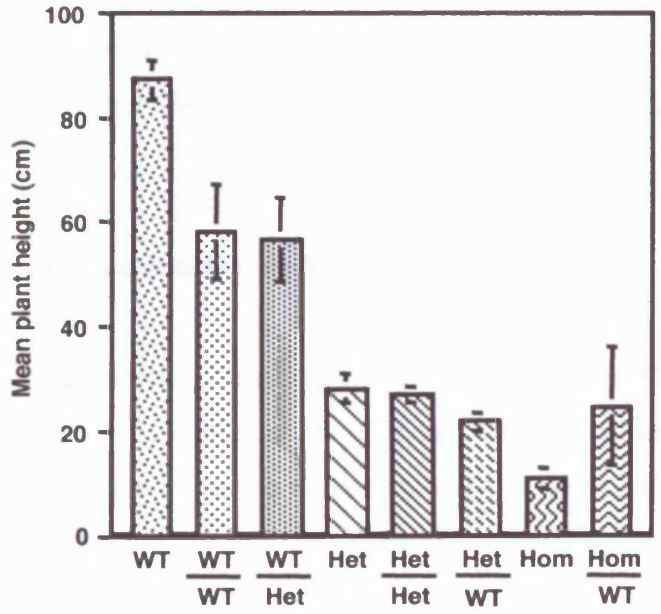
Mean plant height (cm)
100
80
60
40
20
0
WT
WT / WT
WT / Het
Het
Het / Het
Het / WT
Hom
Hom / WT

homozygote and heterozygote *NtmybAS1* scions demonstrated that dwarfing in *NtmybAS1* overexpressing plants is a cell autonomous phenomenon.

Results derived from reciprocal grafting clearly demonstrated that the *NtmybAS1* root system has no effect on wild type shoots. Eleven wild type scions grafted onto heterozygote *NtmybAS1* rootstocks grew to the same height as wild type plants grafted onto wild type (Figure 4. 2. c). This further indicated that the constitutive expression of *NtmybAS1* in roots is not sufficient for dwarfing, which was in good agreement with the results derived from root-specific expression of *NtmybAS1* using the –90 region of CaMV35S promoter (section 3. 2. 4).

4. 6 Analysis of cell morphology

Phenotypic alterations in *NtmybAS1* plants particularly reduced size and reduced growth rate (section 3. 3) could be the consequence of defects in cell division or cell expansion. To identify any such defects in *NtmybAS1* plants, sections from hypocotyls, cotyledons and first true leaves were analysed by light microscopy (section 2. 17). Results described below demonstrate that overproduction of NtMybAS1 protein in tobacco differentially affects cell expansion in different organs.

4. 6. 1 Cell elongation is blocked in *NtmybAS1* hypocotyls

Analysis of sections from hypocotyls of wild type (Figure 4. 3. a) and *NtmybAS1* (Figure 4. 3. b) seedlings revealed that the overproduction of NtMybAS1 protein in tobacco results in severe reduction of cell expansion in hypocotyls. This reduction in cell expansion gave the *NtmybAS1* hypocotyl cells an isodiametric shape. To quantify the changes in cell expansion, cell size in hypocotyls was measured both parallel (Figure 4. 3. c) and perpendicular (Figure 4. 3. d) to the apical-basal axis. Results derived from these analyses demonstrated that mean cell size parallel to the apical-basal axis was reduced to 50% of wild type, whereas this reduction perpendicular to the apical-basal axis was 15% of wild type. The effect of

Figure 4. 3

Comparison of cell morphology and cell size in wild type and *NtmybAS1* hypocotyls

(a) Wild type hypocotyl

(b) Homozygote *NtmybAS1* hypocotyl

(c) Mean cell size parallel to apical-basal axis

(d) Mean cell size perpendicular to apical-basal axis

E1, E2: Epidermal layers

1-6: Cell layers 1 to 6

Results shown in (c) and (d) are the mean cell size ± SD measured for four hypocotyl sections.

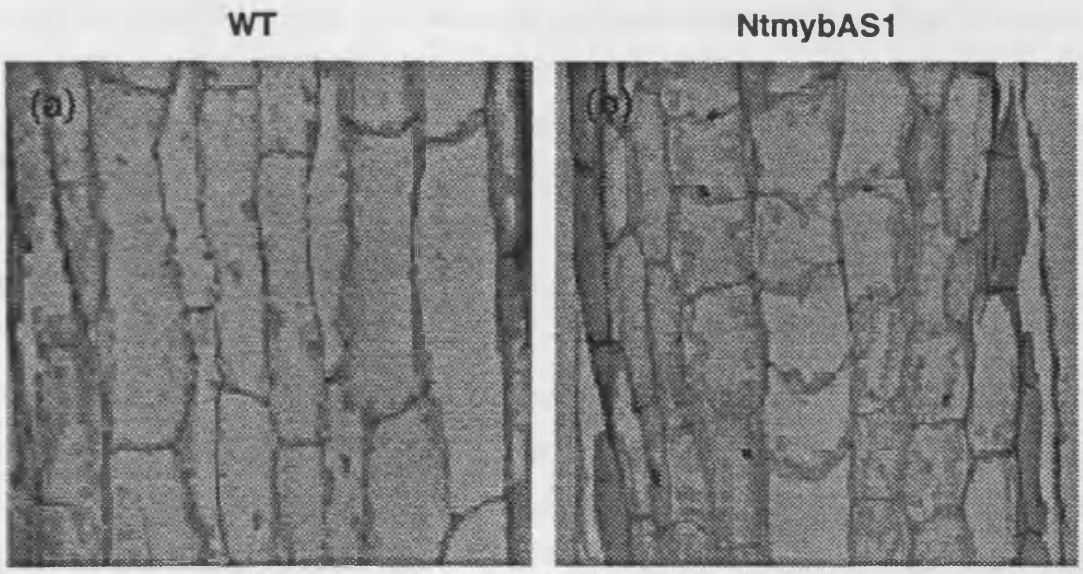
WT
NtmybAS1
(a)
(b)

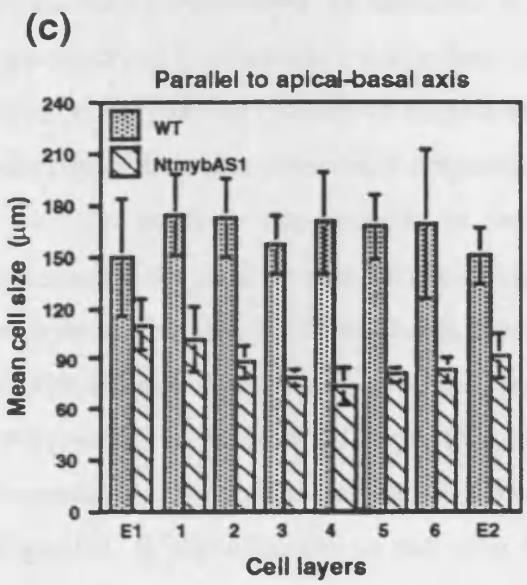
(c)
Parallel to apical-basal axis
WT
NtmybAS1
Mean cell size (μm)
240
210
180
150
120
90
60
30
0
E1
1
2
3
4
5
6
E2
Cell layers

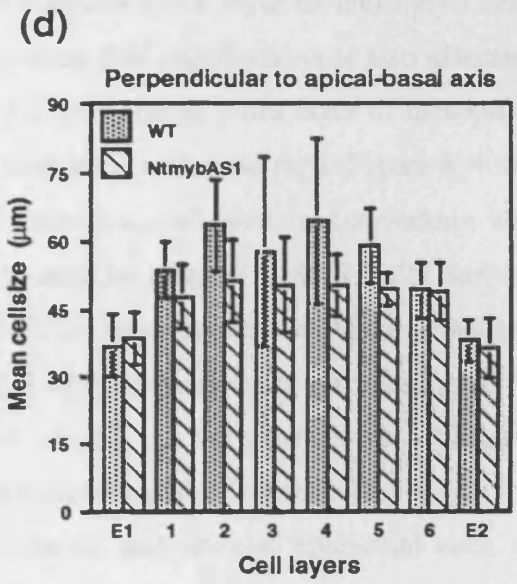
(d)
Perpendicular to apical-basal axis
WT
NtmybAS1
Mean cellsize (μm)
90
75
60
45
30
15
0
E1
1
2
3
4
5
6
E2
Cell layers

NtmybAS1 overexpression on reduction of cell size in epidermal cells of the hypocotyl was lower (33%) than in cortical cells. The *NtmybAS1* epidermal cell size perpendicular to the apical-basal axis was not significantly different from wild type (Figure 4. 3. d). The fact that cell numbers in *NtmybAS1* hypocotyls examined was not significantly different from wild type indicated that the major cause of reduced size of *NtmybAS1* plants is a reduction in cell size due to a block in cell elongation.

4. 6. 2 Overexpression of *NtmybAS1* induces cell elongation in cotyledons

Analysis of cell anatomy in sections from cotyledons of wild type (Figure 4. 4. a) and *NtmybAS1* (Figure 4. 4. b) seedlings revealed that overproduction of NtMybAS1 protein in tobacco caused an increase in cell expansion both in palisade and mesophyll cells of cotyledons, which was in sharp contrast with the reduced cell expansion in hypocotyls. In addition, an incomplete extra layer of mesophyll cells was observed in *NtmybAS1* cotyledons indicating that cell division is also affected. Both cell expansion parallel to adaxial-abaxial axis and an extra layer of mesophyll cells result in thicker *NtmybAS1* cotyledons compared with wild type (Figure 4. 4. b).

To quantify the changes in cell expansion, cell size in cotyledons was measured both parallel and perpendicular to adaxial-abaxial axis. Results derived from these analyses indicated that in *NtmybAS1* cotyledons mean cell size parallel to adaxial-abaxial axis in palisade and layer 1-3 of mesophyll cells increases to 33%, 49%, 46%, 62% of wild type (Figure 4. 4. c). In contrast, mean cell size perpendicular to adaxial-abaxial axis was not significantly different from wild type (Figure 4. 4. d). Changes in cell size in adaxial and abaxial epidermal cells of *NtmybAS1* cotyledons in both axes were not significantly different from wild type (Figures 4. 4. c and 4. 4. d).

4. 6. 3 The *NtmybAS1* leaves contain more elongated cells and two layers of palisade

Analysis of cell anatomy in sections from leaves of wild type (Figure 4. 5. a) and *NtmybAS1* (Figure 4. 5. b) seedlings revealed that the palisade and mesophyll

cells in *NtmybAS1* leaves are more elongated than in cotyledons (4. 6. 2). In addition, the presence of an incomplete extra layer of palisade cells, which was the most conspicuous feature of *NtmybAS1* leaves demonstrated that the overexpression of *NtmybAS1* in tobacco also affects cell division.

To quantify the changes in cell expansion, cell size (parallel and perpendicular to adaxial-abaxial axis) in *NtmybAS1* leaves was compared with wild type. Results derived from these analyses indicated that mean cell size parallel to adaxial-abaxial axis in palisade (layer 1) and layer 1-3 of mesophyll cells increases to 45%, 49%, 78% and 99% of wild type (Figure 4. 4. c). Increase in mean cell size perpendicular to adaxial-abaxial axis in palisade, layer 1 and 2 of mesophyll cells was 6%, 18% and 3% of wild type, whereas in layer 3 of mesophyll cells a decrease to 0.5% of wild type was measured (Figure 4. 4. d). Adaxial and abaxial epidermal cells of *NtmybAS1* leaves showed a 46% and 34% increase (Figure 4. 4. c) in mean cell size perpendicular to adaxial-abaxial axis and this increase parallel to adaxial-abaxial axis was 46% and 21% respectively (Figure 4. 4. d).

4. 7 Overexpression of *NtmybAS1* in tobacco does not affect the overall leaf shape

The altered phenotype of *NtmybAS1* leaves particularly reduced leaf area, increased cell expansion, and reduced cell numbers, suggesting that the overproduction of NtMybAS1 protein in tobacco may affect the overall leaf shape. The changes in leaf shape can easily be expressed as an increase or a decrease in leaf length: leaf width ratio. To quantify the changes in leaf shape of *NtmybAS1* plants, the length: width ratios of 14 leaves of two wild type plants were compared with two heterozygote *NtmybAS1* plants at first flower stage. The mean length: width ratios of leaf 1-14 (from shoot apex to stem base) in wild type and heterozygote *NtmybAS1* plants (WT, *NtmybAS1*) were (1) 4.55, 4.55; (2) 2.25, 2.25; (3) 1.90, 1.80; (4) 1.80, 1.70; (5) 1.85, 1.65; (6) 1.75, 1.65; (7) 1.75, 1.70; (8) 1.70, 1.70; (9) 1.65, 1.65; (10) 1.55, 1.60; (11) 1.50, 1.55; (12) 1.60, 1.60; (13) 1.70, 1.50; (14) 1.50, 1.60. Results revealed that the length: width ratios of *NtmybAS1* leaves are similar to the wild type,

Figure 4. 4

Comparison of cell morphology and cell size in wild type and *NtmybAS1* cotyledons

(a) Wild type cotyledon

(b) Homozygote *NtmybAS1* cotyledon

(c) Mean cell size parallel to adaxial-abaxial axis

(d) Mean cell size perpendicular to adaxial-abaxial axis

E1: Adaxial epidermis

Pl: Palisade cells

M1-M4: Mesophyll cells layer 1-4

E2: Abaxial epidermis

Results shown in (c) and (d) are the mean cell size ± SD measured for four cotyledon sections.

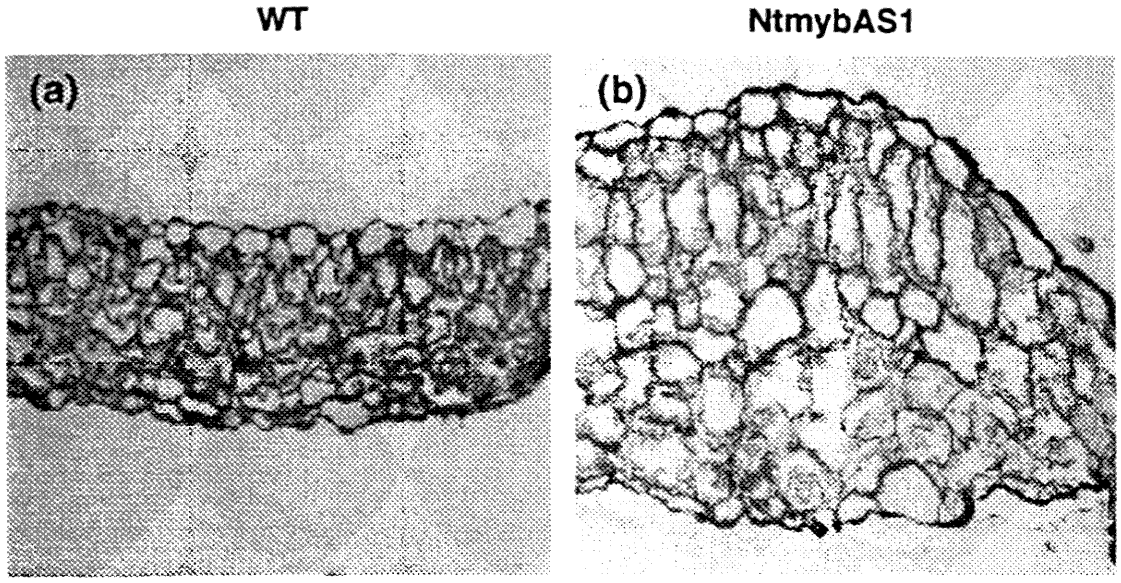
WT
NtmybAS1
(a)
(b)

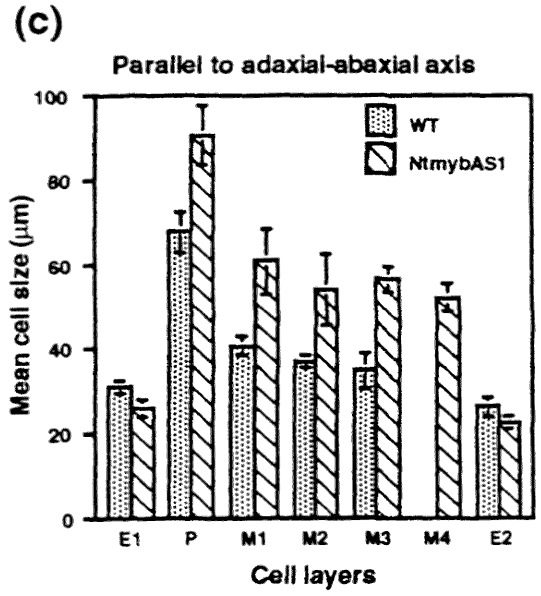
(c)
Parallel to adaxial-abaxial axis
Mean cell size (μm)
100
80
60
40
20
0
WT
NtmybAS1
E1
P
M1
M2
M3
M4
E2
Cell layers

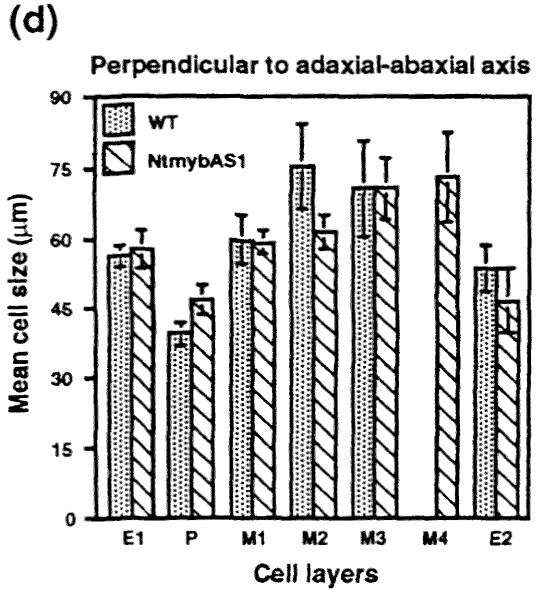
(d)
Perpendicular to adaxial-abaxial axis
Mean cell size (μm)
90
75
60
45
30
15
0
WT
NtmybAS1
E1
P
M1
M2
M3
M4
E2
Cell layers

Figure 4. 5

Comparison of cell morphology and cell size in wild type and *NtmybAS1* leaves

(a) Wild type leaf

(b) Homozygote *NtmybAS1* leaf

(c) Mean cell size parallel to adaxial-abaxial axis

(d) Mean cell size perpendicular to adaxial-abaxial axis

E1: Adaxial epidermis

P1: Palisade cells layer 1

P2: Palisade cells layer 2

M1-M3: Mesophyll cells layer 1 to 3

E2: Abaxial epidermis

Results shown in (c) and (d) are the mean cell size ± SD measured for four leaf sections.

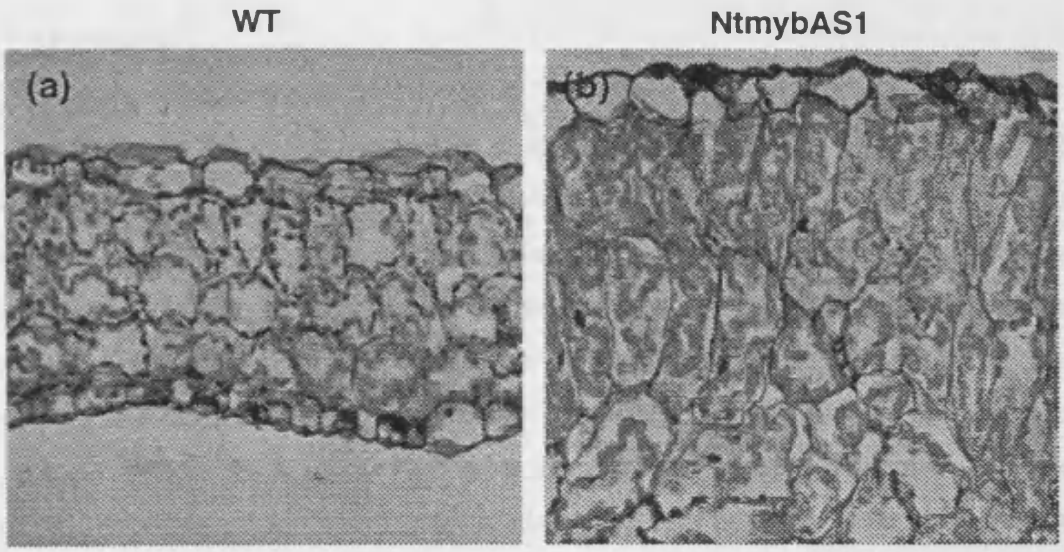
WT
NtmybAS1
(a)
(b)

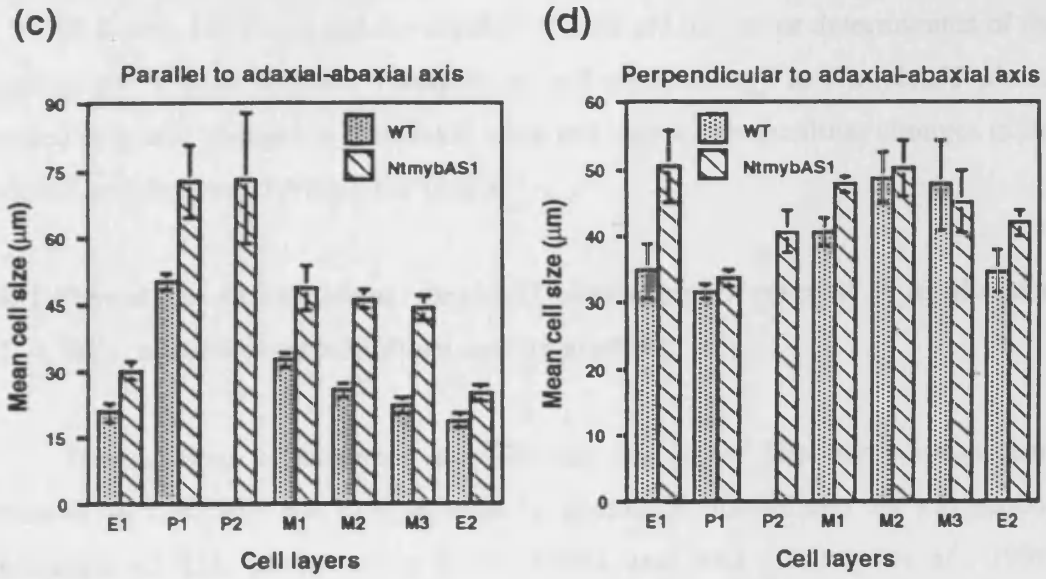
(c)
Parallel to adaxial-abaxial axis
Mean cell size (μm)
90
75
60
45
30
15
0
WT
NtmybAS1
E1
P1
P2
M1
M2
M3
E2
Cell layers
(d)
Perpendicular to adaxial-abaxial axis
Mean cell size (μm)
60
50
40
30
20
10
0
WT
NtmybAS1
E1
P1
P2
M1
M2
M3
E2
Cell layers

and this similarity, which was consistent in leaf 1-14, demonstrated that despite the reduced size and dramatic changes in cell morphology, the overall leaf pattern in *NtmybAS1* plants is not affected.

4. 8 Discussion

Plant growth and development are tightly regulated by environmental stimuli such as light and photoperiod and internal regulatory factors including gene expression and phytohormones. Morphological changes in *NtmybAS1* plants were broadly similar to those reported for a wide range of GA and BR deficient mutants. However, detailed analyses of responses of *NtmybAS1* plants to phytohormones revealed that the morphological defects in *NtmybAS1* plants could not be overcome by phytohormone feeding. Further evidence to support this finding was obtained through grafting experiments, which also demonstrated the cell autonomy of dwarfing.

Cell size, cell shape and the number of cells are the major determinants of the morphology of plant organs. Analysis of cell morphology in *NtmybAS1* plants revealed dramatic changes in *NtmybAS1* cells and linked these cellular changes to the modified architecture of *NtmybAS1* plants.

4. 8. 1 Phenotypic alterations in *NtmybAS1* plants are not rescued by application of GA, BRs, and ethylene inhibitors and by grafting

Several lines of evidence indicate that the dwarf phenotype of mutants defective in GA and BR biosynthesis is generally normalised by exogenous application of GA (reviewed in Reid, 1986) and BRs (Bishop *et al.*, 1996; Kauschmann *et al.*, 1996; Li *et al.*, 1996; Szekeres *et al.*, 1996; Klahre *et al.*, 1997; Nomura *et al.*, 1997; Azpiroz *et al.*, 1998). In some cases the dwarf features of GA deficient mutants in which a specific step in GA biosynthesis pathway is blocked have been reverted by grafting. For example in *na* lines of pea, the dwarf phenotype, which results from a block in conversion of *ent*-7α-hydroxykaurenic acid to GA_{12}-aldehyde (Ingram and Reid, 1987) has been rescued by grafting (Allison-Creese *et*

al., 1985; Reid *et al.*, 1983) whereas the dwarf phenotype of *le* lines of pea which, results from a block in conversion of GA_{20} to GA_1 (Ingram *et al.*, 1984; Ingram *et al.*, 1983) has not been rescued by grafting (Lockard and Grunwald, 1970, McComb and McComb, 1970, Reid *et al.*, 1983). Study on translocation of GAs from the rootstocks to the scions in GA deficient mutants of pea has revealed that the levels of transport of different GAs from rootstock to scion differ dramatically and GA_{20} seems to translocate to the scions at the highest level in peas (Proebsting *et al.*, 1992).

Reduced levels of active GAs in tobacco leaves by overexpression of *NTH15*, a tobacco homeobox gene, which results in suppression of GA_{20} oxidase and blocks conversion of GA_{19} to GA_{20} has been reported to alter the leaf and flower morphology (Tamaoki *et al.*, 1997; Tanaka-Ueguchi *et al.*, 1998). Despite a reduction in leaf and flower size, *NtmybAS1* plants do not show the morphological abnormalities resulting from reduced levels of active GA in *NTH15* overexpressing lines.

Apart from partial elongation of *NtmybAS1* stems in response to GA_3 (Figure 4. 1), none of the dwarfing features of *NtmybAS1* plants (section 3. 3) was reverted to wild type through GA_3 feeding (section 4. 2) or grafting (section 4. 5). This evidence strongly suggested that the overproduction of NtMybAS1 protein in tobacco does not interfere with GA biosynthesis.

Several lines of evidence indicate that application of BRs induces a wide range of cellular responses in plants. Characterisation of mutants deficient in biosynthesis and perception/signal transduction of BRs has revealed that this group of phytohormones, which derive from plant sterols and are structurally similar to animal steroid hormones play a major role in plant development (reviewed in Altmann, 1998a, b). It has been shown that the morphological defects resulting from BR deficiency can be overcome by exogenous application of BRs. However, results described in section 4. 3 did not support the hypothesis that the dwarf feature of *NtmybAS1* plants may result from brassinosteroid deficiency, which suggested that the NtMybAS1 protein does not interfere with BR biosynthesis.

Dwarf phenotype could result from elevated levels of ethylene in plants. The *ctr1* mutants of *Arabidopsis* with constitutive activation of ethylene response show a dwarf phenotype (Kieber *et al.*, 1993). Some of the phenotypic characteristics of *NtmybAS1* plants including reduced size, less extended roots system and reduced size of flowers were similar to those described for *ctr1* mutants. In addition, the epinastic curvature of *NtmybAS1* leaves was similar to a characteristic ethylene response. Several inhibitors of ethylene including $CoCl_2$, STS, aminoethoxyvinylglycine (AVG), α-aminoisobutyric acid (AIB), *trans*-cyclooctene and silver (Ag^{+2}) have been widely used to block ethylene biosynthesis in plants. It has been shown that the phenotypes associated with the overproduction of ethylene in *Arabidopsis* can be reverted by ethylene inhibitors (Guzman and Ecker, 1990; Kieber *et al.*, 1993). Neither $CoCl_2$, nor STS, (section 4. 4) were able to revert the phenotype of *NtmybAS1* seedlings to that of wild type. In addition these inhibitors did not rescue the epinastic curvature of *NtmybAS1* leaves.

The reduced height and increased lateral branches of *NtmybAS1* plants resembles the auxin resistant (*axr1*) mutants *of Arabidopsis* (Lincoln *et al.*, 1990). Unlike *axr1* mutants, the *NtmybAS1* hypocotyls and leaves show dramatic alterations in cell size and cell shape. In addition, the *NtmybAS1* leaves are not irregular in shape. The reduced apical dominance, increased axillary shoots and stunted growth of *NtmybAS1* plants is to some extent similar to tobacco plants overproducing cytokinin by expression of the *ipt* (isopentenyl transferase) gene of *Agrobacterium tumefaciens* (Li *et al.*, 1992). However, the *NtmybAS1* plants do not show reduced root initiation and delayed senescence.

The fact that the GA_3, BRs, ethylene inhibitors and grafting were not able to normalise the phenotype of *NtmybAS1* plants suggests that the non-hormonal factors may be involved in the dwarfing phenomenon. Since the plant cell wall is a heterogeneous polymer, a block in synthesis or integration of cell wall components may prevent cell expansion leading to dwarfing. In addition cell walls generally grow by a mechanism known as acid growth (Cosgrove, 1997) which is largely mediated by expansins (Cosgrove, 1997) and other factors involved in cell wall loosening such as endoglucanases, xyloglucanendotransglycosylase (XET) and

hydroxyl radicals (Cosgrove, 1999). Suppression of genes encoding these factors may prevent cell enlargement required for plant growth consequently leading to a dwarf phenotype.

4. 8. 2 Dramatic changes in cell expansion and cell division do not affect the overall leaf pattern of *NtmybAS1* plants

Analysis of cell morphology in *NtmybAS1* seedlings revealed that the overproduction of NtMybAS1 protein in tobacco affects both cell expansion and cell division (section 4. 6). The results presented in Figure 4. 3 clearly demonstrated a block in cell elongation and a reduction of cell size in *NtmybAS1* hypocotyls. The fact that the number of internodes (section 3. 3) in mature *NtmybAS1* plants and also the number of cells in the *NtmybAS1* hypocotyl sections examined were not significantly different from wild type, suggested that the reduced plant height in *NtmybAS1* overexpressing lines does not result from reduced cell division and therefore, is more likely a consequence of reduced cell elongation in stem.

A model is presented in Figure 4. 6 to illustrate the major cellular changes in *NtmybAS1* plants. In this model, inhibition of cell expansion in hypocotyls and increased cell expansion associated with enhanced cell division in cotyledons and leaves are the most conspicuous features of *NtmybAS1* cells. Despite the cellular changes represented in this model the overall body organisation of *NtmybAS1* plants is not affected. In *NtmybAS1* cotyledons and leaves, most cell expansion and cell division events, described in section 4. 6 occur in the proximal region of leaf lamina and gradually decrease towards the distal region. These pieces of evidence suggest that the gradient of cell expansion and cell division along the proximal-distal axis of leaves, which alters the flat shape of leaves, could be the major cause of epinastic curvature of leaves (section 3. 5. b). Enhanced cell division in *NtmybAS1* cotyledons and leaves leading to formation of incomplete extra layers of mesophyll and palisade cells (Figures 4. 4, 4. 5, 4. 6) may be a part of compensatory mechanism in response to massive increase in cell expansion. Such a balancing mechanism in leaf morphogenesis has been suggested for the *warty* mutant of maize (Reynolds *et al.*,

Figure 4. 6

Schematic representation of cell anatomy in wild type and *NtmybAS1* plants

Left: Hypocotyl

Middle: Cotyledon

Right: Leaf

E: Epidermis

M: Mesophyll cells

P: palisade cells

A-B: Apical –Basal axis

Ad-Ab: Adaxial-Abaxial axis

L: Length

W: Width

Major changes in *NtmybAS1* cell morphology:

-Reduced cell expansion in hypocotyl.

-Increased cell expansion and an incomplete extra layer of mesophyll cells.

-Increased cell expansion and an incomplete extra layer of palisade cells.

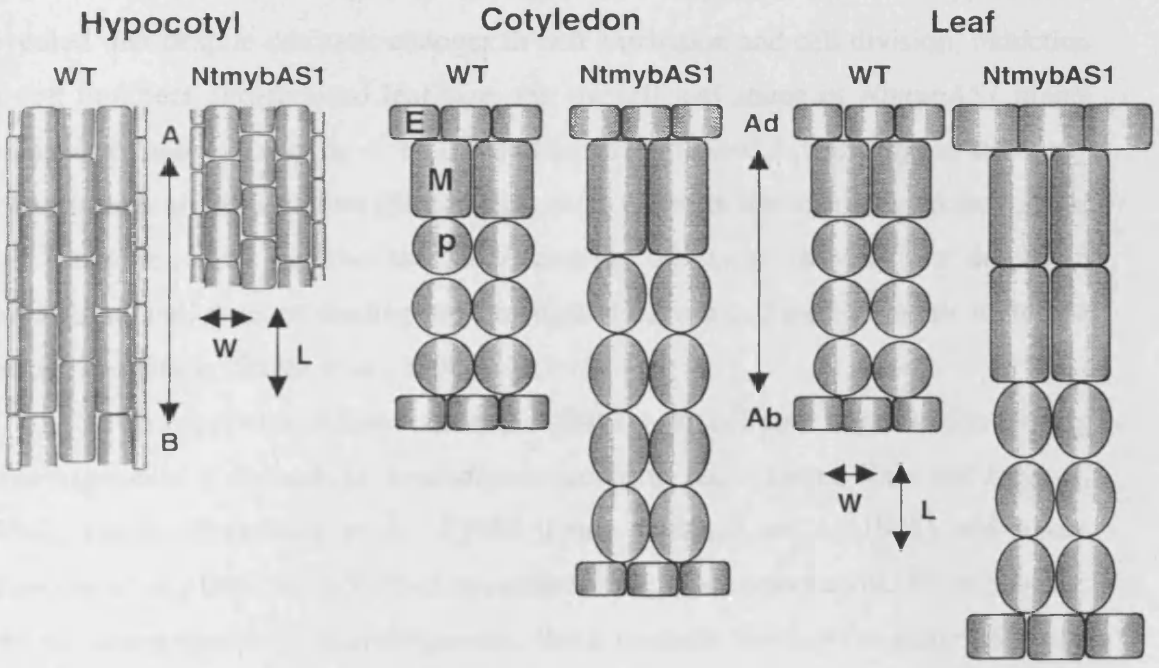
Hypocotyl
WT
NtmybAS1
A
B
W
L
Cotyledon
WT
NtmybAS1
E
M
p
Leaf
WT
NtmybAS1
Ad
Ab
W
L

1998).

It was shown that the fresh weight per unit leaf area in *NtmybAS1* leaves was about 50% higher than that of wild type, whereas dry weight per unit leaf area in these plants was not significantly different from wild type (section 3. 4). The reason for this difference can be explained by the results derived from analysis of cell morphology in *NtmybAS1* leaves (section 4. 6. 3). As illustrated in figure 4. 5. b and 4. 6, one obvious consequence of the dramatic elongation of cells in *NtmybAS1* leaves is a considerable increase in cell volume and this cell enlargement normally requires the uptake of water. Therefore, the higher fresh weight per unit leaf area of *NtmybAS1* leaves could be due to the higher water content of leaf cells.

Comparison of length: width ratios of *NtmybAS1* and wild type leaves revealed that despite dramatic changes in cell expansion and cell division, reduction in cell numbers and reduced leaf size, the overall leaf shape of *NtmybAS1* plants remains unchanged (section 4. 7). In addition the *NtmybAS1* plants do not show any defect in apical-basal pattern. Similarities exist between the results described above and those reported for the *tangled-1* mutant of maize in which a defect in longitudinal cell division leading to formation of curved cell walls does not affect the overall leaf shape (Smith *et al.*, 1996).

Several reports indicate that the defects in cellular organisation during embryogenesis in mutants of *Arabidopsis* including *fass* (Torres-Ruiz and Jürgens, 1994), knolle (Lukowitz *et al.*, 1996), keule (Assaad *et al.*, 1996) and hydra (Topping *et al.*, 1997) do not affect the establishment of correct apical-basal polarity. Despite abnormalities in morphogenesis, these mutants develop the major elements of the apical-basal pattern including cotyledons, hypocotyl and root in their proper position. These pieces evidence has led to this suggestion that the regulation of establishment of apical-basal pattern is independent of the mechanisms controlling correct cell morphogenesis and cell division.

The pathway of leaf development in plants has been studied in detail (reviewed in Sinha, 1999). Mutation analysis, overexpression and antisense suppression approaches have been widely used to investigate the mechanisms by which leaf shape and leaf size are regulated. In *Arabidopsis* the *asymmetric* (Tsukaya *et al.*, 1997) and *curly leaf* (Goodrich *et al.*, 1997; Sieburth *et al.*, 1997; Kim *et al.*,

1998) mutations affect leaf shape. Overexpression of class I *KNOX* genes in tobacco and *Arabidopsis* (Sinha *et al.*, 1993; Lincoln *et al.*, 1994; Chuck *et al.*, 1996) and antisense suppression of *Arabidopsis* methyltransferase (MET1) (Finnegan *et al.*, 1996) results in abnormal leaf shape.

Mutations affecting cell division and cell expansion have been identified in *Arabidopsis* and maize. *Arabidopsis* mutants defective in establishing the microtubule preprophase band show abnormalities in cell division and cell expansion but, despite these changes organogenesis in the correct position is not affected (Traas *et al.*, 1995). The *DIM* gene of *Arabidopsis* is involved in regulation of cell elongation. The *diminuto* (*dim*) mutants with altered expression of β-tubulin (*TUB1*) gene show a short phenotype due to reduced cell expansion along the apical-basal axis. (Takahashi *et al.*, 1995). Two loci in *Arabidopsis*, *ANGUSTIFOLIA* and *ROTUNDIFOLIA3* independently regulate cell expansion in transverse and longitudinal directions respectively (Tsuge *et al.*, 1996). In the *tangled-1* mutant of maize alterations in plane of cell division does not affect the overall leaf shape (Smith *et al.*, 1996). In the *warty* mutants of maize, abnormal cell enlargement is associated with abnormalities in cytokinesis leading to a higher rate of cell division and the altered cell cycle in this mutant may be part of a compensatory mechanism for growth defects (Reynolds *et al.*, 1998). These data support the independence of morphogenesis from the outcome of altered cell division but not altered cell expansion. The fact that the epinastic curvature (Figure 3. 5. b) and thickness of *NtmybAS1* cotyledons and leaves (Figures 4. 4 and 4. 5) largely result from increased cell expansion along the longitudinal axis is in agreement with this conclusion.

Morphological characteristics of *NtmybAS1* plants show similarities to some of the mutants described above suggesting that the involvement of similar mechanism(s) in the *NtmybAS1* phenotype can not be excluded.

Chapter 5

Molecular analysis of NtMybAS1 target genes

5. 1 Introduction

Identification of the genes that are differentially expressed in *NtmybAS1* overexpressing lines is fundamental in understanding mechanisms underlying dwarfing. It was shown by Northern blot analysis that the constitutive expression of *NtmybAS1* in tobacco results in an increase in *gPAL1* expression (section 3. 11). However, the complex modification of plant architecture in *NtmybAS1* overexpressing lines does not seem to arise simply from a single change in gene expression. To identify the genes and changes in the corresponding pathways responsible for dwarfing, altered gene expression can be analysed both at mRNA and protein levels. The differential mRNA display technique has been widely used in animals and in plants to identify and isolate the genes that are differentially expressed during development, in different environments and in response to hormones (McClelland *et al.*, 1995; Sharma and Davis, 1995; Shen *et al.*, 1995; van der Knaap and Kende, 1995). However, study of differentially transcribed genes alone, is not sufficient to determine gene function. Studying on large scale, the protein properties including expression level, post-translational modification, interactions and sub cellular location can provide fundamental insights into gene function.

Global protein products of genomes can be visualised using two-dimensional gel electrophoresis, which allows determining the changes in protein profile. The proteins that are differentially expressed can be further identified by traditional methods of protein sequencing including Edman degradation (section 2. 13. 4) or highly sensitive mass-spectrometric techniques including matrix assisted laser desorption ionization–time of flight (MALDI-TOF) (Yates *et al.*, 1998).

To determine the genes that are differentially expressed in *NtmybAS1* lines, total protein expression was analysed both in wild type and in *NtmybAS1* lines using one and two dimensional gel electrophoresis. This chapter describes identification of two pathogenesis-related (PR) proteins that are highly induced as a result of overexpression of *NtmybAS1* in tobacco and demonstrates a positive correlation between the levels of *NtmybAS1* expression and induction of expression of the PR genes both at mRNA and protein levels. Based on the results derived from these

analyses, a model is proposed to link the induction of *gPAL1* expression (section 3. 11) to activation of PR proteins.

5. 2 Two proteins are highly induced in *NtmybAS1* overexpressing lines

In order to primarily identify the proteins that are differentially expressed in *NtmybAS1* and *NtmybAS1-DBD* overexpressing lines, total protein expression was analysed in tobacco leaves using SDS-PAGE (section 2. 12. 3). In comparison to wild type leaves (W1 and W2), two major proteins with an estimated size of ca. 27 kDa and ca. 17 kDa (Figure 5. 1. a) were identified to be highly induced in two *NtmybAS1* overexpressing lines (lines 3 and 7). The levels of expression of both proteins in homozygote lines (3 Hom and 7 Hom) were higher than in heterozygotes (3 Het and 7 Het). In addition, the older leaves of homozygote lines showed a relatively higher level of expression of both proteins (L3-L6: leaf no. 3 to leaf no. 6 from the shoot apex).

No differential expression of proteins was identified in nine homozygote lines overexpressing the *NtmybAS1-DBD* (Figure 5. 1. b). Results indicated that the induction of expression of the ca. 17 kDa and ca. 27 kDa proteins in *NtmybAS1* overexpressing plants requires the putative transcription activator domain. Furthermore, the high level expression of the NtMybAS1 DNA binding domain alone does not interfere with normal cellular functions or induce the ca. 17 kDa and ca. 27 kDa proteins.

5. 3 Several proteins are differentially expressed in *NtmybAS1* overexpressing lines

To gain a better view of the differential protein expression in *NtmybAS1* overexpressing lines, the global protein expression of wild type and *NymybAS1* plants was visualised through 2-dimensional polyacrylamide gel electrophoresis (2-D PAGE) (section 2. 12. 4).

Total protein was extracted from 18 day-old wild type and homozygote *NtmybAS1* seedlings and quantified by Bradford assay (section 2. 12. 2). A 30 μg

aliquot of each sample was separated on a large format gel (180x245 mm ExcelGel XL) using a Pharmacia Multiphor II electrophoresis unit (section 2. 12. 4). The gels were silver stained (section 2. 12. 5) and the spots on each gel (Figure 5. 2) were visualised. Comparison of the spots derived from wild type (Figure 5. 2. a) and *NtmybAS1* (Figure 5. 2. b) overexpressing seedlings revealed that a multitude of proteins are differentially expressed in *NtmybAS1* overexpressing plants. Arrows in Figure 5. 2 show the most dramatic changes in protein expression.

5. 4 The ca. 27 kDa protein is tobacco acidic chitinase P (PR-P)

The complete sequence of a tryptic peptide derived from the ca.27 Kd protein was determined using automated Edman degradation method (section 2. 13. 4). A Blast search revealed that the 13 amino acids, GPIQLTNQNNYEK, of this peptide are exactly matched with amino acids 123-135 of the tobacco acidic chitinase P (PR-P) and show one amino acid mismatch (arginine at position 130) with the tobacco acidic chitinase Q (PR-Q) (Figure 5. 3. a). The trypsin cleavage sites are located at positions 122 (arginine) and 135 (lysine). This short motif corresponds to the nucleotides 403-441 of tobacco acidic chitinase P in λch28 clone (Payne *et al.*, 1990). The PR-P and its acidic isoform, PR-Q proteins consist of 253 amino acid residues with a 24 amino acid signal peptide. The mature PR-P and PR-Q proteins consist of 229 amino acid with a calculated mass of 24.859 kDa and 25.033 kDa and charges (pH 7.0) -4.9 and -3.8 respectively. The estimated molecular weight of ca. 27 kDa protein from the SDS gel was in good agreement with the molecular weight of the PR-P protein.

5. 5 The ca. 17 kDa protein is tobacco pathogenesis-related (PR) protein 1a (PR-1a)

An incomplete sequence of a tryptic peptide derived from the ca. 17 kDa protein was determined using automated Edman degradation method (section 2. 13. 4). A blast search revealed that the 14 amino acids, ADVGVEPLTWDDQV, of this

Figure 5. 1

Total protein profile of wild type, *NtmybAS1* and *NtmybAS1-DBD* overexpressing lines

(a) Total protein profile in wild type (W1, W2), heterozygote (3 Het, 7 Het) and homozygote (3 Hom, 7 Hom) lines overexpressing the *NtmybAS1* gene. Arrows show the two proteins of ca. 27 kDa and ca. 17 kDa, which are induced in *NtmybAS1* overexpressing lines. L3-L6 represents the leaf no. 3 to leaf no. 6 from the shoot apex.

(b) Total protein profile in 9 homozygote lines (lanes 3-11) overexpressing the *Ntmy*bAS1 DNA binding domain was not significantly different from wild type (W1, W2).

(a)

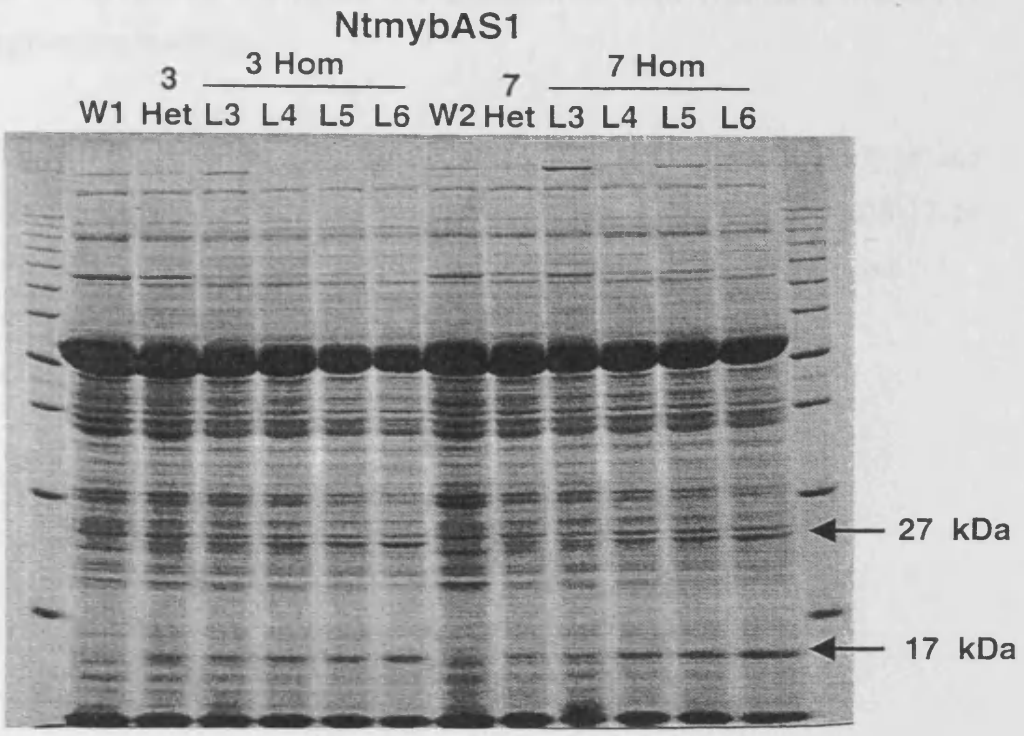
NtmybAS1
3
3 Hom
7
7 Hom
W1 Het L3 L4 L5 L6 W2 Het L3 L4 L5 L6
27 kDa
17 kDa

(b)

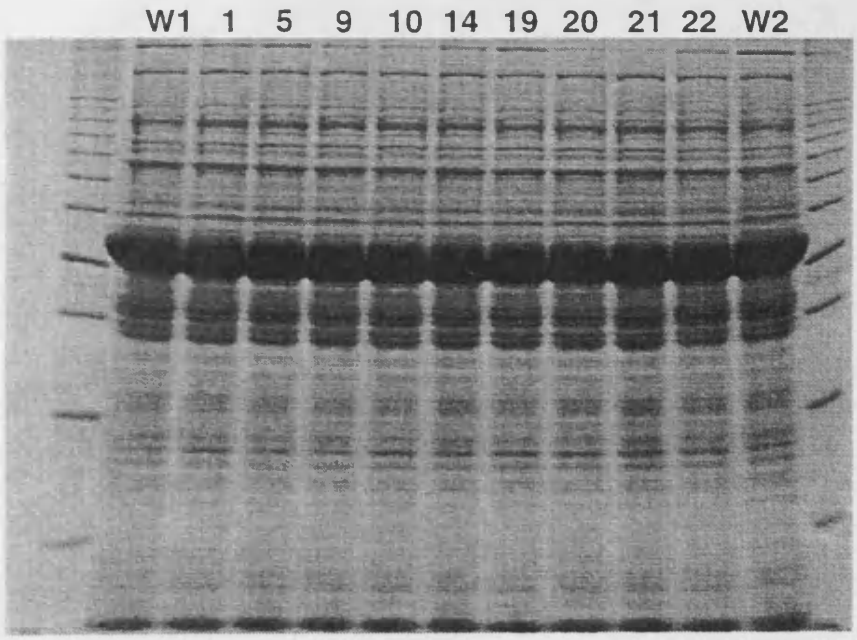
NtmybAS1-DBD (Hom)
W1 1 5 9 10 14 19 20 21 22 W2

Figure 5. 2

2-D gel analysis of total protein expression in wild type and *NtmybAS1* overexpressing seedlings

Total soluble proteins (30 μg) extracted from 18 day-old wild type and homozygote *NtmybAS1* seedlings were separated on Excel Gel XL SDS 12-14 (Section 2. 12. 4). Arrows indicate the major changes in protein expression.

(a) Wild type

(b) Homozygote *NtmybAS1*

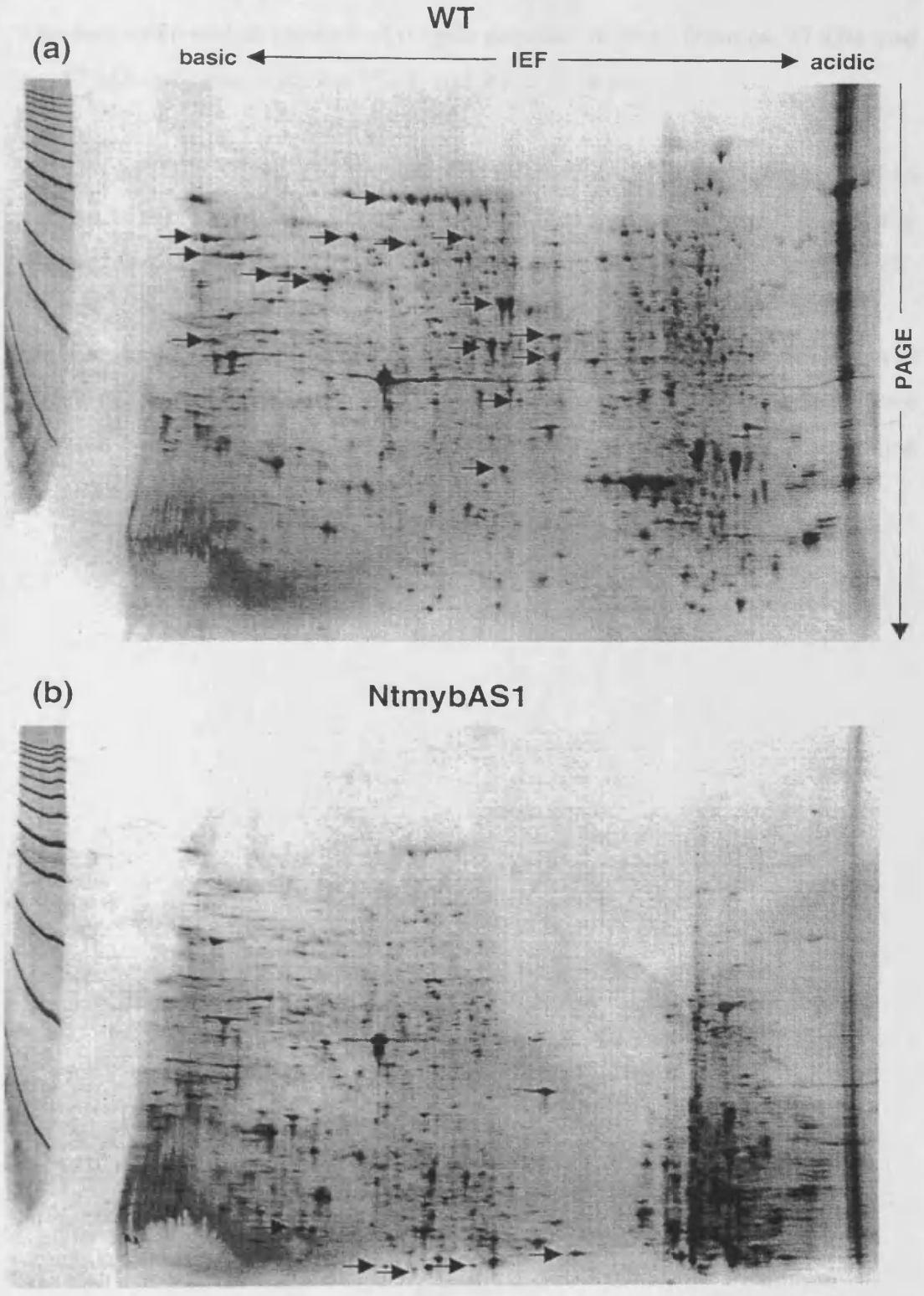
WT
(a)
basic
IEF
acidic
PAGE
(b)
NtmybAS1

Figure 5. 3

The sequence and alignment of tryptic peptides derived from ca. 27 kDa and ca. 17 kDa proteins with the PR-P and PR-1 proteins

(a) The GPIQLTNQNNYEK peptide derived from ca. 27 kDa protein showed an exact match with the residues 123-135 of the tobacco chitinase P (PR-P) and one amino acid mismatch (R at position 130) with PR-Q. The arginine (R) and lysine cleavage sites are at positions 122 and 135.

(b) The ADVGVEPLTWDDQV peptide derived from ca. 17 kDa protein showed an exact match with the residues 46-59 of tobacco PR-1a and PR-1c and two amino acids mismatches (N, G at positions 57, 58) with PR-1b. The arginine (R) cleavage site is at position 45.

(a)

PR-P

```
                                  GPIQLTNQNNYEK
                                  :::::::::::::
TTGGSLSAEPFTGGYCFVRQNDQSDRYYGRGPIQLTNQNNYEKAGNAIRQDLVNNPDLVA
       |         |         |         |         |         |
      100       110       120       130       140       150
```

PR-Q

```
                                  GPIQLTNQNNYEK
                                  ::::::::.:::::
TTGGSLSAEPFTGGYCFVRQNDQSDRYYGRGPIQLTNRNNYEKAGTAIGQELVNNPDLVA
       |         |         |         |         |         |
      100       110       120       130       140       150
```

(b)

PR-1a

```
                                  ADVGVEPLTWDDQV
                                  ::::::::::::::
STLLLFLVISHSCRAQNSQQDYLDAHNTARADVGVEPLTWDDQVAAYAQNYASQLAADCN
    |         |         |         |         |         |
   20        30        40        50        60        70
```

PR-1c

```
                                  ADVGVEPLTWDDQV
                                  ::::::::::::::
STLLLFLIISHSCHAQNSQQDYLDAHNTARADVGVEPLTWDDQVAAYAQNYASQLAADCN
    |         |         |         |         |         |
   20        30        40        50        60        70
```

PR-1b

```
                                  ADVGVEPLTWDDQV
                                  ::::::::::::. :
STLLLFLIISHSSHAQNSQQDYLDAHNTARADVGVEPLTWDNGVAAYAQNYVSQLAADCN
    |         |         |         |         |         |
   20        30        40        50        60        70
```

peptide are exactly matched with amino acids 46-59 of tobacco PR-1a and tobacco PR-1c proteins and show two amino acid mismatches (asparagine and glycine at positions 57 and 58) with tobacco PR-1b (Cornelissen *et al.*, 1987; Pfitzner and Goodman, 1987) (Figure 5. 3. b). The first trypsin cleavage site (arginine) is at position 45. The PR-1a, PR-1b and PR-1c are highly homologous with a molecular weight of 15 kDa (Pfitzner and Goodman, 1987). The PR-1a is induced during systemic acquired resistance (SAR) in tobacco and implicated in pathogen resistance. The estimated molecular weight of ca. 17 kDa protein from the SDS gel was in good agreement with the molecular weight of PR-1a.

5. 6 Analysis of expression of PR-P and PR-1a

5. 6. 1 Tobacco chitinase P (PR-P) mRNA is induced in *NtmybAS1* plants

Analysis of total protein expression in *NtmybAS1* overexpressing lines revealed that a ca. 27 kDa protein which was identified as tobacco PR-P (section 5. 4) is induced in these plants. To establish the relationship between the levels of *NtmybAS1* expression and induction of PR-P mRNA, expression of PR-P in *NtmybAS1* and *NtmybAS1-DBD* overexpressing lines was investigated by Northern blot analysis (section 2. 9). A 0.79 kb fragment of PR-P cDNA was amplified by reverse transcription and PCR amplification of PR-P mRNA (section 2. 6. 4) using two oligonucleotide primers including 5' -GAGAGGAAAATGGAGTTTTCTGGA TCACCAC -3' and 5' – CATAACATGATCTAACGAATCCTAGCCTTGGG -3' corresponding to the nucleotides 28-58 (coding strand) and 788-819 (complementary strand) of the PR-P in λcht28 clone (Payne *et al.*, 1990). The 0.79 kb amplified fragment was gel purified (section 2. 4. 4), radioactively labelled by $\alpha\ ^{32}$P-dCTP (sections 2. 10. 1 and 2. 10. 2) and used as a probe to hybridise the same RNA gel blot used for analysis of expression of *NtmybAS1* and *NtmybAS1-DBD* (section 3. 6).

Analysis of expression of PR-P revealed that in *NtmybAS1* overexpressing lines the PR-P mRNA is induced in a gene dosage dependent manner (Figure 5. 4). Homozygote lines (3 Hom, 7 Hom) showed higher levels of induction PR-P mRNA than heterozygotes (3 Het, 7 Het). Induction of PR-P mRNA in *NtmybAS1*

overexpressing lines was positively correlated with the level of expression of *NtmybAS1* (Figure 3. 7). The PR-P transcript was detectable at a basal level in wild type (WT1, WT2) and in four homozygote lines (9, 10, 14, 21) overexpressing *NtmybAS1-DBD*, which indicates that overexpression of *NtmybAS1-DBD* alone is not sufficient for induction of PR-P. The results derived from this analysis supported the results of protein analysis (Figure 5. 1) and confirmed that overexpression of *NtmybAS1* in tobacco induces expression of PR-P both at mRNA and protein levels.

5. 6. 2 Tobacco PR-1a mRNA is induced in *NtmybAS1* plants

To establish the relationship between the levels of *NtmybAS1* expression and induction of PR-1a mRNA, expression of PR-1a in *NtmybAS1* and *NtmybAS1-DBD* overexpressing lines was investigated by Northern blot analysis (section 2. 9). To prepare a probe for hybridisation, reverse transcription and PCR amplification (section 2. 6. 4) of PR-1a mRNA was performed using two oligonucleotide primers including 5'–ATACAACATTTCTCCTATAGTCATGGG-3' and 5'– ATTAACGT GAAATGGAC GTAGGTCG -3' to amplify a 0.56 kb fragment of PR-1a cDNA. These oligonucleotides correspond to the nucleotides 1486-1512 (coding strand) and 2021-2045 (complementary strand) of the PR-1a cDNA (Cornelissen *et al.*, 1987). The 0.56 kb amplified fragment was gel purified (section 2. 4. 4), radioactively labelled with $\alpha\ ^{32}$P-dCTP (sections 2. 10. 1 and 2. 10. 2) and used as a probe to hybridise the same RNA gel blot used for analysis of expression of *NtmybAS1* and *NtmybAS1-DBD* (section 3. 6).

This analysis revealed that the PR-1a mRNA is induced in a gene dosage dependent manner (Figure 5. 4) similar to PR-P (section 5. 6. 1). Induction of PR-1a mRNA in homozygote lines (3 Hom, 7 Hom) was higher than heterozygotes (3 Het, 7 Het) and showed a positive correlation with the levels of expression of *NtmybAS1* (Figure 3. 7). The PR-1a transcript was not detectable in wild type (WT1, WT2) and in four homozygote lines (9, 10, 14, and 21). These results were in good agreement with the results of protein analysis (Figure 5. 1) and confirmed induction of PR-1a expression both at mRNA and protein levels.

Figure 5. 4

Northern blot analysis of PR-P and PR-1a gene expression

Total RNA (30 μg per lane) was prepared from mature leaves of wild type (WT1, WT2), heterozygote (Het) and homozygote (Hom) lines overexpressing *NtmybAS1* and homozygote lines overexpressing *NtmybAS1* DNA binding domain. RNA gel blot was hybridised with a 0.79 kb fragment of PR-P and a 0.56 kb fragment of PR-1a cDNAs.

Induction of PR-P (top) and PR-1a (bottom) mRNAs in transgenic lines overexpressing the *NtmybAS1* gene. Homozygote lines (3 Hom and 7 Hom) show higher level of induction of PR-P and PR-1a mRNAs than heterozygotes (3 Het and 7 Het). The PR-P and PR-1a mRNAs are not induced in homozygote lines (9, 10, 14 and 21) overexpressing the *NtmybAS1* DNA binding domain.

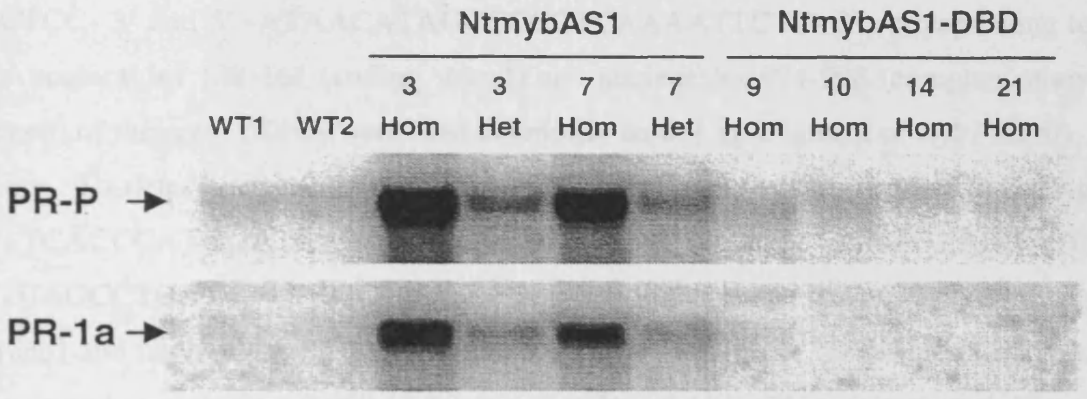
NtmybAS1
NtmybAS1-DBD
3 3 7 7 9 10 14 21
WT1 WT2 Hom Het Hom Het Hom Hom Hom Hom
PR-P
PR-1a

5. 7 Tobacco *myb1*, a SA-inducible gene, is induced in *NtmybAS1* plants

Two pathogenesis-related proteins, PR-P and PR-1a, are the components of an integrated defence system in plants that are induced in response to pathogen attack or elevated levels of SA. Application of SA activates a wide range of defence responses, which are associated with the induction of expression of PR genes (Ward *et al.*, 1991). Therefore, it was hypothesised that the induction of PR-P and PR-1a in *NtmybAS1* overexpressing lines may result from an increase in endogenous SA levels. To test this hypothesis, a RT-PCR-based approach was adopted to examine the induction of tobacco *myb1* mRNA, which encodes a component of SA signal transduction pathway leading to induction of PR-1a (Yang and Klessig, 1996).

Two oligonucleotide primers including 5' –GCAAAAGAAAATGGTGAGA GCTCC- 3' and 5' -ATAACATAGCCCCCTCAAAATTCTG- 3' corresponding to the nucleotides 138-161 (coding strand) and nucleotides 974-998 (complementary strand) of the *myb1* cDNA were used to amplify an 861 bp fragment of *myb1* cDNA.

To detect expression of *NtmybAS1*, two oligonucleotide primers including 5'–TCACCCATGGATAATAATCCCCAAAACTC- 3' and 5' –TTTGAAGGATC CTCAGCCTGATTTTGAGC- 3' corresponding to the nucleotides 638-666 (coding strand) and nucleotides 1578-1606 (complementary strand) of the *NtmybAS1* cDNA were used to amplify a 0.969 kb fragment of *NtmybAS1* cDNA as a control. These primers contain a *NcoI* site and a *BamHI* site respectively. Induction of *NtmybAS1* mRNA in wild type leaves injected with sterile water and 1 mM aqueous solution of SA was investigated in RNA samples extracted 18-24 hours after injection.

RT-PCR analyses revealed that the *NtmybAS1* transcript is not detectable in wild type leaves without any treatment or injected with sterile water and 1 mM aqueous solution of SA (Figure 5. 5. a, lanes 1-3), which indicated that the *NtmybAS1* is not an SA inducible gene. The *NtmybAS1* transcript was easily detectable in *NtmyAS1* overexpressing plants (29 Hom) and mature pollen (Figure 5. 5. a, lanes 4-5), which were used as positive controls. The *myb1* transcript was detected in *NtmybAS1* overexpressing lines without any treatment. Homozygote

NtmybAS1 overexpressing lines showed a higher level of *myb1* induction than heterozygotes (Figure 5. 5. a, lanes 6-7).

5. 8 *NtmybAS1* is not a wound-inducible gene

Induction of *myb1* mRNA in *NtmybAS1* overexpressing lines (section 5. 7) suggested that the Myb1 may act downstream of NtMybAS1 and activation of PR-P and PR-1a expression in these lines may be mediated by the action of Myb1 protein. Therefore, it was hypothesised that the bombardment of wild type tobacco leaves with a plasmid DNA expressing the *NtmybAS1* in leaves may lead to induction of *myb1* mRNA. To test this hypothesis, tobacco leaf discs were bombarded with the pRT2mybAS1 plasmid (Figure 3. 1) and tungsten particles alone (no DNA control) and the expression of *NtmybAS1*, *myb1*, *PR-P* and *PR-1a* in the bombarded leaves was analysed using RT-PCR (section 2. 6. 4). Total RNA extracted from the leaf disks 18-24 hours after bombardment and the primers described in sections 5. 6. 1, 5. 6. 2 and 5. 7 were used to investigate expression of PR-P, PR-1a, *myb1* and *NtmybAS1* in the RT-PCR analysis.

The *NtmybAS1* transcript was detectable in leaf discs bombarded with pRT2-mybAS1 plasmid (Figure 5. 5. b, lane 1). In contrast, no *NtmybAS1* transcript was detected in leaf discs bombarded with tungsten alone, indicating that the *NtmybAS1* is not a wound inducible gene (Figure 5. 5. b, lane 2). Induction of the *myb1* transcript in the control leaf discs bombarded with tungsten alone (Figure 5. 5. B, lane 3) indicated that the *myb1* is a wound inducible gene and therefore, induction of *myb1* mRNA by expression of *NtmybAS1* can not be unambiguously detected following particle bombardment.

The PR-P and PR-1a transcripts were detected in leaf discs bombarded with tungsten alone indicating that transcription of both genes are induced in response to wounding caused by bombardment (Figure 5. 5. b, lane 4-5).

5. 9 Overexpression of *NtmybAS1* in tobacco does not induce callose deposition

Figure 5. 5

RT-PCR analysis of the *NtmybAS1* and *myb1* expression

(a) *NtmybAS1* mRNA is not detected in wild type leaf (lane 1). Injection of sterile water and salicylic acid (SA) into wild type leaves does not induce *NtmybAS1* expression (lanes 2 and 3) indicating that the *NtmybAS1* is not SA inducible. The *NtmybAS1* mRNA is detected in homozygote *NtmybAS1* leaf and wild type pollen (lanes 4 and 5). Tobacco *myb1* mRNA is constitutively induced in *NtmybAS1* leaves (lanes 6 and 7). Hom: homozygote *NtmybAS1* plant; Het: heterozygote *NtmybAS1* plant.

(b) *NtmybAS1* mRNA is detected in wild type leaf bombarded with pRT2-mybAS1 plasmid DNA (lane 1), whereas in leaves bombarded with tungsten alone (no DNA control), the *NtmybAS1* mRNA is not detected (lane 2) indicating that the *NtmybAS1* is not wound inducible. Induction of tobacco *myb1*, PR-P and PR-1a mRNAs (lanes 3-5) indicates that they are wound inducible.

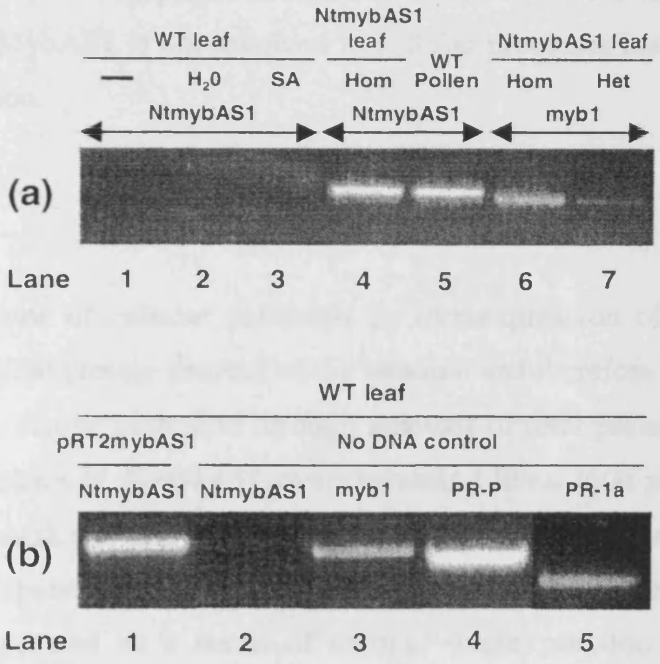
WT leaf
NtmybAS1 leaf
NtmybAS1 leaf
—
H2O
SA
Hom
WT Pollen
Hom
Het
NtmybAS1
NtmybAS1
myb1
(a)
Lane 1 2 3 4 5 6 7
WT leaf
pRT2mybAS1
No DNA control
NtmybAS1
NtmybAS1
myb1
PR-P
PR-1a
(b)
Lane 1 2 3 4 5

Induction of expression of pathogenesis-related proteins in response to pathogen invasion is generally associated with the deposition of callose (β–1,3 glucan). Synthesis of callose is catalysed by callose synthase, which is localised in the plasma membrane. Wounding, stress, elicitors and toxicity also induce callose deposition (Bowles *et al.*, 1990).

To determine whether overexpression of *NtmybAS1* in tobacco induces callose formation, leaves from wild type and *NtmybAS1* overexpressing plants were stained to visualise callose deposition through aniline blue-induced fluorescence of callose (section 2. 19). No increase in callose formation was detected in leaves of *NtmybAS1* overexpressing plants examined, which indicates that the high level expression of NtMybAS1 is not involved in cellular processes leading to activation of callose formation.

5. 10 Discussion

Perturbations of cellular pathways by overexpression of a gene or other stimuli affects global protein product of the genome and therefore potential markers for each stimulus can be identified through analysis of total protein expression. To identify such markers in *NtmybAS1* overexpressing lines, total protein expression was analysed through one and two-dimensional polyacrylamide gel electrophoresis. This approach opened up the possibility of identifying the genes that are differentially expressed as a result of ectopic overexpression of *NtmybAS1* in tobacco. These analyses consistently visualised two marker proteins that are differentially activated in *NtmybAS1* overexpressing lines. Classical Edman sequencing approach (section 2. 13. 4) was adopted to identify the sequence of these markers and thereby the biological pathways, affected by the ectopic overexpression of *NtmybAS1* were determined.

5. 10. 1 Overexpression of *NtmybAS1* in tobacco differentially activates expression of PR-P and PR-1a

The results presented in Figures 5. 1, 5. 3 and 5. 4 clearly demonstrate that the constitutive expression of *NtmybAS1* in tobacco by the CaMV35S promoter results in induction of expression of tobacco PR-P and PR-1a in a gene dosage dependent manner.

The three members of PR-1 gene family consist of PR-1a, PR-1b and PR-1c encode highly homologous acidic extracellular proteins of about 15 kDa. Biochemical function and cellular target of the PR-1 gene family are unknown.

The PR-P and PR-Q genes from the PR-3 family of pathogenesis-related proteins encode acidic extracellular chitinases (Payne *et al.*, 1990). Chitinase activity has been shown for the genes of this group in tobacco (Legrand *et al.*, 1987). Expression of PR-1a, PR-P and the genes belonging to seven other groups (PR-2, PR-4, PR-5, basic form of PR-1, basic class III chitinase, acidic class III chitinase, extracellular β-1,3-glucanase PR-Q) of pathogenesis-related proteins in tobacco are induced during the development of systemic acquired resistance in response to tobacco mosaic virus and by exogenous application of SA (Ward *et al.*, 1991).

PR-P and PR-1a are the two markers of SA-dependent resistant in plants. Studies of *cpr1* (Bowling *et al.*, 1994), *lsd* (Dietrich *et al.*, 1994, Weymann *et al.*, 1995) *acd* (Greenberg *et al.*, 1994), *npr1* (Cao *et al.*, 1994; Cao *et al.*, 1997), *eds* (Glazebrook *et al.*, 1996; Parker *et al.*, 1996; Rogers and Ausubel, 1997) and *ndr1-1* (Century *et al.*, 1995) mutants in *Arabidopsis* have established that the development of SAR and consequently plant resistance to pathogen attack depends on accumulation of SA and further induction of PR proteins.

Considering the SA-inducibility of PR-P and PR-1a, one possible explanation for the activation of PR-P and PR-1a expression in *NtmybAS1* overexpressing lines was an increase in endogenous SA levels. It was expected that an increase in endogenous SA levels would increase expression of the components of SA signal transduction pathway that act down stream of SA. One of these components, which is encoded by the tobacco *myb1* gene has been shown to be rapidly induced by exogenous application of SA (Yang and Klessig, 1996). Demonstration of induction of tobacco *myb1* mRNA in a gene dosage dependent manner in *NtmybAS1* overexpressing lines (Figure 5. 5. a) provided further evidence of the involvement of SA in activation of PR-P and PR-1a. The higher levels of induction of PR-P, PR-1a

and myb1 expression in homozygote plants overexpressing the *NtmybAS1* suggests that the increase in endogenous SA levels in these plants may be higher than heterozygotes.

In *Arabidopsis*, mutations in two genes *cpr1* and *cpr5* that lead to elevated levels of SA and constitutive expression of plant defence response genes have been shown to cause a dwarf phenotype (Bowling *et al.*, 1994; Bowling *et al.*, 1997). The *cpr1* mutant of *Arabidopsis* shows reduced plant size, leaves with dark green color and increased trichome numbers. Suppression of these phenotypes in the progeny of crosses between the *cpr1* and *nahG* plants (overexpressing salicylate hydroxylase which converts salicylic acid to catechol) has led to this suggestion that the phenotypes described for the *cpr1* mutation results from an increase in SA levels (Bowling *et al.*, 1994).

This evidence suggests that the dwarf features of *NtmybAS1* overexpressing plants may also result from elevated levels of SA. It is unlikely that the constitutive expression of PR-P and PR-1a in *NtmybAS1* overexpressing plants causes the dwarf features of these plants. This conclusion is supported by evidence demonstrating that the overexpression of PR-1a, GRP and PR-S in tobacco does not result in reduced growth rate or abnormal growth (Linthorst *et al.*, 1989).

5. 10. 2 NtMybAS1 acts upstream of gPAL1 to activate PR expression

Establishment of a relationship between the expression of *NtmybAS1* and *gPAL1* (Fukasawa-Akada *et al.*, 1996) during anther development (Figure 3. 12) and further demonstration of induction of *gPAL1* expression in *NtmybAS1* overexpressing lines (Figure 3. 13) suggest that the *NtmybAS1* acts upstream of *gPAL1* as a transcription activator.

Two separate sets of results including induction of gPAL1 expression (Figure 3. 13) and activation of PR-P, PR-1a (Figures 5. 1, 5. 4) and *myb1* (Figure 5. 5) expression in *NtmybAS1* overexpressing lines can be linked via the action of SA. The PR-P, PR-1a, and *myb1* are SA inducible (Ward *et al.*, 1991, Yang and klessig, 1996) and SA is formed in the phenylpropanoid pathway (Lee *et al.*, 1995; Leon *et al.*, 1993, Yalpani *et al.*, 1993; Dixon and Paiva, 1995). The first enzyme of this

pathway, PAL, catalyses the conversion of phenylalanine to *trans*-cinnamic acid which serve as a precursor of SA. It has been shown that the synthesis of SA from *trans*-cinnamic in tobacco occurs via benzoic acid and *o*-coumaric acid is not used as a precursor of SA (Yalpani *et al.*, 1993). The synthesis of SA from cinnamic acid via benzoic acid has also been shown in rice seedlings (Silverman *et al.*, 1995)

A model is proposed in Figure 5. 6 to illustrate the role of NtMybAS1 protein in activation of *gPAL1* expression and the possible mechanisms of induction of PR expression in *NtmybAS1* overexpressing lines. In this model, the NtMybAS1 protein binds to the MBSI and MBSII motifs in *gPAL1* promoter and activates transcription of gPAL1. Several pieces of evidence indicate that an increase in PAL transcription generally results in an increase in PAL activity (Edwards *et al.*, 1985; Fritzemeier *et al.*, 1987; Lawton and Lamb, 1987; Orr *et al.*, 1993). Induction of gPAL1 expression and consequently increased gPAL1 activity in *NtmybAS1* overexpressing lines causes a flux through a branch of phenylpropanoid pathway in which SA is synthesised. Elevated SA levels induces expression of the components of SA signal transduction pathway such as tobacco *myb1* (Figure 5. 5) leading to induction of PR proteins.

This model is supported by the finding that the NtMybAS1 protein binds to MBSI and MBSII motifs in two PAL promoters and transactivates GUS expression in tobacco protoplast (Yang *et al.*, 2000). However, the possibility of a SA-independent mechanism for the induction of PR-P and PR-1a by the NtMybAS1 protein can not be excluded. In this case the NtMybAS1 protein directly or via a cofactor binds to MBS motifs in the promoters of PR-P and PR-1a and activates transcription of PR-P and PR-1a. In addition to MBSI and MBSII, the promoter of PR-1a contains four MBSI-like motifs showing a five-nucleotide match with the consensus MBSI motif (Yang and Klessig, 1996).

The promoter sequence of PR-P has not been published. Therefore, the presence of MBS motifs in this promoter is unknown. However, the MBS and MBS-like motifs are found in the promoters of other tobacco chitinases. For example, a search for the presence of MBS motifs in the tobacco class I chitinase, chn50 (van Buuren *et al.*, 1992) promoter revealed that it contains one MBSII motif (GTTTGTT), seven MBSI-like and four MBSII-like motifs. Currently, transcription

Figure 5. 6

Schematic representation of the regulatory function of NtMybAS1 protein

MBSI and MBSII: Myb binding sequences
PAL: Phenylalanine ammonia-lyase
BA2H: Benzoic acid 2-hydroxylase

The NtMybAS1 protein binds to MBSI and MBSII motifs in *gPAL1* promoter and induces *gPAL1* expression. Increase in gPAL1 activity induces SA synthesis from *trans*-cinnamic acid via benzoic acid. The elevated SA levels leads to induction of PR-1a and PR-P via SA signal transduction pathway. The tobacco Myb1 protein as a component of SA signal transduction pathway is involved in the process of induction of PR-1a expression. Alternatively, the NtMybAS1 protein may directly or via cofactors such as Myb1 bind to MBSs in PR-1a and PR-P promoters and induce PR-1a and PR-P expression.

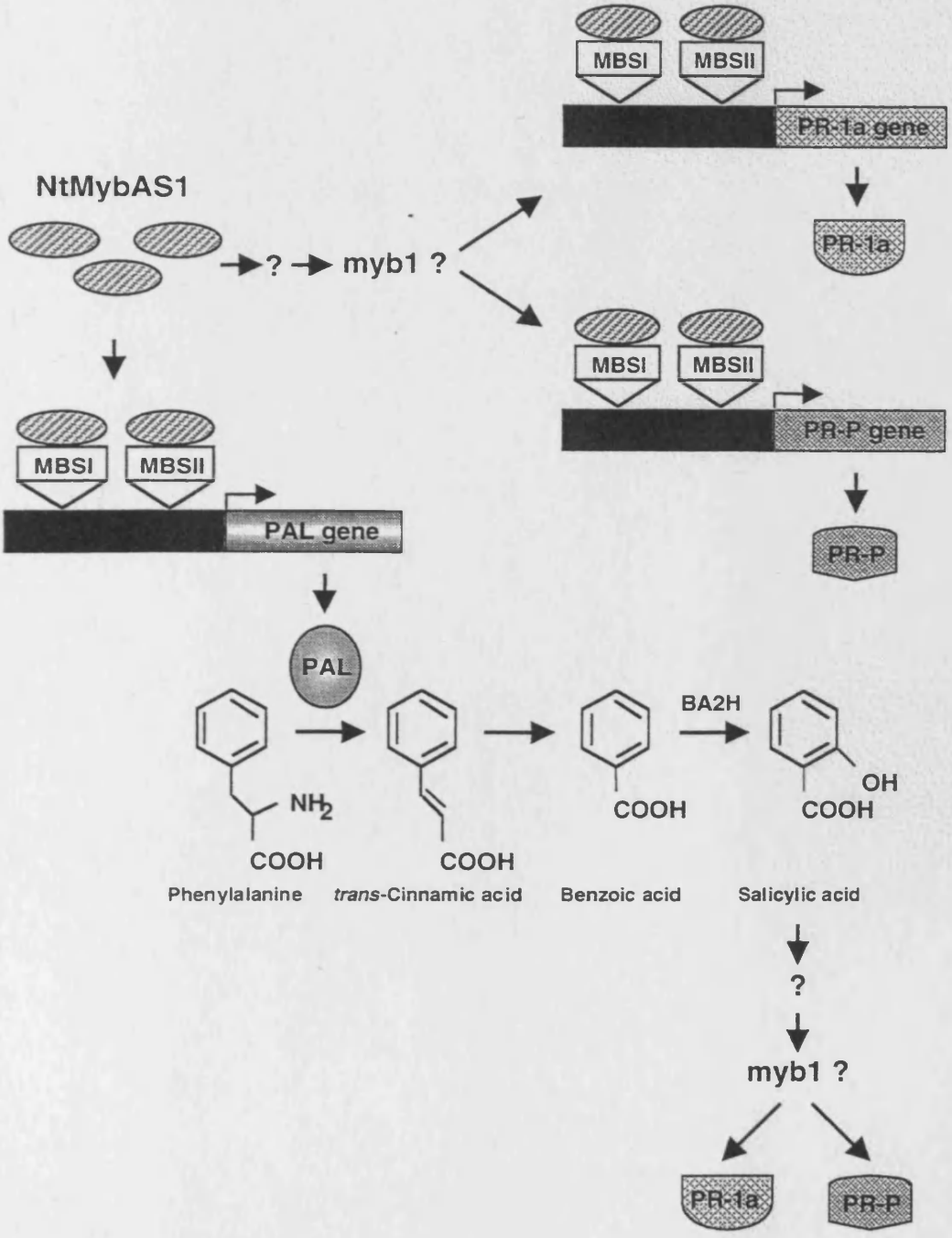
MBSI
MBSII
PR-1a gene
NtMybAS1
?
myb1 ?
PR-1a
MBSI
MBSII
PR-P gene
PR-P
MBSI
MBSII
PAL gene
PAL
BA2H
NH2
COOH
COOH
COOH
OH
COOH
Phenylalanine
trans-Cinnamic acid
Benzoic acid
Salicylic acid
?
myb1 ?
PR-1a
PR-P

factors regulating PR gene expression are unknown and among the members of *myb* gene family, only tobacco Myb1 has been shown to bind the MBS motifs in PR-1a promoter and therefore, potentially play a direct role in regulation of PR-1a expression (Yang and Klessig, 1996).

Chapter 6

General discussion

6. 1 The tobacco *NtmybAS1* is a novel anther specific member of the plant *myb* gene family

The first evidence for the involvement of plant Myb proteins in regulation of gene expression in pollen was provided by the isolation and characterisation of two cDNA clones (*NtmybAS1* and *NtMybAS2*) encoding Myb-related proteins from a tobacco pollen cDNA library (Sweetman, 1996). Initially, similarity searches revealed that the NtMybAS1 protein shares the highest sequence homology to plant Myb-related proteins including PhMYB3 and PhMYB2 (Avila *et al.*, 1993) from *Petunia hybrida*, ZmP1 (Grotewold *et al.*, 1994) from maize and GAMyb (Gubler *et al.*, 1995) from barley (Sweetman, 1996). However, during the course of this study a large number of *myb*-related sequences particularly from *Arabidopsis thaliana* were submitted to current databases. A recent similarity search using FASTA version 3 (ExPASy Molecular Biology Server, www.expasy.ch) revealed that NtMybAS1 protein shows higher sequence identity (%) to a number of plant Myb proteins different from those previously reported (Sweetman. 1996). Apart from PhMYB3 (Q02994; 63.7%) with the highest sequence identity to NtMybAS1 the most closely related plant Myb proteins to NtMybAS1 include Myb-related proteins (O80883, 38.3%; and BAB10576, 40.8%) from *Arabidopsis thaliana*, GAMyb (Q9XEP0; 36.5%) from *Lolium temulentum* (Gocal *et al.*, 1999) and GAMyb (P93417; 40.7%) from rice (Oryza sativa).

Considering the functions of PhMYB3, which is strongly implicated in control of flavonoid biosynthesis (Avila *et al.*, 1993; Solano *et al.*, 1995) and the two GAMyb proteins described above, which are involved in the GA signalling pathway, it is evident that this group of structurally similar Myb proteins do not perform similar functions in plants.

Analysis of temporal and spatial expression patterns of *NtmybAS1* led to the conclusion that *NtmybAS1* is pollen-specific and may play a regulatory role during pollen development (Sweetman, 1996). In this work analysis of expression of *NtmybAS1* during five stages of anther development and in mature pollen (Figure 3. 12) revealed that the *NtmybAS1* transcript is detectable at the early stages of anther development when flower buds are 10-12 and 12-16 mm. The level of *NtmybAS1*

transcript reached a maximum level at the mature pollen stage (section 3. 10). Furthermore, *in situ* localisation of *NtmybAS1* mRNA detected *NtmybAS1* transcripts in the tapetum, stomium and vascular tissues of anthers at the same developmental stages described above and also in developing pollen (Yang *et al.*, 2000), which was consistent with the results of Northern blot analysis (Figure 3. 12). These data provided a broader view of the temporal and spatial pattern of *NtmybAS1* expression and clearly demonstrated that the *NtmybAS1* is anther-specific and its expression is developmentally regulated in sporophytic and gametophytic cell types.

Recently, an anther-specific member of the *myb* gene family (*Atmyb103*) has been reported in *Arabidopsis*, which is expressed specifically in the tapetum and middle layer of anthers but not in pollen (Li *et al.*, 1999). These findings indicate the involvement of plant Myb-related proteins in regulation of gene expression during anther development and also add a new function to the list of previously known functions of plant Myb proteins (reviewed in Jin and Martin, 1999).

6. 2 Overexpression of *NtmybAS1* results in cell autonomous and gene dosage dependent dwarfing in tobacco

The most outstanding effect of overproduction of NtMybAS1 in tobacco was a general reduction in plant growth leading to a dwarf phenotype (section 3. 3). Identification of two distinct classes of dwarf phenotype in the progeny of four primary transformants and further analysis of *NtmybAS1* expression (Figure 3. 7) in these plants demonstrated that the levels of dwarfing were directly related to the levels of *NtmybAS1* transcripts. The effect of overproduction of NtMybAS1 on plant development was not limited to a specific stage. Phenotypic alterations including reduced root and shoot growth, epinastic curvature of leaves (section 3. 3) and changes in cell morphology (section 4. 6) were detectable at the seedling stage. The growth rates of the heterozygote and homoygote *NtmybAS1* plants were constantly lower than wild type (Figure 3. 6. a). Furthermore, *NtmybAS1* plants showed reduced size of flowers and seed capsules.

To gain further insight into the functional domains of NtMybAS1, the DNA binding domain (*NtmybAS1-DBD*) and a C-terminally truncated (*NtmybAS1-ClaI*)

version of *NtmybAS1* (sections 3.5, 3.7) were overexpressed in tobacco and the phenotype of resulting transformants were characterised. The finding that plants overexpressing the truncated versions of NtMybAS1 were phenotypically normal indicated that the induction of dwarfing requires the expression of a full-length NtMybAS1 protein and further suggested that the *trans*-activation activity of NtMybAS1 is dependent on the function of its C-terminus. This conclusion was supported by the results of transient expression analysis using GUS reporter gene (Yang *et al.*, 2000) demonstrating that the C-terminus of the NtMybAS1 is required for *trans*-activation of two PAL promoters including *PALA* (Pellegrini *et al.*, 1994) and *gPAL1* (Fukasawa-Akada *et al.*, 1996). Further support was provided by the finding that the sequence between amino acids 264 and 318 is essential for *trans*-activation activity of NtMybAS1 protein (Yang *et al.*, 2000), which was truncated both in *NtmybAS1-DBD* and *NtmybAS1-ClaI* constructs.

Analysis of distribution of charges in the NtMybAS1 protein using SAPS (Statistical Analysis of Protein Sequences) software (ExPASy Molecular Biology Server, www.expasy.ch) to determine the regions with a relatively high charge concentration detected a cluster of negative charge, EEYGLSEEAEDIILTEESTFSFAQQGGED, at position 361-389. Further analysis of this motif using the secondary structure predictions within MacVector Sequence Analysis Software (Oxford Molecular Group PLC) predicted a α-helical structure for this motif, which is characteristic of a *trans*-activation domain. However the results of transient expression assay indicated that deletion of the NtMybAS1 C-terminus containing this motif does not significantly reduce *trans*-activation of *PALA* and *gPAL1* (Yang *et al.*, 2000).

Demonstration of localisation of NtMybAS1 in the pollen nucleus (section 3. 9) was in good agreement with its *trans*-activation function. Localisation of plant Myb proteins in the nucleus has been shown by immunocytochemical analysis in the case of petunia PhMyb3 (Avila *et al.*, 1993) and by transient expression assay in the onion epidermal cells for the *Arabidopsis* Myb-related protein CCA1 (Wang *et al.*, 1997). However, in neither case has the signal responsible for nuclear targeting been identified. Although analysis of NtMybAS1 protein sequence using PSORT software (ExPASy Molecular Biology Server, www.expasy.ch) did not detect any nuclear

signal motif, transient expression of the N-terminal Myb domain derivatives fused to sGFP reporter gene demonstrated the importance of RLKRRQR motif (aa.119-125) in targeting sGFP reporter protein to the pollen nucleus (section 3. 9. 5). Removing this motif from the N-terminal Myb domain dramatically reduced nuclear localisation of sGFP. The finding that RLKRRQR motif alone is not sufficient to fully direct sGFP to the pollen nucleus clearly demonstrated that the NtmybAS1 nuclear localisation signal is not monopartite. Furthermore, the RLKRRQR motif alone partially directed sGFP to the nucleolus (Figure 3. 11. d). This motif basic in nature to some extent resembles nucleolar targeting signals of rat ribosomal protein L31 (RLSRKR) (Quaye *et al.*, 1996), and the human fragile X-related proteins FXR2P (RPQRRNRSRRRRFR) belonging to the family of RNA binding proteins (Tamanini *et al.*, 2000). Furthermore, the finding that the arginine rich motifs bind RNA and their binding affinity is dramatically enhanced by the presence of a single glutamine (Q) or asparagine (N) mainly due to the specific contact of carboxamide group of these amino acids with the AG bases of RNA by hydrogen bonds (Tan and Frankel, 1998) raises the possibility that partial localisation of RLKRRQR motif in nucleolus is mediated by a similar mechanism via RNA binding.

Analysis of expression of *NtmybAS1* revealed that the intensity of radioactive signals (Figure 3. 7) corresponding to the *NtmybAS1* transcripts in two homozygote *NtmybAS1* lines (3 Hom and 7 Hom) were approximately three times higher than in heterozygotes (3 Het and 7 Het). However, it can not be unambiguously concluded that the difference in levels of *NtmybAS1* transcripts between the homozygote and heterozygote *NtmybAS1* plants is non-linear. Reduction of plant height (section 3. 3; Figure 3. 6. a) and internode length (section 3. 3; Figure 3. 6. b) in homozygote and heterozygote *NtmybAS1* plants were not linear. The non-linear reduction of plant height in homozygote plants may be a consequence of increased level of co-operative interaction of NtMybAS1 protein with the *cis*-acting elements in the target promoters. Such co-operativity leading to a dramatic increase in occupancy of the target *cis*-acting elements has been shown for the yeast (*Saccharomyces cerevisiae*) heat shock factor (HSF) (Erkine *et al.*, 1999). In addition co-operative binding and synergistic *trans*-activation of the α-coixin gene promoter has been shown for the maize Opaque2 (Yunes *et al.*, 1998).

The finding that the mean internode number in heterozygote and homozygote *NtmybAS1* plants was not significantly different from wild type (Figure 3. 6. b) and further demonstration of a severe reduction in hypocotyl cell expansion parallel to the apical-basal axis (Figure 4. 3) demonstrated that the *NtmybAS1*-induced dwarfing is a consequence of dramatic reduction in cell elongation.

Analysis of effect of phytohormones and their inhibitors on *NtmybAS1* phenotype led to the conclusion that neither GA and BR deficiency nor elevated level of ethylene cause the dwarf features of *NtmybAS1* plants (sections 4. 2 and 4.3 and 4. 4). The dwarf phenotype of *NtmybAS1* plants was not also normalised by grafting (section 4. 5). Grafting provides a route for translocation of signals such as phytohormones and the evidence discussed in section 4. 8. 1 indicates that translocation of different GAs through grafting vary to a great extent. The fact that no transmissible signal through grafting normalised the *NtmybAS1* phenotype demonstrated that the dwarfing is cell autonomous.

Results derived from reciprocal grafting (section 4. 5) were consistent with the results of root–specific expression of *NtmybAS1* (section 3. 8) using the –90 region of the *CaMV35S* promoter and demonstrated that the root-specific expression of *NtmybAS1* is not sufficient for the induction of dwarfing.

The effect of overproduction of NtMybAS1 can be examined in other plant species to determine whether it causes a similar dwarf phenotype as in *NtmybAS1* plants. Overexpression of *myb* genes with known functions in heterologous species does not necessarily lead to a similar phenotype. The *GLABROUS 1* (*GL1*) gene of *Arabidopsis* encodes a Myb-related protein, which is necessary for the initiation of trichome development (Oppenheimer *et al.*, 1991). Overexpression of *GL1* in tobacco does not affect the phenotype of trichomes. In contrast, overexpression of the *MIXTA* gene of *Antirrhinum* in tobacco results in formation of numerous multicellular trichomes and development of conical cells of leaf epidermis (Glover *et al.*, 1998). These pieces of evidence led to the conclusion that trichomes in *Arabidopsis* and *Nicotiana* are not structurally homologous and different regulatory proteins control their differentiation. Similarly, overexpression of *NtmybAS1* in other plant species would not necessarily result in a dwarf phenotype. However, *NtmybAS1*

overexpression may induce dwarfing in certain plant species and therefore, could be of value for commercial applications.

Incorporation of dwarfing genes into commercial varieties of crop plants has had a great impact on agricultural production. This dramatic increase in crop yield has been mainly due to reduced lodging of semi-dwarf varieties of crop plants, which resist wind and rain damage (Hoisington *et al.*, 1999; Silverstone and Sun, 2000). Modification of plant architecture by manipulation of expression of a dominant gene such as *NtmybAS1* could potentially be applicable for crop improvement. This strategy has the advantage that the expression of transgene could be targeted to the specific tissue/organ using tissue/organ-specific promoters.

6. 3 The NtMybAS1 protein activates PR gene expression via a salicylic acid-dependent signal transduction pathway

Fundamental insights into the molecular basis of *NtmybAS1*-induced dwarfing were provided by comparing the total protein profile of *NtmybAS1* plants with wild type using one and two-dimensional gel electrophoresis (sections 5. 2 and 5.3; Figures 5. 1 and 5. 2). These analyses led to the identification of two marker proteins of approximately 17 kDa and 27 kDa, which were differentially activated as a result of *NtmybAS1* overexpression. A detailed characterisation of these two proteins using in-gel digestion with trypsin (section 2. 13. 1), reversed-phase HPLC (section 2. 13. 2) and N-terminal sequencing by Edman degradation method (section 2. 13. 4) demonstrated that the two induced proteins are PR-P (section 5. 4) and PR-1a (section 5. 5). Induction of expression of PR-P and PR-1a in *NtmybAS1* plants were also demonstrated at mRNA level by Northern blot analysis (Figure 5. 4). Interestingly, both PR-P and PR-1a mRNAs were induced in a gene dosage-dependent manner and showed a positive correlation with the level of *NtmybAS1* transcripts. Moreover, the relationship between the levels of PR-P and PR1a mRNAs in heterozygote and homozygote genotypes similar to *NtmybAS1* transcripts (section 6. 2) was not linear.

The PR-P and PR-1a are among the nine classes of pathogenesis-related proteins, which are co-ordinately activated in tobacco during the onset of SAR

(Ryals *et al.*, 1994) in response to tobacco mosaic virus (TMV) and to exogenous application of SA (Ward *et al.*, 1991). Development of SAR depends on elicitation of a hypersensitive response (HR) upon viral, bacterial or fungal infection. Once SAR is established it enhances a long lasting resistance to subsequent pathogen attack both locally at the initial infection site and systemically in the uninfected tissues distant from the primary site of pathogen attack. SAR is not necessarily specific to the primary pathogen and confers enhanced resistance against a wide spectrum of plant pathogens. A considerable body of evidence indicates that the induction of a large number of defence-related genes (Reymond and Farmer, 1998) in higher plants is regulated via a small number of signal transduction pathways including SA (Durner *et al.*, 1997), jasmonic acid (JA) (Creelman and Mullet, 1997) and ethylene (Ecker, 1995). It has been shown that SA is an absolutely essential signal for the induction of SAR. Tobacco plants expressing the *nahG* gene of *Pseudomonas putida*, the product of which converts salicylic acid to catechol fail to establish SAR (Gaffney *et al.*, 1993).

Although the evidence described above implies that the activation of PR-P and PR-1a in *NtmybAS1* plants is via a SA-dependent signal transduction pathway, the other SA-inducible PR proteins (Ward *et al.*, 1991) were not detectable by one-dimensional SDS-PAGE (Figure 5. 1). Further characterisation of differentially expressed proteins identified in two-dimensional gels (Figure 5. 2) using the highly sensitive mass spectrometry could provide more insights into the molecular basis of *NtmybAS1*-induced gene expression.

The reports concerning the mechanism of SA signal transduction leading to activation of PR proteins are not consistent. Purification of SA binding protein (SABP) from tobacco, the similarity of SABP sequence to plant catalases and demonstration of catalase activity of SABP *in vitro* led to the conclusion that the SA acts as an inhibitor of catalase and therefore, the induction of PR proteins during SAR is a consequence of elevated level of H_2O_2 (Chen *et al.*, 1993a; Chen *et al.*, 1993b). However, demonstration of binding of SA to a number of iron containing enzymes has strongly argued against the hypothesis described above (Rüffer *et al.*, 1995).

Further evidence of involvement of SA in *NtmybAS1*-induced dwarfing was provided by demonstration of induction of tobacco *myb1* mRNA (section 5. 7), which encodes a Myb-related component of SA signal transduction pathway and is activated upon TMV infection and by the exogenous application of SA (Yang and Klessig, 1996). Induction of *myb1* mRNA in homozygote *NtmybAS1* plants with a severe dwarf phenotype was higher than heterozygotes with a semi-dwarf phenotype (Figure 5. 5) and showed a positive correlation with level of *NtmybAS1* expression (Figure 3. 7). These data suggested that the overproduction of NtMybAS1 protein in tobacco might result in a rise in the endogenous SA levels, which in turn triggers the induction of PR-P and PR-1a expression.

The mechanisms of triggering SAR gene expression by SA have been under intense investigation. The *PR* genes as markers of SAR have been used to isolate the genes encoding components of SA-mediated PR gene expression. The *NPR1* mutant of *Arabidopsis* is defective in SA- or INA (2,6-dichloroisonicotinic acid)-induced PR expression. The *NPR1* (Cao *et al.*, 1997; Cao *et al.*, 1998) product, which contains an ankyrin, repeat domain is the key component of SA signal transduction pathway leading to PR expression. It has been shown by yeast two-hybrid assay that the NPR1 interacts with the basic leucine zipper proteins (AHBP-1b and TGA6). Furthermore, demonstration of specific binding of AHBP-1b to *as-1* element, a SA responsive elements in the PR-1 gene promoter (Lebel *et al.*, 1998) led to the suggestion that regulation of PR-1 expression by NPR1 is via interaction with the basic leucine zipper transcription factors (Zhang *et al.*, 1999).

The evidence described in section 5. 10. 1 supports the idea that the dwarf features of *NtmybAS1* plants are not a direct consequence of elevated levels of PR-P and PR-1a proteins and more likely result from elevated level of endogenous SA. This is further supported by several lines of evidence indicating the growth inhibitory effects of SA both in animal and plant systems. In animal systems much attention has been focused on the effect of SA on growth of cancer cells. It has been shown that SA and its derivatives inhibit cell growth and proliferation and induce apoptosis in human and animal cancer cells (Aas *et al.*, 1995; Viljoen *et al.*, 1995; Elder *et al.*, 1996; Bus *et al.*, 1999; Sotiriou *et al.*, 1999). In plants the sulfur-containing derivatives of SA including thiosalicylic acid and methyl acetylthiosalicylate have

inhibitory effects on root growth and seed germination and cause a reduction in chlorophyll level (Inamori *et al.*, 1993). Furthermore, it has been reported that treatment of *acd6–nahG* plants with BTH, benzo (1,2,3) thiadiazole-7-carbothioic acid, which induces SA signaling pathway results in abnormal growth and formation of clusters of enlarged cells along the abaxial leaf surface (Rate *et al.*, 1999). These pieces of evidence suggest that SA may play a role in modulation of cell growth. However, the mechanisms by which SA affects cell growth are unknown. Based on the evidence described above the possibility that the severe alterations of cell morphology in *NtmybAS1* plants described in sections 4. 6. 1, 4. 6. 2 and 4. 6. 3 may be a direct consequence of elevated endogenous SA levels or sensitivity to SA can not be excluded.

Two sets of experiments could provide more direct evidence for the involvement of SA in *NtmybAS1*-induced dwarfing. First the endogenous SA levels in *NtmybAS1* plants can be compared with wild type by HPLC analysis. Furthermore, the crosses between the *NtmybAS1* and *nahG* plants (Gaffney *et al.*, 1993) would help to determine whether an arrest in the SA signalling pathway could restore the wild type phenotype in *NtmybAS1* plants.

In eukaryotes and eubacteria SA is synthesised through different pathways. In *Mycobacterium* species SA is initially synthesised from shikimate via chorismate and eventually isochorismate, which apparently is the only intermediate of SA (Marshall and Ratledge, 1972), whereas in plants SA is a product of phenylpropanoid metabolism (Hahlbrock and Scheel, 1989; Dixon and Paiva, 1995). The first enzyme of the phenylpropanoid pathway, PAL, catalyses deamination of phenylalanine to *trans*-cinnamic acid. Following this step SA is synthesised from *trans*-cinnamic acid via two routes. The first route involves side chain decarboxylation of *trans*-cinnamic acid to benzoic acid and further 2-hydroxylation to SA, which is catalysed by benzoic acid 2-hydroxylase. The second route involves 2-hydroxylation of *trans*-cinnamic acid to *ortho*-coumaric acid and further oxidation of the side chain to give SA (reviewed in Lee *et al.*, 1995). Although in some plant species such as *Primula acaulis* and *Gaultheria procumbens* SA is synthesised via both pathways described above (Lee *et al.*, 1995) in tobacco (Yalpani *et al.*, 1993), rice (Silverman *et al.*,

1995), potato (Coquoz *et al.*, 1998) and cucumber (Meuwly *et al.*, 1995) the synthesis of SA from phenylalanine proceeds via benzoic acid.

Unpublished data suggests that SA in concentrations more than 0.1 mM causes phytotoxicity in tobacco (Lee *et al.*, 1995). Furthermore, long exposure of tobacco leaves to 0.5 mM SA has been shown to reduce catalase and ascorbate peroxidase activities and causes phytotoxicity (Rao *et al.*, 1997). It has been shown by HPLC analysis that the treatment of tobacco leaves with 5 mM SA reduces the level of the major photosynthetic pigments (Rao *et al.*, 1997). As described in section 3. 4, the total chlorophyll content of the heterozygote *NtmybAS1* leaves was 24% lower than wild type. Based on the evidence described above the reduction of chlorophyll content, which gave the older *NtmybAS1* leaves a paler appearance and resembled mottling may be a consequence of elevated SA levels in *NtmybAS1* plants.

The high level accumulation of PR-P and PR-1a proteins in *NtmybAS1* plants may confer protection against infection by certain pathogens. Overexpression of the bean chitinase gene in tobacco results in increased protection against *Rhizoctonia solani* (Broglie *et al.*, 1991). It has been shown that the overexpression of *PR-1a* in tobacco results in enhanced tolerance to the fungal pathogens including *Peronospora tabacina* and *Phytophthora parasitica* var. *nicotianae* (Alexander *et al.*, 1993). The product of the osmotin gene of tobacco has a defensive role against infection of potato by the parasitic fungus *Phytophthora infestans* (Liu *et al.*, 1994). Co-expression of the rice RCH10 basic chitinase and the alfalfa AGLU1 acidic glucanase in tobacco confer a greater tolerance against the parasitic fungus *Cercospora nicotianae* than is obtained by expression of any of these genes alone (Zhu *et al.*, 1994). Furthermore, coexpression of barley chitinase and β-1,3-glucanase or chitinase and type I ribosome-inactivating protein (RIP) in tobacco provide a synergistic protection against *Rhizoctonia solani* (Jach *et al.*, 1995). Moreover, it has been reported that the differentiation of infection hyphae of the rust fungus *Uromyces fabae* is inhibited by the PR-1 protein purified from the SA treated leaves of broad bean (Rauscher *et al.*, 1999).

Although the examples presented above supports the idea that the accumulation of specific PR proteins in transgenic plants could provide higher levels of protection against certain pathogens it should be considered that in some cases

accumulation of PR proteins is not associated with increased anti-pathogenic activity. Overproduction of PR proteins including PR-1, GRP and PR-S in tobacco does not result in enhanced protection against tobacco mosaic virus and alfalfa mosaic virus (Linthorst *et al.*, 1989). The high level expression of PR-1b in tobacco does not alleviate systemic symptoms of tobacco mosaic virus infection (Cutt *et al.*, 1989). Accumulation of class I basic chitinase in tobacco leaves does not confer increased protection against *Cercospora nicotianae* (Neuhaus *et al.*, 1991) Furthermore, suppression of β-1,3-glucanase expression does not alter plant susceptibility to *Cercospora nicotianae* (Neuhaus *et al.*, 1992).

Considering the evidence described above the *NtmybAS1* could be overexpressed in heterologous systems to determine the activation of PR gene expression and the spectrum of protection provided against plant pathogens. This approach may also be applicable in certain crop species to engineering enhanced tolerance against plant pathogens. However, it should be noted that the accumulation of specific PR proteins such as PR-P and PR-1a as a result of NtmybAS1 overexpression would not be sufficient to induce a broad-spectrum resistance against plant pathogens.

Taken together, the data presented here strongly support the conclusion that the overproduction of NtMybAS1 in tobacco triggers gene expression upstream of SA signal transduction pathway leading to induction of PR proteins including PR-P and PR-1a.

6. 4 The NtMybAS1 acts as a positive regulator of *gPAL1* transcription in sporophytic tissues of tobacco anthers

The results derived from Northern blot (Figure 3. 12), *in situ* hybridisation and transient expression (Yang *et al.*, 2000) analyses provided compelling evidence to conclude that the NtMybAS1 protein acts as an anther-specific transcription factor and regulates *gPAL1* expression at the early stages of anther development in sporophytic and not in gametophytic tissues of tobacco anthers. These data further suggest that the induction of *gPAL1* expression in sporophytic tissues of anther particularly at a high level in tapetal cells is part of a developmental program to

provide the precursors of the phenylpropanoid metabolites essentially required for pollen development and fertility.

The tapetal layer activity is absolutely essential for pollen development. The functions of tapetum and the metabolites released from this layer during anther development were discussed in sections 1. 11 and 1. 13. Male sterile tobacco and oilseed rape has been generated by disruption of tapetum using the tapetum specific promoter TA29 to drive expression of barnase gene of *Bacillus amyloliquefaciens*, which encodes a cytotoxic extracellular RNase (Mariani *et al.*, 1990). Furthermore, it has been shown that the male fertility can be restored in TA29-barnase expressing plants by tapetum-specific expression of barstar gene, which encodes the corresponding RNase inhibitor (Mariani *et al.*, 1992). Selective disruption of tapetal layer in tobacco by expression of cytotoxic diphteria toxin A-chain (DTA) driven by the tapetum specific TA29 promoter results in male sterile plants lacking pollen grains at dehiscence (Koltunow *et al.*, 1990). In petunia the antisense inhibition of chalcone synthase activity in tapetum results in formation of unpigmented anthers leading to male sterility (van der Meer *et al.*, 1992). The biological significance of NtMybAS1 protein for the development of tobacco anthers could be examined by antisense suppression of *NtmybAS1* expression using its own promoter or a tapetum specific promoter such as TA29 (Koltunow *et al.*, 1990). Downregulation of *NtmybAS1* in tapetum is expected to suppress *gPAL1* activity and this in turn would suppress the synthesis of phenylpropanoid metabolites required for pollen development and fertility. Antisense expression of *NtmybAS1* could be applicable in other plant species for the induction of male sterility and development of hybrid varieties.

An alternative reverse genetic approach, RNA-mediated interference (RNAi) (reviewed in Sharp, 1999), can be adopted to investigate the loss-of-function phenotype of *NtmybAS1*. In this approach, a double-stranded RNA (dsRNA) incorporating part of the targeted gene sequence suppresses the expression of a specific gene at the post-transcriptional level in a sequence-specific manner. This dsRNA triggers the degradation of homologous RNA sequences by an unknown mechanism. RNAi has been used to suppress genes in a number of organisms, including *Caenorhabditis elegans* (Fire *et al.*, 1998; Montgomery *et al.*, 1998; Shi

and Mello, 1998; Tabara *et al.*, 1998; Fraser *et al.*, 2000; Gonczy *et al.*, 2000), *Drosophila* (Kennerdell and Carthew, 1998; Misquitta and Paterson, 1999), *Trypanosoma brucei* (Ngo *et al.*, 1998), the planarian *Schmidtea mediterranea* (Sanchez Alvarado and Newmark, 1999), as well as in the plants *Nicotiana tabacum* and *Oryza sativa* (Waterhouse *et al.*, 1998) and *Arabidopsis thaliana* (Chuang and Meyerowitz, 2000). These studies have proved the efficiency of RNAi for targeted repression of gene expression and large-scale functional genomic analysis.

The finding that the level of *gPAL1* transcript in two homozygote *NtmybAS1* plants was above the wild type (Figure 3. 13) further supported the regulatory role of NtMybAS1 protein in activation of *gPAL1* expression. Based on this evidence and that described in section 6. 3 the most plausible way of linking the induction of *gPAL1* mRNA with the activation of *PR-P*, *PR-1a* and *myb1* expression is via a rise in salicylic acid level, which depends on the increased gPAL1 activity. The mechanism of activation of PR-P and PR-1a via SA signalling pathway was discussed in detail by a model presented in section 5. 10. 2.

Demonstration of induction of *gPAL1* mRNA is not sufficient to make a conclusion concerning the changes in levels of gPAL1 enzyme activity in *NtmybAS1* plants. However, this finding implies that the activation of *gPAL1* mRNA in *NtmybAS1* plants is more likely associated with an increase in gPAL1 enzyme activity. The level of gPAL1 activity in *NtmybAS1* plants could be compared with wild type using radiometric (Legrand *et al.*, 1976) or spectrophotometric (Lamb *et al.*, 1979) assays. Increased PAL activity in *NtmybAS1* plants may dramatically alter the overall flux into phenylpropanoid pathway. The effect of perturbations of PAL activity on the levels of phenylpropanoid products has been studied in tobacco plants in which overexpression of bean *PAL2* resulted in cosuppression of PAL activity (Elkind *et al.*, 1990). The recovery of PAL activity in homozygous progenies of a primary transformant (YE6-16) overexpressing bean *PAL2* in subsequent generations allowed determining the effect of increased PAL activity on phenylpropanoid metabolite accumulation. These analyses revealed a direct relationship between PAL activity and accumulation of major phenolics of tobacco leaves including CGA (3-caffeoylquinic acid) and rutin (quercetin 3-β-D-rutinoside). Despite recovery of PAL activity in these plants the total PAL activity did not exceed wild type levels after

four generations (Bate *et al.*, 1994). Further study of PAL enzyme activity in the progeny of another primary transformant (YE10-6) overexpressing bean *PAL2* revealed a change from sense suppression to increased PAL activity up to 5 and 2 times that of wild type levels in leaf and stem tissues respectively. This increase in PAL activity above the wild type levels resulted in increased levels of CGA but not rutin. These analyses revealed the role of PAL as a key rate-limiting enzyme for CGA biosynthesis and the involvement of additional flux control points into the flavonoid branch pathway (Howles *et al.*, 1996). The *NtmybAS1* plants provide a good source of plant material to investigate the effect of increase in endogenous gPAL1 enzyme activity above the wild type level on phenylpropanoid metabolites accumulation and on overall flux through phenylpropanoid pathway. In this regard it would be noteworthy to examine whether the induction of *gPAL1* expression affects the level of lignification in *NtmybAS1* plants. This could be investigated by Northern blot analysis of expression of genes encoding the enzymes of lignin biosynthesis (reviewed in Whetthen and Sederoff, 1995) such as cinnamyl alcohol dehydrogenase (CAD) or directly by quantification of lignin using thioglycolic acid (Doster and Bostock, 1988) or nitrobenzene oxidation (Chen, 1992) methods. However, in this case the results of Northern blot analyses should be interpreted cautiously as CAD is expressed in cells not synthesising lignin and in response to stress, pathogen attack and wounding (Whetthen and Sederoff, 1995).

Although the results presented here and those reported by Yang *et al.* (2000) established the primary function of NtMybAS1 protein in regulation of *gPAL1* transcription in sporophytic tissues of tobacco anthers the possibility of transcriptional regulation of other phenylpropanoid biosynthetic genes by the NtMybAS1 protein can not be ruled out. This hypothesis is supported by the fact that the consensus Myb biding sites is also present in the promoters of other phenylpropanoid biosynthetic genes including chalcone synthase (CHS), chalcone isomerase (CHI), dihydroflavonol reductase (DFR), 4-coumarate: coenzyme A ligase (4CL) and Bronze (Bz1) (Sablowski *et al.*, 1994). Among these genes *CHS* encodes the first enzyme of the flavonoid biosynthetic pathway, the products of which are essential for the pollen development, germination and fertility (section 1. 13). In anthers tapetal cells are the major site of localisation of PAL and chalcone synthase

(Rittscher and Wiermann, 1983; Kehrel and Wiermann, 1985; Beerhues *et al.*, 1989; Kishitani *et al.*, 1993). Therefore, CHS may be a second target of NtMybAS1 protein. Northern blot and *in situ* hybridisation analyses could provide insight into the role of NtMybAS1 in regulation of *CHS* transcription in tobacco anthers.

Modulation of DNA binding and *trans*-activation activities of Myb proteins by post-translational modifications including phosphorylation and acetylation has been well documented (section 1. 8). Analysis of NtMybAS1 protein sequence using ScanProsite software (ExPASy Molecular Biology Server, www.expasy.ch) revealed the presence of four N-glycosylation sites, (NISN,184-187; NFSQ, 240-243; NSSS, 403-406; NTSN, 450-453) seven N-myristoylation sites (GGLKAR, 6-11; GNWNAV, 43-48; GLMRCG, 53-58; GNKWAR, 94-99; GLILGM, 277-282; GLSRGN, 318-323; GGEDAT, 386-391) and several phosphorylation sites including five protein kinase C phosphorylation sites (SCR, 60-62; TMK, 179-181; SIR, 224-226; TTR, 264-266; TTK, 409-411), ten casein kinase II phosphorylation sites (TATE, 26-29; SLEE, 79-82; TDNE, 108-111; SPFD, 153-156; SLLD, 170-173; SIPE, 293-296; TSSD, 305-308; SSDD, 306-309; TRAE, 338-341; TTKE, 409-412) and a tyrosine kinase phosphorylation site (RTDNEIKNY, 107-115). These data imply that that the NtMybAS1 may undergo post-translational modifications. These modifications may be a determining factor in regulation of *trans*-activation activity and cellular function of NtMybAS1 protein. Considering the recent finding that the CDK9, a cyclin T associated kinase, specifically repress B-Myb gene autoregulation (DeFalco *et al.*, 2000) such modifications may be part of a mechanism to repress *gPAL1* activity in mature pollen (section 3. 12. 3). Study of phosphorylation of NtMybAS1 in conjunction with mutation analysis of the predicted phosphorylation sites, electrophoretic mobility shift assay and transient expression analysis could provide insight into the role of phosphorylation in modulation of DNA binding, activation potential and cellular function of NtMybAS1 protein.

It is not yet clear whether specific *trans*-activation activity of the NtMybAS1 protein in tobacco anthers depends on co-operation with other cofactors. Cell type specificity of *trans*-activation activity has been reported for the B-Myb. It has been shown using an affinity resin that the proteins which bind to the conserved region of B-Myb in specific cells types showing B-Myb *trans*-activation activity are different

from those in cells showing no B-Myb *trans*-activation activity. This finding led to the suggestion that the B-Myb interacting proteins are a determining factor in cell type specificity of *trans*-activation by the B-Myb. (Tashiro *et al.*, 1995). Recently it was shown that a nuclear protein, which interacts with the B-Myb DNA binding domain is poly (ADP-ribose) polymerase (PARP) and this interaction synergistically enhances *trans*-activation activity of B-Myb (Cervellera and Sala, 2000). The v-Myb and c/EBPβinteract via their DNA binding domains and this interaction on a composite response element containing both v-Myb and c/EBPβbinding sites is necessary for the synergistic activation of *mim1* promoter (Mink *et al.*, 1996). Furthermore, interaction of v-Myb with retinoic acid (RA) receptors (RAR/RXR) has been shown both *in vitro* and *in vivo* and this interaction suppress RA-dependent *trans*-activation (Pfitzner *et al.*, 1998). In maize *trans*-activation by the Myb-related proteins C1 or P1 requires interaction with one member of the basic helix-loop-helix family B or R (Goff *et al.*, 1990; Goff *et al.*, 1992).

Two methods including yeast two hybrid (Fields and Song, 1989; Chien *et al.*, 1991; Fields and Sternglanz, 1994) and the glutathione S-transferase-pull down assays have been used to characterise the cofactors interacting with the C-Myb (Pfitzner *et al.*, 1998), B-Myb (Cervellera and Sala, 2000) and the *Arabidopsis* Myb-related protein CCA1 (Sugano *et al.*, 1998). Similarly, these method could be adopted to identify potential cofactors interacting with both the NtMybAS1 DNA binding and transcriptional activator domain. Identification of such cofactors and analysis of their temporal and spatial expression patterns could provide clues about the mechanism of suppression of *gPAL1* expression in mature pollen.

Taken together, the *NtmybAS1* represents the most well characterised anther-specific transcription factor reported so far, which is involved in regulation of *gPAL1* transcription in sporophytic tissues of tobacco anthers. Ectopic overexpression of *NtmybAS1* upregulates *gPAL1* expression, induces a cell autonomous and gene dosage-dependent dwarfing and activates *PR* gene expression via a salicylic acid-dependent signal transduction pathway.

Bibliography

Aas, A. T., Tonnessen, T. I., Brun, A. and Salford, L. G. (1995) Growth inhibition of rat glioma cells *in vitro* and *in vivo* by aspirin. J. Neurooncol. 24, 171-180.

Abate, C., Patel, L., Rauscher, F. J. and Curran, T. (1990) Redox regulation of fos and jun DNA-binding activity in vitro. Science 249, 1157-1161.

Alexander, D., Goodman, R. M., Gut-Rella, M., Glascock, C., Weymann, K., Friedrich, L., Maddox, D., Ahl-Goy, P., Luntz, T., Ward, E. and Ryals, J. (1993) Increased tolerance to two oomycete pathogens in transgenic tobacco expressing pathogenesis-related protein 1a. Proc. Natl. Acad. Sci. USA 90, 7327-7331.

Allison-Creese, K., Duchene, C. and Murfet, I. C. (1985) Internode length in *Pisum*: the response of *le na* scions grafted to *Na* stocks. Ann. Bot. 55, 121-123.

Altmann, T. (1998a) A tale of dwarfs and drugs: brassinosteroids to the rescue. Trends Genet. 14, 490-495.

Altmann, T. (1998b) Recent advances in brassinosteroid molecular genetics. Curr. Opin. Plant Biol. 1, 378-383.

Amaravadi, L. and King, M. W. (1994) Characterization and expression of the Xenopus c-Myb homolog. Oncogene 9, 971-974.

Assaad, F. F., Mayer, U., Wanner, G. and Jurgens, G. (1996) The KEULE gene is involved in cytokinesis in *Arabidopsis*. Mol Gen. Genet. 253, 267-277.

Avila, J., Nieto, C., Canas, L., Benito, M. J. and Paz-Ares, J. (1993) *Petunia hybrida* genes related to the maize regulatory *C1* gene and to animal *myb* proto-oncogenes. Plant J. 3, 553-562.

Azpiroz, R., Wu, Y. W., LoCascio, J. C. and Feldmann, K. A. (1998) *Arabidopsis* brassinosteroid-dependent mutant is blocked in cell elongation. Plant Cell 10, 219-230.

Baltz, R., Domon, C., Pillay, D. T. and Steinmetz, A. (1992) Characterization of a pollen-specific cDNA from sunflower encoding a zinc finger protein. Plant J. 2, 713-721.

Baltz, R., Evrard, J. L., Bourdon, V. and Steinmetz, A. (1996) The pollen-specific LIM protein PLIM-1 from sunflower binds nucleic acids in vitro. Sex. Plant Reprod. 9, 264-268.

Baltz, R., Schmit, A. C., Kohnen, M., Hentges, F. and Steinmetz, A. (1999) Differential localization of the LIM domain protein PLIM-1 in microspores and mature pollen grains from sunflower. Sex. Plant Reprod. 12, 60-65.

Baluda, M. A. and Reddy, E. P. (1994) Anatomy of an integrated avian myeloblastosis provirus: structure and function. Oncogene 9, 2761-2774.

Banks, J. A., Masson, P. and Fedoroff, N. (1988) Molecular mechanisms in the developmental regulation of the maize suppressor-mutator transposable element. Genes Dev. 2, 1364-1380.

Baranowskij, N., Frohberg, C., Prat, S. and Willmitzer, L. (1994) A novel DNA binding protein with homology to Myb oncoproteins containing only one repeat can function as a transcriptional activator. EMBO J. 13, 5383-5392.

Barnabas, B. and Fridvalszky, L. (1984) Adhesion and germination of differently treated maize pollen grains on the stigma. Acta Bot. Hung. 30, 329-332.

Bartsch, O., Horstmann, S., Toprak, K., Klempnauer, K. H. and Ferrari, S. (1999) Identification of cyclin A/Cdk2 phosphorylation sites in B-Myb. Eur. J. Biochem. 260. 384-391.

Baskaran, R., Dahmus, M. E. and Wang, J. Y. (1993) Tyrosine phosphorylation of mammalian RNA polymerase II carboxyl-terminal domain. Proc. Natl. Acad. Sci. USA 90, 11167-11171.

Bate, N. (1997) Transcriptional and translational control of gene expression during pollen development. Ph.D. Thesis, University of Leicester, UK.

Bate, N. J., Orr, J., Ni, W., Meromi, A., Nadler-Hassar, T., Doerner, P. W., Dixon, R. A., Lamb, C. J. and Elkind, Y. (1994) Quantitative relationship between phenylalanine ammonia-lyase levels and phenylpropanoid accumulation in transgenic tobacco identifies a rate-determining step in natural product synthesis. Proc. Natl. Acad. Sci. USA 91, 7608-7612.

Bate, N. and Twell, D. (1998) Functional architecture of a late pollen promoter: pollen-specific transcription is developmentally regulated by multiple stage-specific and co-dependent activator elements. Plant Mol. Biol. 37, 859-869.

Baumann, P., Qureshi, S. A. and Jackson, S. P. (1995) Transcription: new insights from studies on Archaea. Trends Genet. 11, 279-283.

Bedinger, P. (1992) The remarkable biology of pollen. Plant Cell 4, 879-887.

Bedinger, P. A. and Edgerton, M. D. (1990) Developmental staging of maize microspores reveals a transition in developing microspore proteins. Plant Physiol. 92, 474-479.

Beerhues, L., Forkmann, G., Schopker, H., Stotz, G. and Wiermann, R. (1989b) Flavanone 3-hydroxylase and dihydroflavonol oxygenase activities in anthers of Tulipa. The significance of the tapetum fraction in flavonoid metabolism. J. Plant Physiol. 133, 743-746.

Bender, J. and Fink, G. R. (1998) A Myb homologue, ATR1, activates tryptophan gene expression. Proc. Natl. Acad. Sci. USA 95, 5655-5660.

Benfey P. N. and Chua, N. H. (1990) The cauliflower mosaic virus 35S promoter: Combinatorial regulation of transcription in plants. Science 250: 959-966.

Bevan, M. (1984) Binary *Agrobacterium* vectors for plant transformation. Nucl. acids Res. 12, 8711-8721.

Bih, F. Y., Wu, S. S., Ratnayake, C., Walling, L. L., Nothnagel, E. A. and Huang, A. H. (1999) The predominant protein on the surface of maize pollen is an endoxylanase synthesized by a tapetum mRNA with a long 5' leader. J. Biol. Chem. 274, 22884-22894.

Bin, X. and Lipsick, J. S. (1993) Individual repeats of *Drosophila* Myb can function in transformation by v-Myb. J. Virol. 67, 7332-7339.

Bishop, G. J., Harrison, K. and Jones, J. D. G. (1996) The tomato Dwarf gene isolated by heterologous transposon tagging encodes the first member of a new cytochrome P450 family. Plant Cell, 8, 959-969.

Bouwmeester, T., Guehmann, S., el-Baradi,T., Kalkbrenner, F., van Wijk, I., Moelling, K. and Pieler, T. (1992) Molecular cloning, expression and in vitro functional characterization of Myb-related proteins in Xenopus. Mech. Dev. 37, 57-68.

Bowles, D. J. (1990) Defense-related proteins in higher plants. Annu. Rev. Biochem. 59,873-907.

Bowling, S. A., Clarke, J. D., Liu, Y., Klessig, D. F. and Dong, X. (1997) The *cpr5* mutant of *Arabidopsis* expresses both NPR1-dependent and NPR1-independent resistance. Plant Cell 9, 1573-1584.

Bowling, S. A., Guo, A., Cao, H., Gordon, A. S., Klessig, D. F. and Dong, X. (1994) A mutation in *Arabidopsis* that leads to constitutive expression of systemic acquired resistance. Plant Cell 6, 1845-1857.

Bradford, M. M. (1976) A refined and sensitive method for the quantitation of microgram quantities of protein utilising the principle of protein-dye binding. Anal. Biochem. 72, 248-254.

Braun, E. L. and Grotewold, E. (1999) Newly discovered plant *c-myb*-like genes rewrite the evolution of the plant *myb* gene family. Plant Physiol. 121, 21-24.

Brewbaker, J. L. (1967) The distribution and phylogenetic significance of binucleate and trinucleate pollen grains in angiosperms. Am. J. Bot. 54, 1069-1083.

Broglie, K., Chet, I., Holliday, M., Cressman, R., Biddle, P., Knowlton, S., Mauvais, C. J. and Broglie, R. (1991) Transgenic plants with enhanced resistance to the fungal pathogen *Rhizoctonia solani*. Science 254, 1194-1197.

Bullock, W. O., Fermandez, J. M. and Short, J. M. (1987) XL1-blue, a high efficiency plasmid transforming *RecA Escherichia coli* strain with ß-galactosidase selection. Biotechniques 5, 376.

Buratowski, S., Hahn, S., Guarente, L. and Sharp, P. A. (1989) Five intermediate complexes in transcription initiation by RNA polymerase II. Cell 56, 549-561.

Burbulis, I. E., Iacobucci, M. and Shirley, B. W. (1996) A null mutation in the first enzyme of flavonoid biosynthesis does not affect male fertility in Arabidopsis. Plant Cell 8, 1013-1025.

Burk, O., Mink, S., Ringwald, M. and Klempnauer, K. H. (1993) Synergistic activation of the chicken *mim-1* gene by v-myb and C/EBP transcription factors. EMBO J. 12, 2027-2038.

Bus, P. J., Nagtegaal, I. D., Verspaget, H. W., Lamers, C. B., Geldof, H., Van, Krieken, J. H. and Griffioen, G. (1999) Mesalazine-induced apoptosis of colorectal cancer: on the verge of a new chemopreventive era? Aliment. Pharmacol. Ther. 13, 1397-1402.

Van Buuren, M., Neuhaus, J. M. Shinshi, H., Ryals, J. and Meins, F. (1992) The structure and regulation of homeologous tobacco endochitinase genes of *Nicotiana sylvestris* and *N. tomentosiformis* origin. Mol. Gen. Genet. 232, 460-469.

Cadena, D. L. and Dahmus, M. E. (1987) Messenger RNA synthesis in mammalian cells is catalyzed by the phosphorylated form of RNA polymerase II. J. Biol. Chem. 262, 12468-12474.

Cao, H., Bowling, S. A., Gordon, A. S. and Dong, X. (1994) Characterization of an *Arabidopsis* mutant that is nonresponsive to inducers of systemic acquired resistance. Plant Cell 6, 1583-1592.

Cao, H., Glazebrook, J., Clarke, J. D., Volko, S. and Dong, X. (1997) The *Arabidopsis NPR1* gene that controls systemic acquired resistance encodes a novel protein containing ankyrin repeats. Cell 88, 57-63.

Cao, H., Li, X. and Dong, X. (1998) Generation of broad-spectrum disease resistance by overexpression of an essential regulatory gene in systemic acquired resistance. Proc. Natl. Acad. Sci. USA 95, 6531-6536.

Carlson, M. and Laurent, B. C. (1994) The SNF/SWI family of global transcriptional activators. Curr Opin. Cell Biol. 6, 396-402.

Carrington, J. C. and Freed, D. D. (1990) Cap-independent enhancement of translation by a plant potyvirus 5' nontranslated region. J. Virol. 64, 1590-1597.

Carrington, J. C., Freed, D. D. and Leinicke, A. J. (1991) Bipartite signal sequence mediates nuclear translocation of the plant potyviral NIa protein. Plant Cell 3, 953-962.

Century, K. S., Holub, E. B. and Staskawicz, B. J. (1995) *NDR1*, a locus of *Arabidopsis thaliana* that is required for disease resistance to both a bacterial and a fungal pathogen. Proc. Natl. Acad. Sci. USA 92, 6597-6601.

Cervellera, M. N. and Sala, A. (2000) Poly(ADP-ribose) polymerase is a B-MYB coactivator. J. Biol. Chem. 275, 10692-10696.

Chen, C. L. (1992) Nitrobenzene and cupric oxide oxidations. In Methods in Lignin Chemistry, S. Y. Lin and C. W. Dence, eds (Berlin: Springer Verlag), pp. 301-321.

Chen, Z., Ricigliano, J. W. and Klessig, D. F. (1993a) Purification and characterization of a soluble salicylic acid-binding protein from tobacco. Proc. Natl. Acad. Sci. USA 90, 9533-9537.

Chen, Z, Silva, H. and Klessig, D. F. (1993b) Active oxygen species in the induction of plant systemic acquired resistance by salicylic acid. Science 262, 1883-1886.

Chesnut, J. D., Stephens, J. H. and Dahmus, M. E. (1992) The interaction of RNA polymerase II with the adenovirus-2 major late promoter is precluded by phosphorylation of the C-terminal domain of subunit IIa. J. Biol. Chem. 267, 10500-10506.

Cheung, Man-Kim (1998) A study of genetic transformtion systems for groundnut (*Arachis hypogaea* L.) with the objective to genetically engineering resistance to Indian peanut clump virus. Ph.D Thesis, University of Leicester, UK.

Chien, C. T., Bartel, P. L., Sternglanz, R. and Fields, S. (1991) The two-hybrid system: a method to identify and clone genes for proteins that interact with a protein of interest. Proc. Natl. Acad. Sci. USA 88, 9578-9582.

Chiu, W. L., Niwa, Y., Zeng, W., Hirano, T., Kobayashi, H. and Sheen, J. (1996) Engineered GFP as a vital reporter in plants. Current Biology 6, 325-330.

Chuang, C. F. and Meyerowitz, E. M. (2000) Specific and heritable genetic interference by double-stranded RNA in *Arabidopsis thaliana*. Proc. Natl. Acad. Sci USA 97, 4985-4990.

Chuck, G., Lincoln, C. and Hake, S. (1996) *KNAT1* induces lobed leaves with ectopic meristems when overexpressed in *Arabidopsis*. Plant Cell 8, 1277-1289.

Chung, Y. Y., Kim, S. R., Finkel, D., Yanofsky, M. F. and An, G. H. (1994) Early flowering and reduced apical dominance result from ectopic expression of a rice MADS box gene. Plant Mol. Biol. 26, 657-665.

Chung, Y. Y., Kim, S. R., Kang, H. G., Noh, Y. S., Park, M. C., Finkel, D. and An, G. H. (1995) Characterization of two rice MADS box genes homologous to *GLOBOSA*. Plant Science 109, 45-56.

Church, G. M. and Gilbert, W. (1984) Genomic sequencing. Proc. Natl. Acad. Sci. USA 81, 1991-1995.

Clarke, M. C. Wei, W. and Lindsey, K. (1992) High-frequency transformation of *Arabidopsis thaliana* by *Agrobacterium tumefaciens*. Plant Mol. Biol. Rep. 10, 178-189.

Coe, E. H., McCormick, S. M. and Modena, S. A. (1981) White pollen in maize. J. Hered. 72, 318-320.

Coles, J. P., Phillips, A. L., Croker, S. J., GarciaLepe, R., Lewis, M. J. and Hedden, P. (1999) Modification of gibberellin production and plant development in *Arabidopsis* by sense and antisense expression of gibberellin 20-oxidase genes. Plant J. 17, 547-556.

Conaway, R. C. and Conaway, J. W. (1997) General transcription factors for RNA polymerase II. Prog. Nucleic Acid Res. Mol. Biol. 56, 327-346.

Cone, K. C., Burr, F. A. and Burr, B. (1986) Molecular analysis of the maize anthocyanin regulatory locus *C1*. Proc. Natl. Acad. Sci. USA 83, 9631-9635.

Cone, K. C., Cocciolone, S. M., Burr, F. A. and Burr, B. (1993) Maize anthocyanin regulatory gene *pl* is a duplicate of *c1* that functions in the plant. Plant Cell 5, 1795-1805.

Coquoz, J. L., Buchala, A. and Metraux, J. P. (1998) The biosynthesis of salicylic acid in potato plants. Plant Physiol. 117, 1095-1101.

Cornelissen, B. J., Horowitz, J., van Kan, J. A., Goldberg, R. B. and Bol, J. F. (1987) Structure of tobacco genes encoding pathogenesis-related proteins from the PR-1 group. Nucleic acids Res. 15, 6799-6811.

Cosgrove, D. J. (1997) Relaxation in a high-stress environment: The molecular bases of extensible cell walls and cell enlargement. Plant Cell 9, 1031-1041.

Cosgrove, D. J. (1998) Cell wall loosening by expansins. Plant Physiol. 118, 333-339.

Cosgrove, D. J. (1999) Enzymes and other agents that enhance cell wall extensibility. Annu. Rev. Plant Physiol. Plant Mol. Biol. 50, 391-417.

da Costa e Silva, O., Klein, L., Schmelzer, E., Trezzini, G. F. and Hahlbrock, K. (1993) BPF-1, a pathogen-induced DNA-binding protein involved in the plant defense response. Plant J. 4, 125-135.

Creelman, R. A. and Mullet, J. E. (1997) Biosynthesis and action of jasmonates in plants. Annu. Rev. Plant Physiol. Plant Mol. Biol. 48, 355-381.

Currier, H. and Strugger, S. (1956) Aniline blue and fluorescence microscopy of callose in bulb scales of *Allium cepa* L. Protoplasma 45, 552-559.

Cutt, J. R., Harpster, M. H., Dixon, D. C., Carr, J. P., Dunsmuir, P. and Klessig, D. F. (1989) Disease response to tobacco mosaic virus in transgenic tobacco plants that constitutively express the pathogenesis-related PR1b gene. Virology 173, 89-97.

Dahmus, M. E. (1981) Phosphorylation of eukaryotic DNA-dependent RNA polymerase. Identification of calf thymus RNA polymerase subunits phosphorylated by two purified protein kinases, correlation with in vivo sites of phosphorylation in HeLa cell RNA polymerase II. J. Biol. Chem. 256, 3332-3339.

Daniel, X., Lacomme, C., Morel, J. B. and Roby, D. (1999) A novel *myb* oncogene homologue in Arabidopsis thaliana related to hypersensitive cell death. Plant J. 20, 57-66.

De Falco, G., Bagella, L., Claudio, P. P., De Luca, A., Fu, Y., Calabretta, B., Sala, A. and Giordano, A. (2000) Physical interaction between CDK9 and B-Myb results in suppression of B-Myb gene autoregulation. Oncogene 19, 373-379.

Dietrich, R. A., Delaney, T. P., Uknes, S. J., Ward, E. R., Ryals, J. A. and Dangl, J. L. (1994) *Arabidopsis* mutants simulating disease resistance response. Cell 77, 565-577.

Dixon, R. A. and Paiva, N. L. (1995) Stress-induced phenylpropanoid metabolism. Plant Cell 7, 1085-1097.

Dixon, R. A. and Steele, C. L. (1999) Flavonoids and isoflavonoids- a gold mine for metabolic engineering. Trends Plant Sci. 4, 394-400.

Doster, M. A. and Bostock, R. M. (1988) Quantification of lignin formation in almond bark in response to wounding and infection by *Phytophthora* species. Phytopathology 78, 473-477.

Drapkin, R. and Reinberg, D. (1994) The multifunctional TFIIH complex and transcriptional control. Trends Biochem. Sci. 19, 504-508.

Durner, J., Shah, J. and Klessig, D. F. (1997) Salicylic acid and disease resistance in plants. Trends Plant Sci. 2, 266-274.

Eady, C., Lindsey, K. and Twell, D. (1994) Differential activation and conserved vegetative cell-specific activity of a late pollen promoter in species with bicellular and tricellular pollen. Plant J. 5, 543-550.

Ecker, J. R. (1995) The ethylene signal transduction pathway in plants. Science 268, 667-675.

Edwards, K., Cramer, C. L., Bolwell, G. P., Dixon, R. A., Schuch, W. and Lamb, C. J. (1985) Rapid transient induction of phenylalanine ammonia-lyase mRNA in elicitor- treated bean cells. Proc. Natl. Acad. Sci. USA 82, 6731-6735.

Elder, D. J., Hague, A., Hicks, D. J. and Paraskeva, C. (1996) Differential growth inhibition by the aspirin metabolite salicylate in human colorectal tumor cell lines: enhanced apoptosis in carcinoma and in vitro-transformed adenoma relative to adenoma relative to adenoma cell lines. Cancer Res. 56, 2273-2276.

Elkind, Y., Edwards, R., Mavandad, M., Hedrick, S. A., Ribak, O., Dixon, R. A. and Lamb, C. J. (1990) Abnormal plant development and down-regulation of phenylpropanoid biosynthesis in transgenic tobacco containing a heterologous phenylalanine ammonia-lyase gene. Proc. Natl. Acad. Sci. USA 87, 9057-9061.

England, B. P., Admon, A. and Tjian, R. (1992) Cloning of Drosophila transcription factor Adf-1 reveals homology to Myb oncoproteins. Proc. Natl. Acad. Sci. USA 89 683-687.

Erkine, A. M., Magrogan, S. F., Sekinger, E. A. and Gross, D. S. (1999) Cooperative binding of heat shock factor to the yeast HSP82 promoter in vivo and in vitro. Mol. Cell Biol. 19, 1627-1639.

Esch, J. J., Oppenheimer, D. G. and Marks, M. D. (1994) Characterization of a weak allele of the *GL1* gene of *Arabidopsis thaliana*. Plant Mol. Biol. 24, 203-207.

Eyal, Y., Curie, C. and McCormick, S. (1995) Pollen specificity elements reside in 30 bp of the proximal promoters of two pollen-expressed genes. Plant Cell 7, 373-384.

Fairall, L., Schwabe, J. W., Chapman, L., Finch, J. T. and Rhodes, D. (1993) The crystal structure of a two zinc-finger peptide reveals an extension to the rules for zinc-finger DNA recognition. Nature 366, 483-487.

Feaver, W. J., Gileadi, O., Li, Y. and Kornberg, R. D. (1991) CTD kinase associated with yeast RNA polymerase II initiation factor b. Cell 67, 1223-1230.

Fedoroff, N. V. (1999) The Suppressor-mutator element and the evolutionary riddle of transposons. Genes to Cells 4, 11-19.

Feldbrügge, M., Sprenger, M., Hahlbrock, K. and Weisshaar, B. (1997) PcMYB1, a novel plant protein containing a DNA-binding domain with one MYB repeat, interacts in vivo with a light-regulatory promoter unit. Plant J. 11, 1079-1093.

Feldmann, K. A. (1992) T-DNA insertion mutagenesis in *Arabidopsis*: Seed infection/transformation. In Methods in Arabidopsis Research (Koncz, C., Chua, N. H. and Schell, J., eds). World Scientific Publishing Co. Pte. Ltd. Singapore, New Jersey, London, Hong Kong, pp. 274-289.

Feldmann, K. A., Marks, M. D., Christianson, M. L. and Quatrano, R. S. 1989) A dwarf mutant of *Arabidopsis* generated by T-DNA insertion mutagenesis. Science 243, 1351-1354.

Fields, S. and Song, O. (1989) A novel genetic system to detect protein-protein interactions. Nature 340, 245-246.

Fields, S. and Sternglanz, R. (1994) The two-hybrid system: an assay for protein-protein interactions. Trends Genet. 10, 286-292.

Finnegan, E. J., Peacock, W. J. and Dennis, E. S. (1996) Reduced DNA methylation in *Arabidopsis thaliana* results in abnormal plant development. Proc. Natl. Acad. Sci. USA 93, 8449-8454.

Fire, A., Xu, S., Montgomery, M. K., Kostas, S. A., Driver, S. E. and Mello, C. C. (1998) Potent and specific genetic interference by double-stranded RNA in *Caenorhabditis elegans*. Nature 391, 806-811.

Fladung, M. (1990) Transformation of diploid and tetraploid potato clones with the *rol C* gene of *Agrobacterium rhizogenes* and characterization of transgenic plants. Plant Breeding 104, 295-304.

Flores, O., Lu, H., Killeen, M., Greenblatt, J., Burton, Z. F. and Reinberg, D. (1991) The small subunit of transcription factor IIF recruits RNA polymerase II into the preinitiation complex. Proc. Natl. Acad. Sci. USA 88, 9999-10003.

Foos, G., Grimm, S. and Klempnauer, K. H. (1992) Functional antagonism between members of the myb family: B-myb inhibits v-myb-induced gene activation. EMBO J. 11, 4619-4629.

Frampton, J., Gibson, T. J., Ness, S. A., Doderlein, G. and Graf, T. (1991) Proposed structure for the DNA-binding domain of the Myb oncoprotein based on model building and mutational analysis. Protein Eng. 4, 891-901.

Franken, P., Schrell, S., Peterson, P. A., Saedler, H. and Wienand, U. (1994) Molecular analysis of protein domain function encoded by the myb-homologous maize genes *C1*, *Zm 1* and *Zm 38*. Plant J. 6, 21-30.

Fraser, A. G., Kamath, R. S., Zipperlen, P., Martinez-Campos, M., Sohrmann, M. and Ahringer, J. (2000) Functional genomic analysis of *C. elegans* chromosome I by systematic RNA interference. Nature 408, 325-330.

Fray, R. G., Wallace, A., Fraser, P. D., Valero, D., Hedden, P., Bramley, P. M. and Grierson, D. (1995) Constitutive expression of a fruit phytoene synthase gene in transgenic tomatoes causes dwarfism by redirecting metabolites from the gibberellin pathway. Plant J. 8, 693-701.

Fritzemeier, K. H., Cretin, C., Kombrink, E., Rohwer, F., Taylor, J., Scheel, D. and Hahlbrock, K. (1987) Transient induction of phenylalanine ammonia-lyase and 4-coumarate:CoA ligase mRNAs in potato leaves infected with

virulent or avirulent races of *Phytophthora infestans*. Plant Physiol. 85, 34-41.

Fukasawa-Akada, T., Kung, S. and Watson, J. C. (1996) Phenylalanine ammonia-lyase gene structure, expression, and evolution in *Nicotiana*. Plant Mol. Biol. 30, 711-722.

Gabrielsen, O. S., Sentenac, A. and Fromageot, P. (1991) Specific DNA binding by c-Myb: evidence for a double helix-turn-helix-related motif. Science 253, 1140-1143.

Gaffney, T., Friedrich, L., Vernooij, B., Negrotto, D., Nye, G., Uknes, S., Ward, E., Kessmann, H. and Ryals, J. (1993) Requirement of salicylic-acid for the induction of systemic acquired resistance. Science 261, 754-756.

Gerondakis, S. and Bishop, J. M. (1986) Structure of the protein encoded by the chicken proto-oncogene c-myb. Mol. Cell. Biol. 6, 3677-3684.

Ghoshal, K., Majumder, S., Li, Z. L., Dong, X. C. and Jacob, S. T. (2000) Suppression of metallothionein gene expression in a rat hepatoma because of promoter-specific DNA methylation. J. Biol. Chem. 275, 539-547.

Gibson, S. and Somerville, C. (1993) Isolating plant genes. Trends Biotechnol. 11, 306-313.

Glazebrook, J., Rogers, E. E. and Ausubel, F. M. (1996) Isolation of *Arabidopsis* mutants with enhanced disease susceptibility by direct screening. Genetics 143, 973-982.

Glover, B. J., Perez-Rodriguez, M. and Martin, C. (1998) Development of several epidermal cell types can be specified by the same MYB-related plant transcription factor. Development 125, 3497-3508.

Gocal, G. F., Poole, A. T., Gubler, F., Watts, R. J., Blundell, C. and King, R.W. (1999) Long-day up-regulation of a GAMYB gene during *Lolium temulentum* inflorescence formation. Plant Physiol. 119, 1271-1278.

Goff, S. A., Cone, K. C. and Chandler, V. L. (1992) Functional analysis of the transcriptional activator encoded by the maize B gene: evidence for a direct functional interaction between two classes of regulatory proteins. Genes Dev. 6, 864-875.

Goff, S. A., Klein, T. M., Roth, B. A., Fromm, M. E., Cone, K. C., Radicella, J. P. and Chandler, V. L. (1990) Transactivation of anthocyanin biosynthetic genes following transfer of B regulatory genes into maize tissues. EMBO J. 9, 2517-2522.

Gonczy, P., Echeverri, G., Oegema, K., Coulson, A., Jones, S. J., Copley, R. R., Duperon, J., Oegema, J., Brehm, M., Cassin, E., Hannak, E., Kirkham, M., Pichler, S., Flohrs, K., Goessen, A., Leidel, S., Alleaume, A. M., Martin, C., Ozlu, N., Bork, P. and Hyman, A. A. (2000) Functional genomic analysis of cell division in *C. elegans* using RNAi of genes on chromosome III. Nature 408, 331-336.

Gonda, T. J. and Bishop, J. M. (1983) Structure and transcription of the cellular homolog (c-myb) of the avian myeloblastosis virus transforming gene (v-myb). J Virol. 46, 212-220.

Gonda, T. J., Gough, N. M., Dunn, A. R. and de Blaquiere, J. (1985) Nucleotide sequence of cDNA clones of the murine myb proto-oncogene. EMBO J. 4, 2003-2008.

Gong, Z. Z., Yamazaki, M. and Saito, K. (1999) A light-inducible Myb-like gene that is specifically expressed in red Perilla frutescens and presumably acts as a determining factor of the anthocyanin forma. Mol. Gen. Genet. 262, 65-72.

Goodrich, J., Puangsomlee, P., Martin, M., Long, D., Meyerowitz, E. M. and Coupland, G. (1997) A polycomb-group gene regulates homeotic gene expression in *Arabidopsis*. Nature 386, 44-51.

Graf, T., McNagny, K., Brady, G. and Frampton, J. (1992) Chicken "erythroid" cells transformed by the Gag-Myb-Ets-encoding E26 leukemia virus are multipotent. Cell 70, 201-213.

Grässer, F. A., LaMontagne, K., Whittaker, L., Stohr, S. and Lipsick J. S. (1992) A highly conserved cystein in the v-Myb DNA-binding domain is essential for transformation and transcriptional *trans*-activation. Oncogene 7, 1005-1009.

Greenberg, J. T., Guo, A., Klessig, D. F. and Ausubel, F. M. (1994) Programmed cell death in plants: A pathogen triggered response activated coordinately with multiple defense functions. Cell 7, 551-563.

Grotewold, E., Drummond, B. J., Bowen, B. and Peterson, T. (1994) The myb-homologous P gene controls phlobaphene pigmentation in maize floral organs by directly activating a flavonoid biosynthetic gene subset. Cell 76, 543-553.

Gubler, F., Kalla, R., Roberts, J. K. and Jacobsen, J. V. (1995) Gibberellin-regulated expression of a *myb* gene in barley aleurone cells: evidence for Myb transactivation of a high-pI a-amylase gene promoter. Plant Cell 7, 1879-1891.

Guzman, P. and Ecker, J. R. (1990) Exploiting the triple response of *Arabidopsis* to identify ethylene-related mutants. Plant Cell 2, 513-523.

Ha, I., Roberts, S., Maldonado, E., Sun, X., Kim, L. U., Green, M. and Reinberg, D. (1993) Multiple functional domains of human transcription factor IIB: distinct interactions with two general transcription factors and RNA polymerase II. Genes Dev. 7, 1021-1032.

Hahlbrock, K. and Scheel, D. (1989) Physiology and molecular biology of phenylpropanoid metabolism. Annu. Rev. Plant Phys. Plant. Mol. Biol. 40, 347-369.

Hanahan, D. (1983) Studies on transformation of *Escherichia coli* with plasmids. J. Mol. Biol. 166, 557-580.

Hedden, P. and Kamiya, Y. (1997) Gibberellin biosynthesis: Enzymes, genes and their regulation. Annu. Rev. Plant Phys. Plant Mol. Biol. 48, 431-460.

Hirayama, T. and Shinozaki, K. (1996) A cdc5+ homolog of a higher plant, *Arabidopsis thaliana*. Proc. Natl. Acad. Sci. USA 93, 13371-13376.

Hoisington, D., Khairallah, M., Reeves, T., Ribaut, J. M., Skovmand, B., Taba, S. and Warburton, M. (1999) Plant genetic resources: What can they contribute toward increased crop productivity? Proc. Natl. Acad. Sci. USA 96, 5937-5943.

Hooley, R. (1994) Gibberellins: perception, transduction and responses. Plant Mol. Biol. 26, 1529-1555.

Howles, P. A., Sewalt, V. J. H., Paiva, N. L., Elkind, Y., Bate, N. J., Lamb, C. and Dixon, R. A. (1996) Overexpression of L-phenylalanine ammonia-lyase in transgenic tobacco plants reveals control points for flux into phenylpropanoid biosynthesis. Plant Physiol. 112, 1617-1624.

Inamori, Y., Muro, C., Yoshioka, M., Yamada, M., Tsujibo, H., Kusano, G., Watanabe, M. and Fujimoto, M. (1993) Phytogrowth-inhibitory activities of sulfur-containing compounds. II. The inhibitory activities of thiosalicylic acid and dihydro-2(3H)-thiophenone-related compounds on plant growth. Biol. Pharm. Bull. 16, 813-816.

Inamori, Y., Ogawa, M., Nishiguchi, K., Koyama, S., Tsujibo, H., Miki, Y. and Takemura, S. (1991) Phytogrowth-inhibitory and antimicrobial activities of 3,4'-dihydroxy-alpha,beta-diethylstilbene, the isomer of diethylstilbestrol. Chem. Pharm. Bull. 39, 218-220.

Ingram, T. J. and Reid, J. B. (1987) Internode length in Pisum. Gene *na* may block gibberellin synthesis between *ent*-7α-hydroxykaurenoic acid and gibberellin A_{12}-aldehyde. Plant Physiol. 83, 1048-1053.

Ingram, T. J., Reid, J. B., Murfet, I. C., Gaskin, P., Willis, C. L. and Macmillan, J. (1984) Internode length in *Pisum*. The *Le* gene controls the 3β-hydroxylation of gibberellin A_{20} to gibberellin A_1. Planta 160, 455-463.

Ingram, T. J., Reid, J. B., Potts, W. C. and Murfet, I. C. (1983) Internode length in *Pisum*. IV. The effect of the *Le* gene on gibberellin metabolism. Physiol. Plant. 59, 607-616.

Inostroza, J., Flores, O. and Reinberg, D. (1991) Factors involved in specific transcription by mammalian RNA polymerase II. Purification and functional analysis of general transcription factor IIE. J. Biol. Chem. 266, 9304-9308.

Introna, M., Golay, J., Frampton, J., Nakano, T., Ness, S. A. and Graf, T. (1990) Mutations in v-*myb* alter the differentiation of myelomonocytic cells transformed by the oncogene. Cell 63, 1289-1297.

Ishiguro, N., Ohzono, T., Shinagawa, T., Horiuchi, M. and Shinagawa, M. (1994) A spontaneous internal deletion of the c-myb protooncogene

enhances transcriptional activation in bovine T lymphoma cells. J. Biol. Chem. 269, 26822-26829.

Iturriaga, G., Leyns, L., Villegas, A., Gharaibeh, R., Salamini, F. and Bartels, D. (1996) A family of novel *myb*-related genes from the resurrection plant *Craterostigma plantagineum* are specifically expressed in callus and roots in response to ABA or desiccation. Plant Mol. Biol. 32, 707-716.

Jach, G., Gornhardt, B., Mundy, J., Logemann, J., Pinsdorf, E., Leah, R., Schell, J. and Maas, C. (1995) Enhanced quantitative resistance against fungal disease by combinatorial expression of different barley antifungal proteins in transgenic tobacco. Plant J. 8, 97-109.

Jackson, D., Culianez-Macia, F., Prescott, A. G., Roberts, K. and Martin, C. (1991) Expression patterns of myb genes from Antirrhinum flowers. Plant Cell 3, 115-125.

Jamin, N., Gabrielsen, O. S., Gilles, N., Lirsac, P. N. and Toma, F. (1993) Secondary structure of the DNA-binding domain of the c-Myb oncoprotein in solution. A multidimensional double and triple heteronuclear NMR study. Eur. J. Biochem. 216, 147-154.

Jin, H. and Martin, C. (1999) Multifunctionality and diversity within the plant MYB-gene family. Plant Mol Biol. 41, 577-85.

Jofuku, K. D., den Boer, B. G. W., Van Montagu, M. and Okamuro, J. K. (1994) Control of *Arabidopsis* flower and seed development by the homeotic gene *APETALA2*. Plant Cell 6, 1211-1225.

Johnson, T. K., Schweppe, R. E., Septer, J. and Lewis, R. E. (1999) Phosphorylation of B-Myb regulates its transactivation potential and DNA binding. J. Biol. Chem. 274, 36741-36749.

Ju, Q. D., Morrow, B. E. and Warner, J. R. (1990) REB1, a yeast DNA-binding protein with many targets, is essential for growth and bears some resemblance to the oncogene myb. Mol. Cell Biol. 10, 5226-5234.

Kamalay, J. C. and Goldberg, R. B. (1980) Regulation of structural gene expression in tobacco. Cell 19, 934-946.

Katzen, A. L., Kornberg, T. B. and Bishop, J. M. (1985) Isolation of the proto-oncogene *c-myb* from *D. melanogaster*. Cell 41, 449-456.

Katzen, A. L., Jackson, J., Harmon, B. P., Fung, S. M., Ramsay, G. and Bishop, J. M. (1998) *Drosophila myb* is required for the G2/M transition and maintenance of diploidy. Genes Dev. 12, 831-843.

Kauschmann, A., Jessop, A., Koncz, C., Szekeres, M., Willmitzer, L. and Altmann, T. (1996) Genetic evidence for an essential role of brassinosteroids in plant development. Plant J. 9, 701-713.

Keeling, P. J. and Doolittle, W. F. (1995) Archaea: narrowing the gap between prokaryotes and eukaryotes. Proc. Natl. Acad. Sci. USA 92, 5761-5764.

Kefeli, V. I. and Dashek, W. V. (1984) Non-hormonal stimulators and inhibitors of plant-growth and development. Biol. Rev. 59, 273-288.

Kehrel, B. and Wierman, N. R. (1985) Immunochemical localization of phenylalanine ammonia-lyase and chalcone synthase in anthers. Planta 163, 183-190.

Kennerdell, J. R. and Carthew, R. W. (1998) Use of dsRNA-mediated genetic interference to demonstrate that *frizzled* and *frizzled 2* act in the wingless pathway. Cell 95, 1017-1026.

Kieber, J. J., Rothenberg, M., Roman, G., Feldmann, K. A. and Ecker, J. R. (1993) *CTR1*, a negative regulator of the ethylene response pathway in *Arabidopsis*, encodes a member of the Raf family of protein-kinases. Cell 72, 427-441.

Killeen, M. T. and Greenblatt, J. F. (1992) The general transcription factor RAP30 binds to RNA polymerase II and prevents it from binding nonspecifically to DNA. Mol. Cell. Biol. 12, 30-37.

Kim, G. T., Tsukaya, H. and Uchimiya, H. (1998) The *CURLY LEAF* gene controls both division and elongation of cells during the expansion of the leaf blade in *Arabidopsis thaliana*. Planta 206, 175-183.

Kirik, V. and Baumlein, H. (1996) A novel leaf-specific myb-related protein with a single binding repeat. Gene 183, 109-113.

Kirik, V., Kolle, K., Wohlfarth, T., Misera, S. and Baumlein, H. (1998) Ectopic expression of a novel MYB gene modifies the architecture of the *Arabidopsis* inflorescence. Plant J. 13, 729-742.

Kishitani, S., Yomoda, A., Konno, N. and Tanaka, Y. (1993) Involvement of phenylalanine ammonia-lyase in the development of pollen in broccoli (*Brassica oleracea* L.). Sex. Plant Reprod. 6, 244-248.

Klahre, U., Noguchi, T., Fujioka, S., Takatsuto, S., Yokota, T., Nomura, T., Yoshida, S. and Chua, N. H. (1998) The *Arabidopsis DIMINUTO/DWARF1* gene encodes a protein involved in steroid synthesis. Plant Cell 10, 1677-1690.

Klein, T. M., Wolf, E. D., Wu, R. and Sanford, J. C. (1987) High velocity microprojectiles for delivering nucleic acids into living cells. Nature 327, 71-73.

Klempnauer, K. H., Gonda, T. J. and Bishop, J. M. (1982) Nucleotide sequence of the retroviral leukemia gene v-myb and its cellular progenitor c-myb: the architecture of a transduced oncogene. Cell 31, 453-63.

van der Knaap, E. and Kende, H. (1995) Identification of a gibberellin-induced gene in deepwater rice using differential display of mRNA. Plant Mol. Biol. 28, 589-592.

Kobayashi, A., Sakamoto, A., Kubo, K., Rybka, Z., Kanno, Y. and Takatsuji, H. (1998) Seven zinc-finger transcription factors are expressed sequentially during the development of anthers in petunia. Plant J. 13, 571-576.

Koltunow, A. M., Truettner, J., Cox, K. H., Wallroth, M. and Goldberg, R. B. (1990) Different temporal and spatial gene-expression patterns occur during anther development. Plant Cell 2, 1201-1224.

Kranz, H. D., Denekamp, M., Greco, R., Jin, H., Leyva, A., Meissner, R. C., Petroni, K., Urzainqui, A., Bevan, M., Martin, C., Smeekens, S., Tonelli, C., Paz-Ares, J. and Weisshaar, B. (1998) Towards functional characterisation of the members of the *R2R3- MYB* gene family from *Arabidopsis thaliana*. Plant J. 16, 263-276.

Kranz, H., Scholz, K. and Weisshaar, B. (2000) *c-MYB* oncogene-like genes encoding three MYB repeats occur in all major plant lineages. Plant J. 21, 231-235.

Kusaba, S., Kano-Murakami, Y., Matsuoka, M., Tamaoki, M., Sakamoto, T., Yamaguchi, I. and Fukumoto, M. (1998) Alteration of hormone levels in

transgenic tobacco plants overexpressing the rice homeobox gene *OSH1*. Plant Physiol. 116, 471-476.

Kusano, G., Takahira, M., Shibano, M., Kusano, A., Okamoto, Y., Tsujibo, H., Numata, A. and Inamori, Y. (1998) Studies on inhibitory activities of fukiic acid esters on germination, alpha-amylase and carboxypeptidase A. Biol. Pharm. Bull. 21, 997-999.

Lam, E. W., Robinson, C. and Watson, R. J. (1992) Characterization and cell cycle-regulated expression of mouse B-myb. Oncogene 7, 1885-1890.

Lamb, C. J., Merritt, T. K. and Butt, V. S. (1979) Synthesis and removal of phenylalanine ammonia-lyase activity in illuminated discs of potato tuber parenchyme. Biochim. Biophys. Acta 582, 196-212.

Lane, S., Farlie, P. and Watson, R. (1997) B-Myb function can be markedly enhanced by cyclin A-dependent kinase and protein truncation. Oncogene 14, 2445-2453.

Langer, D., Hain, J., Thuriaux, P., and Zillig, W. (1995) Transcription in archaea: similarity to that in eucarya. Proc. Natl. Acad. Sci. USA. 92, 5768-5772.

Lawton, M. A. and Lamb, C. J. (1987) Transcriptional activation of plant defense genes by fungal elicitor, wounding and infection. Mol. Cell. Biol. 7, 335-341.

Lebel, E., Heifetz, P., Thorne, L., Uknes, S., Ryals, J. and Ward, E. (1998) Functional analysis of regulatory sequences controlling PR-1 gene expression in *Arabidopsis*. Plant J. 16, 223-233.

Lee, H., Leon, J. and Raskin, I. (1995) Biosynthesis and metabolism of salicylic acid. Proc. Natl. Acad. Sci. USA 92, 4076-4079.

Lee, M. M. and Schiefelbein, J. (1999) WEREWOLF, a MYB-related protein in *Arabidopsis*, is a position-dependent regulator of epidermal cell patterning. Cell 99, 473-483.

Leech, M. J., Kammerer, W., Cove, D. J., Martin, C. and Wang, T. L. (1993) Expression of *myb*-related genes in the moss, *Physcomitrella patens*. Plant J. 3, 51-61.

Legrand, M., Fritig, B. and Hirth, L. (1976) Enzymes of the phenylpropanoid pathway and the necrotic reaction of hypersensitive tobacco mosaic virus. Phytochemistry 15, 1353-1359.

Legrand, M., Kauffmann, S., Geoffroy, P. and Fritig, B. (1987) Biological function of pathogenesis-related proteins: Four tobacco pathogenesis-related proteins are chitinases. Proc. Natl. Acad. Sci. USA 84, 6750-6754.

Leon, J., Yalpani, N., Raskin, I. and Lawton, M. A. (1993) Induction of benzoic acid 2-hydroxylase in virus-inoculated tobacco. Plant Physiol. 103, 323-328.

Li, Y., Flanagan, P. M., Tschochner, H. and Kornberg, R. D. (1994) RNA polymerase II initiation factor interactions and transcription start site selection. Science 263, 805-807.

Li, Y., Hagen, G. and Guilfoyle, T. J. (1992) Altered morphology in transgenic tobacco plants that overproduce cytokinins in specific tissues and organs. Dev. Biol. 153, 386-395.

Li, S. F., Higginson, T. and Parish, R. W. (1999) A novel MYB-related gene from *Arabidopsis thaliana* expressed in developing anthers. Plant Cell Physiol. 40, 343-347.

Li, J. M., Nagpal, P., Vitart, V., McMorris, T. C. and Chory, J. (1996) A role for brassinosteroids in light-dependent development of *Arabidopsis*. Science 272, 398-401.

Lin, Q., Hamilton, W. D. and Merryweather, A. (1996) Cloning and initial characterization of 14 myb-related cDNAs from tomato (*Lycopersicon esculentum* cv. Ailsa Craig). Plant Mol. Biol. 30, 1009-1020.

Lincoln, C., Britton, J. H. and Estelle, M. (1990) Growth and development of the *axr1* mutants of *Arabidopsis*. Plant Cell 2, 1071-1080.

Lincoln, C., Long, J., Yamaguchi, J., Serikawa, K. and Hake, S. (1994) A *knotted1*-like homeobox gene in *Arabidopsis* is expressed in the vegetative meristem and dramatically alters leaf morphology when overexpressed in transgenic plants. Plant Cell 6, 1859-1876.

Linthorst, H. J., Meuwissen, R. L., Kauffmann, S. and Bol, J. F. (1989) Constitutive expression of pathogenesis-related proteins PR-1, GRP, and PR-S in tobacco has no effect on virus infection. Plant Cell 1, 285-291.

Lipsick, J. S. (1996) One billion years of Myb. Oncogene 13, 223-235.

Liu, D., Raghothama, K. G., Hasegawa, P. M. and Bressan, R. A. (1994) Osmotin overexpression in potato delays development of disease symptoms. Proc. Natl. Acad. Sci. USA 91, 1888-1892.

Lockard, R. G. and Grunwald, C. (1970) Grafting and gibberellin effects on the growth of tall and dwarf peas. Plant Physiol. 45, 160-162.

Loguerico, L. L., Zhang, J. Q. and Wilkins, T. A. (1999) Differential regulation of six novel MYB-domain genes defines two distinct expression patterns in allotetraploid cotton (*Gossypium hirsutum* L.). Mol. Gen. Genet. 261, 660-6671.

Lu, H., Flores, O., Weinmann, R. and Reinberg, D. (1991) The nonphosphorylated form of RNA polymerase II preferentially associates with the preinitiation complex. Proc. Natl. Acad. Sci. USA 88, 10004-10008.

Lu, H., Zawel, L., Fisher, L., Egly, J. M. and Reinberg, D. (1992) Human general transcription factor IIH phosphorylates the C-terminal domain of RNA polymerase II. Nature 358, 641-645.

Lugert, T. and Werr, W. (1994) A novel DNA-binding domain in the Shrunken initiator-binding protein (IBP1). Plant Mol. Biol. 25, 493-506.

Lukowitz, W., Mayer, U. and Jurgens, G. (1996) Cytokinesis in the *Arabidopsis* embryo involves the syntaxin-related KNOLLE gene product. Cell 84, 61-71.

Majello, B., Kenyon, L. C. and Dalla-Favera, R. (1986) Human *c-myb* protooncogene: nucleotide sequence of cDNA and organization of the genomic locus. Proc. Natl. Acad. Sci. USA 83, 9636-9640.

Maldonado, E., Ha, I., Cortes, P., Weis , L. and Reinberg, D. (1990) Factors involved in specific transcription by mammalian RNA polymerase II: role of transcription factors IIA, IID, and IIB during formation of a transcription-competent complex. Mol. Cell. Biol. 10, 6335-6347.

Mariani, C., De Beuckeleer, M., Truettner, J., Leemans, J. and Goldberg, R. B. (1990) Induction of male-sterility in plants by a chimeric ribonuclease gene. Nature 347, 737-741.

Mariani, C., Gossele, V., De Beuckeleer, M., De Block, M., Goldberg, R. B., De Greef, W. and Leemans, J. (1992) A chimeric ribonuclease-inhibitor gene restores fertility to male sterile plants. Nature 357, 384-387.

Marshall, B. J. and Ratledge, C. (1972) Salicylic acid biosynthesis and its control in *Mycobacterium smegmatis*. Biochim. Biophys. Acta. 264,106-116.

Martin, C. and Paz-Ares, J. (1997) MYB transcription factors in plants. Trends Genet. 13, 67-73.

Mascarenhas, J. P. (1989) The male gametophyte of flowering plants. Plant Cell 1, 657-664.

Mascarenhas, J. P. (1990) Gene activity during pollen development. Annu. Rev. Plant Physiol. Plant Mol. Biol. 41, 317-338.

Matsuda, N., Tsuchiya, T., Kishitani, S., Tanaka, Y. and Toriyama, K. (1996) Partial male sterility in transgenic tobacco carrying antisense and sense PAL cDNA under the control of a tapetum-specific promoter. Plant Cell Physiol. 37, 215-222.

Maxon, M. E. and Goodrich, J. A. and Tjian, R. (1994) Transcription factor IIE binds preferentially to RNA polymerase IIa and recruits TFIIH: a model for promoter clearance. Genes Dev. 8, 515-524.

McClelland, M., Mathieu-Daude, F. and Welsh, J. (1995) RNA fingerprinting and differential display using arbitrarily primed PCR. Trends Genet. 11, 242-246.

McComb, A. J. and McComb, J. A. (1970) Growth substances and the relation between phenotype and genotype in *Pisum sativum*. Planta 91, 235-245.

McCormick, S. (1991) Molecular analysis of male gametogenesis in plants. Trends Genet. 7, 298-303.

McCourt, P. (1999) Genetic analysis of hormone signaling. Annu. Rev. Plant Physiol. Plant Mol. Biol. 50, 219-243.

McIntosh, P. B., Frenkiel, T. A., Wollborn, U., McCormick, J. E., Klempnauer, K. H., Feeney, J. and Carr, M. D. (1998) Solution structure of the B-Myb DNA-binding domain: a possible role for conformational instability of the protein in DNA binding and control of gene expression. Biochemistry 37, 9619-9629.

van der Meer, I. M., Stam, M. E., van Tunen, A. J., Mol, J. N. and Stuitje, A. R. (1992) Antisense inhibition of flavonoid biosynthesis in petunia anthers results in male sterility. Plant Cell 4, 253-262.

Merkle, T. and Nagy, F. (1997) Nuclear import of proteins: putative import factors and development of in vitro import systems in higher plants. Trends Plant Sci. 2, 458-464.

Meuwly, P., Molders, W., Buchala, A. and Metraux, J. P. (1995) Local and systemic biosynthesis of salicylic acid in infected cucumber plants. Plant Physiol. 109, 1107-1114.

Mink, S., Kerber, U. and Klempnauer, K. H. (1996) Interaction of C/EBPβ and v-Myb is required for synergistic activation of the *mim*-1 gene. Mol. Cell Biol. 16, 1316-1325.

Misquitta, L. and Paterson, B. M. (1999) Targeted disruption of gene function in *Drosophila* by RNA interference (RNA-i): a role for nautilus in embryonic somatic muscle formation. Proc. Natl. Acad. Sci. USA 96, 1451-1456.

Mo, Y. Y., Nagel, C. and Taylor, L. P. (1992) Biochemical complementation of chalcone synthase mutants defines a role for flavonols in functional pollen. Proc. Natl. Acad. Sci. USA 89, 7213-7217.

Montgomery, M. K., Xu, S. and Fire, A. (1998) RNA as a target of double-stranded RNA-mediated genetic interference in *Caenorhabditis elegans*. Proc. Natl. Acad. Sci. USA 95, 15502-15507.

Montminy, M. (1997) Transcriptional regulation by cyclic AMP. Annu. Rev. Biochem. 66, 807-822.

Moran, R. (1982) Formulae for determination of chlorophyllous pigments extracted with N, N-dimethylformamide. Photochem. Photobiol. 69, 1376-1381.

Moyano, E., Martinez-Garcia, J. F. and Martin C. (1996) Apparent redundancy in *myb* gene function provides gearing for the control of flavonoid biosynthesis in *Antirrhinum* flowers. Plant Cell 8, 1519-1532.

Murashige, T. and Skoog, F. (1962) A revised medium for rapid growth and bioassays with tobacco tissue cultures. Physiol. Plant. 15. 473-497.

Myrset, A. H., Bostad, A., Jamin, N., Lirsac, P. N., Toma, F. and Gabrielsen, O. S. (1993) DNA and redox state induced conformational changes in the DNA-binding domain of the Myb oncoprotein. EMBO J. 12, 4625-4633.

Neuhaus, J. M., Ahl-Goy, P., Hinz, U., Flores, S. and Meins, F. Jr. (1991) High-level expression of a tobacco chitinase gene in *Nicotiana sylvestris*. Susceptibility of transgenic plants to *Cercospora nicotianae* infection. Plant Mol. Biol. 16, 141-151.

Neuhaus, J. M., Flores, S., Keefe, D., Ahl-Goy, P. and Meins, F. Jr. (1992) The function of vacuolar beta-1,3-glucanase investigated by antisense transformation. Susceptibility of transgenic *Nicotiana sylvestris* plants to *Cercospora nicotianae* infection. Plant Mol. Biol. 19, 803-813.

Ngo, H., Tschudi, C., Gull, K. and Ullu, E. (1998) Double-stranded RNA induces mRNA degradation in *Trypanosoma brucei*. Proc. Natl. Acad. Sci. USA 95, 14687-14692.

Noda, K, I., Glover, B, J., Linstead, P. and Martin, C. (1994) Flower colour intensity depends on specialized cell shape controlled by a Myb-related transcription factor. Nature 369, 661-664.

Nomura, T., Nakayama, M., Reid, J. B., Takeuchi, Y. and Yokota, T. (1997) Blockage of brassinosteroid biosynthesis and sensitivity causes dwarfism in garden pea. Plant Physiol. 113, 31-37.

Nomura, N., Takahashi, M., Matsui, M., Ishii, S., Date, T., Sasamoto, S. and Ishizaki, R. (1988) Isolation of human cDNA clones of *myb*-related genes, A-*myb* and B-*myb*. Nucleic Acids Res. 16, 11075-11089.

O'Brien, T., Hardin, S., Greenleaf, A. and Lis, J. T. (1994) Phosphorylation of RNA polymerase II C-terminal domain and transcriptional elongation. Nature 370, 75-77.

Ogata, K., Hojo, H., Aimoto, S., Nakai, T., Nakamura, H., Sarai, A., Ishii, S. and Nishimura, Y. (1992) Solution structure of a DNA-binding unit of Myb: a helix-turn-helix-related motif with conserved tryptophans forming a hydrophobic core. Proc. Natl. Acad. Sci. USA 89, 6428-6432.

Ogata, K., Kanei-Ishii, C., Sasaki, M., Hatanaka, H., Nagadoi, A., Enari, M., Nakamura, H., Nishimura, Y., Ishii, S. and Sarai , A. (1996) The cavity

in the hydrophobic core of Myb DNA-binding domain is reserved for DNA recognition and trans-activation. Nat. Struct. Biol. 3, 178-187.

Ogata, K., Morikawa, S., Nakamura, H., Hojo, H., Yoshimura, S., Zhang, R., Aimoto, S., Ametani, Y., Hirata, Z., Sarai, A., Ishii, S. and Nishimura, Y. (1995) Comparison of the free and DNA-complexed forms of the DNA-binding domain from c-Myb. Nat. Struct. Biol. 2, 309-20.

Ogata, K., Morikawa, S., Nakamura, H., Sekikawa, A., Inoue, T., Kanai, H., Sarai, A., Ishii, S. and Nishimura, Y. (1994) Solution structure of a specific DNA complex of the Myb DNA-binding domain with cooperative recognition helices. Cell 79, 639-48.

Ohi, R., McCollum, D., Hirani, B., Den Haese, G. J., Zhang, X., Burke, J. D., Turner, K., and Gould, K. L. (1994) The *Schizosaccharomyces pombe cdc5+* gene encodes an essential protein with homology to c-Myb. EMBO J. 13, 471-483.

Ohkuma, Y. and Roeder, R. G. (1994) Regulation of TFIIH ATPase and kinase activities by TFIIE during active initiation complex formation. Nature 368, 160-103.

Ohkuma, Y., Sumimoto, H., Horikoshi, M. and Roeder, R. G. (1990) Factors involved in specific transcription by mammalian RNA polymerase II: purification and characterization of general transcription factor TFIIE. Proc. Natl. Acad. Sci. USA 87, 9163-9167.

Ooms, G., Hooykaas, P. J. J., Van Veen, R. J. M., Van Beelen, P., Regensburg-Tuink, T. J. G. and Schilperoort, R. A. (1982) Octopine Ti-plasmid deletion mutants of *Agrobacterium tumefaciens* with emphasis on the right side of the T-DNA region. Plasmid 7, 15-29.

Oppenheimer, D. G., Herman, P. L., Sivakumaran, S., Esch, J. and David Marks, M. (1991) A *myb* gene required for leaf trichome differentiation in Arabidopsis is expressed in stipules. Cell 67, 483-493.

Orr, J. D., Edwards, R. and Dixon, R. A. (1993) Stress responses in alfalfa (*Medicago-sativa* L.). XIV. Changes in the levels of phenylpropanoid pathway intermediates in relation to regulation of L-phenylalanine

ammonia-lyase in elicitor-treated cell-suspension cultures. Plant Physiol. 101, 847-856.

Owen, H. A. and Makaroff, C. A. (1995) Ultrastructure of microsporogenesis and microgametogenesis in *Arabidopsis thaliana* (L.) Heynh ecotype Wassilewskija (Brassicaceae). Protoplasma 185, 7-21.

Pacini, E. (1990) Tapetum and microspore function. In: Microspores: evolution and ontogeny (Blackmore, S. and Knox, R. B., eds). Academic Press, Lonon, pp. 213-237.

Parker, J. E., Holub, E. B., Frost, L. N., Falk, A., Gunn, N. D. and Daniels, M. J. (1996) Characterization of *eds1*, a mutation in *Arabidopsis* suppressing resistance to *Peronospora parasitica* specified by several different *RPP* genes. Plant Cell 8, 2033-2046.

Pavletich, N. P. and Pabo, C. O. (1991) Zinc finger-DNA recognition: crystal structure of a Zif268-DNA complex at 2.1 A°. Science 252, 809-817.

Pavletich, N. P. and Pabo. C. O. (1993) Crystal structure of a five-finger GLI-DNA complex: new perspectives on zinc fingers. Science 261, 1701-1707.

Payne, G., Ahl, P., Moyer, M., Harper, A., Beck, J., Meins, F. and Ryals, J. (1990) Isolation of complementary DNA clones encoding pathogenesis-related proteins P and Q, two acidic chitinases from tobacco. Proc. Natl. Acad. Sci. USA 87, 98-102.

Paz-Ares, J., Ghosal, D., Wienand, U., Peterson, P. A. and Saedler, H. (1987) The regulatory c1 locus of Zea mays encodes a protein with homology to myb proto-oncogene products and with structural similarities to transcriptional activators. EMBO J. 6, 3553-3558.

Pellegrini, L., Rohfritsch, O., Fritig, B. and Legrand, M. (1994) Phenylalanine ammonia-lyase in tobacco. Molecular cloning and gene expression during the hypersensitive reaction to tobacco mosaic virus and the response to a fungal elicitor. Plant Physiol. 106, 877-886.

Pfitzner, U. M. and Goodman, H. M (1987) Isolation and characterization of cDNA clones encoding pathogenesis-related proteins from tobacco mosaic virus infected tobacco plants. Nucleic Acids Res. 15, 4449-4465.

Pfitzner, E., Kirfel, J., Becker, P., Rolke, A. and Schule, R. (1998) Physical interaction between retinoic acid receptor and the oncoprotein myb inhibits retinoic acid-dependent transactivation. Proc. Natl. Acad. Sci. USA 95, 5539-5544.

Pollak, P. E., Hansen, K., Astwood, J. D. and Taylor, L. P. (1995) Conditional male-fertility in maize. Sex. Plant Reprod. 8, 231-241.

Pollak, P. E., Vogt, T., Mo, Y. Y. and Taylor, L. P. (1993) Chalcone synthase and flavonol accumulation in stigmas and anthers of *Petunia hybrida.* Plant Physiol. 102, 925-932.

Proebsting, W. M., Hedden, P., Lewis, M. J., Croker, S. J. and Proebsting, L. N. (1992) Gibberellin concentration and transport in genetic lines of pea, Effects of grafting. Plant Physiol. 100, 1354-1360.

Quattrocchio, F., Wing, J., van der Woude, K., Souer, E., de Vetten, N., Mol, J. and Koes, R. (1999) Molecular analysis of the anthocyanin2 gene of petunia and its role in the evolution of flower color. Plant Cell 11, 1433-1444.

Quaye, I. K. E., Toku, S. and Tanaka, T. (1996) Sequence requirement for nucleolar localization of rat ribosomal protein L31. Eur. J. Cell Biol. 69, 151-155.

Rabinowicz, P. D., Braun, E. L., Wolfe, A. D., Bowen, B. and Grotewold, I. (1999) Maize R2R3 Myb genes: Sequence analysis reveals amplification in the higher plants. Genetics 153, 427-444.

Raikhel, N. (1992) Nuclear targeting in plants. Plant Physiol. 100, 1627-1632.

Rao, M. V., Paliyath, G., Ormrod, D. P., Murr, D. P. and Watkins, C. B. (1997) Influence of salicylic acid on H_2O_2 production, oxidative stress, and H_2O_2-metabolizing enzymes. Salicylic acid-mediated oxidative damage requires H2O2. Plant Physiol. 115, 137-149.

Rate, D. N., Cuenca, J. V., Bowman, G. R., Guttman, D. S. and Greenberg, J. T. (1999) The gain-of-function Arabidopsis *acd6* mutant reveals novel regulation and function of the salicylic acid signaling pathway in controlling cell death, defenses, and cell growth. Plant Cell 11, 1695-1708.

Rauscher, M., Adam, A. L., Wirtz, S., Guggenheim, R., Mendgen, K. and Deising, H. B. (1999) PR-1 protein inhibits the differentiation of rust infection hyphae in leaves of acquired resistant broad bean. Plant J.19, 625-633.

Redei, G. P. and Koncz, C. (1992) Classical mutagenesis. In Methods in Arabidopsis Research (Koncz, C., Chua, N. H. and Schell, J., eds). World Scientific Publishing Co. Pte. Ltd. Singapore, New Jersey, London, Hong Kong, pp. 16-82.

Regan, S. M. and Moffatt, B. A. (1990) Cytochemical analysis of pollen development in wild-type *Arabidopsis* and a male-sterile mutant. Plant Cell 2, 877-889.

Reid, J. B. (1986) Gibberellin mutants. In: A Genetic Approach to Plant Biochemistry (Blonstein, A. D. and King, P. J., eds). Springer-Verlag Wien, New York, pp 1-34.

Reid, J. B., Murfet, I. C. and Potts, W. C. (1983) Internode length in *Pisum*. II. Additional information on the relationship and action of loci *Le*, *La*, *Cry*, *Na* and *Lm*. J. Exp. Bot. 34, 349-364.

Reymond, P. and Farmer, E. E. (1998) Jasmonate and salicylate as global signals for defense gene expression. Curr. Opin. Plant Biol. 1, 404-411.

Reynolds, J. O., Eisses, J. F. and Sylvester, A. W. (1998) Balancing division and expansion during maize leaf morphogenesis: analysis of the mutant, *warty-1*. Development 125, 259-268.

Rittscher, M. and Wiermann, R. (1983) Occurrence of phenylalanine ammonia-lyase (PAL) in isolated tapetum cells of tulipa anthers. Protoplasma 118, 219-224.

Roberts, S. G., Ha, I., Maldonado, E., Reinberg, D. and Green, M. R. (1993) Interaction between an acidic activator and transcription factor TFIIB is required for transcriptional activation. Nature 363, 741-744.

Robertson, K. D. and Jones, P. A. (2000) DNA methylation: past, present and future directions. Carcinogenesis 21, 461-467.

Robinson, C., Light, Y., Groves, R., Mann, D., Marias, R. and Watson, R. (1996) Cell-cycle regulation of B-Myb protein expression: specific phosphorylation during the S phase of the cell cycle. Oncogene 12, 1855-1864.

Roeder, R. G. (1996) The role of general initiation factors in transcription by RNA polymerase II. Trends Biochem. Sci. 9, 327-335.

Rogers, E. E. and Ausubel, F. M. (1997) *Arabidopsis* enhanced disease susceptibility mutants exhibit enhanced susceptibility to several bacterial pathogens and alterations in PR-1 gene expression. Plant Cell 9, 305-316.

Romero, I., Fuertes, A., Benito, M. J., Malpica, J. M., Leyva, A. and Paz-Ares, J. (1998) More than 80 *R2R3-MYB* regulatory genes in the genome of *Arabidopsis thaliana*. Plant J. 14, 273-284.

Rosinski, J. A. and Atchley, W. R. (1998) Molecular evolution of the Myb family of transcription factors: Evidence for polyphyletic origin. J. Mol. Evol. 46, 74-83.

Rosson, D. and Reddy, E. P. (1986) Nucleotide sequence of chicken c-myb complementary DNA and implications for myb oncogene activation. Nature 319, 604-606.

Rüffer, M., Steipe, B. and Zenk, M. H. (1995) Evidence against specific binding of salicylic acid to plant catalase. FEBS Letters 377, 175-180.

Ryals, J., Uknes, S. and Ward, E. (1994) Systemic acquired resistance. Plant Physiol. 104, 1109-1112.

Sablowski, R. W. M., Moyano, E., Culianez-Macia, F. A., Schuch, W., Martin, C. and Bevan, M. (1994) A flower-specific MYB protein activates transcription of phenylpropanoid biosynthetic genes. EMBO J. 13, 128-137.

Saikumar, P., Murali, R. and Reddy, E. P. (1990) Role of tryptophan repeats and flanking amino acids in Myb-DNA interactions. Proc. Natl. Acad. Sci. USA. 87, 8452-8456.

Sala, A., Kundu, M., Casella, I., Engelhard, A., Calabretta, B., Grasso, L., Paggi, M. G., Giordano, A., Watson, R. J., Khalili, K. and Peschle, C. (1997) Activation of human B-MYB by cyclins. Proc. Natl. Acad. Sci. USA 94, 532-536.

Sanchez Alvarado, A. and Newmark, P. A. (1999) Double-stranded RNA specifically disrupts gene expression during planarian regeneration. Proc. Natl. Acad. Sci. USA 96, 5049-5054.

Saville, M. K. and Watson, R. J. (1998) The cell-cycle regulated transcription factor B-Myb is phosphorylated by cyclin A/Cdk2 at sites that enhance its transactivation properties. Oncogene 17, 2679-2689.

Sawadogo, M. and Van Dyke, M.W. (1991) A rapid method for the purification of deprotected oligodeoxynucleotides. Nucleic Acids Res. 19, 674.

Schaeffer, L., Moncollin, V., Roy, R., Staub, A., Mezzina, M., Sarasin, A., Weeda, G., Hoeijmakers, J. H. and Egly, J. M. (1994) The ERCC2/DNA repair protein is associated with the class II BTF2/TFIIH transcription factor. EMBO J. 13, 2388-2392.

Schaffer, R., Ramsay, N., Samach, A., Corden, S., Putterill, J., Carre, I. A. and Coupland, G. (1998) The *late elongated hypocotyl* mutation of *Arabidopsis* disrupts circadian rhythms and the photoperiodic control of flowering. Cell 93, 1219-1229.

Schmülling, T., Fladung, M., Grossmann, K. and Schell, J. (1993) Hormonal content and sensitivity of transgenic tobacco and potato plants expressing single *rol* genes of *Agrobacterium rhizogenes* T-DNA. Plant J. 3, 371-382.

Schmülling, T., Schell, J. and Spena, A. (1988) Single genes from *Agrobacterium rhizogenes* influence plant development. EMBO J. 7, 2621-2629.

Schrauwen, J. A. M., de Groot, P. F. M., van Herpen, M. M. A., van der Lee, T., Reynen W. H., Weterings, K. A. P. and Wullems, G. J. (1990) Stage-related expression of mRNAs during pollen development in lily and tobacco. Planta 182, 298-304.

Scott, R. J. (1994) Pollen exine- the sporopollenin enigma and the physics of pattern. In:. Molecular and cellular aspects of plant reproduction (Scott, R. J. and Stead, A. D., eds). Camridge University Press, pp. 49-81.

Serizawa, H., Conaway, J. W. and Conaway, R. C. (1994) An oligomeric form of the large subunit of transcription factor (TF) IIE activates phosphorylation of the RNA polymerase II carboxyl-terminal domain by TFIIH. J. Biol. Chem. 269, 20750-20756.

Serizawa, H., Conaway, R. C. and Conaway, J. W. (1992) A carboxyl-terminal-domain kinase associated with RNA polymerase II transcription factor delta from rat liver. Proc. Natl. Acad. Sci. USA 89, 7476-7480.

Sharma, Y. K. and Davis, K. R. (1995) Isolation of a novel *Arabidopsis* ozone-induced cDNA by differential display. Plant. Mol. Biol. 29, 91-98.

Sharp, P. A. (1999) RNAi and double-strand RNA. Genes Dev. 13, 139-141.

Shen, R., Su, Z. Z., Olsson, C. A. and Fisher, P. B. (1995) Identification of the human prostatic carcinoma oncogene PTI-1 by rapid expression cloning and differential RNA display. Proc. Natl. Acad. Sci. USA 92, 6778-6782.

Shi, Y. and Mello, C. (1998) A CBP/p300 homolog specifies multiple differentiation pathways in *Caenorhabditis elegans*. Genes Dev. 12, 943-955.

Shirley, B. W., Kubasek, W. L., Storz, G., Bruggemann, E., Koornneef, M., Ausubel, F. M. and Goodman, H. M. (1995) Analysis of *Arabidopsis* mutants deficient in flavonoid biosynthesis. Plant J. 8, 659-671.

Sieburth, L. E. and Meyerowitz, E. M. (1997) Molecular dissection of the *AGAMOUS* control region shows that cis-elements for spatial regulation are located intragenically. Plant Cell 9, 355-365.

Silverman, P., Seskar, M., Kanter, D., Schweizer, P., Metraux, J. P. and Raskin, I (1995) Salicylic acid in rice: biosynthesis, conjugation, and possible role. Plant Physiol. 108, 633-639.

Silverstone, A. L. and Sun, T. (2000) Gibberellins and the Green Revolution. Trends Plant Sci. 5, 1-2.

Sinha, N. (1999) Leaf development in angiosperms. Annu. Rev. Plant Physiol. Plant Mol. Biol. 50, 419-446.

Sinha, N. R., Williams, R. E. and Hake, S. (1993) Overexpression of the maize homeo box gene, *KNOTTED-1*, causes a switch from determinate to indeterminate cell fates. Genes Dev. 7, 787-795.

Sinkar, V. P., Pythoud, F., White, F. F., Nester, E. W. and Gordon, M. P. (1988) *rolA* locus of the Ri plasmid directs developmental abnormalities in transgenic tobacco plants. Genes Dev. 2, 688-697.

Slamon, D. J., Boone,T. C., Murdock, D. C., Keith, D. E., Press, M. F., Larson, R. A. and Souza, L. M. (1986) Studies of the human c-*myb* gene and its product in human acute leukemias. Science 233, 347-351.

Sleeman, J. P. (1993) Xenopus A-myb is expressed during early spermatogenesis. Oncogene 8, 1931-1941.

Smale, S. T. and Baltimore, D. (1989) The "initiator" as a transcription control element. Cell 57, 103-113.

Smith, L. G., Hake, S. and Sylvester, A. W. (1996) The *tangled-1* mutation alters cell division orientations throughout maize leaf development without altering leaf shape. Development 122, 481-489.

Solano, R., Nieto, C., Avila, J., Canas, L., Diaz, I. and Paz-Ares, J. (1995) Dual DNA binding specificity of a petal epidermis-specific MYB transcription factor (MYB.Ph3) from *Petunia hybrida*. EMBO J. 14, 1773-1784.

Sotiriou, C., Lacroix, M., Lagneaux, L., Berchem, G. and Body, J. J. (1999) The aspirin metabolite salicylate inhibits breast cancer cells growth and their synthesis of the osteolytic cytokines interleukins-6 and -11. Anticancer Res. 19, 2997-3006.

Stinson, J. R., Eisenberg, A. J., Willing, R. P., Pe, M. E., Hanson, D. D. and Mascarenhas, J. P. (1987) Genes expressed in the male gametophyte of flowering plants and their isolation. Plant Physiol. 83, 442-447.

Stober-Grasser, U., Brydolf, B., Bin, X., Grasser, F., Firtel, R. A. and Lipsick, J. S. (1992) The Myb DNA-binding domain is highly conserved in Dictyostelium discoideum. Oncogene 7, 589-596.

Struhl, K. (1996) Chromatin structure and RNA polymerase II connection: implications for transcription. Cell 84, 179-182.

Sugano, S., Andronis, C., Green, R. M., Wang, Z. Y. and Tobin, E. M. (1998) Protein kinase CK2 interacts with and phosphorylates the *Arabidopsis* circadian clock-associated 1 protein. Proc. Natl. Acad. Sci. USA. 95, 11020-11025.

Swain, S. M. and Olszewski, N. E. (1996) Genetic analysis of gibberellin signal transduction. Plant Physiol. 112, 11-17.

Sweetman, J. P. (1996) Characterisation and functional analysis of pollen-specific cDNAs encoding putative transcriptional regulators from *Nicotiana tabacum*. Ph.D Thesis, University of Leicester, UK.

Sweetman, J., Spurr, C., Eliasson, A., Gass, N., Steinmetz, A. and Twell, D. (2000) Isolation and characterisation of two pollen-specific LIM domain protein cDNAs from *Nicotiana tabacum*. Sex. Plant Reprod. 12, 339-345.

Szekeres, M., Nemeth, K., Koncz-Kalman, Z., Mathur, J., Kauschmann, A., Altmann, T., Redei, G. P., Nagy, F., Schell, J. and Koncz, C. (1996) Brassinosteroids rescue the deficiency of CYP90, a cytochrome P450, controlling cell elongation and de-etiolation in *Arabidopsis*. Cell 85, 171-182.

Tabara, H., Grishok, A. and Mello, C. C. (1998) RNAi in *C. elegans*: soaking in the genome sequence. Science 282, 430-431.

Takahashi, T., Gasch, A., Nishizawa, N. and Chua, N. H. (1995) The *DIMINUTO* gene of *Arabidopsis* is involved in regulating cell elongation. Genes Dev. 9, 97-107.

Takemoto, Y., Tashiro, S., Handa, H. and Ishii, S. (1994) Multiple nuclear localization signals of the B-myb gene product. FEBS Letters 350, 55-60.

Tamagnone, L., Merida, A., Parr, A., Mackay, S., Culianez-Macia, F. A., Roberts, K. and Martin, C. (1998) The AmMYB308 and AmMYB330 transcription factors from antirrhinum regulate phenylpropanoid and lignin biosynthesis in transgenic tobacco. Plant Cell 10, 135-154.

Tamanini, F., Kirkpatrick, L. L., Schonkeren, J., Unen, Lv., Bontekoe, C., Bakker, C., Nelson, D. L., Galjaard, H., Oostra, B. A. and Hoogeveen, A. T. (2000) The fragile X-related proteins FXR1P and FXR2P contain a functional nucleolar-targeting signal equivalent to the HIV-1 regulatory proteins. Hum. Mol. Genet. 9, 1487-1493.

Tamaoki, M., Kusaba, S., Kano-Murakami, Y. and Matsuoka, M. (1997) Ectopic expression of a tobacco homeobox gene, *NTH15*, dramatically alters leaf morphology and hormone levels in transgenic tobacco. Plant Cell Physiol. 38, 917-927.

Tan, R. and Frankel, A. D. (1998) A novel glutamine-RNA interaction identified by screening libraries in mammalian cells. Proc. Natl. Acad. Sci. USA 95, 4247-4252.

Tanaka-Ueguchi, M., Itoh, H., Oyama, N., Koshioka, M. and Matsuoka M. (1998) Over-expression of a tobacco homeobox gene, *NTH15*, decreases the expression of a gibberellin biosynthetic gene encoding GA 20-oxidase. Plant J. 15, 391-400.

Tanikawa, J., Yasukawa, T., Enari, M., Ogata, K., Nishimura, Y., Ishii, S. and Sarai, A. (1993) Recognition of specific DNA sequences by the c-myb protooncogene product: role of three repeat units in the DNA-binding domain. Proc. Natl. Acad. Sci. USA 90, 9320-9324.

Tashiro, S., Takemoto, Y., Handa, H. and Ishii, S. (1995) Cell type-specific trans-activation by the B-myb gene product: requirement of the putative cofactor binding to the C-terminal conserved domain. Oncogene 10, 1699-1707.

Taylor, L. P. and Jorgensen, R. (1992) Conditional male-fertility in chalcone synthase-deficient petunia. J. Hered. 83, 11-17.

Tebbutt, S. J., Rogers, H. J. and Lonsdale, D. M. (1994) Characterization of a tobacco gene encoding a pollen-specific polygalacturonase. Plant Mol. Biol. 25, 283-297.

Tice-Baldwin, K., Fink, G. R. and Arndt, K. T. (1989) BAS1 has a Myb motif and activates HIS4 transcription only in combination with BAS2. Science 246, 931-935.

Timmermans, M. C., Hudson, A., Becraft, P. W. and Nelson, T. (1999) ROUGH SHEATH2: a Myb protein that represses knox homeobox genes in maize lateral organ primordia. Science 284, 151-153.

Timpte, C. S., Wilson, A. K. and Estelle, M. (1992) Effects of the *axr2* mutation of *Arabidopsis* on cell-shape in hypocotyl and inflorescence. Planta 188, 271-278.

Tomita, A., Towatari, M., Tsuzuki, S., Hayakawa, F., Kosugi, H., Tamai, K., Miyazaki, T., Kinoshita, T. and Saito, H. (2000) c-Myb acetylation at the carboxyl-terminal conserved domain by transcriptional co-activator p300. Oncogene 19, 444-451.

Töpfer, R., Matzeit, V., Gronenborn, B., Schell, J. and Steinbiss, H. H. (1987) A set of plant expression vectors for transcriptional and translational fusions. Nucleic Acids Res. 15, 5890.

Topping, J. F., May, V. J., Muskett, P. R. and Lindsey, K. (1997) Mutations in the *HYDRA1* gene of *Arabidopsis* perturb cell shape and disrupt embryonic and seedling morphogenesis. Development 124, 4415-4424.

Torres-Ruiz, R. A. and Jürgens, G. (1994) Mutations in the *FASS* gene uncouple pattern-formation and morphogenesis in *Arabidopsis* development. Development 120, 2967-2978.

Traas, J., Bellini, C., Nacry, P., Kronenberger, J., Bouchez, D. and Caboche, M. (1995) Normal differentiation patterns in plants lacking microtubular preprophase bands. Nature 375, 676-677.

Tsuchiya, T., Toriyama, K., Ejiri, S. and Hinata, K. (1994) Molecular characterization of rice genes specifically expressed in the anther tapetum. Plant Mol. Biol. 26, 1737-1746.

Tsuge, T., Tsukaya, H. and Uchimiya, H. (1996) Two independent and polarized processes of cell elongation regulate leaf blade expansion in *Arabidopsis thaliana* (L) Heynh. Development 122, 1589-1600.

Tsukaya, H. and Uchimiya, H. (1997) Genetic analyses of the formation of the serrated margin of leaf blades in *Arabidopsis*: combination of a mutational analysis of leaf morphogenesis with the characterization of a specific marker gene expressed in hydathodes and stipules. Mol. Gen. Genet. 256, 231-238.

van Tunen, A.J., Koes, R. E., Spelt, C. E., van der Krol, A. R., Stuitje, A. R. and Mol, J. N. (1988) Cloning of the two chalcone flavanone isomerase genes from Petunia hybrida: Coordinate, light-regulated and differential expression of flavonoid genes. EMBO J. 7, 1257-1263.

Tupy, J., Rihova, L. and Zarsky, V. (1991) production of fertile tobacco pollen from microspores in suspension-culture and its storage for *in situ* pollination. Sex. Plant Reprod. 4, 284-287.

Tupy, J., Suss, J., Hrabetova, E. and Rihova, L. (1983) Developmental changes in gene expression during pollen differentiation and maturation in *Nicotiana tabacum* L. Biologia Plantarum. 25, 231-237.

Twell, D. (1994) The diversity and regulation of gene expression in the pathway of male gametophyte development. In:.Molecular and cellular aspects of plant reproduction (Scott, R. J. and Stead, A. D., eds). Camridge: Camridge University Press, pp. 83-135.

Twell, D. and Howden, R. (1998) Cell polarity, asymmetric division and cell fate determination in developing pollen. In: S. J. Owens and P. J. Rudall (Editors) Reproductive Biology, PP. 197-218. Royal Botanic Gardens, Kew.

Twell, D., Klein, T. M., Fromm, M.E. and McCormick, S. (1989a) Transient expression of chimeric genes delivered into pollen by microprojectile bombardment. Plant Physiol. 91, 1270 1274.

Twell, D., Park, S. K. and Lalanne, E. (1998) Asymmetric division and cell-fate determination in developing pollen. Trends Plant Sci. 3, 305-310.

Twell, D., Wing, R. A., Yamaguchi, J. and McCormick, S. (1989b) Isolation and expression of an anther-specific gene from tomato. Mol. Gen. Genet. 217, 240-245.

Uimari, A. and Strommer, J. (1997) Myb26: a MYB-like protein of pea flowers with affinity for promoters of phenylpropanoid genes. Plant J. 12, 1273-1284.

Urao, T., Yamaguchi-Shinozaki, K., Urao, S. and Shinozaki, K. (1993) An Arabidopsis *myb* homolog is induced by dehydration stress and its gene product binds to the conserved MYB recognition sequence. Plant Cell 5, 1529-1539.

Usheva, A., Maldonado, E., Goldring, A., Lu, H., Houbavi, C., Reinberg, D. and Aloni, Y. (1992) Specific interaction between the nonphosphorylated form of RNA polymerase II and the TATA-binding protein. Cell 69, 871-881.

Viljoen, T. C., van Aswegen, C. H. and du Plessis, D. J. (1995) Influence of acetylsalicylic acid and metabolites on DU-145 prostatic cancer cell proliferation. Oncology 52, 465-469.

Vogt, T., Pollak, P., Tarlyn, N. and Taylor, L. P. (1994) Pollination-induced or wound-induced kaempferol accumulation in petunia stigmas enhances seed production. Plant Cell 6, 11-23.

Vorbrueggen, G., Lovric, J. and Moelling, K. (1996) Functional analysis of phosphorylation at serine 532 of human c-Myb by MAP kinase. Biol. Chem. 377, 721-730.

Wada, T., Tachibana, T., Shimura, Y. and Okada, K. (1997) Epidermal cell differentiation in *Arabidopsis* determined by a *Myb* homolog, *CPC*. Science 277, 1113-1116.

Waites, R., Selvadurai, H. R., Oliver, I. R. and Hudson, A. (1998) The *PHANTASTICA* gene encodes a MYB transcription factor involved in growth and dorsoventrality of lateral organs in *Antirrhinum*. Cell 93, 779-789.

Wang, Z. Y., Kenigsbuch, D., Sun, L., Harel, E., Ong, M. S. and Tobin, E. M. (1997) A Myb-related transcription factor is involved in the phytochrome regulation of an Arabidopsis *Lhcb* gene. Plant Cell 9, 491-507.

Wang, Z. Y. and Tobin, E. M. (1998) Constitutive expression of the *CIRCADIAN CLOCK ASSOCIATED 1* (*CCA1*) gene disrupts circadian rhythms and suppresses its own expression. Cell 93, 1207-1217.

Ward, E. R., Uknes, S. J., Williams, S. C., Dincher, S. S., Wiederhold, D. L., Alexander, D. C., Ahl-Goy, P., Metraux, J . P. and Ryals, J. A. (1991) Coordinate gene activity in response to agents that induce systemic acquired resistance. Plant Cell 3, 1085-1094.

Waterhouse, P. M., Graham, M. W. and Wang, M. B. (1998) Virus resistance and gene silencing in plants can be induced by simultaneous expression of sense and antisense RNA. Proc. Natl. Acad. Sci. USA 95, 13959-13964.

Weeks, J. R., Hardin, S. E., Shen, J., Lee, J. M. and Greenleaf, A. L. (1993) Locus-specific variation in phosphorylation state of RNA polymerase II in vivo: correlations with gene activity and transcript processing. Genes Dev. 7, 2329-2344.

Westin, E. H., Gorse, K. M. and Clarke, M. F. (1990) Alternative splicing of the human c-myb gene. Oncogene 5, 1117-1124.

Weterings, K., Schrauwen, J., Wullems, G. and Twell, D. (1995) Functional dissection of the promoter of the pollen-specific gene *NTP303* reveals a novel pollen-specific, and conserved *cis*-regulatory element. Plant J. 8, 55-63.

Weymann, K., Hunt, M., Uknes, S., Neuenschwander, U., Lawton, K., Steiner, H. Y. and Ryals, J. (1995) Suppression and restoration of lesion formation in *Arabidopsis lsd* mutants. Plant Cell 7, 2013-2022.

Whetten, R. and Sederoff, R. (1995) Lignin biosynthesis. Plant Cell 7, 1001-1013.

Wieser, J. and Adams, T. H. (1995) *flbD* encodes a Myb-like DNA-binding protein that coordinates initiation of *Aspergillus nidulans* conidiophore development. Genes Dev. 9, 491-502.

Willing, R. P., Bashe, D. and Mascarenhas, J. P. (1998) An analysis of the quantity and diversity of messenger RNAs from pollen and shoots of *Zea mays*. Theor. Appl. Genet. 75, 751-753.

Willing, R. P. and Mascarenhas, J. P. (1984) Anlysis of the complexity and diversity of mRNAs from pollen and shoots of *Tradescantia*. Plant Physiol. 75, 865-868.

Wilson, K., Long, D., Swinburne, J. and Coupland, G. (1996) A *Dissociation* insertion causes a semidominant mutation that increases expression of *TINY*, an *Arabidopsis* gene related to *APETALA2*. Plant Cell 8, 659-671.

Wilson, A. K., Pickett, F. B., Turner, J. C. and Estelle, M. (1990) A dominant mutation in *Arabidopsis* confers resistance to auxin, ethylene and abscisic acid. Mol. Gen. Genet. 222, 377-383.

Yalpani, N., Leon, J., Lawton, M. A. and Raskin, I. (1993) Pathway of salicylic acid biosynthesis in healthy and virus-inoculated tobacco. Plant Physiol. 103, 315-321.

Yang, Y. and Klessig, D. (1996) Isolation and characterization of a tobacco mosaic virus -inducible *myb* oncogene homolog from tobacco. Proc. Natl. Acad. Sci. USA 93, 14972 14977.

Yang, S., Sweetman, J., Amirsadeghi, S., Barghchi, M., Huttly, A. K., Chung, W. I. and Twell, D. (2000) Novel anther-specific *myb* genes from tobacco as regulators of phenylalanine ammonia-lyase expression. In Prep.

Yates, J. R. (1998) Mass spectrometry and the age of the proteome. J. Mass Spectrom. 33, 1-19.

Ylstra, B., Busscher, J., Franken, J., Hollman, P. C. H., Mol, J. N. M. and van Tunen, A. J. (1994) Flavonols and fertilization in petunia hybrida: localization and mode of action during pollen tube growth. Plant J. 6, 201-212.

Ylstra, B., Muskens, M. and Van Tunen, A. J. (1996) Flavonols are not essential for fertilization in Arabidopsis thaliana. Plant Mol. Biol. 32, 1155-1158.

Ylstra, B., Touraev, A., Benito-Moreno, R. M., Stöger, E., van Tunen, A. J., Vicente, O., Mol, J. N. M. and Heberle-Bors, E. (1992) Flavonols stimulate development, germination, and tube growth of tobacco pollen. Plant Physiol. 100, 902-907.

Yunes, J. A., Vettore, A. L., da Silva, M. J., Leite, A. and Arruda, P. (1998) Cooperative DNA binding and sequence discrimination by the Opaque2 bZIP factor. Plant Cell 10, 1941-1955.

Zachgo, S., Saedler, H., and Schwarz-Sommer, Z. (1997) Pollen-specific expression of DEFH125, a MADS-box transcription factor in *Antirrhinum* with unusual features. Plant J. 11,1043-1050.

Zawel, L., Lu, H., Cisek, L. J., Corden, J. L. and Reinberg, D. (1993); The cycling of RNA polymerase II during transcription. Cold Spring Harbor Symp. Quant. Biol. 58:187-198.

Zawel, L. and Reinberg, D. (1992) Advances in RNA polymerase II transcription. Curr. Opin. Cell Biol. 4, 488-495.

Zawel, L. and Reinberg, D. (1995) Common themes in assembly and function of eukaryotic transcription complexes. Annu. Rev. Biochem. 64, 533-561.

Zhang, Y., Fan, W., Kinkema, M., Li, X., and Dong, X. (1999) Interaction of NPR1 with basic leucine zipper protein transcription factors that bind sequences required for salicylic acid induction of the PR-1 gene. Proc. Natl. Acad. Sci. USA 96, 6523-5628.

Zhu, Q., Maher, E. A., Masoud, S., Dixon, R. A. and Lamb, C. J. (1994) Enhanced protection against fungal attack by constitutive coexpression of

chitinase and glucanase genes in transgenic tobacco. Bio-Technology 12, 807-812.

Ziebold, U. and Klempnauer, K. H. (1997) Linking Myb to the cell cycle: cyclin-dependent phosphorylation and regulation of A-Myb activity. Oncogene 15, 1011-1019.